**Title**
Development of Late Transition Metal Catalysts for the Hydroamination of Unactivated Alkenes



**Author**
Ma, Senjie

**Publication Date**
2023

Peer reviewed|Thesis/dissertation

# Development of Late Transition Metal Catalysts for the Hydroamination of Unactivated Alkenes

By

Senjie Ma

A dissertation submitted in partial satisfaction of the

requirements for the degree of

Doctor of Philosophy

in

Chemistry

in the

Graduate Division

of the

University of California, Berkeley

Committee in charge:

Professor John F. Hartwig, Chair
Professor Richmond Sarpong
Professor Alexis T. Bell

Spring 2023

Abstract

Development of Late Transition Metal Catalysts for the Intermolecular Hydroamination of Unactivated Alkenes

by

Senjie Ma

Doctor of Philosophy in Chemistry

University of California, Berkeley

Professor John F. Hartwig, Chair

The following dissertation discusses the development of ruthenium and iridium catalysts for the intermolecular hydroamination of unstrained and unconjugated alkenes with amines. These reactions involved the direct addition of the N–H bond of derivatives of 2-aminopyridine to unactivated terminal alkenes and the remote addition of the N–H bond of derivatives of 2-aminopyridine to unactivated disubstituted alkenes. These reactions occurred with high chemo- and regioselectivity to install the amino group at the subterminal position of an aliphatic chain. Experimental and computational mechanistic studies have shed light on the mechanism of these reactions and common side pathways during catalytic hydroamination.

Chapter 1 provides an overview of the hydroamination of alkenes catalyzed by late transition metals. This review includes information regarding the importance and the challenges of catalytic hydroamination, representative examples of catalytic hydroamination of different classes of alkenes, including vinylarenes, conjugated dienes and trienes, strained alkenes as well as unactivated alkenes, and the mechanisms of those reactions. Discussion of photocatalytic hydroamination of alkenes and the future of catalytic hydroamination is also included in this chapter.

Chapter 2 describes the development of ruthenium-catalyzed hydroamination of unactivated terminal alkenes. A cationic ruthenium complex catalyzes the intermolecular hydroamination of a variety of unactivated terminal alkenes with 2-aminopyridine as an ammonia surrogate. Detailed mechanistic studies show that this reaction occurs by a new mechanism comprising initial formation of an imine by oxidative amination, followed by reduction of the imine.

Chapter 3 describes the development of iridium-catalyzed enantioselective hydroamination of unactivated terminal alkenes. A combination of a specific iridium precatalyst containing a

monodentate, labile ethylene ligand and NaBArF catalyzes enantioselective hydroaminations with equimolar amounts of a 2-aminopyridine and unactivated alkenes containing a wide range of functional groups. This catalytic system suppresses competing side reactions, such as the isomerization of the terminal alkene and the racemization of the product of hydroamination.

Chapter 4 describes the development of iridium-catalyzed remote hydroamination of unactivated disubstituted alkenes to place the amino group at the unactivated subterminal carbon of an alkyl chain. The electronic properties of the substituent on the aminopyridine and the development of a new ligand are critical to the high regioselectivity and reaction rates of the reaction.

Table of Content

Acknowledgement

常无本事世说诉 响声钟舍精园祇

First and most importantly, I am sincerely grateful to my parents, my grandparents, and my other family members for their love and support. I am certain that I would not have made it through and obtained a PhD degree without them.

I would like to thank my PhD supervisor Professor John Hartwig. His enthusiasm for chemistry is remarkable, and I have learned a lot about chemistry, research, and writing over the past five year in the group. I also want to thank Professor Richmond Sarpong, Professor Peter Vollhardt, and Professor Alexis Bell for serving as my committee members and offering me with suggestions about chemistry. In addition, I am very grateful to my undergraduate supervisors Matt Whited and Clark Landis. As professors, they not only offered me with excellent mentorship but were also super approachable and friendly. My experiences in the Whited and Landis lab were fantastic and these experiences definitely convinced me to pursue a PhD degree in chemistry and equipped me with the knowledge needed to succeed.

It has been a great pleasure to be part of a group with so many bright, friendly, and supportive coworkers. Group members have talents in diverse areas of life, including stylish designs of phenanthrolines and phosphines, foreign languages and linguistics, as well as various aspects of chemistry, of course. I would like to thank members of the group for insights regarding chemistry, for maintaining a wonderful working environment, and for random discussions and mental supports.

In particular, I would like to thank Yehao Qiu for being a good friend of mine and my roommate for four years, Yumeng Xi, Bo Su, and Alex Fawcett for their mentorship, Isaac Yu, Kyan D'Angelo, Eric Kalkman, Jenna Manske, and Daniel Atanes for making 702 one of the best rooms in the group, my collaborators Haoyu Fan and Craig Day for their help with my projects, Nico Ciccia and Shirley Guo for their assistance during my job search, John Brunn for being the nicest person in the lab, and Adrian Aca, Pengfei Ji, Liye Chen, Zhitao He, Xingyu Jiang, Jeremy Nicolai, Jake Shi, Yuanzhe Xie, Reichi Chen, and many others for being my good friends. The above list is by no means exhaustive and please forgive me if I forget to include your name to the list.

I am also fortunately and grateful to have many friends outside the group to support me during my PhD. They include my undergraduate roommate and best friend, Jia Zhang, Jia’s wife, Weitong Wu, my high school friend, Xin Gu, Gen Li from the Chang group, as well as Yi Xie, Beth Zhu, and Shang Ning from the Maimone group.

In the end, I want to wish everyone the best of luck with their future, and I will miss you and my time in the group.

# CHAPTER 1
# Overview of Late Transition Metal-Catalyzed Intermolecular Hydroamination of Alkenes

## 1.1 Overview of Intermolecular Hydroamination of Alkenes

The intermolecular hydroamination of alkenes is the addition of an N–H bond across a C=C double bond and is an atom- and step-economical method for the synthesis of alkylamines.[1-4] Due to their Lewis basicity and hydrogen-bond acceptor properties, alkylamines are common substructures in pharmaceuticals, agrochemicals, catalysts, and materials. Because amines and unconjugated alkenes are both nucleophilic, the hydroamination of alkenes generally does not occur without a catalyst.[3] Since the first observation of catalytic hydroamination of ethylene with ammonia in the presence of metallic sodium or lithium in 1954,[5] a series of catalysts, including alkali metals, early transition-metal complexes, and late transition-metal complexes, have been reported for the hydroamination of alkenes,[1-4] but only recently have catalysts for the thermal and photocatalytic[6-7], intermolecular addition of amines to unactivated alkenes been disclosed.

Several challenges needed to be overcome to create highly selective and active catalysts for hydroamination. First, the reaction is close to thermoneutral or even endergonic,[8] as shown by experimental measurements of equilibria, thereby limiting the conversion of certain combinations of N–H donors and alkenes and making enantioselective intermolecular hydroaminations difficult to achive.[9-12] Second, systems that catalyze hydroamination often catalyze accompanying side reactions, such as the isomerization and telomerization of alkenes as well as oxidative amination,[9-10, 13] making precise control of the chemoselectivity during hydroamination essential. Third, the hydroamination of alkenes can form constitutional isomers, and the challenge confronting regioselective hydroamination is especially pronounced for the intermolecular addition of unsymmetrical internal alkenes.[9, 14] Lastly, for metal catalyzed hydroaminations, poisoning of the catalyst by amines is common because they are stronger σ-donors and usually bind more strongly to metals than alkenes do.[3]

Since 2000, our group has extensively studied the intermolecular hydroamination of alkenes and has discovered a variety of catalysts based on late-transition metals for the hydroamination of vinylarenes, dienes and trienes, bicyclic strained alkenes, and unactivated terminal and internal alkenes. We focused on creating catalysts based on late transition metals for these reactions because such catalysts are easier to handle and are more tolerant of polar functional groups than those based on alkali metals, early transition-metals, or rare-earth metals. As part of this work, we reported a series of asymmetric hydroaminations to form highly enantioenriched amines from feedstock alkenes, as well as complex alkenes. Detailed mechanistic studies have elucidated the steps of the catalytic cycles, which included novel complexes and elementary reactions. This information has been used to develop more active and selective catalysts for a wide range of hydroaminations. This chapter describes our development of intermolecular hydroamination reactions, from our initial examples with activated alkenes, such as vinylarenes and dienes, to our more recent reactions with unstrained and unconjugated terminal and internal alkenes. Interleaved with these studies on catalyst development are mechanistic information and accompanying features of our design that led to selective catalysis. Because a portion of this chapter will be submitted for potential publication in an accounts-style format, the first series of sections focuses on work from our own laboratory in the context of concurrent work in the field, and the second half of section 1.7 describes research during my Ph.D. work. To complete this introductory chapter, the final sections briefly summarize alternative systems for hydroamination from other laboratories.

## 1.2 Overview of Hydroamination of Vinylarenes Catalyzed by Complexes of Late Transition Metals

The hydroamination of vinylarenes is a valuable reaction for the synthesis of phenethylamines as building blocks for pharmaceuticals.[15] The intermolecular hydroamination of vinylarenes is widely studied, and both Markovnikov and Anti-Markovnikov hydroamination of vinylarenes have been reported to proceed in the presence of transition metals,[16-18] rare-earth metals,[19] alkali metals,[20] and acids.[14, 21]

## 1.3 Markovnikov Hydroamination of Vinylarenes Catalyzed by Complexes of Late Transition Metals

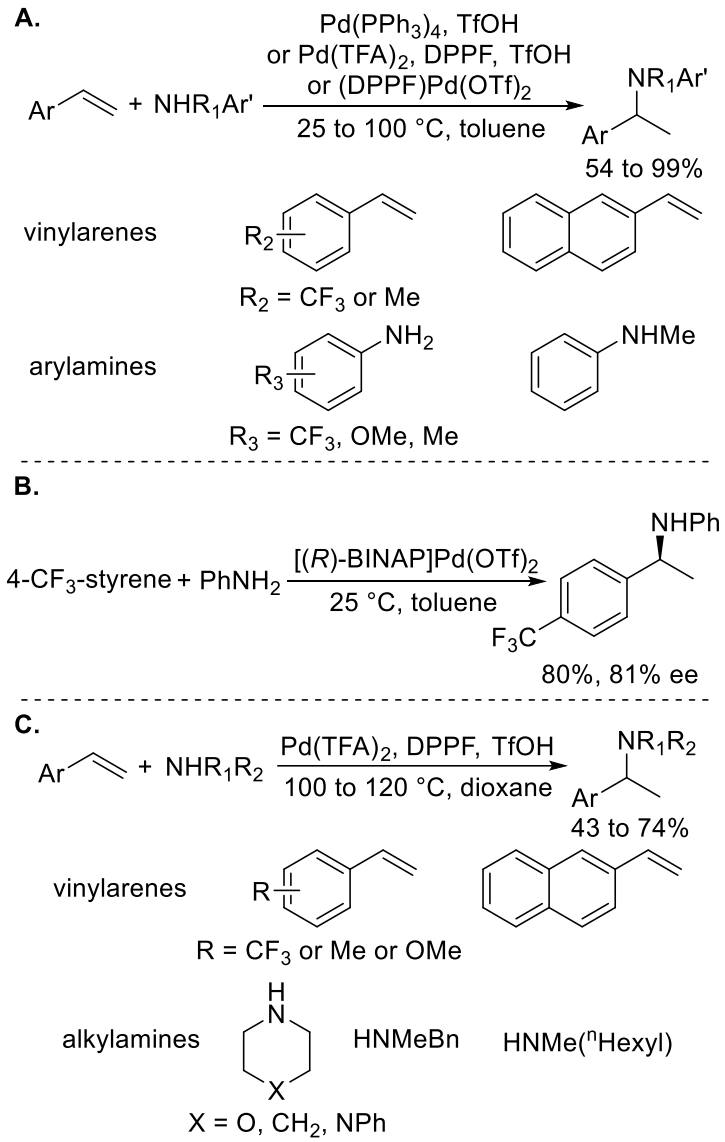


**Figure 1.1.** (A) Pd-catalyzed Markovnikov hydroamination of vinylarenes with arylamines.[15] (B) Pd-catalyzed enantioselective Markovnikov hydroamination of vinylarenes with arylamines.[15] (C) Pd-catalyzed Markovnikov hydroamination of vinylarenes with alkylamines.[22]

In 2000, we reported the discovery of Pd-catalyzed Markovnikov hydroamination of vinylarenes with arylamines discovered by Dr. Motoi Kawatsura (Figure 1.1a).[15] The combination of $Pd(TFA)_2$, DPPF, and TfOH was found to catalyze the hydroamination of both electron-poor and electron-neutral vinylarenes to afford *sec*-phenethylamines in high yield. This reaction was compatible with primary anilines containing methoxy and trifluoromethyl substituents, as well as secondary *N*-methylanilines. The addition of aniline to para-trifluoromethylstyrene was rendered enantioselective to afford the corresponding product in 81% ee when [(*R*)-BINAP]$Pd(OTf)_2$ was used as the catalyst (Figure 1.1b). Acid cocatalyst and the counteranion of the acid were important to achieve a high rate of the reaction. The scope of the Pd-catalyzed Markovnikov hydroamination of vinylarenes was extended to secondary aliphatic amines and benzylic amines by the replacement of toluene with dioxane as the solvent (Figure 1.1c).[22]

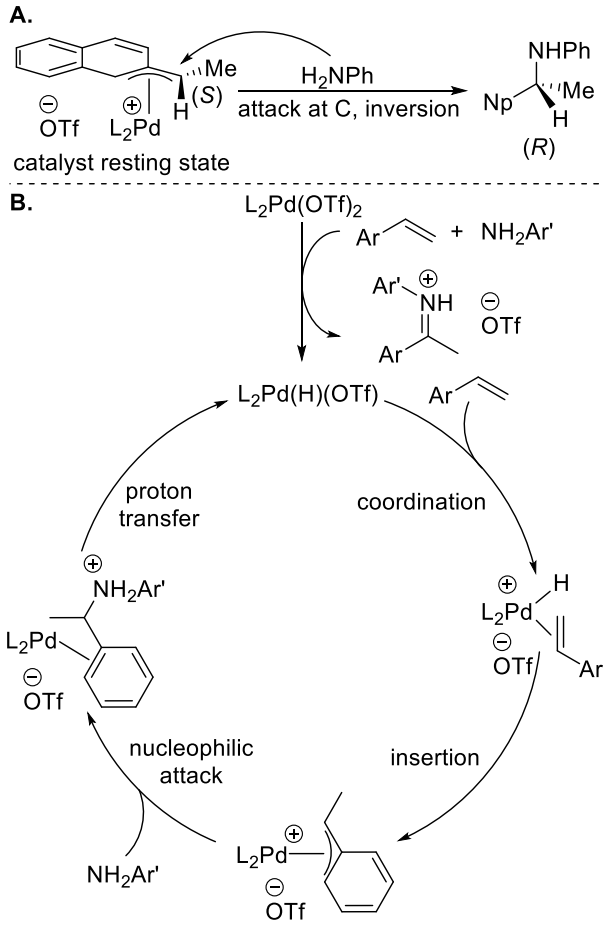


**Figure 1.2.** (A) Catalyst resting state for the Pd-catalyzed Markovnikov hydroamination of vinylarenes with arylamines and stochiometric experiment to probe the possible pathway for the formation of the C–N bond. (B) Proposed mechanism for the Pd-catalyzed enantioselective Markovnikov hydroamination of vinylarenes with arylamines.[23]

Dr. Ulrike Netekoven conducted mechanistic studies to understand the possible pathway for this Pd-catalyzed hydroamination of vinylarenes (Figure 1.2).[23] The resting state of the reaction

catalyst for the reaction of vinylnaphthalene with aniline in the presence of [(*R*)-Tol-BINAP]Pd(OTf)$_2$ was determined, by NMR spectroscopy, to be a mixture of diastereomeric forms of [(*R*)-Tol-BINAP][1-(2-naphthyl-ethyl)]Pd(OTf) (Figure 1.2a). The major diastereomer was characterized crystallographically, and the hydroamination of vinylnaphthalene with aniline catalyzed by the isolated diastereomeric mixture afforded product in comparable yield and at comparable rate as that catalyzed by the species generated from [(*R*)-Tol-BINAP]Pd(OTf)$_2$. Treatment of [(*R*)-Tol-BINAP][(*S*)-1-(2-naphthyl-ethyl)]Pd(OTf) with aniline afforded the (*R*)-*N*-1-(2-naphthyl)ethylamine in 71% ee. This result suggested that the C–N bond in the product primarily formed by external nucleophilic attack of aniline at the benzylic position, rather than by a concerted reductive elimination from a (phenethyl)Pd anilide complex (Figure 1.2a). Consequently, the following catalytic cycle was proposed for the hydroamination of vinylarenes with arylamines. $L_2Pd(OTf)_2$ entered the catalytic cycle by reacting with the vinylarene and the amine to form $L_2Pd(H)(OTf)$. Coordination of the vinylarene to the Pd center, followed by migratory insertion of the alkene into the Pd–H bond, affords the Pd($\eta^3$-benzyl) complex as the catalyst resting state. Turnover-limiting nucleophilic attack of the Pd($\eta^3$-benzyl) complex with aniline, followed by proton transfer, generates the hydroamination product and regenerates $L_2Pd(H)(OTf)$ to complete the catalytic cycle (Figure 1.2b).

Further improvement in the rate of the hydroamination of vinylarenes with arylamines was achieved by accelerating the turnover-limiting, C–N bond-forming step occurring by nucleophilic attack of the arylamine on the Pd($\eta^3$-benzyl) complex. Stoichiometric reactions of isolated $L_2Pd(\eta^3\text{-}CH_2Ph)(OTf)$ complexes with aniline occurred with a positive relationship between the rate of the nucleophilic attack and the bite angle of the bidentate ligand. Consequently, (Xantphos)Pd(OTf)$_2$ was identified as a more active catalyst for the hydroamination of vinylarenes because the bite angle of Xantphos (108°) is larger than that of DPPF (102°). As a result, the reaction between *para*-cyanoaniline and styrene catalyzed by a combination of (Xantphos)Pd(OTf)$_2$ and TfOH occurred to form the product in 93% yield which was 7 times greater than the yield obtained with (DPPF)Pd(OTf)$_2$ and TfOH as catalyst. With the newly developed (Xantphos)Pd(OTf) as the catalyst in the presence of catalytic amount of TfOH, the hydroamination of styrene occurred with anilines bearing sensitive functional groups, including alcohol, amine, ester, acid, and amide groups (Figure 1.3).[11]

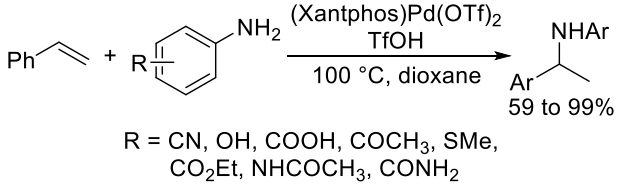


**Figure 1.3.** Improved scope of arylamines for Pd-catalyzed Markovnikov hydroamination of vinylarenes with arylamines.[11]

The development of an efficient catalytic hydroamination of vinylarenes enabled the direct measurement of the thermodynamic parameters of this reaction (Figure 1.4). Measurements of the

equilibrium constants showed that the hydroamination of vinylarenes with anisidine and N-methylaniline were nearly ergoneutral and Van't Hoff analysis showed that a favorable enthalpy was counterbalanced by the unfavorable entropy of an intermolecular reaction.[8] Consequently, the use of excess alkene was required to achieve a high yield for the hydroamination of certain vinylarenes, such as indene and dihydronaphthalene, due to the unfavorable thermodynamics of the reaction.

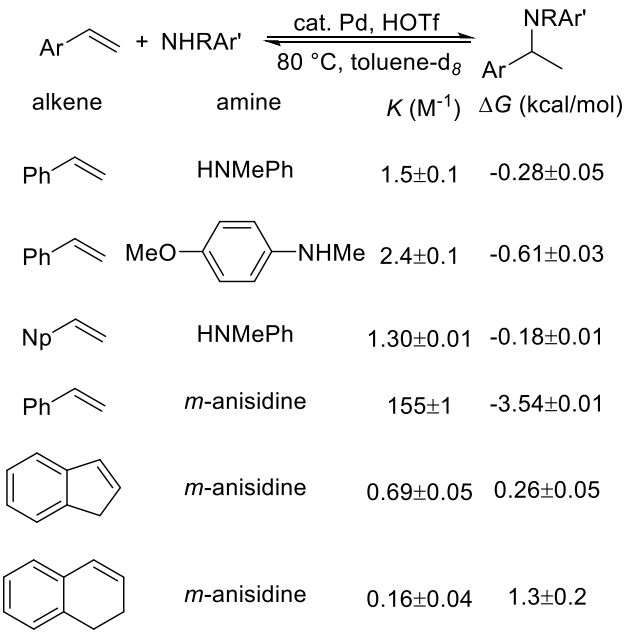


**Figure 1.4.** Measurements of the thermodynamics of the Markovnikov hydroamination of vinylarenes with arylamines.[8]

## 1.4 Anti-Markovnikov Hydroamination of Vinylarenes Catalyzed by Complexes of Late Transition Metals

Vinylarenes also react with amines through organometallic intermediates to form products from anti-Markovnikov aminations. Beller reported the oxidative amination of vinylarenes with alkylamines with anti-Markovnikov selectivity to form enamines as the major product catalyzed by $[Rh(cod)_2]BF_4$ and $PPh_3$.[24] Masaru Utsunomiya in our group later showed that vinylarenes reacted with secondary alkylamines catalyzed by $[Rh(cod)(DPEphos)]BF_4$ with the same anti-Markovnikov selectivity, but to form amines by hydroamination[25]. The scope of the reaction catalyzed by $[Rh(cod)(DPEphos)]BF_4$ encompassed cyclic and acyclic secondary alkylamines as well as both electron-poor and electron-rich vinylarenes (Figure 1.5a). Enamines formed by oxidative amination were the major side product. The selectivity for hydroamination over the oxidative amination depended on the alkene and was higher with more electron-rich vinylarenes and at lower concentration of vinylarene. These results suggested that the vinylarene served as both a reactant and an ancillary ligand and a possible mechanism that accounted for the observations was proposed (Figure 1.5b). It involves the formation of a $\beta$-amino, $\alpha$-alkyl rhodacycle from either the migratory insertion of the vinylarene into a Rh–N bond or the

nucleophilic attack of aniline on a Rh-bound vinylarene. Due to the rigidity of the four-membered rhodacycle, reductive elimination from the rhodacycle to form the hydroamination product was preferred over the $\beta$-hydrogen elimination from this rhodacycle to form the oxidative amination product. If this rhodacycle equilibrated with a Rh-alkyl complex containing vinylarene as a dative ligand, $\beta$-hydrogen elimination could occur, thereby accounting for the lower selectivity for hydroamination with more electron-poor vinylarenes (which would bind more tightly to the Rh(III) species) and at higher concentrations of the vinylarene.

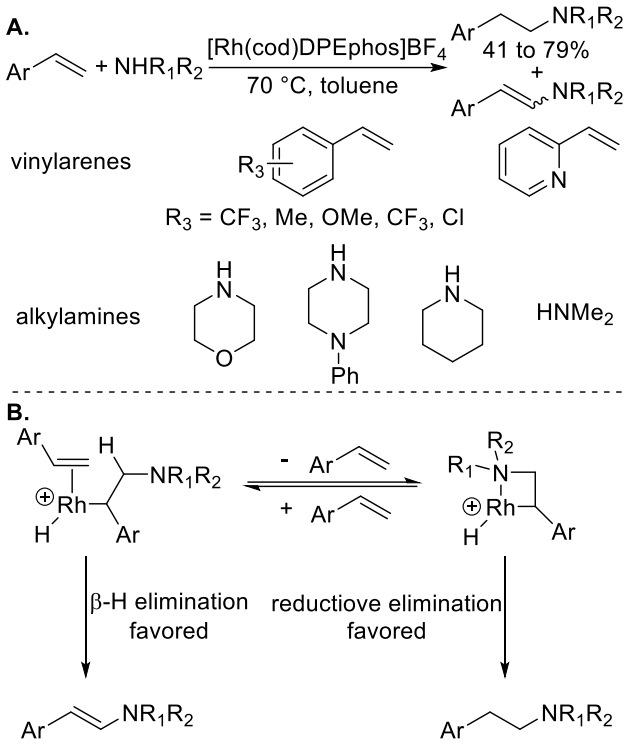


**Figure 1.5.** (A) Rh-catalyzed Anti-Markovnikov hydroamination of vinylarenes with alkylamines. (B) Possible explanation for the low selectivity for hydroamination with more electron-poor vinylarenes and at higher concentrations of vinylarene.[25]

Seeking to suppress the formation of enamine side products, Masaru discovered a ruthenium catalyst for the anti-Markovnikov hydroamination of vinylarenes with secondary alkylamines to form amines without competing oxidative amination.[26] A combination of Ru(cod)(methylallyl)$_2$, DPPPent, and TfOH catalyzes the anti-Markovnikov hydroamination of electron-poor and electron-rich vinylarenes with secondary alkylamines (Figure 1.6a), as well as α-methylstyrene for the first time.

Detailed mechanistic studies revealed a new pathway for hydroamination and an unusual example of catalysis through π-arene metal complexes. The combination of Ru(cod)(methylallyl)$_2$, DPPPent, and TfOH generates a PCP-pincer ligand in the active form of the catalyst by cleavage of the C-H bond on the central carbon, and the remaining coordination sites are occupied by the arene of the vinylarene (Figure 1.6b).[27] [Ru(DPPPent)(styrene)](OTf) synthesized independently

was found to be chemically and kinetically competent to be the active catalyst. Furthermore, treatment of this complex with excess morpholine formed a new Ru π-arene complex by nucleophilic attack of morpholine on the coordinated styrene at the terminal position. The π-bound hydroamination product in the resulting complex was subsequently released by ligand exchange with excess styrene. While this system was not designed to react through π-arene complexes, it was one of the first examples of a catalytic process that occurred by this class of complex.[28-29]

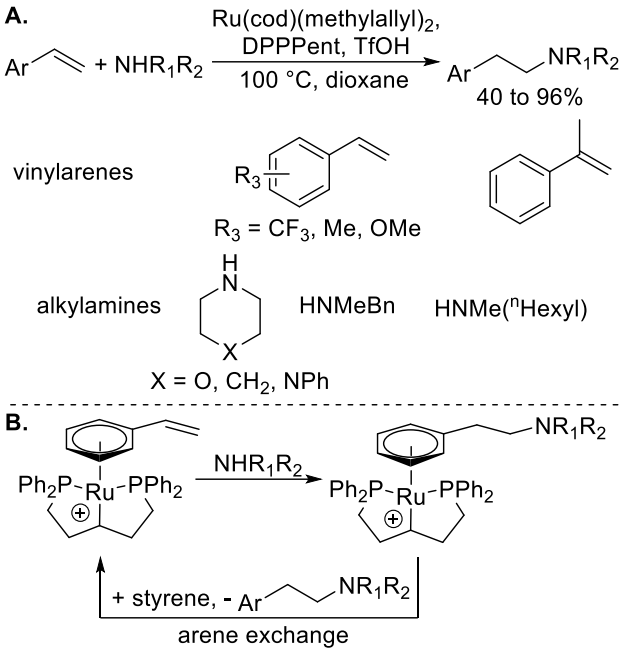


**Figure 1.6.** (A) Ru-catalyzed Anti-Markovnikov hydroamination of vinylarenes with alkylamines.[26] (B) Proposed mechanism for the Ru-catalyzed Anti-Markovnikov hydroamination of vinylarenes with alkylamines.[27]

## 1.5 Hydroamination of Conjugated Dienes and Trienes Catalyzed by Complexes of Late Transition Metals

The hydroamination of dienes and trienes forms allylamines and has been reported to occur with transition metals,[30-34] rare-earth metals,[35] and acids.[36] Having observed the hydroamination of vinylarenes and considering the literature on the telomerization of butadiene with amines,[37] the 1:1 addition of amines to dienes was a logical target, and Dr. Oliver Löber in our laboratory developed conditions for the Pd-catalyzed hydroamination of dienes with arylamines. A combination of $Pd(PPh_3)_4$ and TFA was shown by a colorimetric high-throughput screening method to catalyze the 1,4-addition of aniline to cyclohexadiene in high yield (Figure 1.7a).[38] The scope of the reaction encompassed the addition of primary and *N*-methyl anilines bearing electron-donating and electron-withdrawing substituents to cyclic and acyclic 1,3-dienes. However, for acyclic dienes, formation of *N*,*N*-diallylamines as side product was detected with primary arylamines. Enantioselective hydroamination of cyclohexadiene with aniline was achieved with a combination of $[Pd(allyl)Cl]_2$ and a Trost ligand as the catalyst (Figure 1.7b). The authors

postulated that this reaction proceeded through a mechanism similar to that followed by the Pd-catalyzed hydroamination of vinylarenes. A migratory insertion of the diene into the Pd–H bond generated a Pd $\eta^3$-allyl intermediate. The allylamine product was formed by turnover-limiting nucleophilic attack of the arylamine on the Pd $\eta^3$-allyl complex followed by a proton transfer (Figure 1.8).[11, 38]

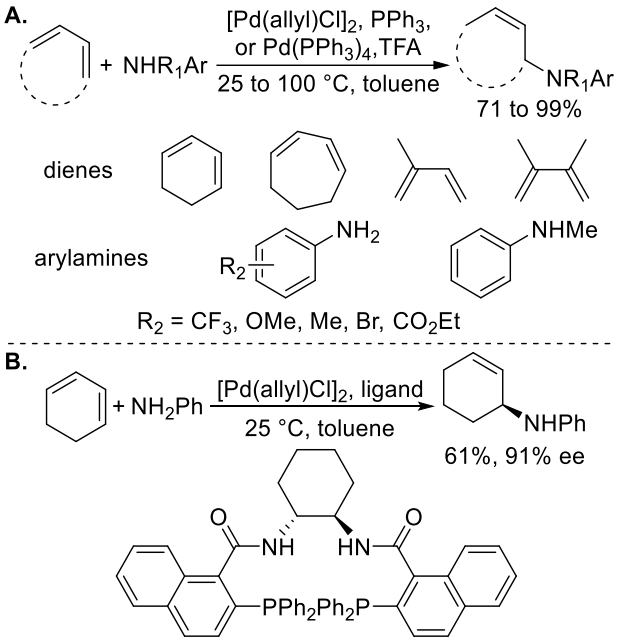


**Figure 1.7.** (A) Pd-catalyzed hydroamination of 1,3-dienes with arylamines. (B) Pd-catalyzed enantioselective hydroamination of 1,3-dienes with arylamines.[38]

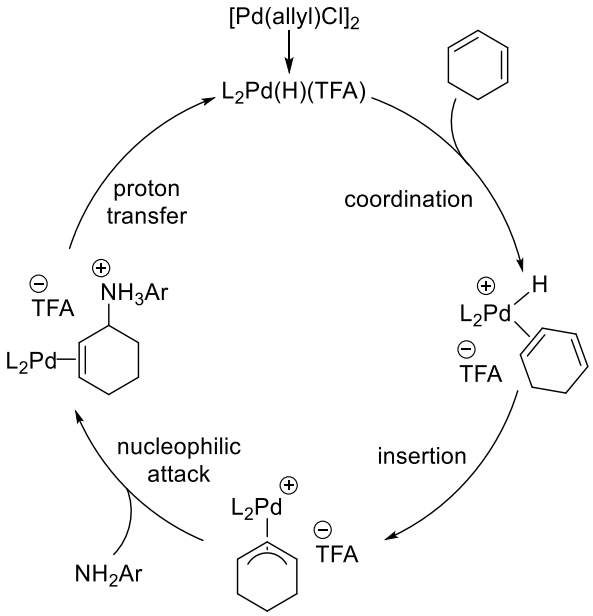

**Figure 1.8.** Proposed mechanism for the Pd-catalyzed hydroamination of 1,3-dienes with arylamines.[11, 38]

Like the hydroamination of vinylarenes, the hydroamination of dienes was improved with a Pd catalyst containing a bidentate ligand possessing a large bite-angle (Figure 1.9a).[11] For example, a five-fold increase in the rate of the reaction between *para*-cyanoaniline and cyclohexadiene was observed when $[Pd(allyl)Cl]_2$ and Xantphos were used instead of $[Pd(allyl)Cl]_2$ and $PPh_3$ as the catalyst. Moreover, the combination of $[Pd(allyl)Cl]_2$ and Xantphos catalyzes the reactions of additional N–H donors, such as hydrazones, hydrazines, and hydroxyamines, with a variety of cyclic and acyclic dienes (Figure 1.9b).[39] The synthesis of tropene derivatives from a sequential intermolecular and subsequent transannular, intramolecular hydroamination of cycloheptatriene was also reported with a combination of $Pd(TFA)_2$, Xantphos, and benzoic acid as the catalyst (Figure 1.9c).[40]

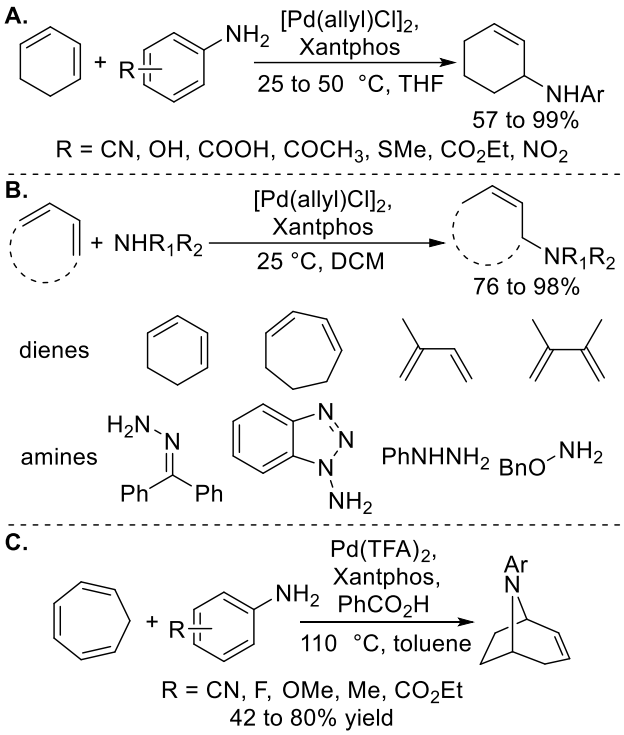


**Figure 1.9.** (A) Improved scope of arylamines for the Pd-catalyzed hydroamination of 1,3-dienes with arylamines.[11] (B) Pd-catalyzed hydroamination of 1,3-dienes with hydrazones, hydrazines, and hydroxyamines.[39] (C) Synthesis of tropene derivatives by Pd-catalyzed Markovnikov hydroamination of cycloheptatrienes.[40]

During the Pd-catalyzed hydroamination of dienes, the population of catalytically active [(bisphosphine)Pd($\eta^3$-allyl)(Cl)] was higher than that of the inactive (bisphosphine)$PdCl_2$ when the bisphosphine possessed a larger bite angle.[11] This difference in the speciation of the catalyst, together with the faster turnover-limiting nucleophilic attack when the metal bears the large bite-angle of Xantphos, contributed to the observed high rate of catalysis.[11]

A nickel-catalyzed hydroamination of 1,3-dienes with alkylamines was discovered by Motoi Kawatsura using high-throughput screening methods and was developed and studied mechanistically by Jan Pawlas and visiting scholar Yoshiaki Nakao.[12] A combination of $Ni(cod)_2$, DPPF, and TFA was found to catalyze the hydroamination of cyclic dienes with alkyl and benzyl amines (Figure 1.10a). For reactions of butadiene, the product from 1,2-addition of the amine was favored kinetically, and the product from 1,4-addition was favored thermodynamically.

This result, together with the observation that allylic amines reacted with primary or secondary alkyl or arylamines in the presence of this catalyst to generate mixtures of allylic amines, suggested that the hydroamination of 1,3-dienes with alkylamines was reversible. The thermodynamic stability of a variety of allylamines derived from a series of amines was determined by the exchange process, and the order of stability was cyclic secondary amines > primary alkylamines > primary benzylamines > primary arylamines > acyclic secondary amines (Figure 1.10b).

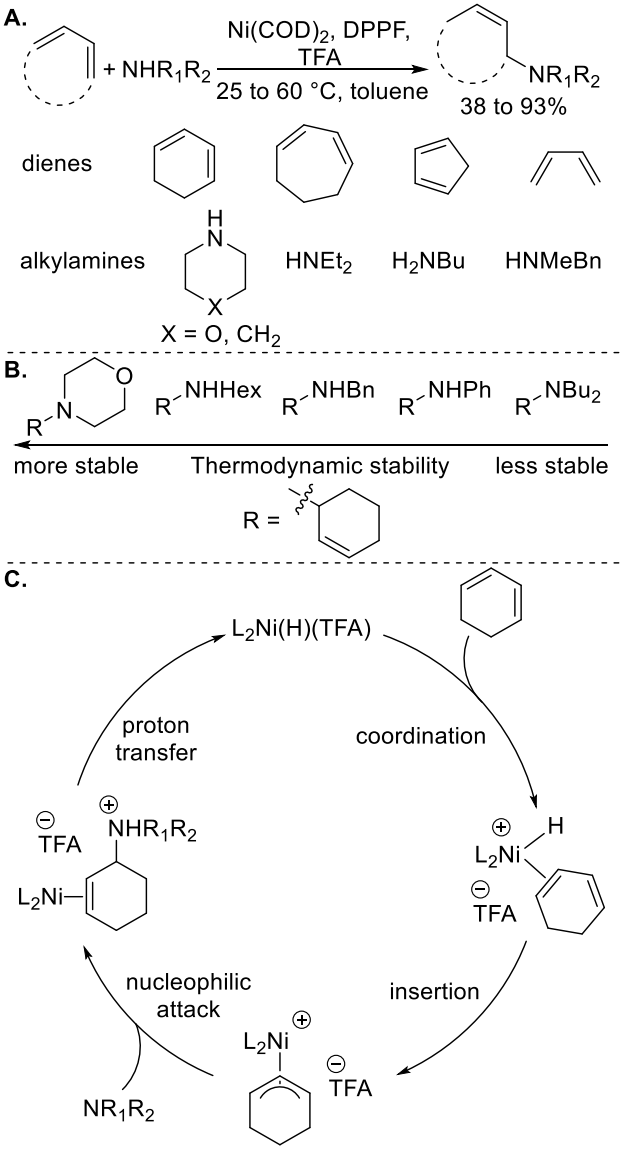

**Figure 1.10.** (A) Ni-catalyzed hydroamination of 1,3-dienes with alkylamines. (B) Evaluation of the thermodynamic stability of allylamines. (C) Proposed mechanism for the Ni-catalyzed hydroamination of 1,3-dienes with alkylamines.[12]

Mechanistic studies revealed the pathway for this Ni-catalyzed hydroamination of dienes (Figure 1.10c).[12] The catalyst resting state in the reaction between cyclohexadiene and methylbenzylamine was determined to be [(DPPF)Ni($\eta^3$-cyclohexenyl)](TFA) by $^{31}$P NMR spectroscopy and independent synthesis. The reaction between a 1:1 ratio of [(DPPF)Ni($\eta^3$-cyclohexenyl)](TFA) and methylbenzylamine afforded the allylamine in only 15% yield, but the same reaction in the presence of excess cyclooctadiene afforded the allylamine in 90% yield, indicating that the nucleophilic attack of the allylnickel complex by amines was feasible but endogenic and that the diene was needed to make the reaction exergonic by trapping the Ni–H intermediate as the allyl complex. These studies on catalytic hydroamination of conjugated dienes seeded further development of enantioselective hydroamination of dienes[34, 41-42] and hydroamination of internal dienes[43] by groups including those of Mazet, Malcolmson, and Dong.

## 1.6 Hydroamination of Bicyclic Strained Alkenes Catalyzed by Complexes of Late Transition Metals

The hydroamination of strained alkenes, such as cyclopropene,[44-45] cyclobutene,[46] and bicyclic alkenes,[47-51] is an attractive method for the synthesis for amine-substituted carbocyclic compounds. Milstein reported the first hydroaminations of strained, bicyclic alkenes, which occurred with six turnovers in the presence of an iridium catalyst containing $PEt_3$ as the ligand.[51] Togni reported the first enantioselective examples in high yield but with low enantioselectivity or low yield but with high enantioselectivity in the presence of iridium and chiral bisphosphine.[47]

An iridium system that catalyzes the enantioselective hydroamination of strained bicyclic alkenes and dienes in both high yield and high ee was discovered in our laboratory by Jianrong (Steve) Zhou (Figure 1.11a).[52] A combination of $[Ir(coe)_2Cl]_2$, DTBM-SEGPHOS and KHMDS catalyzed the enantioselective addition of arylamines to norbornenes in high yield and selectivity. While fluoride was important for catalyst activity in prior work by Togni,[47] the key to achieving activity in Steve Zhou's systems was the replacement of the chloride ligand with an anilido ligand by aniline and KHMDS. Bisphosphines possessing biaryl backbones with smaller dihedral angles and bulky, electron-donating aryl groups on phosphorus increased the yield and enantioselectivity of the reaction over those with larger dihedral angles and less bulky aryl groups on phosphorus. The scope of the reaction encompassed arylamines with both electron-donating and electron-withdrawing substituents and the bicyclic alkenes norbornene, norbornadiene, and benzo- as well as imide-fused norbornenes.

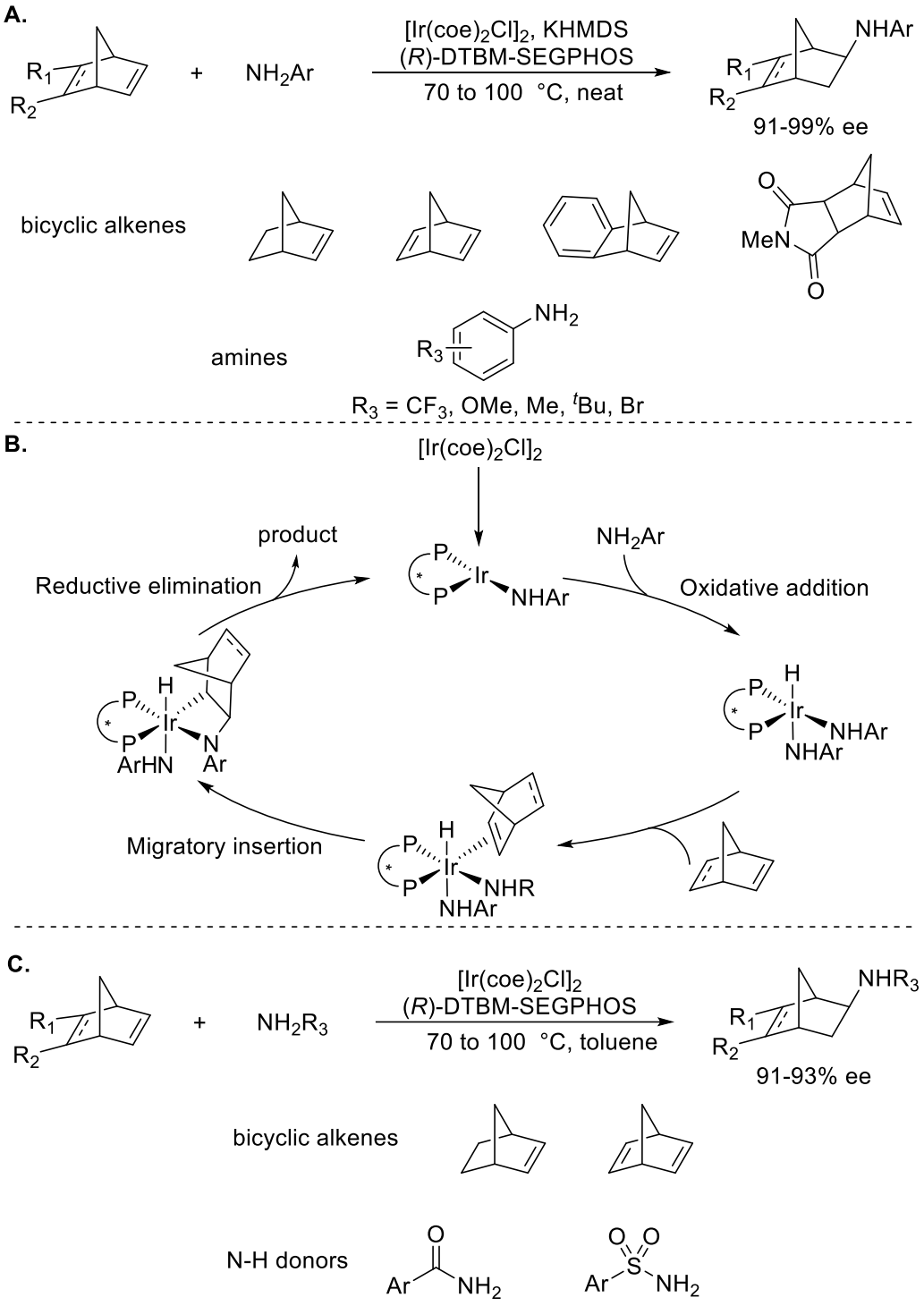


**Figure 1.11.** (A) Ir-catalyzed enantioselective hydroamination of bicyclic alkenes with arylamines.[52] (B) Proposed mechanism for the Ir-catalyzed enantioselective hydroamination of bicyclic alkenes with arylamines. (C) Ir-catalyzed enantioselective hydroamination of bicyclic alkenes with arylamides and arylsulfonamides.[13]

In addition to prior work, our studies with iridium catalysts were motivated by our direct observation of the oxidative addition of N–H bonds in aryl amines and ammonia to well-defined Ir(I) complexes to from hydrido amido complexes.[53-54] Consistent with these studies on N–H activation, mechanistic studies implied that the catalytic reactions occurred by oxidative addition of an N–H bond, followed by alkene insertion into the Ir–N bond. The reaction between *N*-deuterated *m*-xylylamine and norbornene formed the product from *syn* addition of the deuterium and the amino group across the alkene. The anionic bis-anilide complex K[Ir(DM-SEGPHOS)(NH*m*-Xylyl)$_2$] catalyzed the reaction of *m*-xylylamine with norbornene in high yield only in the presence of an equimolar amount of *m*-XylylNH$_3^+$, which would generate the neutral, five-coordinate complex [Ir(DM-SEGPHOS)(H)(NH*m*-Xylyl)$_2$]. The neutral dimeric complex [Ir(DM-SEGPHOS)(NHmXylyl)]$_2$ did not catalyze the hydroamination, implying that the monomeric unsaturated complex, [Ir(DM-SEGPHOS)(H)(NH*m*-Xylyl)$_2$] was the active catalyst for the reaction and that the anilide dimer resisted dissociation to a monomer. [Ir(DM-SEGPHOS)(H)(NH*m*-Xylyl)$_2$] was presumably generated in the catalytic reaction by oxidative addition of aniline to the species generated from [Ir(coe)$_2$Cl]$_2$, DTBM-SEGPHOS, and potassium anilide. Norbornene would then coordinate to [Ir(DM-SEGPHOS)(H)(NH*m*-Xylyl)$_2$], as depicted in the catalytic cycle of Figure 1.11b,[52] and undergo migratory insertion into the Ir–N bond. Reductive elimination would form the C–H bond. These studies set the stage for reactions of N–H bonds with unactivated alkenes catalyzed by iridium complexes, and Christo Sevov in our group showed that a similar system comprising [Ir(coe)$_2$Cl]$_2$ and DTBM-SEGPHOS catalyzed the addition of benzamides and sulfonamides to norbornene and norbornadiene in high yield and enantioselectivity (Figure 1.11c).[13]

## 1.7 Markovnikov Hydroamination of Unactivated Alkenes Catalyzed by Complexes of Late Transition Metals

The hydroamination of unactivated alkenes could be a straightforward, atom-economical method for the preparation of aliphatic amines. However, unlike conjugated alkenes, for which insertion can generate $\eta^3$-allyl or benzyl intermediates, and strained alkenes, for which migratory insertion is promoted by release of ring-strain, unactivated aliphatic alkenes had rarely been shown to undergo migratory insertion into late-transition-metal–nitrogen bonds.[55-58] Consequently, reports of direct N–H additions to unactivated alkenes are uncommon and these reactions often required a large excess of alkene, and occurred with limited tolerance of functional groups.[59-61] Several alternative strategies for the hydroamination of unactivated alkenes have also been developed, including the reactions of alkenes bearing a directing group,[62-63] formal hydroaminations with silanes and esters of hydroxylamines[64-68] or dioxazolones as the source of an amino group,[69] and hydroamination under photocatalytic conditions.[6-7] Our group has sought to achieve the hydroamination of unactivated alkenes by the oxidative addition or deprotonation of the N–H bond to generate metal amido complexes that can form the C–N bond by insertion of the alkene.

Christo Sevov built upon initial results of Dr. Steve Zhou in our group to achieve Ir-catalyzed hydroamination of unactivated terminal alkenes with arylamides and arylsulfonamides catalyzed by a combination of $[Ir(coe)_2Cl]_2$ and DTBM-SEGPHOS in neat alkene (Figure 1.12a).[13] Enamides from oxidative amination were the major side product, but high yield of the *N*-alkylamide was achieved by addition of $H_2$ or isopropanol to the reaction mixture after the amination process.

The resting state of the catalyst during the reaction was determined to be $(L_2)Ir(H)(Cl)(NHCOAr)(NH_2COAr)$, which was formed by oxidative addition one molecule of the arylamide to the iridium center and dative coordination of a second arylamide. This complex was determined to be chemically and kinetically competent for the catalyst hydroamination. Kinetic measurements showed that the reaction was first order in the concentration of the Ir catalyst, inverse first order in the concentration of the arylamide, and first order in the concentration of the terminal alkene. Consequently, this reaction was proposed to occur by the dissociation of the dative arylamide from $(L_2)Ir(H)(Cl)(NHCOAr)(NH_2COAr)$, followed by sequential migratory insertion of the terminal alkene into the Ir–N bond and reductive elimination to form the alkylamide product (Figure 1.12b).

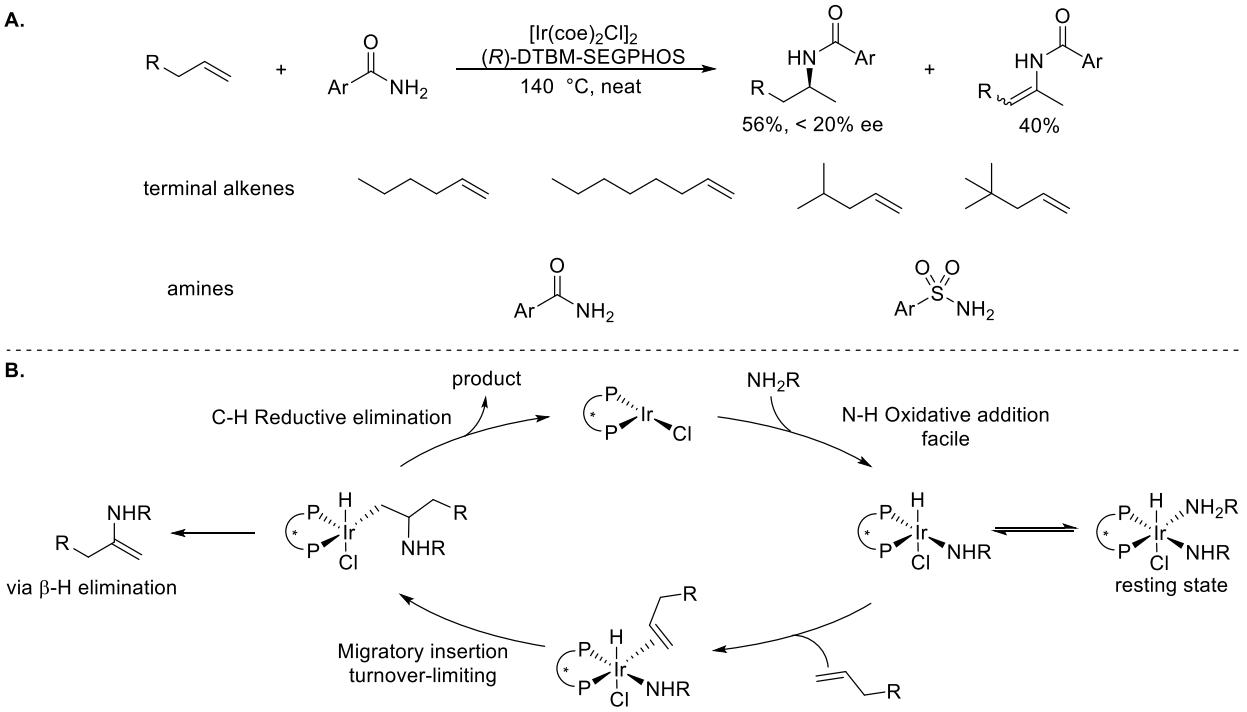


**Figure 1.12.** (A) Ir-catalyzed hydroamidation of unactivated terminal alkenes with arylamides and arylsulfonamides. (B) Proposed mechanism for the Ir-catalyzed hydroamidation of unactivated terminal alkenes with arylamides and arylsulfonamides.[13]

Sevov and Zhou also showed that the combination of $[Ir(cod)Cl]_2$ and DTBM-SEGPHOS catalyzed the hydroamination of unactivated alkenes with indoles (Figure 1.13a).[70] The reaction

occurred through selective addition of the N–H bond of the indole to the alkene, and side products from the addition of the indoyl C–H bond to the alkene were not observed. With ethyl acetate as a cosolvent, the reaction occurred with as few as 1.5 equiv of alkene versus indole.

Mechanistic analysis showed that the resting state of the reaction, unexpectedly, was a C-bound iridium indolyl alkene complex. This observed complex isomerized to its reactive N-bound isomer before undergoing migratory insertion and reductive elimination to generate the product from hydroamination. Computational studies by DFT indicated that addition of the N–H bond over the C–H bond to the alkene occurred because the transition state for migratory insertion of the alkene into the Ir–N bond was lower in energy than that for the migratory insertion of the alkene into the Ir–C bond of the Ir-indolyl isomers (Figure 1.13b). These relative barriers would not be predicted by the vast prior literature on insertions of alkenes into metal-carbon bonds and scarce literature on insertions into metal-nitrogen bonds. However, it is consistent with the growing literature on the insertions of alkenes into metal-heteroatom bonds and analyses of the factors controlling these relative rates.[71]

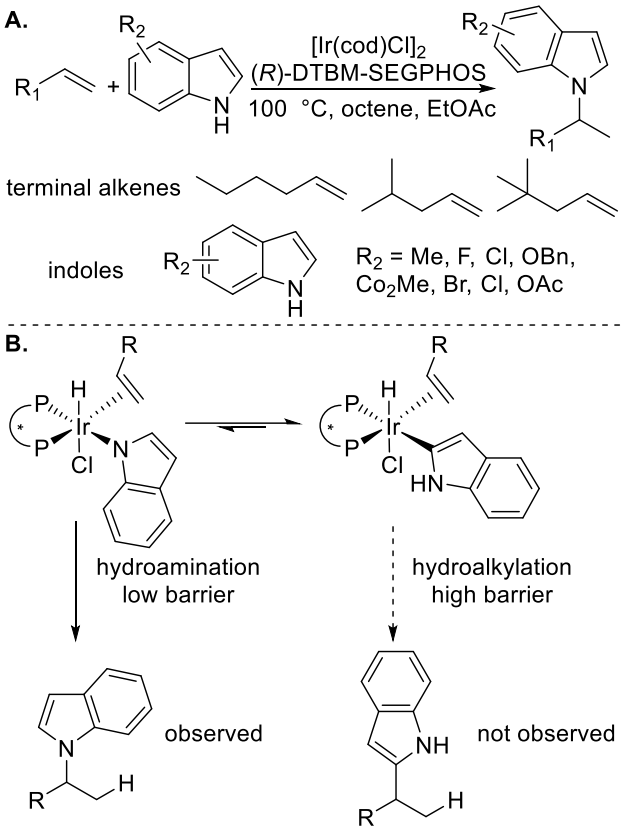


**Figure 1.13.** (A) Ir-catalyzed hydroamination of unactivated terminal alkenes with indoles. (B) Explanation for the selectivity of hydroamination over hydroalkylation.[70]

While this work showed that the intermolecular hydroamination of unactivated alkenes catalyzed by late transition metals was possible, the reactions required excess alkene and did not occur with

internal alkenes. Thus, Yumeng Xi and Chris Hill in our group sought to redesign the catalysts and amines to address these shortcomings.

Achieving enantioselective intermolecular hydroamination of unactivated internal alkenes is particularly challenging because internal alkenes tend to bind more weakly to transition metals than do terminal alkenes, undergo migratory insertion less readily, and undergo isomerization and oxidation by $\beta$-hydrogen elimination after the insertion event. To tackle these challenges, Yumeng focused on systems comprising a cationic Ir catalyst and a judiciously designed amine that collectively promoted the key alkene coordination, migratory insertion, and reductive elimination steps of the catalytic cycle for hydroamination (Figure 1.14a). Cationic iridium catalysts were used because they readily bind and insert internal alkenes, as shown by Crabtree's hydrogenation systems many years ago,[72] and an amine possessing a second coordinating group was used to favor the thermodynamics of oxidative addition.

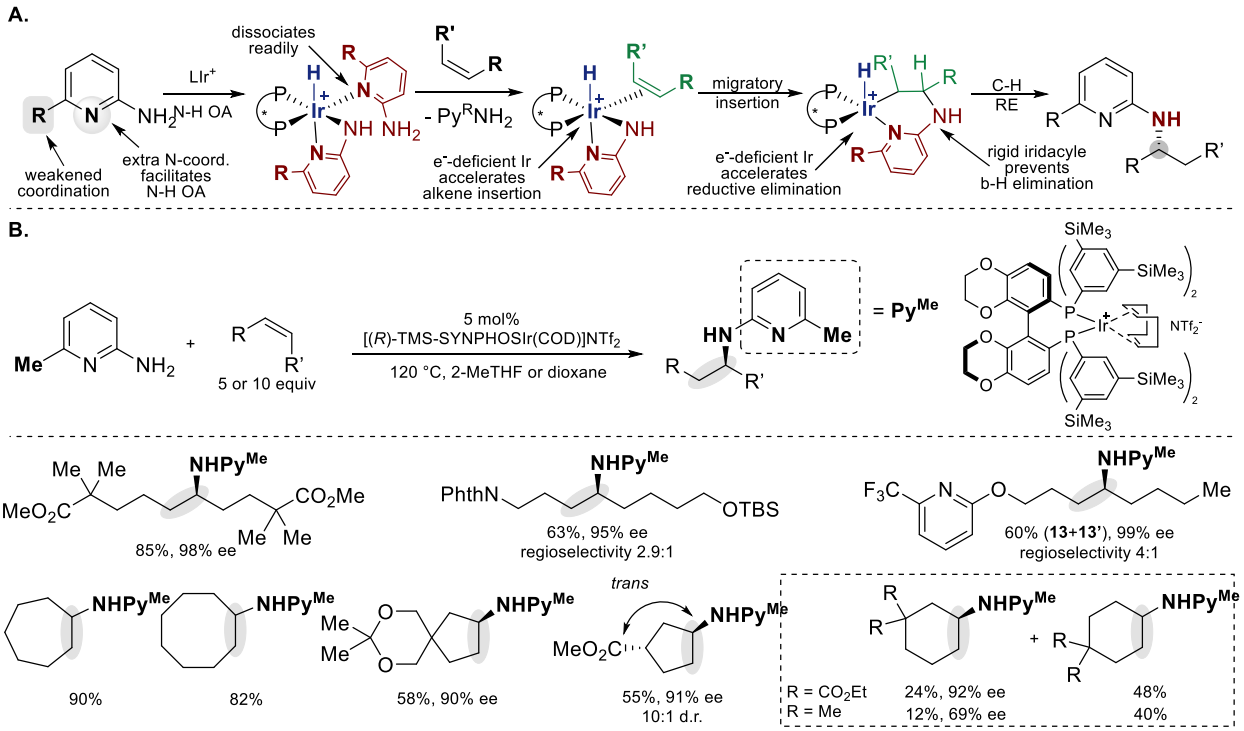


**Figure 1.14.** (A) Design elements for catalytic hydroamination of unactivated internal alkenes. (B) Ir-catalyzed enantioselective hydroamination of unactivated internal alkenes with 6-methyl-2-aminopyridine.

Following this design, the enantioselective hydroamination of unactivated symmetric and unsymmetrical linear *Z*-alkenes, as well as cyclic internal alkenes, occurred with 6-methyl-2-aminopyridine catalyzed by [(*R*)-TMS-SYNPHOSIr(COD)]$NTf_2$ (Figure 1.14b). The products of this hydroamination were converted into primary amines with little to no erosion of enantiopurity by sequential hydrogenation and reduction. Due to competing alkene isomerization, an excess of alkene was required for this reaction to occur with high regioselectivity, and further development

was needed to address this limitation. Mechanistic experiments showed that this reaction occurred by turnover-limiting migratory insertion of the alkene into the Ir–N bond, and DFT computations suggested that both steric and electronic properties of the ligand contributed to the high enantioselectivity of this transformation.

This design was also applicable to the hydroamination of terminal alkenes, but further modifications of the catalysts by Senjie Ma was needed to increase the functional-group tolerance and to enable reactions to be conducted without excess of alkene. Initial mechanistic experiments on the reactions of terminal alkenes, including deuterium-labelling and $^1$H NMR spectroscopy analysis of the reaction revealed three undesired pathways: (1) the retrohydroamination of the product amine (Figure 1.15a, path i), (2) the irreversible isomerization of allylbenzene to *β*-methylstyrene (path ii), and (3) the reversible dehydrogenation of the product amine (path iii). A catalytic system comprising [Ir[(*S*)-DTBM-SEGPHOS](ethylene)(Cl)], which contains a monodentate, unstrained, and volatile alkene, and NaBArF to generate the cation, was discovered to catalyze the hydroamination of allylbenzene with 6-methyl-2-aminopyridine at 60 °C with no detectable side products.[10] The hydroamination occurred with equimolar 6-methyl-2-aminopyridine, and >40 structurally diverse terminal alkenes (Figure 1.15b). This reaction occurred equally well on gram-scale, and even with 0.2 mol % catalyst for selected substrates.

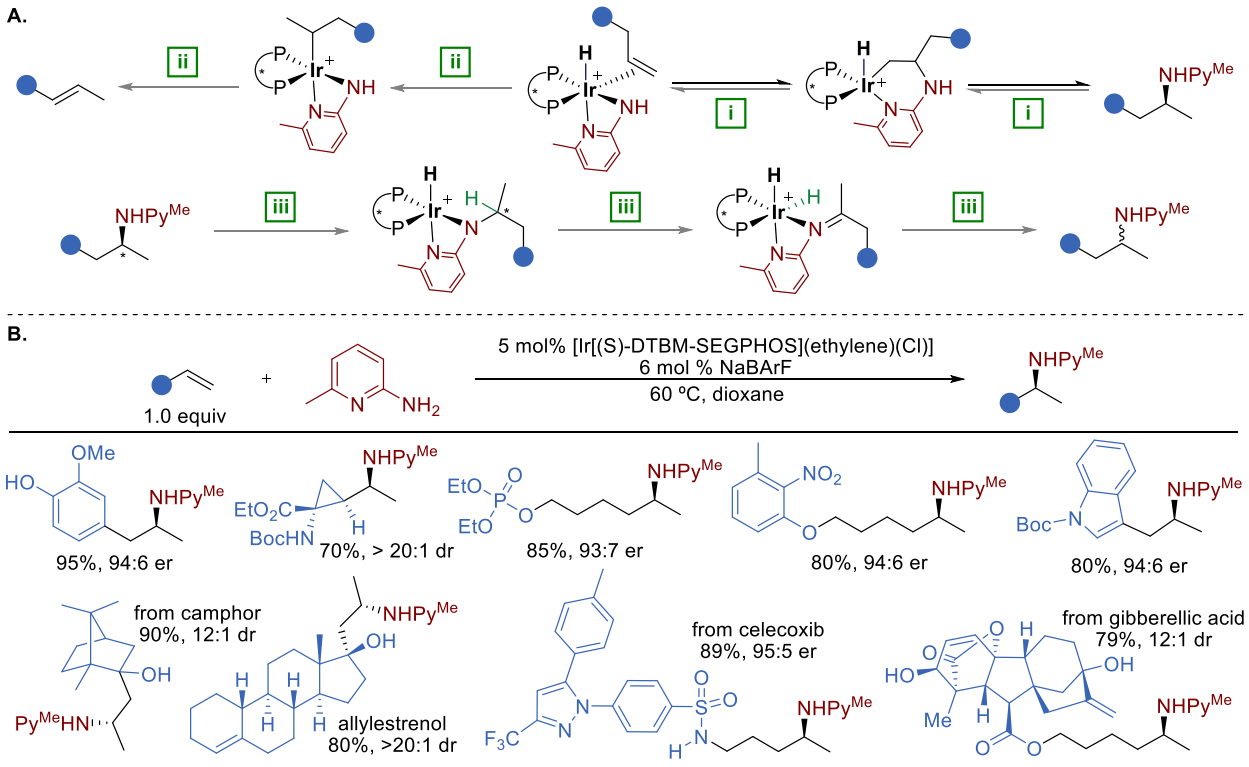


**Figure 1.15.** (A) Undesired pathways for the isomerization of the alkene and the racemization of the product. (B) Ir-catalyzed enantioselective hydroamination of unactivated terminal alkenes with 6-methyl-2-aminopyridine.

Prior to the discovery of this iridium-catalyzed hydroamination of terminal alkenes, Chris Hill in our group discovered a ruthenium-catalyzed, intermolecular Markovnikov hydroamination of unactivated terminal alkenes with equimolar 2-aminopyridines and this reaction occurred via an unusual mechanism involving sequential oxidative amination and transfer hydrogenation (Figure 1.16). Studies on the mechanism by Senjie Ma showed that the catalyst resting state was the Ru-amido complex $Ru(PEt_3)_3(amido)(NTf_2)$ formed by coordination of the 2-aminopyridine to ruthenium, followed by deprotonation of acidic N–H bond of the aminopyridine. Kinetic measurements and DFT computations revealed that this reaction occurred by a turnover-limiting migratory insertion of the alkene into the Ru–N bond, and deuterium labeling studies implied that the product forms by initial oxidative amination, followed by reduction of the resulting imine (Figure 1.17).

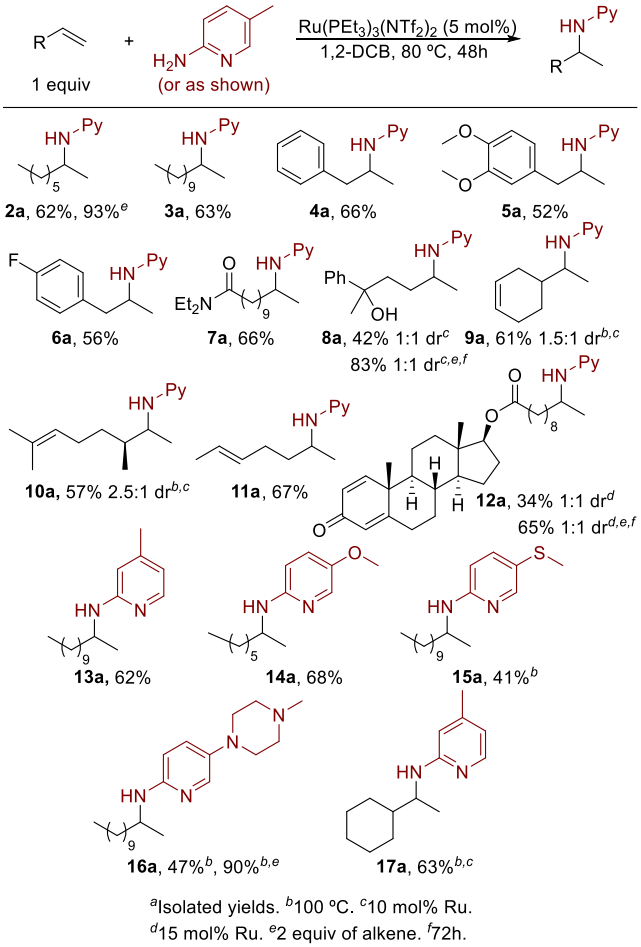


**Figure 1.16.** Ru-catalyzed hydroamination of unactivated terminal alkenes with 2-aminopyridine.

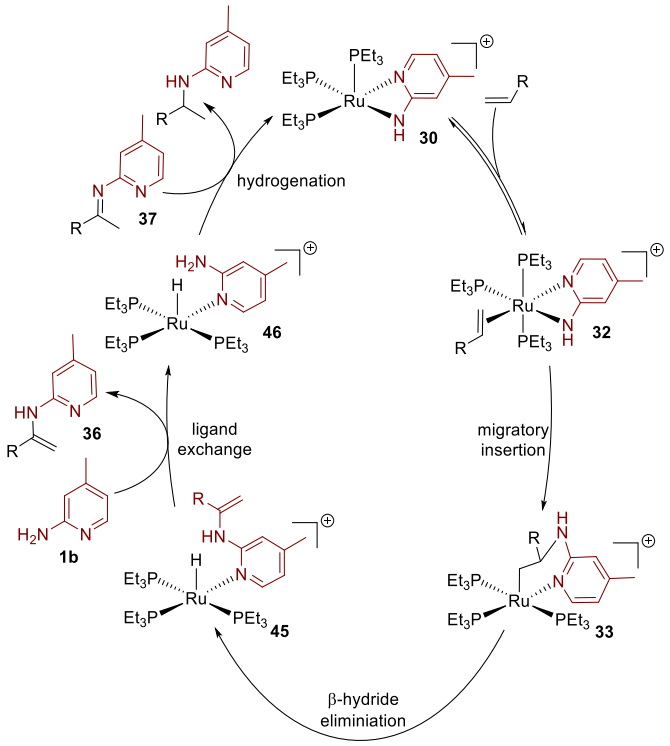


Figure 1.17. Proposed mechanism for Ru-catalyzed hydroamination of unactivated terminal alkenes with 2-aminopyridine.

### 1.8 Photocatalytic Intermolecular Hydroamination of Unactivated Alkenes

Recently, organic and Ir-based photocatalysts have been demonstrated to catalyze intermolecular hydroamination of unactivated alkenes. These reactions have been shown to occur through the activation of the alkenes to form alkenyl radical cations as well as through the activation of the amines to form amino radical cations or amino radicals. One advantage of photocatalytic hydroamination is that it usually proceeds with Anti-Markovnikov selectivity and this selectivity is complementary to the Markovnikov selectivity of most transition-metal catalyzed hydroamination. Additionally, photocatalytic hydroamination, which proceeds through radical intermediates, is often more tolerant of multi-substituted alkenes compared to transition-metal catalyzed hydroamination.

Nicewicz reported the first photocatalytic intermolecular Anti-Markovnikov hydroamination of unactivated alkenes in 2013 (Figure 1.18a).[73] During the investigation of the intramolecular hydroamination of alkenes, the authors discovered that, under 450 nm irradiation, a combination of 9-mesityl-10-methylacridinium tetrafluoroborate (Mes-Acr-Me$^+$), phenylthiol, and 2,6-lutidine catalyzed the intermolecular hydroamination of cyclic trisubstituted alkenes with triflylamide. A year later, Nicewicz showed that acyclic trisubstituted alkenes also undergo hydroamination with triflylamide under similar conditions (Figure 1.18b).[74] This reaction was proposed to occur through oxidation of the alkene by the photocatalyst to generate an alkenyl radical cation and nucleophilic attack of the resulting alkenyl radical cation by the amine. In 2021, Shu showed that 9-mesityl-10-phenylacridinium tetrafluoroborate (Mes-Acr-Ph$^+$) and 2-aminothiophenol catalyzed the Anti-

Markovnikov hydroamination of vinylarenes and unactivated alkenes with ammonium carbonate as the amine source (Figure 1.18c).[75]

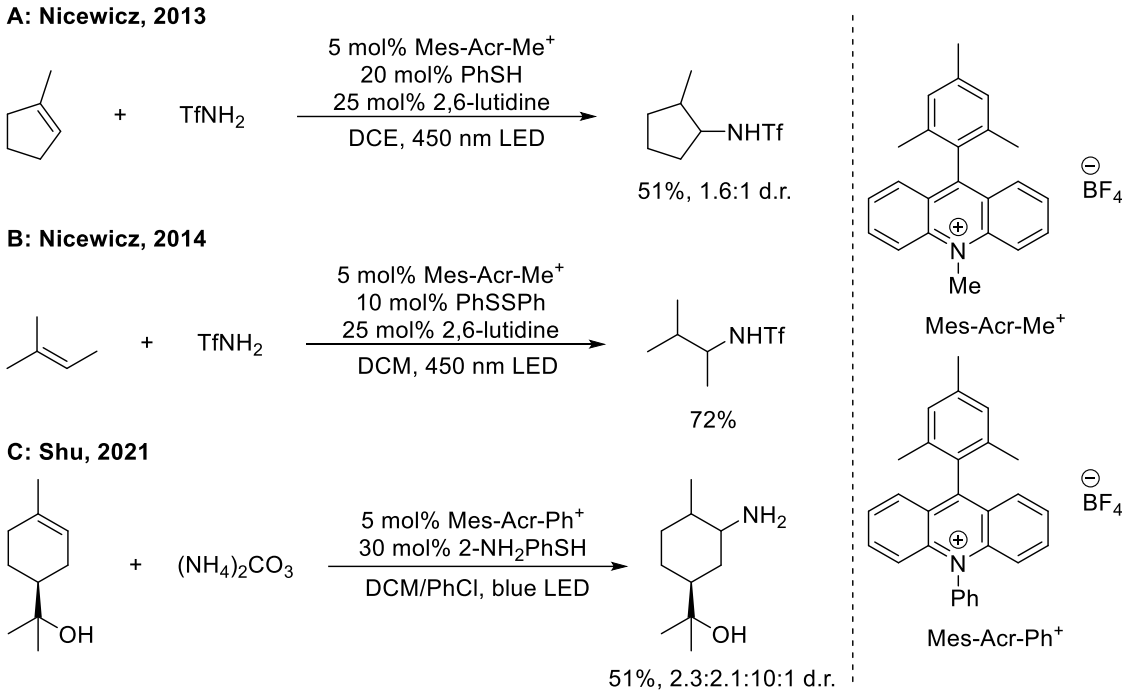


**Figure 1.18.** (A) Photocatalytic Anti-Markovnikov hydroamination of unactivated cyclic alkenes with triflylamide. (B) Photocatalytic Anti-Markovnikov hydroamination of unactivated acyclic alkenes with triflylamide. (C) Photocatalytic Anti-Markovnikov hydroamination of unactivated alkene with ammonium carbonate.

In 2017, Knowles disclosed photocatalytic intermolecular Anti-Markovnikov hydroamination of unactivated alkenes with secondary amines in the presence of an iridium photocatalyst (Figure 1.19a).[6] This reaction was compatible with mono- to tetrasubstituted alkenes and a variety of cyclic and acyclic secondary amines bearing polar functional groups. Mechanistic studies, including Stern-Volmer analysis, NMR spectroscopy, and DFT computations, suggested that this reaction proceeded through oxidation of the amine to generate the amino radical cation and nucleophilic attack of the amino radical cation by the alkene. With the use of a more oxidizing photocatalyst, the scope of amine was extended to primary alkylamines by Knowles in 2019 (Figure 1.19b).[76]

In 2018, Knowles reported photocatalytic intermolecular Anti-Markovnikov hydroamidation of mono- to tetrasubstituted unactivated alkenes with primary and secondary arylsulfonamides in the presence of an iridium photocatalyst (Figure 1.20a). Unlike the photocatalytic hydroamination with alkylamines, the hydroamidation with arylsulfonamides occurred via concerted PCET of the amide to form an amidyl radical and addition of the amidyl radical to the unactivated alkene.[77] In 2021, Doyle also reported a similar transformation in the presence of an iridium photocatalyst and a phosphine cocatalyst (Figure 1.20b). Amidyl radical was also invoked as the intermediate for this reaction and this radical was proposed to result from scission of a P–N bond.[7]

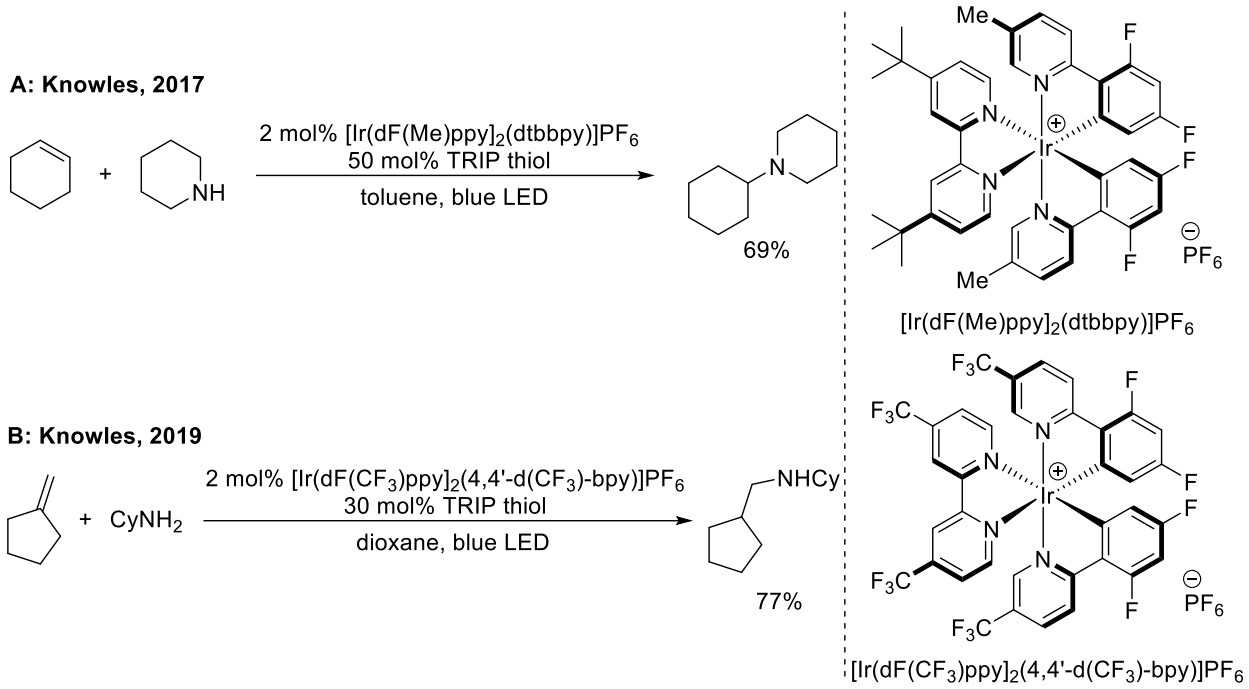


**Figure 1.19.** (A) Photocatalytic hydroamination of unactivated alkenes with secondary alkylamines. (B) Photocatalytic hydroamination of unactivated alkenes with primary alkylamines.

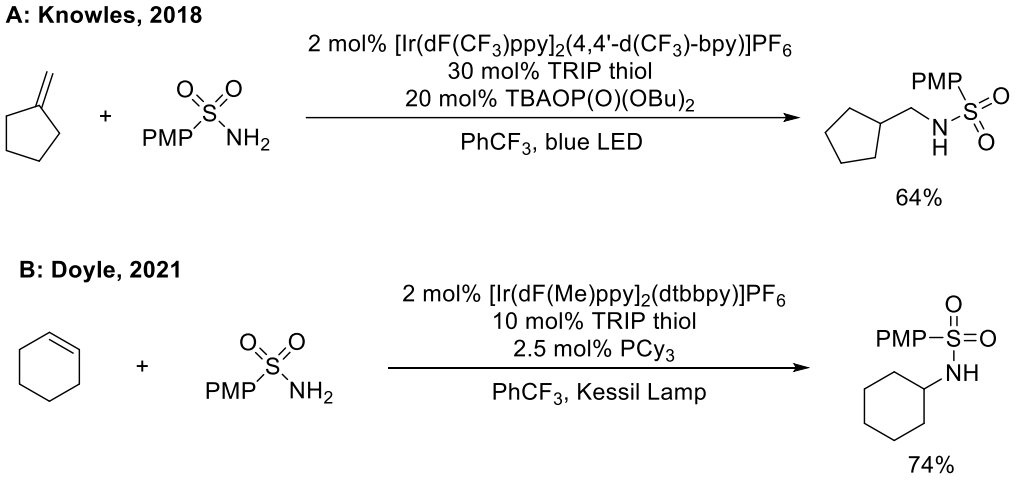


**Figure 1.20.** (A) Photocatalytic hydroamidation of unactivated alkenes with arylsulfonamides by Knowles. (B) Photocatalytic hydroamidation of unactivated alkenes with arylsulfonamides by Doyle.

### 1.9 Undirected Intermolecular Hydroamination of Unactivated Alkenes Catalyzed by Transition-Metal Complexes

In 2005, Tilley and Bell reported hydroamination of norbornene and unactivated alkenes with sulfonamides and weakly basic anilines in the presence of electrophilic platinum complexes

(Figure 1.21a).[78] Mechanistic studies showed that this reaction proceeded through protonation of the alkene by the acidic platinum sulfonamide complex and nucleophilic attack of the resulting carbocation by another molecule of sulfonamide.[50] In 2006, gold-catalyzed intra- and intermolecular hydroamination of unactivated alkene was reported by He (Figure 1.21b).[79] ($PPh_3$)Au(OTf) was found to catalyze the intermolecular hydroamination of a variety of cyclic and acyclic unactivated alkenes with *p*-toluenesulfonamide. In 2009, an enantioselective hydroamination of unactivated alkenes with cyclic ureas in the presence of a combination of (DTBM-MEOBIPHEP)AuCl and AgOTf was realized by Widenhoefer (Figure 1.21c).[61] Hultzsch disclosed the enantioselective hydroamination of unactivated alkenes with primary alkyl and benzyl amines catalyzed by complexes of rare-earth metals in 2010 (Figure 1.21d).[60]

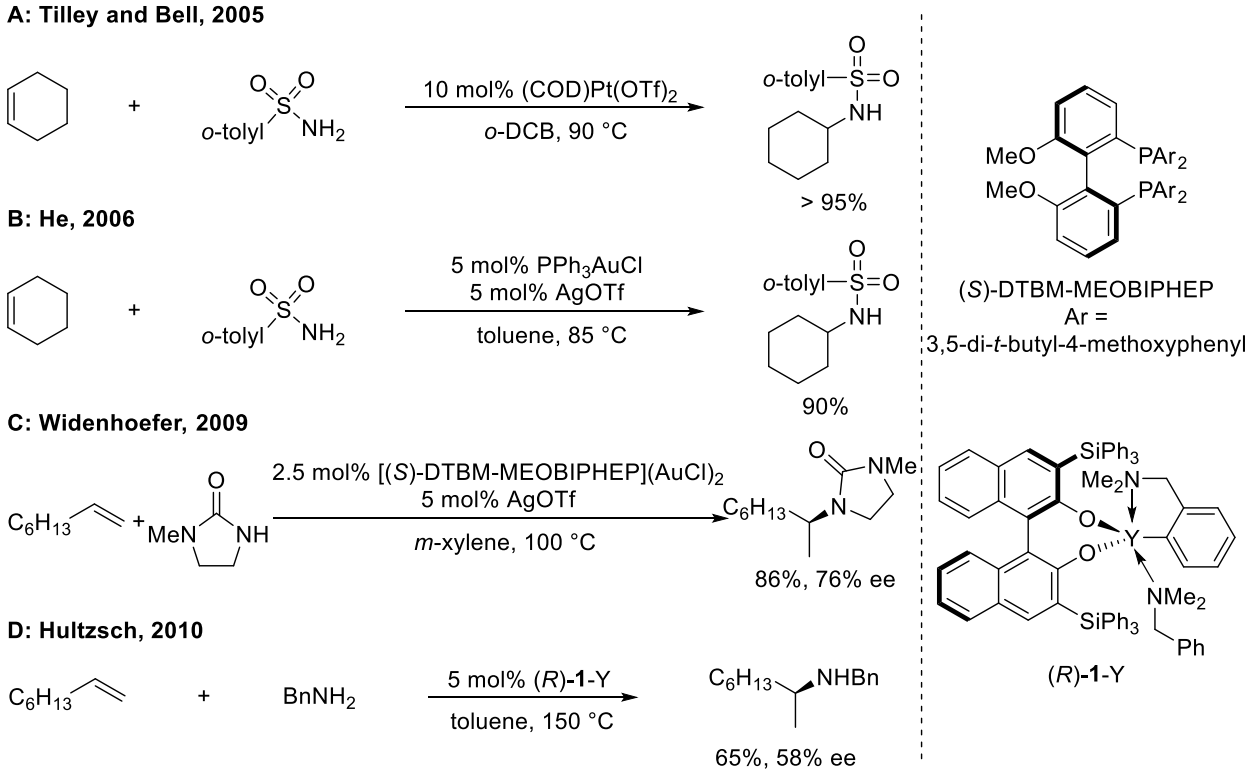


**Figure 1.21.** (A) Hydroamidation of unactivated alkenes with arylsulfonamides in the presence of electrophilic platinum complexes. (B) Au-catalyzed hydroamidation of unactivated alkenes with arylsulfonamides. (C) Au-catalyzed enantioselective hydroamination of unactivated alkenes with cyclic ureas. (D) Enantioselective hydroamination of unactivated alkenes with alkylamines catalyzed by complexes of rare-earth metals.

## 1.10 Directed Intermolecular Hydroamination of Unactivated Alkenes Catalyzed by Transition-Metal Complexes

In 2014, Hull reported Rh-catalyzed directed Markovnikov hydroamination of terminal allyl imines with secondary alkylamines (Figure 1.22a).[80] Deuterium labeling experiments suggested that this reaction proceeded through the following steps: (1) coordination of the allyl imine to the cationic Rh center, (2) nucleophilic attack of the coordinated alkene by alkylamine, and (3) proton

transfer. In 2019, an enantioselective directed Markovnikov hydroamination of terminal allyl amines with secondary alkylamines was achieved by Hull using a cationic rhodium complex containing a chiral MEOBIPHEP ligand (Figure 1.22b).[63] In 2016, Pd-catalyzed Anti-Markovnikov hydroamination of terminal alkenes bearing an aminoquinoline directing group with imides, carbamates, and sulfonamides was reported by Engle (Figure 1.22c).[62] This reaction was proposed to occur through a sequence of coordination of the alkene to the Pd center, aminopalladation, and proto-depalladation.

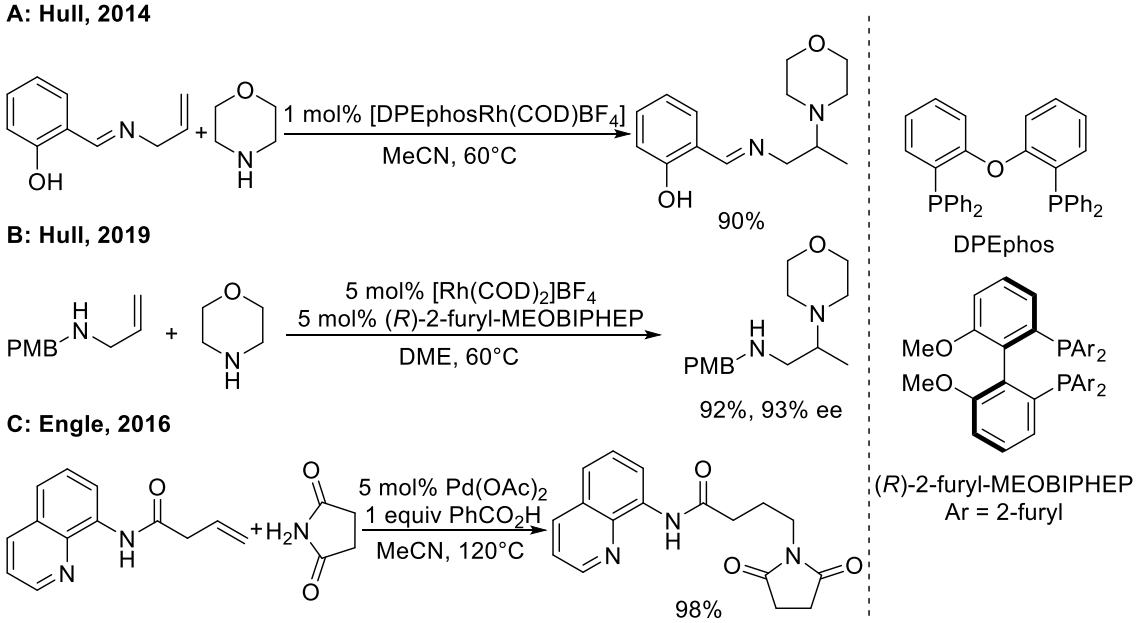


**Figure 1.22.** (A) Rh-catalyzed hydroamination of allyl imines with secondary alkylamines. (B) Rh-catalyzed enantioselective hydroamination of allyl amines with secondary alkylamines. (C) Pd-catalyzed hydroamination of alkenes with imides, carbamates, and sulfonamides.

## 1.11 Formal Intermolecular Hydroamination of Unactivated Alkenes Catalyzed by Transition-Metal Complexes

Recently, a series of copper-catalyzed formal hydroamination of unactivated terminal and internal alkenes in the presence of silanes and esters of hydroxylamine was disclosed by Buchwald, and enantioselective formal hydroamination was also achieved with the use of copper catalysts containing chiral bisphosphine ligands (Figure 1.23).[68, 81-82] Similar transformations were also reported by Lalic[64] and Miura.[65] These formal hydroamination reactions were proposed to occur via initial formation of a copper hydride intermediate, insertion of the alkene into the Cu–H bond, and electrophilic amination of the generated copper alkyl intermediate. More recently, Ni- and Co-catalyzed formal hydroaminations of alkenes have been developed by Hong,[67, 83] Niu,[84] and Shu.[85]

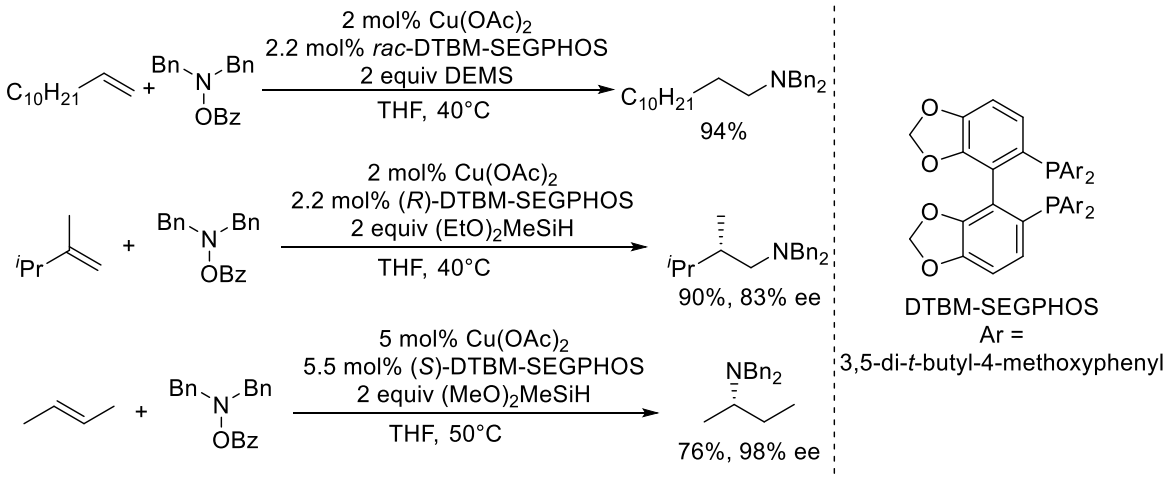


**Figure 1.23.** Copper-catalyzed formal hydroamination of unactivated terminal and internal alkenes.

## 1.12 Conclusions and Outlook

This chapter described the progression of hydroamination catalyzed by late transition-metal complexes in our laboratory from the additions of N–H bonds to conjugated alkenes to the additions to unconjugated and unstrained internal and terminal alkenes. While reactions of the conjugated alkenes catalyzed by palladium, rhodium, and ruthenium occur by nucleophilic attack of the amine on a coordinated benzyl, allyl, alkene or arene ligand, the reactions of unconjugated alkenes occur by migratory insertion into metal-nitrogen bonds in complexes formed by oxidative addition of the N-H bond. Fundamental studies have shown that the oxidative addition of N–H bonds to Ir(I) is close to thermoneutral and is influenced by subtle properties of the ancillary ligand,[71] causing reactions to be more favorable with substrates containing more acidic N–H bonds or secondary binding groups.[86] The hydroamination of alkenes also was shown experimentally to be close to thermoneutral, and common side products were found to result from oxidative amination and alkene isomerization. The facility of alkene insertions into metal-nitrogen bonds during these reaction runs counter to the rarity of this reaction in prior literature and presages multiple possible future alkene amination processes. On the basis of these principles, future catalytic systems for the addition of N–H donors that are more directly relevant to synthetic applications than aminopyridines to unactivated alkenes, for the regioselective hydroamination of unsymmetrical internal alkenes, and for the hydroamination of hindered, multi-substituted alkenes will be sought. In parallel the application of these principles to create intramolecular reactions to form a variety of saturated nitrogen heterocycles that avoid the translational, entropic penalty of intermolecular processes will be sought.

## 1.13 References

1. Müller, T. E.; Beller, M., Metal-Initiated Amination of Alkenes and Alkynes. *Chem. Rev.* **1998,** *98* (2), 675-704.
2. Müller, T. E.; Hultzsch, K. C.; Yus, M.; Foubelo, F.; Tada, M., Hydroamination: Direct Addition of Amines to Alkenes and Alkynes. *Chem. Rev.* **2008,** *108* (9), 3795-3892.

3. Huang, L.; Arndt, M.; Gooßen, K.; Heydt, H.; Gooßen, L. J., Late Transition Metal-Catalyzed Hydroamination and Hydroamidation. *Chem. Rev.* **2015,** *115* (7), 2596-2697.
4. Trowbridge, A.; Walton, S. M.; Gaunt, M. J., New Strategies for the Transition-Metal Catalyzed Synthesis of Aliphatic Amines. *Chem. Rev.* **2020,** *120* (5), 2613-2692.
5. Howk, B. W.; Little, E. L.; Scott, S. L.; Whitman, G. M., Alkali Metal-catalyzed Amination of Olefins. *J. Am. Chem. Soc.* **1954,** *76* (7), 1899-1902.
6. Musacchio, A. J.; Lainhart, B. C.; Zhang, X.; Naguib, S. G.; Sherwood, T. C.; Knowles, R. R., Catalytic intermolecular hydroaminations of unactivated olefins with secondary alkyl amines. *Science* **2017,** *355* (6326), 727-730.
7. Chinn, A. J.; Sedillo, K.; Doyle, A. G., Phosphine/Photoredox Catalyzed Anti-Markovnikov Hydroamination of Olefins with Primary Sulfonamides via α-Scission from Phosphoranyl Radicals. *J. Am. Chem. Soc.* **2021,** *143* (43), 18331-18338.
8. Johns, A. M.; Sakai, N.; Ridder, A.; Hartwig, J. F., Direct Measurement of the Thermodynamics of Vinylarene Hydroamination. *J. Am. Chem. Soc.* **2006,** *128* (29), 9306-9307.
9. Xi, Y.; Ma, S.; Hartwig, J. F., Catalytic asymmetric addition of an amine N–H bond across internal alkenes. *Nature* **2020,** *588* (7837), 254-260.
10. Ma, S.; Xi, Y.; Fan, H.; Roediger, S.; Hartwig, J. F., Enantioselective hydroamination of unactivated terminal alkenes. *Chem* **2022,** *8* (2), 532-542.
11. Johns, A. M.; Utsunomiya, M.; Incarvito, C. D.; Hartwig, J. F., A Highly Active Palladium Catalyst for Intermolecular Hydroamination. Factors that Control Reactivity and Additions of Functionalized Anilines to Dienes and Vinylarenes. *J. Am. Chem. Soc.* **2006,** *128* (6), 1828-1839.
12. Pawlas, J.; Nakao, Y.; Kawatsura, M.; Hartwig, J. F., A General Nickel-Catalyzed Hydroamination of 1,3-Dienes by Alkylamines: Catalyst Selection, Scope, and Mechanism. *J. Am. Chem. Soc.* **2002,** *124* (14), 3669-3679.
13. Sevov, C. S.; Zhou, J.; Hartwig, J. F., Iridium-Catalyzed Intermolecular Hydroamination of Unactivated Aliphatic Alkenes with Amides and Sulfonamides. *J. Am. Chem. Soc.* **2012,** *134* (29), 11960-11963.
14. Rosenfeld, D. C.; Shekhar, S.; Takemiya, A.; Utsunomiya, M.; Hartwig, J. F., Hydroamination and Hydroalkoxylation Catalyzed by Triflic Acid. Parallels to Reactions Initiated with Metal Triflates. *Org. Lett.* **2006,** *8* (19), 4179-4182.
15. Kawatsura, M.; Hartwig, J. F., Palladium-Catalyzed Intermolecular Hydroamination of Vinylarenes Using Arylamines. *J. Am. Chem. Soc.* **2000,** *122* (39), 9546-9547.
16. Qian, H.; Widenhoefer, R. A., Platinum-Catalyzed Intermolecular Hydroamination of Vinyl Arenes with Carboxamides. *Org. Lett.* **2005,** *7* (13), 2635-2638.
17. Hu, A.; Ogasawara, M.; Sakamoto, T.; Okada, A.; Nakajima, K.; Takahashi, T.; Lin, W., Palladium-Catalyzed Intermolecular Asymmetric Hydroamination with 4,4′-Disubstituted BINAP and SEGPHOS. *Adv. Synth. Catal.* **2006,** *348* (15), 2051-2056.
18. Kaspar, L. T.; Fingerhut, B.; Ackermann, L., Titanium-Catalyzed Intermolecular Hydroamination of Vinylarenes. *Angew. Chem. Int. Ed.* **2005,** *44* (37), 5972-5974.
19. Hong, S.; Marks, T. J., Organolanthanide-Catalyzed Hydroamination. *Acc. Chem. Res.* **2004,** *37* (9), 673-686.
20. Horrillo-Martínez, P.; Hultzsch, K. C.; Gil, A.; Branchadell, V., Base-Catalyzed Anti-Markovnikov Hydroamination of Vinylarenes – Scope, Limitations and Computational Studies. *Eur. J. Org. Chem.* **2007,** *2007* (20), 3311-3325.

21. Seshu Babu, N.; Mohan Reddy, K.; Sai Prasad, P. S.; Suryanarayana, I.; Lingaiah, N., Intermolecular hydroamination of vinyl arenes using tungstophosphoric acid as a simple and efficient catalyst. *Tetrahedron Lett.* **2007,** *48* (43), 7642-7645.
22. Utsunomiya, M.; Hartwig, J. F., Intermolecular, Markovnikov Hydroamination of Vinylarenes with Alkylamines. *J. Am. Chem. Soc.* **2003,** *125* (47), 14286-14287.
23. Nettekoven, U.; Hartwig, J. F., A New Pathway for Hydroamination. Mechanism of Palladium-Catalyzed Addition of Anilines to Vinylarenes. *J. Am. Chem. Soc.* **2002,** *124* (7), 1166-1167.
24. Beller, M.; Eichberger, M.; Trauthwein, H., Anti-Markovnikov Functionalization of Olefins: Rhodium-Catalyzed Oxidative Aminations of Styrenes. *Angew. Chem. Int. Ed.* **1997,** *36* (20), 2225-2227.
25. Utsunomiya, M.; Kuwano, R.; Kawatsura, M.; Hartwig, J. F., Rhodium-Catalyzed Anti-Markovnikov Hydroamination of Vinylarenes. *J. Am. Chem. Soc.* **2003,** *125* (19), 5608-5609.
26. Utsunomiya, M.; Hartwig, J. F., Ruthenium-Catalyzed Anti-Markovnikov Hydroamination of Vinylarenes. *J. Am. Chem. Soc.* **2004,** *126* (9), 2702-2703.
27. Takaya, J.; Hartwig, J. F., Mechanistic Studies of Ruthenium-Catalyzed Anti-Markovnikov Hydroamination of Vinylarenes: Intermediates and Evidence for Catalysis through π-Arene Complexes. *J. Am. Chem. Soc.* **2005,** *127* (16), 5756-5757.
28. Otsuka, M.; Yokoyama, H.; Endo, K.; Shibata, T., Ru-catalyzed β-selective and enantioselective addition of amines to styrenes initiated by direct arene-exchange. *Org. Biomol. Chem.* **2012,** *10* (19), 3815-3818.
29. Takemoto, S.; Matsuzaka, H., Recent topics on catalytic transformations of aromatic molecules via η6-arene transition metal complexes. *Tetrahedron Lett.* **2018,** *59* (8), 697-703.
30. Minami, T.; Okamoto, H.; Ikeda, S.; Tanaka, R.; Ozawa, F.; Yoshifuji, M., (η3-Allyl)palladium Complexes Bearing Diphosphinidenecyclobutene Ligands: Highly Active Catalysts for the Hydroamination of 1,3-Dienes. *Angew. Chem. Int. Ed.* **2001,** *40* (23), 4501-4503.
31. Brouwer, C.; He, C., Efficient Gold-Catalyzed Hydroamination of 1,3-Dienes. *Angew. Chem. Int. Ed.* **2006,** *45* (11), 1744-1747.
32. Goldfogel, M. J.; Roberts, C. C.; Meek, S. J., Intermolecular Hydroamination of 1,3-Dienes Catalyzed by Bis(phosphine)carbodicarbene–Rhodium Complexes. *J. Am. Chem. Soc.* **2014,** *136* (17), 6227-6230.
33. Yang, X.-H.; Lu, A.; Dong, V. M., Intermolecular Hydroamination of 1,3-Dienes To Generate Homoallylic Amines. *J. Am. Chem. Soc.* **2017,** *139* (40), 14049-14052.
34. Tran, G.; Shao, W.; Mazet, C., Ni-Catalyzed Enantioselective Intermolecular Hydroamination of Branched 1,3-Dienes Using Primary Aliphatic Amines. *J. Am. Chem. Soc.* **2019,** *141* (37), 14814-14822.
35. Ryu, J.-S.; Li, G. Y.; Marks, T. J., Organolathanide-Catalyzed Regioselective Intermolecular Hydroamination of Alkenes, Alkynes, Vinylarenes, Di- and Trivinylarenes, and Methylenecyclopropanes. Scope and Mechanistic Comparison to Intramolecular Cyclohydroaminations. *J. Am. Chem. Soc.* **2003,** *125* (41), 12584-12605.
36. Pradhan, S.; Das, S.; Kumar, G.; Chatterjee, I., Transition-Metal-Free Regioselective Intermolecular Hydroamination of Conjugated 1,3-Dienes with Heterocyclic Amines. *Org. Lett.* **2022,** *24* (12), 2452-2456.
37. Takahashi, S.; Shibano, T.; Hagihara, N., The Dimerization of Butadiene by Palladium Complex Catalysts. *Bull. Chem. Soc. Jpn.* **1968,** *41* (2), 454-460.

38. Löber, O.; Kawatsura, M.; Hartwig, J. F., Palladium-Catalyzed Hydroamination of 1,3-Dienes: A Colorimetric Assay and Enantioselective Additions. *J. Am. Chem. Soc.* **2001,** *123* (18), 4366-4367.
39. Johns, A. M.; Liu, Z.; Hartwig, J. F., Primary tert- and sec-Allylamines via Palladium-Catalyzed Hydroamination and Allylic Substitution with Hydrazine and Hydroxylamine Derivatives. *Angew. Chem. Int. Ed.* **2007,** *46* (38), 7259-7261.
40. Sakai, N.; Ridder, A.; Hartwig, J. F., Tropene Derivatives by Sequential Intermolecular and Transannular, Intramolecular Palladium-Catalyzed Hydroamination of Cycloheptatriene. *J. Am. Chem. Soc.* **2006,** *128* (25), 8134-8135.
41. Adamson, N. J.; Hull, E.; Malcolmson, S. J., Enantioselective Intermolecular Addition of Aliphatic Amines to Acyclic Dienes with a Pd–PHOX Catalyst. *J. Am. Chem. Soc.* **2017,** *139* (21), 7180-7183.
42. Jiu, A. Y.; Slocumb, H. S.; Yeung, C. S.; Yang, X.-H.; Dong, V. M., Enantioselective Addition of Pyrazoles to Dienes. *Angew. Chem. Int. Ed.* **2021,** *60* (36), 19660-19664.
43.Park, S.; Malcolmson, S. J., Development and Mechanistic Investigations of Enantioselective Pd-Catalyzed Intermolecular Hydroaminations of Internal Dienes. *ACS Catal.* **2018,** *8* (9), 8468-8476.
44. Teng, H.-L.; Luo, Y.; Wang, B.; Zhang, L.; Nishiura, M.; Hou, Z., Synthesis of Chiral Aminocyclopropanes by Rare-Earth-Metal-Catalyzed Cyclopropene Hydroamination. *Angew. Chem. Int. Ed.* **2016,** *55* (49), 15406-15410.
45. Teng, H.-L.; Luo, Y.; Nishiura, M.; Hou, Z., Diastereodivergent Asymmetric Carboamination/Annulation of Cyclopropenes with Aminoalkenes by Chiral Lanthanum Catalysts. *J. Am. Chem. Soc.* **2017,** *139* (46), 16506-16509.
46. Feng, S.; Hao, H.; Liu, P.; Buchwald, S. L., Diastereo- and Enantioselective CuH-Catalyzed Hydroamination of Strained Trisubstituted Alkenes. *ACS Catal.* **2020,** *10* (1), 282-291.
47. Dorta, R.; Egli, P.; Zürcher, F.; Togni, A., The [IrCl(Diphosphine)]2/Fluoride System. Developing Catalytic Asymmetric Olefin Hydroamination. *J. Am. Chem. Soc.* **1997,** *119* (44), 10857-10858.
48. Ackermann, L.; Kaspar, L. T.; Gschrei, C. J., TiCl4-Catalyzed Intermolecular Hydroamination Reactions of Norbornene. *Org. Lett.* **2004,** *6* (15), 2515-2518.
49. Kemper, J.; Studer, A., Stable Reagents for the Generation of N-Centered Radicals: Hydroamination of Norbornene. *Angew. Chem. Int. Ed.* **2005,** *44* (31), 4914-4917.
50. McBee, J. L.; Bell, A. T.; Tilley, T. D., Mechanistic Studies of the Hydroamination of Norbornene with Electrophilic Platinum Complexes: The Role of Proton Transfer. *J. Am. Chem. Soc.* **2008,** *130* (49), 16562-16571.
51. Casalnuovo, A. L.; Calabrese, J. C.; Milstein, D., Rational design in homogeneous catalysis. Iridium(I)-catalyzed addition of aniline to norbornylene via nitrogen-hydrogen activation. *J. Am. Chem. Soc.* **1988,** *110* (20), 6738-6744.
52. Zhou, J.; Hartwig, J. F., Intermolecular, Catalytic Asymmetric Hydroamination of Bicyclic Alkenes and Dienes in High Yield and Enantioselectivity. *J. Am. Chem. Soc.* **2008,** *130* (37), 12220-12221.
53. Zhao, J.; Goldman, A. S.; Hartwig, J. F., Oxidative Addition of Ammonia to Form a Stable Monomeric Amido Hydride Complex. *Science* **2005,** *307* (5712), 1080-1082.
54. Kanzelberger, M.; Zhang, X.; Emge, T. J.; Goldman, A. S.; Zhao, J.; Incarvito, C.; Hartwig, J. F., Distinct Thermodynamics for the Formation and Cleavage of N−H Bonds in Aniline and

Ammonia. Directly-Observed Reductive Elimination of Ammonia from an Isolated Amido Hydride Complex. *J. Am. Chem. Soc.* **2003,** *125* (45), 13644-13645.
55. Zhao, P.; Krug, C.; Hartwig, J. F., Transfer of Amido Groups from Isolated Rhodium(I) Amides to Alkenes and Vinylarenes. *J. Am. Chem. Soc.* **2005,** *127* (34), 12066-12073.
56. Hanley, P. S.; Marković, D.; Hartwig, J. F., Intermolecular Insertion of Ethylene and Octene into a Palladium−Amide Bond. Spectroscopic Evidence for an Ethylene Amido Intermediate. *J. Am. Chem. Soc.* **2010,** *132* (18), 6302-6303.
57. Hanley, P. S.; Hartwig, J. F., Intermolecular Migratory Insertion of Unactivated Olefins into Palladium–Nitrogen Bonds. Steric and Electronic Effects on the Rate of Migratory Insertion. *J. Am. Chem. Soc.* **2011,** *133* (39), 15661-15673.
58. Hanley, P. S.; Hartwig, J. F., Migratory Insertion of Alkenes into Metal–Oxygen and Metal–Nitrogen Bonds. *Angew. Chem. Int. Ed.* **2013,** *52* (33), 8510-8525.
59. Pan, S.; Endo, K.; Shibata, T., Ir(I)-Catalyzed Intermolecular Regio- and Enantioselective Hydroamination of Alkenes with Heteroaromatic Amines. *Org. Lett.* **2012,** *14* (3), 780-783.
60. Reznichenko, A. L.; Nguyen, H. N.; Hultzsch, K. C., Asymmetric Intermolecular Hydroamination of Unactivated Alkenes with Simple Amines. *Angew. Chem. Int. Ed.* **2010,** *49* (47), 8984-8987.
61. Zhang, Z.; Lee, S. D.; Widenhoefer, R. A., Intermolecular Hydroamination of Ethylene and 1-Alkenes with Cyclic Ureas Catalyzed by Achiral and Chiral Gold(I) Complexes. *J. Am. Chem. Soc.* **2009,** *131* (15), 5372-5373.
62. Gurak, J. A., Jr.; Yang, K. S.; Liu, Z.; Engle, K. M., Directed, Regiocontrolled Hydroamination of Unactivated Alkenes via Protodepalladation. *J. Am. Chem. Soc.* **2016,** *138* (18), 5805-5808.
63. Vanable, E. P.; Kennemur, J. L.; Joyce, L. A.; Ruck, R. T.; Schultz, D. M.; Hull, K. L., Rhodium-Catalyzed Asymmetric Hydroamination of Allyl Amines. *J. Am. Chem. Soc.* **2019,** *141* (2), 739-742.
64. Rucker, R. P.; Whittaker, A. M.; Dang, H.; Lalic, G., Synthesis of Tertiary Alkyl Amines from Terminal Alkenes: Copper-Catalyzed Amination of Alkyl Boranes. *J. Am. Chem. Soc.* **2012,** *134* (15), 6571-6574.
65. Miki, Y.; Hirano, K.; Satoh, T.; Miura, M., Copper-Catalyzed Intermolecular Regioselective Hydroamination of Styrenes with Polymethylhydrosiloxane and Hydroxylamines. *Angew. Chem. Int. Ed.* **2013,** *52* (41), 10830-10834.
66. Gao, Y.; Cui, Y.; Huo, Y.; Chen, J.; She, M.; Li, X.; Chen, Q.; Hu, X.-Q., Nickel-Catalyzed Hydroamination of Olefins with Anthranils. *J. Org. Chem.* **2021,** *86* (17), 12107-12118.
67. Lee, C.; Kang, H.-J.; Seo, H.; Hong, S., Nickel-Catalyzed Regio- and Enantioselective Hydroamination of Unactivated Alkenes Using Carbonyl Directing Groups. *J. Am. Chem. Soc.* **2022,** *144* (20), 9091-9100.
68. Yang, Y.; Shi, S.-L.; Niu, D.; Liu, P.; Buchwald, S. L., Catalytic asymmetric hydroamination of unactivated internal olefins to aliphatic amines. *Science* **2015,** *349* (6243), 62-66.
69. Wagner-Carlberg, N.; Rovis, T., Rhodium(III)-Catalyzed Anti-Markovnikov Hydroamidation of Unactivated Alkenes Using Dioxazolones as Amidating Reagents. *J. Am. Chem. Soc.* **2022,** *144* (49), 22426-22432.
70. Sevov, C. S.; Zhou, J.; Hartwig, J. F., Iridium-Catalyzed, Intermolecular Hydroamination of Unactivated Alkenes with Indoles. *J. Am. Chem. Soc.* **2014,** *136* (8), 3200-3207.
71. Tye, J. W.; Hartwig, J. F., Computational Studies of the Relative Rates for Migratory Insertions of Alkenes into Square-Planar, Methyl, −Amido, and −Hydroxo Complexes of Rhodium. *J. Am. Chem. Soc.* **2009,** *131* (41), 14703-14712.

72. Verendel, J. J.; Pàmies, O.; Diéguez, M.; Andersson, P. G., Asymmetric Hydrogenation of Olefins Using Chiral Crabtree-type Catalysts: Scope and Limitations. *Chem. Rev.* **2014,** *114* (4), 2130-2169.
73. Nguyen, T. M.; Nicewicz, D. A., Anti-Markovnikov Hydroamination of Alkenes Catalyzed by an Organic Photoredox System. *J. Am. Chem. Soc.* **2013,** *135* (26), 9588-9591.
74. Nguyen, T. M.; Manohar, N.; Nicewicz, D. A., anti-Markovnikov Hydroamination of Alkenes Catalyzed by a Two-Component Organic Photoredox System: Direct Access to Phenethylamine Derivatives. *Angew. Chem. Int. Ed.* **2014,** *53* (24), 6198-6201.
75. Du, Y.-D.; Chen, B.-H.; Shu, W., Direct Access to Primary Amines from Alkenes by Selective Metal-Free Hydroamination. *Angew. Chem. Int. Ed.* **2021,** *60* (18), 9875-9880.
76. Miller, D. C.; Ganley, J. M.; Musacchio, A. J.; Sherwood, T. C.; Ewing, W. R.; Knowles, R. R., Anti-Markovnikov Hydroamination of Unactivated Alkenes with Primary Alkyl Amines. *J. Am. Chem. Soc.* **2019,** *141* (42), 16590-16594.
77. Zhu, Q.; Graff, D. E.; Knowles, R. R., Intermolecular Anti-Markovnikov Hydroamination of Unactivated Alkenes with Sulfonamides Enabled by Proton-Coupled Electron Transfer. *J. Am. Chem. Soc.* **2018,** *140* (2), 741-747.
78. Karshtedt, D.; Bell, A. T.; Tilley, T. D., Platinum-Based Catalysts for the Hydroamination of Olefins with Sulfonamides and Weakly Basic Anilines. *J. Am. Chem. Soc.* **2005,** *127* (36), 12640-12646.
79. Zhang, J.; Yang, C.-G.; He, C., Gold(I)-Catalyzed Intra- and Intermolecular Hydroamination of Unactivated Olefins. *J. Am. Chem. Soc.* **2006,** *128* (6), 1798-1799.
80. Ickes, A. R.; Ensign, S. C.; Gupta, A. K.; Hull, K. L., Regio- and Chemoselective Intermolecular Hydroamination of Allyl Imines for the Synthesis of 1,2-Diamines. *J. Am. Chem. Soc.* **2014,** *136* (32), 11256-11259.
81. Zhu, S.; Niljianskul, N.; Buchwald, S. L., Enantio- and Regioselective CuH-Catalyzed Hydroamination of Alkenes. *J. Am. Chem. Soc.* **2013,** *135* (42), 15746-15749.
82. Zhu, S.; Buchwald, S. L., Enantioselective CuH-Catalyzed Anti-Markovnikov Hydroamination of 1,1-Disubstituted Alkenes. *J. Am. Chem. Soc.* **2014,** *136* (45), 15913-15916.
83. Jeon, J.; Lee, C.; Seo, H.; Hong, S., NiH-Catalyzed Proximal-Selective Hydroamination of Unactivated Alkenes. *J. Am. Chem. Soc.* **2020,** *142* (48), 20470-20480.
84. Yang, D.; Huang, H.; Zhang, H.; Yin, L.-M.; Song, M.-P.; Niu, J.-L., Regioselective Intermolecular Hydroamination of Unactivated Alkenes: "Co–H" Enabled Remote Functionalization. *ACS Catal.* **2021,** *11* (11), 6602-6613.
85. Yang, P.-F.; Liang, J.-X.; Zhao, H.-T.; Shu, W., Access to Enantioenriched 1,n-Diamines via Ni-Catalyzed Hydroamination of Unactivated Alkenes with Weakly Coordinating Groups. *ACS Catal.* **2022,** *12* (15), 9638-9645.
86. Wang, D. Y.; Choliy, Y.; Haibach, M. C.; Hartwig, J. F.; Krogh-Jespersen, K.; Goldman, A. S., Assessment of the Electronic Factors Determining the Thermodynamics of "Oxidative Addition" of C–H and N–H Bonds to Ir(I) Complexes. *J. Am. Chem. Soc.* **2016,** *138* (1), 149-163.

# CHAPTER 2
# Ruthenium-Catalyzed Hydroamination of Unactivated Terminal Alkenes with Stoichiometric Amounts of Alkene and an Ammonia Surrogate by Sequential Oxidation and Reduction

## 2.1 Introduction

Amines and their derivatives are important as both pharmaceuticals and agrochemicals.[1-3] Traditional methods to synthesize amines include nucleophilic substitution of organic halides,[4] reductive amination of carbonyl compounds,[5] and reduction of amides, nitriles, and azides.[6] The hydroamination of alkenes catalyzed by transition-metal complexes is an attractive alternative to these methods because it occurs directly with alkenes and could be applied to the functionalization of both simple alkenes and complex molecules containing alkene units.[7-9] Despite the potential utility of hydroamination, examples of intermolecular hydroaminations are often limited to conjugated and strained alkenes, such as dienes,[10-11] vinylarenes,[12-13], norbornenes[14-15] , and cyclopropenes.[16-17] Hydroaminations of unactivated alkenes are rare and generally require a large excess of alkene (Scheme 2.1a).[18-26]

Two main strategies have been followed to enable hydroamination to occur without an excess amount of alkene. The first involves catalytic reactions of alkenes possessing a directing group (Scheme 2.1b);[27-28] the second involves a formal catalytic hydroamination achieved by combining a silane reducing agent and a nitrogen-based electrophile (Scheme 2.1c).[29-30] These strategies require special alkenes or generate stoichiometric amounts of waste from the silane and aminating reagents and require synthesis of the aminating reagent. Thus, the development of a method that involves the direct addition of the N–H bond of an amine to unactivated alkenes is needed and would address these drawbacks.

Two general classes of mechanisms have been followed by most late, transition-metal catalysts for the hydroamination of alkenes. The first mechanism involves nucleophilic attack of a nitrogen nucleophile on a coordinated alkene, followed by protonation of the resulting amino-alkyl intermediate. The second involves oxidative addition of an N–H bond, followed by migratory insertion of the alkene into the metal-nitrogen bond and reductive elimination to form the C–H bond. Cationic rhodium[31] and gold[22] systems react by the first pathway, whereas neutral iridium complexes[19] react by the second pathway. Ruthenium complexes, the subject of this work, catalyze the hydroamination of terminal alkynes[32] and vinylarenes,[13] but they have not been shown to catalyze the hydroamination of unconjugated alkenes. We considered that such complexes and a carefully designed amine could catalyze the hydroaminations of alkenes and do so by mechanisms that are distinct from those followed by complexes of other transition metals.

Multidentate coordination of an amine that is tethered to a Lewis basic group, rather than the alkene, can accelerate hydroaminations due to a series of effects. First, the Lewis basic group can stabilize the intermediates resulting from oxidative addition of the N–H bond and products from insertion. Second, such an amine can serve as an ammonia equivalent by removal of the Lewis basic group. Third, an appropriate heteroaryl substituent can alter the thermodynamics of this nearly thermoneutral process[33] to favor addition by rendering the N–H bond of the ammonia surrogate weaker than the N–H bond of ammonia.

We report ruthenium-catalyzed Markovnikov hydroaminations of unactivated, terminal alkenes with 2-aminopyridine as an ammonia surrogate (Scheme 2.1d). Terminal alkenes containing a series of functional groups undergo hydroamination in the presence of this catalyst to afford the corresponding amine products without excess alkene. Detailed experimental and computational mechanistic studies provide strong evidence that this reaction occurs by a new pathway for hydroamination that comprises oxidative amination of the alkene and reduction of the corresponding imine intermediate.

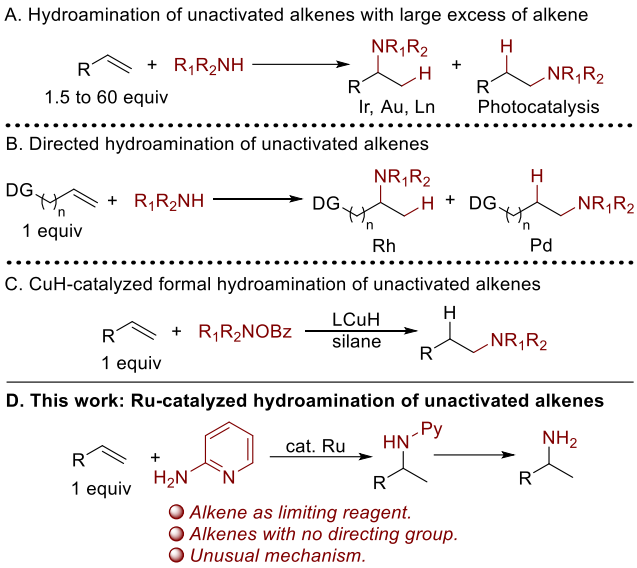


**Scheme 2.1.** Catalytic hydroamination of unactivated Terminal Alkenes.

## 2.2 Results and Discussion

**Reaction Development** Our studies on ruthenium-catalyzed hydroamination of unactivated terminal alkenes began by examining the reaction between 1-dodecene (1.0 equiv) and 2-aminopyridine **1a** (1.0 equiv) in the presence of a variety of electrophilic ruthenium complexes, a class of catalyst previously reported by our group to catalyze the oxidation of alcohols[34] (Table 2.1). 2-Aminopyridine was investigated as the amine component because it could coordinate to the cationic ruthenium complex in a bidentate fashion to form a 4-membered ruthenacycle that would retain reactivity at the Ru-N bond, due to the ring strain.

A survey of a series of phosphine-ligated ruthenium triflimide and triflate complexes showed that the triethylphosphine-ligated ruthenium complex **Ru-1** containing triflimide as the anionic ligand catalyzes the hydroamination of 1-dodecene to afford the amine product **2a** in 67% yield (Table 2.1, entry 1). Entries 2 to 6 show the effect of the phosphine ligand. Ruthenium complexes that contain more sterically demanding phosphine ligands (entry 2) and less electron-rich phosphine ligands (entry 3) catalyzed the reactions to form the addition product in lower yields. Complexes of ruthenium ligated by trimethylphosphine, 1,2-bis(diethylphosphino)-butane and a tripodal phosphine ligand, $N(CH_2PEt_2)_3$, did not catalyze the hydroamination reaction (entries 4-6). Entries 7 and 8 show the effect of the anionic ligand. Hydroamination conducted with the $PEt_3$-ligated ruthenium complex containing triflate counteranion (**Ru-7**) afforded the product in a slightly lower 62% yield (entry 7) than that with **Ru-1** and the $PEt_3$-ligated ruthenium complex containing chlorides (**Ru-8**) did not catalyze the hydroamination reaction (entry 8). This hydroamination reaction proceeded in a variety of polar, non-coordinating solvents, and the reaction in 1,2-DCB (entry 1) occurred in a higher yield than reactions in other solvents of this class (entries 9-14). The reaction performed with 2 mol% of **Ru-1** instead of 5 mol% gave a lower yield of product (entry 15).

Hydroaminations of alkenes catalyzed by electrophilic metal complexes, in some cases, have been suspected to occur by acid generated from the amine and the complex.[35] Although the basicity of the 2-aminopyridine would render such a pathway unlikely, we conducted control experiments to

test this potential. To assess the role of the ruthenium complex in this reaction, we conducted the reaction in the absence of **Ru-1**. Without **Ru-1**, no detectable product formed, indicating that the ruthenium complex is necessary for this transformation (entry 16). The hydroamination of 1-dodecene with sub-stoichiometric amounts of strong acid also did not form detectable amounts of product (entry 17), providing evidence against a pathway for hydroamination with 2-aminopyridine catalyzed by a Brønsted acid.

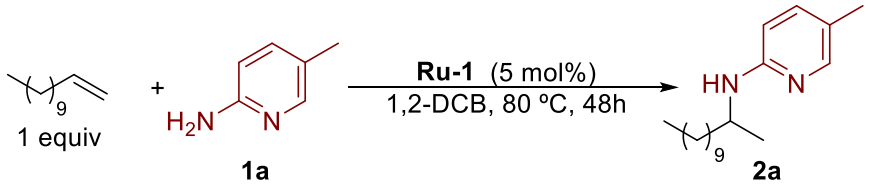


**Ru-1:** $Ru(PEt_3)_3NTf_2$
**Ru-2:** $Ru(P^nPr_3)_3NTf_2$
**Ru-3:** $Ru(PMePh_2)_3NTf_2$
**Ru-4:** $Ru(PMe_3)_4NTf_2$
**Ru-5:** $Ru(Et_2P(CH_2)_4PEt_2)_2NTf_2$
**Ru-6:** $Ru(N(CH_2PEt_2)_3)NTf_2$
**Ru-7:** $[Ru_2(PEt_3)_6(OTf)_3](OTf)$
**Ru-8:** $[Ru_2(PEt_3)_6(Cl)_3]Cl$

| entry | conditions | yield (%)[b] |
|---|---|---|
| 1 | standard | 67% |
| 2 | **Ru-2** as catalyst | 43% |
| 3 | **Ru-3** as catalyst | 18% |
| 4 | **Ru-4** as catalyst | <1% |
| 5 | **Ru-5** as catalyst | <1% |
| 6 | **Ru-6** as catalyst | <1% |
| 7 | **Ru-7** as catalyst | 62% |
| 8 | **Ru-8** as catalyst | <1% |
| 9 | 1,2-DCE as solvent | <1% |
| 10 | toluene as solvent | 29% |
| 11 | PhCl as solvent | 48% |
| 12 | $CH_3CN$ as solvent | <1% |
| 13 | THF as solvent | 56% |
| 14 | dioxane as solvent | 61% |
| 15 | **Ru-1** (2 mol%) | 45% |
| 16 | no **Ru-1** | <1% |
| 17 | $HNTf_2$ (5 mol%) | <1% |

[a]Standard Condition: 1-dodecene (0.2 mmol), **Ru-1** (0.01 mmol), **1a** (0.2 mmol), 1,2-DCB (50 μL), 80 °C, 48h. [b]Determined by $^1H$ NMR spectroscopy of the crude reaction mixture with 1,3,5-trimethoxybenzene as internal standard.

**Table 2.1. Evaluation of the Conditions for the Hydroamination of 1-Dodecene with 1a.**[a]

**Scope of Terminal Alkenes and 2-Aminopyridines for Catalytic Hydroamination.** Studies on the scope of the ruthenium-catalyzed hydroamination under the developed conditions are summarized in Table 2.2. The hydroamination of terminal alkenes with alkyl and aryl substituents occurred to afford products in good yields (**2a**-**4a**). The hydroamination of a series of alkenes

bearing ether, fluoride, amide, and tertiary alcohol functional groups also formed the hydroamination products in good to moderate yields (**5a-8a**). Alkenes containing multiple double bonds underwent hydroamination exclusively at the terminal alkene (**9a-11a**). Even the hydroamination of boldenone undecylenate, an anabolic steroid, occurred, showing the potential of this methodology for late-stage functionalization of architecturally complex molecules containing potential competing functionality (**12a**). An investigation of the scope of 2-aminopyridines for this reaction showed that a variety of 2-aminopyridines containing alkyl, ether, sulfide, and methylpiperazine substituents reacted to give the hydroamination products (**13a-17a**).

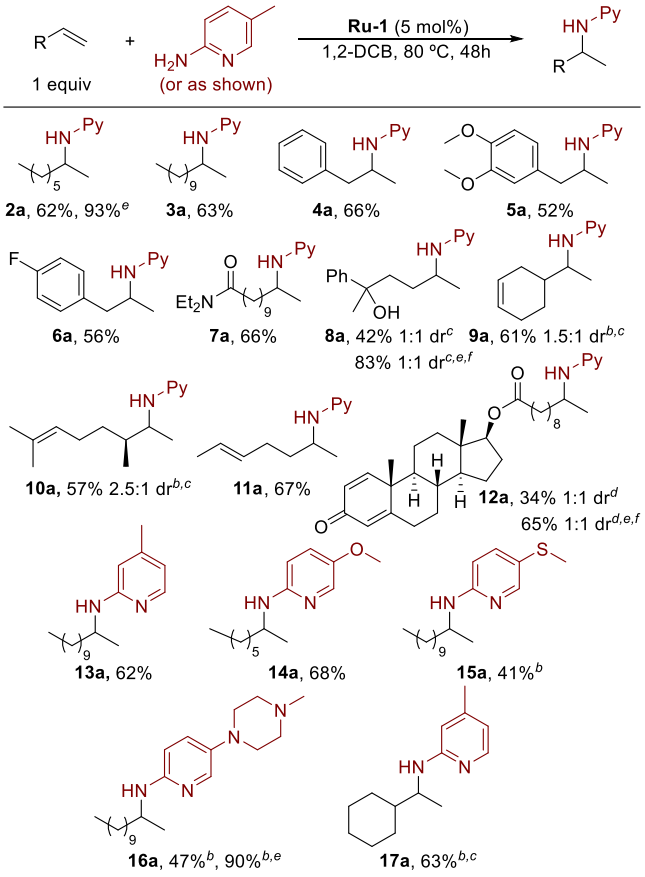


[a]Isolated yields. [b]100 °C. [c]**Ru-1** 10 mol%.
[d]**Ru-1** 15 mol%. [e]2 equiv of alkene. [f]72h.

**Table 2.2. Scope of Unconjugated Alkenes and 2-Aminopyridines for Catalytic Hydroamination.**[a-d]

In addition to unconjugated, terminal alkenes, vinylarenes underwent this hydroamination reaction (Table 2.3). Vinylarenes bearing a variety of electron-donating and electron-withdrawing *para* substituents underwent hydroamination to afford products in good yields (**18a-24a**). However, higher temperatures were required for the hydroaminations of electron-deficient vinylarenes catalyzed by **Ru-1** (**20a**, **22-24a**). A lower yield was observed from the reaction of a vinylarene bearing an *ortho*-substituent (**25a**), indicating that the reaction is sensitive to steric hindrance. The hydroamination of vinylnaphthalene and vinylferrocene also proceeded to afford hydroamination products (**27a-28a**). The major side reaction observed during the hydroamination was the isomerization of the terminal alkene to form internal alkenes, which did not undergo

hydroamination under our reaction conditions. High yields of the amine products **2a**, **8a**, **12a**, **16a**, and **28a** were obtained for reactions with just two equivalents of alkene with respect to the aminopyridine.

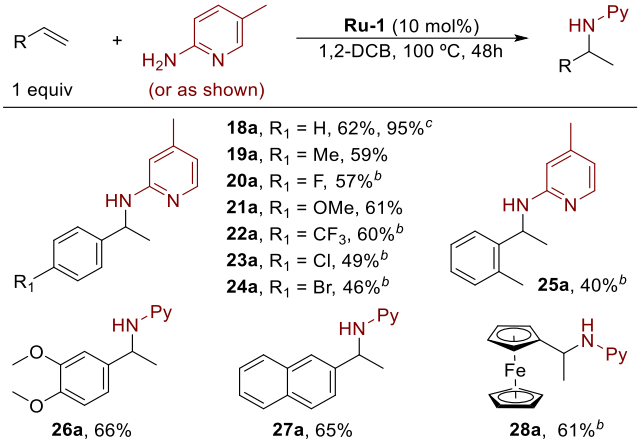


[a]Isolated yields. [b]120 °C. [c] 2 equiv of alkene.

**Table 2.3. Scope of Vinylarenes for Catalytic Hydroamination.**[a,b]

**Removal of Pyridyl Group from the Hydroamination Product.** The product from the hydroamination reaction was converted to a primary amine by a two-step sequence (Scheme 2.2).[36-38] Compound **2a** was first converted to an amidine, and the amidine was cleaved by $NaBH_4$ to form primary amine **2b**. For convenience on laboratory scale, the Boc-protected amine **2c** was isolated instead of the free amine **2b**.

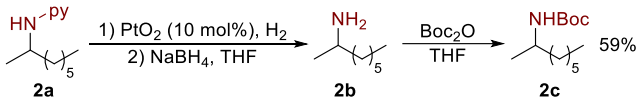


**Scheme 2.2. Removal of the Pyridyl Group from 2a.**

**Mechanistic Studies of Alkene Hydroamination.** Because side reactions, such as alkene isomerization, alkene oligomerization, and oxidative amination compete with alkene hydroamination,[9,19,39] literature protocols for the hydroamination of unactivated alkenes require either the use of alkenes containing a directing group or excess alkene. Our hydroamination protocol represents a rare example of catalytic hydroamination of unactivated alkenes with a stoichiometric amount of alkene. Therefore, a detailed investigation of the mechanism of this ruthenium-catalyzed hydroamination reaction was conducted to provide insight into the features that promote the hydroamination reaction over other side reactions.

**Determination of the Catalyst Resting State**. Our mechanistic investigation began with identifying the catalyst resting state. To obtain preliminary information about this species, we monitored the reaction of 2-amino-4-methylpyridine (**1b**) and 1-dodecene catalyzed by **Ru-1** by $^{31}P$ NMR spectroscopy at 80 °C (spectrum b of Figure 2.1). Aminopyridine **1b** was used for these studies, instead of **1a**, because ruthenium complexes containing **1b** were more crystalline than those containing **1a** (*vide infra*). A broad resonance at 50 ppm, corresponding to the resting state of the catalyst, was observed in the $^{31}P$ NMR spectrum of the reaction mixture.

Further information on the identity of the resting state was obtained by allowing **Ru-1** to react with 1-dodecene and **1b** separately and monitoring the reaction mixtures by $^{31}$P NMR spectroscopy. Treatment of **Ru-1** with excess 1-dodecene led to no new Ru complexes, as determined by $^{31}$P NMR spectroscopy at 80 °C (a and c of Figure 2.1). However, treatment of **Ru-1** with excess aminopyridine **1b** led to the observation of a broad resonance at 50 ppm in the $^{31}$P NMR spectrum of the reaction mixture at 80 °C, and this resonance was identical to that of the resting state of the Ru catalyst (d of Figure 2.1). Therefore, the major ruthenium complex in the reaction system forms from the combination of **Ru-1** with one or more equivalents of aminopyridine **1b**.

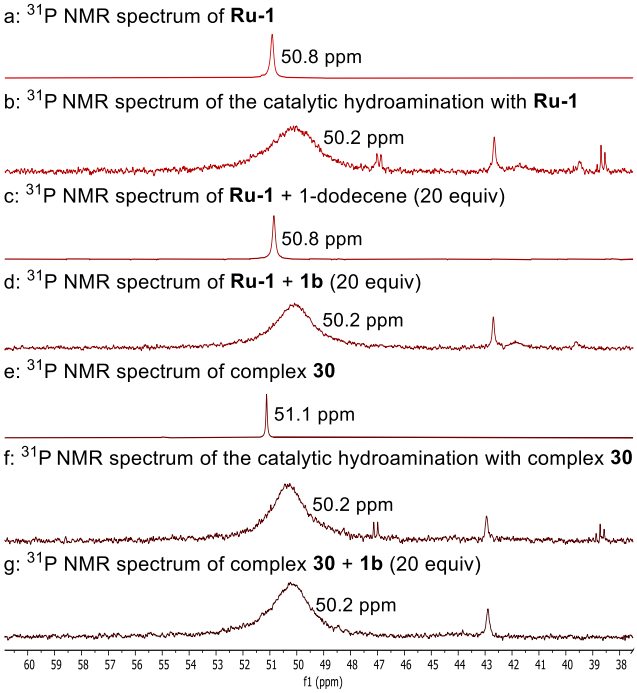


**Figure 2.1.** (a) $^{31}$P NMR spectrum **Ru-1**. (b) $^{31}$P NMR spectrum of the catalytic hydroamination of 1-dodecene with **Ru-1** as the catalyst. (c) $^{31}$P NMR spectrum the mixture of **Ru-1** and 1-dodecene (20 equiv). (d) $^{31}$P NMR spectrum the mixture of **Ru-1** and **1b** (20 equiv). (e) $^{31}$P NMR spectrum complex **30**. (f) $^{31}$P NMR spectrum of the catalytic hydroamination of 1-dodecene with complex **30** as the catalyst. (g) $^{31}$P NMR spectrum the mixture of complex **30** and **1b** (20 equiv). All above spectra were acquired at 80 °C.

An independent synthesis of the resting state was pursued (Figure 2.2) because we were unable to isolate it in pure form directly from the mixture of **Ru-1** and excess **1b**. Treatment of **Ru-1** with one equivalent of **1b** afforded the aminopyridine-coordinated ruthenium complex **29** in 82% yield after recrystallization (Figure 2.2a). The $^{31}$P NMR spectrum of complex **29** contained a single $^{31}$P resonance at 38 ppm, and the structure of **29** was determined by single-crystal X-ray diffraction. The Ru center in **29** is ligated by three $PEt_3$ ligands, one *O*-bound triflimide, and one $\kappa^2$-bound aminopyridine in an octahedral geometry (Figure 2.2c). The $^{31}$P NMR chemical shift of 38 ppm for complex **29** is distinct from that of the catalyst resting state (50 ppm).

Thus, we postulated that coordination of **1b** to the cationic ruthenium center sufficiently acidifies the N-H bonds to cause deprotonation of **29** by another equivalent of aminopyridine. To test this hypothesis, we treated complex **29** with an insoluble base ($K_3PO_4$). This reaction led to the

isolation of the Ru-amido complex **30** in 85% yield after recrystallization (Figure 2.2b). The $^{31}$P NMR spectrum of complex **30** consisted of a single sharp resonance at 51 ppm (e of Figure 2.1). The solid-state structure of complex **30** was determined by X-ray diffraction (Figure 2.2d). This complex adopts a square pyramidal geometry with an empty coordination site trans to a $PEt_3$ ligand.

The hydroamination of 1-dodecene by aminopyridine **1b** catalyzed by 5 mol % of the isolated complex **30** afforded the product **13a** in 65% yield in 48 hours. This result indicates that complex **30** is kinetically competent to be an intermediate in this hydroamination reaction. Furthermore, a broad resonance at 51 ppm, which matched that observed for the catalytic reaction initiated with **Ru-1**, was observed in the $^{31}$P NMR spectrum of the hydroamination reaction initiated with complex **30** as catalyst (f of Figure 2.1).

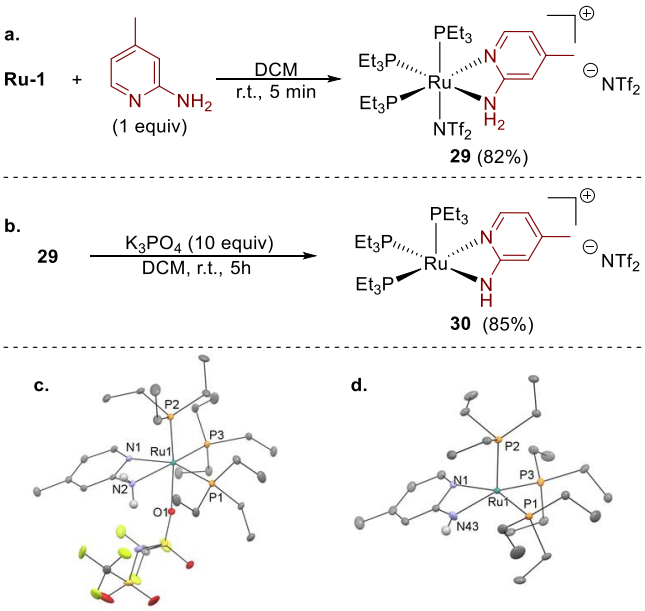


**Figure 2.2.** (a) Synthesis of complex **29**. (b) Synthesis of complex **30**. (c) Solid-state structure of complex **29** with ellipsoids set at 30% and selected hydrogen atoms and free triflimide anion omitted for clarity. (d) Solid-state structure of complex **30** with ellipsoids set at 30% and selected hydrogen atoms and free triflimide anion omitted for clarity.

These data suggest that complex **30** could be the resting state of the catalyst, but the resonance corresponding to isolated **30** is much sharper and slightly more downfield (0.9 ppm) than that of the major ruthenium complex in the catalytic system. We determined that this difference in line shape and chemical shift depends on the presence or absence of an excess of the aminopyridine; the $^{31}$P NMR signal of isolated **30** broadened and shifted slightly upfield in the presence of 20 equiv of aminopyridine **1b** at 80 °C (g of Figure 2.1).

To investigate the origin of this difference in line shape and chemical shift further, we conducted variable temperature NMR spectroscopy with a 20:1 mixture of aminopyridine **1b** and complex **30** (Figure 2.3). At -40 °C, the $^{31}$P NMR spectrum of the mixture contained three triplet resonances. A potential structure for the complex corresponding to the three triplet resonances is **31a** shown at the bottom of Fig 3. This structure contains an additional 2-aminopyridine occupying the sixth coordination site and a hydrogen bond to the amido ligand. The hydrogen-bonding interaction in **31a** is evidenced by the observation of a broad downfield proton resonance (14 ppm) in the $^{1}$H

NMR spectrum of this mixture. The integration of the three triplet resonances in the $^{31}P$ NMR spectrum decreased at higher temperatures, and we were unable to detect the triple resonances when the temperature of the mixture reached 40 °C, indicating that complex **31a** is a minor species in the catalytic reaction at 80 °C.

The chemical shift of the broad resonance corresponding to the major ruthenium complex at 80 °C migrated significantly upfield at lower temperature. The origin of this lineshape and change in chemical shift is not clear, but could result from hydrogen bonding between the amide ligand NH and the aminopyridine without coordination of the pyridine nitrogen to the metal as we suggest is present in complex **31b**. The chemical shift of this resonance lies further upfield in solutions containing higher concentrations of aminopyridine, implying that the resonance results from an equilibrium between **30** and an adduct formed between **30** and the aminopyridine that is distinct from complex **31a.** At the same time, the similarity in chemical shift between pure complex **30** and the resonance in the presence of aminopyridine at the concentration and 80°C temperature of the reaction implies that the major component in the catalytic reaction is complex **30.**

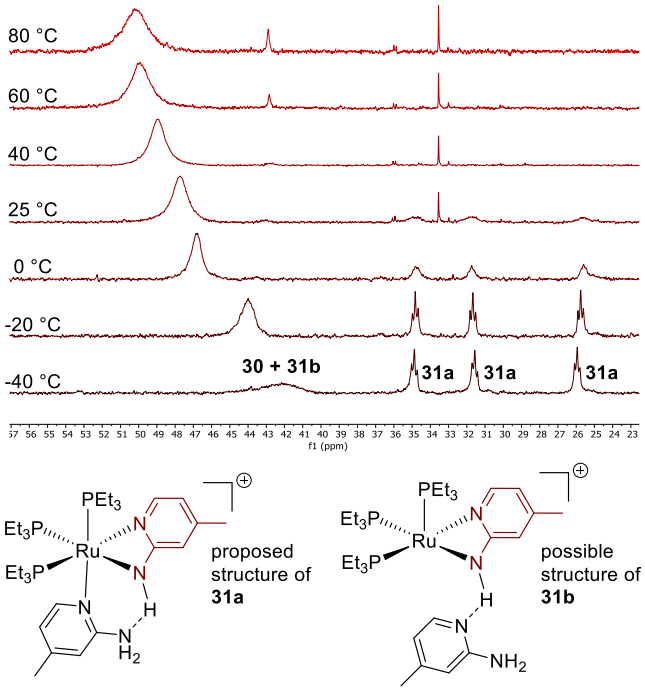


**Figure 2.3.** $^{31}P$ NMR spectra of the mixture of complex **30** and **1b** (20 equiv) at different temperature and possible structures for complex **31a** and **31b**.

**Kinetic Studies on Catalytic Hydroamination.** Kinetic experiments were conducted to gain further information on the mechanism of the hydroamination. Kinetic experiments with 1-dodecene as the substrate were complicated by the observation of alkene isomerization during the reaction. Therefore, we conducted kinetic studies with vinylcyclohexane, which did not undergo competing isomerization.

Initial rates of the hydroamination reaction were measured at a series of concentrations of vinylcyclohexane, aminopyridine **1b**, and catalyst **Ru-1** (See supporting information for details). Plots of initial rates against the concentration of the vinylcyclohexane, **1b,** and **Ru-1** are shown in Figures 2.4a-c. We found that the hydroamination reaction is first order in the concentration of

vinylcyclohexane, zero order in the concentration of **1b**, and first order in the concentration of **Ru-1**. The order in alkene and catalyst imply that these species react in the turnover-limiting step. The zero-order dependence of the reaction on the concentration of aminopyridine **1b** suggests that the hydroamination does not proceed by turnover-limiting nucleophilic attack of **1b** on the alkene in a Ru complex like **32** (Scheme 2.3 pathway a). Instead, the kinetic data are consistent with a migratory insertion of the alkene into the Ru–N bond of the Ru-alkene complex **32** to generate a Ru-alkyl complex **33** (Scheme 2.3, pathway b).

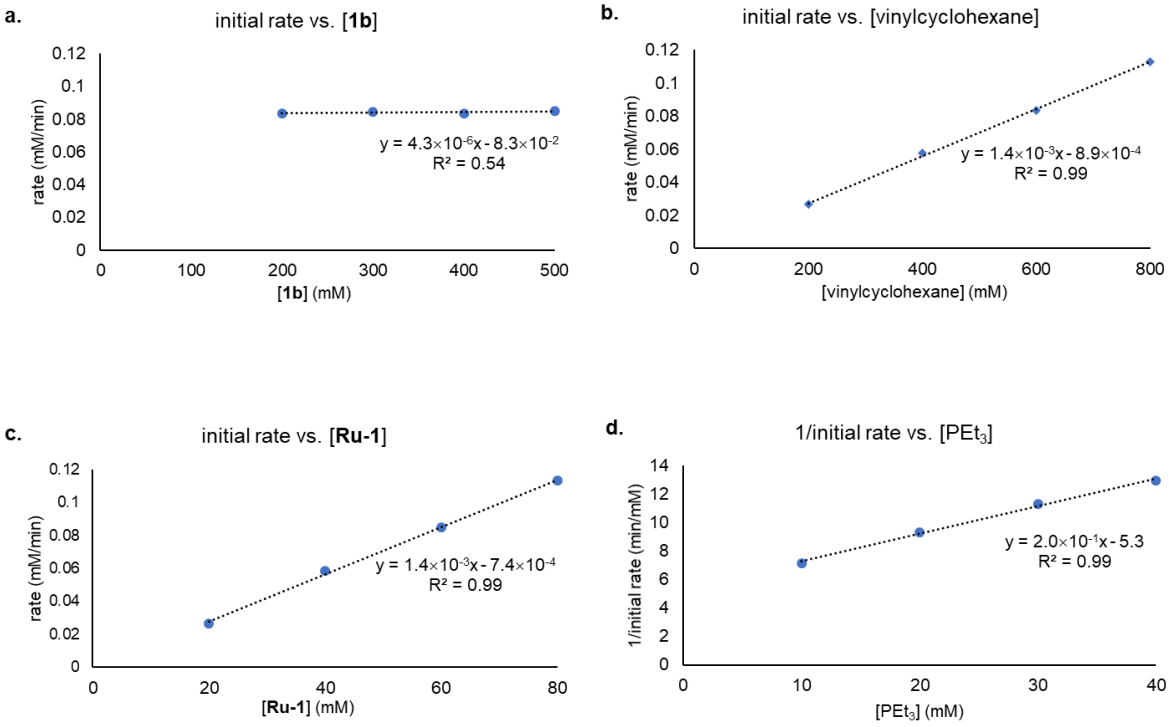


**Figure 2.4.** (a) Initial Rates of Product Formation as a Function of [**1b**]. (b) Initial Rates of Product Formation as a Function of [vinylcyclohexane]. (c) Initial Rates of Product Formation as a Function of [**Ru-1**]. (d) Initial Rates of Product Formation as a Function of [$PEt_3$].

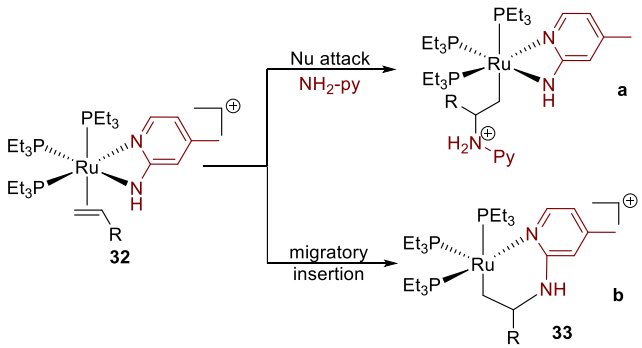


**Scheme 2.3. Possible pathways for the formation of the C–N bond.**

The effect of the concentration of $PEt_3$ on the rate of the catalytic hydroamination was also studied. Added $PEt_3$ inhibited the reaction, and a plot of 1/initial rate against the concentration of $PEt_3$ was linear (Figure 2.4d). To account for this observation, we considered two hypotheses. First, the

added $PEt_3$ could inhibit the reaction by reversibly coordinating to complex **30** to generate complex **34** (Scheme 2.4a). Second, reversible dissociation of $PEt_3$ from complex **30** could generate the catalytically active complex **35** (Scheme 2.4b). To test these hypotheses, variable temperature NMR spectroscopy analysis was conducted with a 5:1 mixture of $PEt_3$ and complex **30**. Full conversion of **30** to complex **34** was observed by $^{31}P$ NMR spectroscopy of this mixture at -20 °C (see supporting information for details). In addition, the association of $PEt_3$ to complex **30** was computed by DFT to be exergonic by 0.3 kcal/mol at -20 °C, whereas the dissociation of $PEt_3$ from complex **30** was calculated to be endergonic by an energy (31.5 kcal/mol at 80 °C) that exceeds the entire 30.5 kcal/mol barrier for the reaction determined from the experimental rates. Therefore, we conclude that the origin of the inhibition of the hydroamination by added $PEt_3$ results from the reversible coordination of $PEt_3$ to complex **30** to form the inactive tetraphosphine complex **34** (Scheme 2.4a).

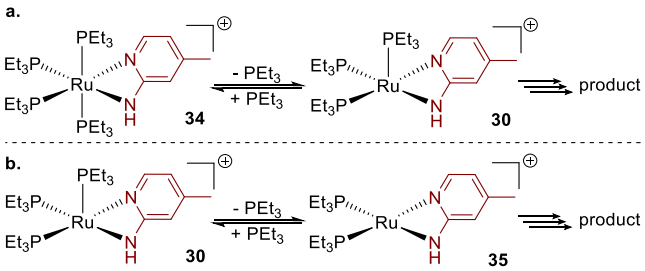


**Scheme 2.4. Two hypotheses to explain the rate inhibition by additional $PEt_3$.**

**Studies on the Pathway for the Formation of the product from Ru-alkyl Complex 33.** To elucidate the pathway by which the product of this hydroamination reaction was formed from the Ru-alkyl complex **33**, the hydroamination of vinylcyclohexane was performed with **1b**-$d_2$ under the standard catalytic conditions (Table 2.4). Deuterium incorporation was observed at four different positions in the product **17a**-$d_n$. The ratios of the percentage of deuterium incorporation at the $H_a$ and $H_b$ positions were 1:1 at various time points during the reaction (Table 2.4), and the accumulation of deuterium into the starting vinylcyclohexane was not observed.

The results of this labeling study are consistent with the pathway in Scheme 2.5. By this pathway, coordination and migratory insertion of the alkene occurs to form Ru-alkyl complex **33**-*d* from the catalyst resting state **30**-*d*, after which complex **33**-*d* undergoes a subsequent β-hydride elimination to generate the ruthenium-hydride species **44** ([Ru–H]) (Figure 2.5a) and enamine **36**-*d*. The enamine **36**-*d* would then undergo tautomerization catalyzed by protonated aminopyridine, which was formed during the generation of the catalyst resting state **30**-*d*. This tautomerization forms the *β*-deuterated imine **37**-*d*. Intramolecular H–D exchange between the Ru–H position and bound aminopyridine in complex **44** would generate a ruthenium-deuteride. Subsequent reduction of imine **37**-*d* by complex **44** containing a Ru–D bond would generate the final hydroamination product **17a**-$d_n$, containing an enhanced level of deuterium at the $H_\alpha$ and $H_\beta$ positions. Because the tautomerization step and H/D exchange of the hydride position of complex **44** occur by reversible proton transfers involving the amino group in **1b**, the amount of deuterium in the $H_a$ and $H_b$ positions of the product are equal to each other. Furthermore, the observation of the incorporation of deuterium at the alpha position of the product **17a**-$d_n$ provides evidence against a nucleophilic attack of **1b** on the metal-bound alkene complex, like **32** (Scheme 2.3 pathway a) because the coordinative saturation of the complex formed after a nucleophilic attack of the aminopyridine would disfavor *β*-hydrogen elimination.

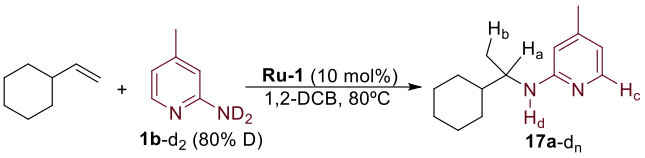


| Reaction time | %D at the $H_a$ position[a] | %D at the $H_b$ position[a] |
|---|---|---|
| 24h | 29% | 29% |
| 36h | 31% | 32% |
| 48h | 29% | 28% |

[a]%D incorporation = moles of D atoms / moles of product.

**Table 2.4. Hydroamination of vinylcyclohexane with 1b-$d_2$.[a]**

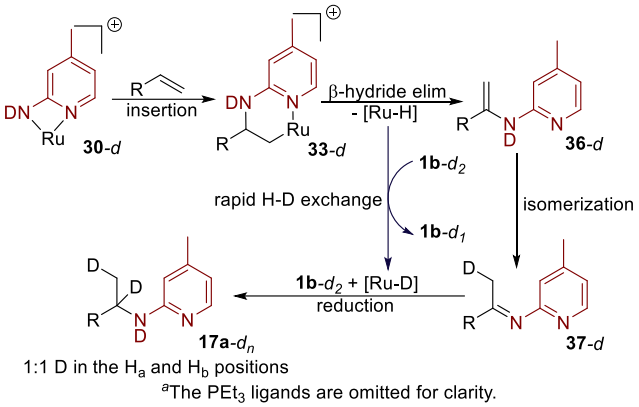


[a]The $PEt_3$ ligands are omitted for clarity.

**Scheme 2.5. Proposed pathway for the formation of hydroamination product from 33.[a]**

To investigate the pathway for the formation of the hydroamination product further**,** we conducted the hydroamination of 1-dodecene with **1b** in the presence of 1 equiv of acetone. 2-Dodecanone **38** and the product from reductive amination of acetone **39** were observed, along with the hydroamination product **13a** (Scheme 2.6). The formation of **38** and **39** imply that the reaction occurs through an imine intermediate. Dodecyl enamine **40** is generated by migratory insertion of the alkene into the amidopyridine complex **30** and *β*-hydride elimination from metallacycle **33**. A subsequent tautomerization of the enamine **40** forms dodecyl imine **42**. Isopropyl imine **41** and water are generated by reversible condensation of acetone with aminopyridine **1b**. The imines **41** and **42** undergo competitive reduction to yield amines **13a** and **39** respectively. The portion of imine **42** that is not reduced is hydrolyzed to give ketone **38**, which is detected by $^1$H NMR spectroscopy.

To elucidate the identity of the proposed [Ru–H] intermediate that would result from *β*-H elimination of the aminoalkyl intermediate, we exposed complex **30** to 1 atm of $H_2$ (Figure 2.5a). Complex **43**, which resulted from the overall addition of $H_2$ across the Ru–N bond of complex **30** and coordination of $H_2$ was observed. The structure of this complex was deduced by the observation of two distinct ruthenium hydride signals in the $^1$H NMR spectrum. The $H_2$ ligand in **43** was slowly replaced by $N_2$ in a nitrogen atmosphere to afford complex **44**, which was characterized by single-crystal X-ray diffraction (Figure 2.5a,b).

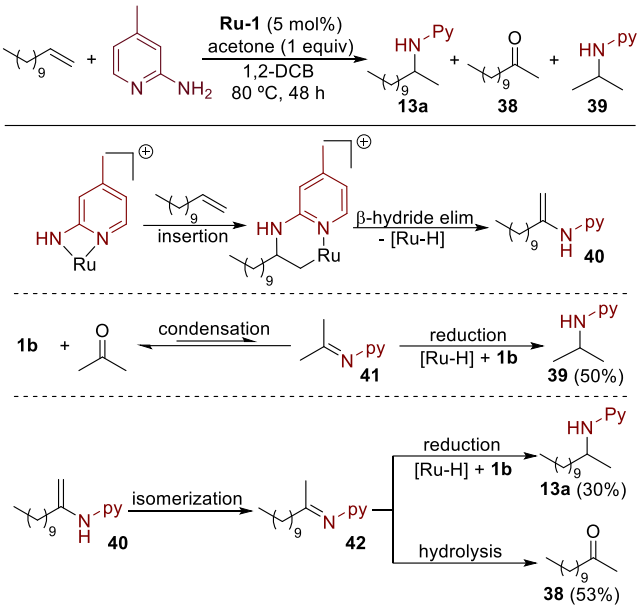


**Scheme 2.6. Hydroamination of 1-dodecene in the presence of acetone.**

Under an atmosphere of $H_2$, the imine generated *in situ* from ketone **38** and aminopyridine **1b** underwent hydrogenation to form amine **13a** catalyzed by the amido complex **30** in 95% yield (Figure 2.5c). This result indicates that the hydridoruthenium complex **43** that would form *in situ* during the catalytic process from complex **30** and $H_2$ catalyzes the reduction of imines, such as **41** that would be formed in the catalytic process, to generate the final amine **13a**.

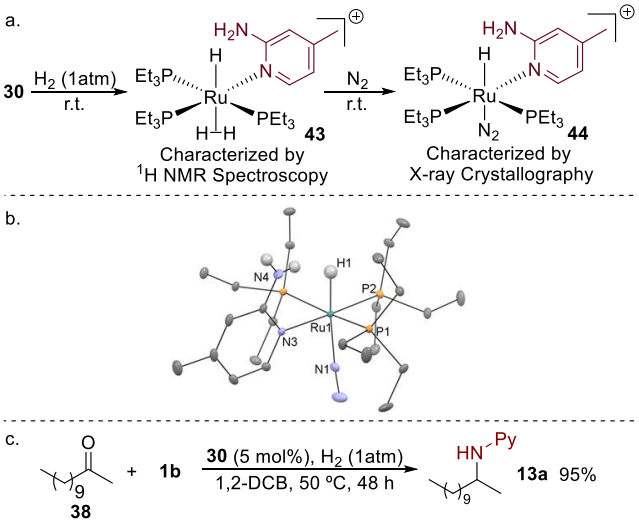


**Figure 2.5.** (a) Synthesis the [Ru–H] intermediate **44**. (b) Solid-state structure of complex **44** with ellipsoids set at 30% and selected hydrogen atoms and free triflimide anion omitted for clarity. (c) Catalytic imine hydrogenation with complex **30** in the presence of $H_2$.

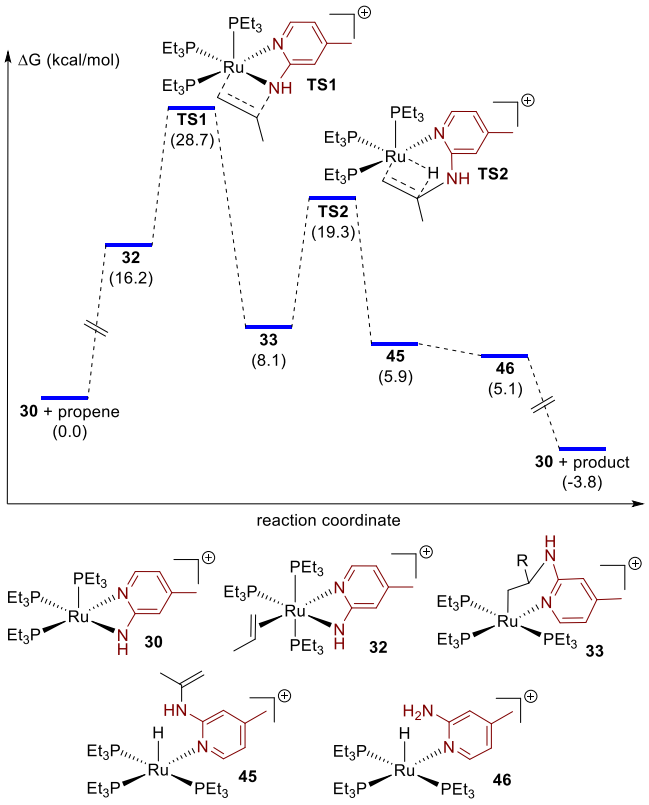


**Figure 2.6.** DFT computational Studies on the Ruthenium-Catalyzed Hydroamination of Terminal Alkenes. Free energies in kcal/mol at 80 °C are provided in parentheses.

**DFT Computational Studies of the Proposed Catalytic Cycle for the Ruthenium-Catalyzed Hydroamination of Terminal Alkenes.** Our mechanistic experiments imply that this Ru-catalyzed hydroamination of terminal alkenes with 2-aminopyridine occurs by coordination of alkene to the catalyst resting state **30**, followed by migratory insertion of the alkene into the Ru–N bond, *β*-hydride elimination to generate an enamine, tautomerization of the enamine to an imine, and reduction of the imine to afford to amine product. Our kinetic studies indicate that the alkene and the ruthenium catalyst are involved in the turnover-limiting step. Hydrogenation of the imine cannot be turnover limiting because this step occurs faster than the overall hydroamination of the alkene (Figure 2.5c). To determine whether migratory insertion or *β*-hydride elimination following a reversible insertion process is turnover-limiting, DFT computations were conducted on the oxidative amination portion of the mechanism.

This mechanism was calculated for the hydroamination of propene, as a model alkene, with aminopyridine **1b**. An energy diagram for this process is shown in Figure 2.6. The coordination of propene to the catalyst resting state **30** was calculated to endergonic be 16.2 kcal/mol. The free-energy barrier to the elementary migratory insertion step of propene into the Ru–N bond was computed to be 12.5 kcal/mol (**32** to **TS1**). These energies lead to an overall barrier for coordination and insertion of 28.7 kcal/mol. The metallacycle **33** formed from insertion was computed to lie 8.1 kcal/mol uphill of the starting complex and free propene, and the barrier for *β*-hydride elimination from complex **33** was computed to be 11.2 kcal/mol (**33** to **TS2**). Thus, the transition state for the β-hydride elimination lies 19.3 kcal/mol uphill of the starting species and nearly 10 kcal/mol below the transition state for migratory insertion. The oxidative amination

portion of the hydroamination reaction was calculated to be uphill by 5.9 kcal/mol, and the overall hydroamination was computed to be exergonic by 3.8 kcal/mol. These calculations strongly suggest that the combination of coordination of alkene and migratory insertion of the alkene into the Ru–N bond is irreversible and the turnover-limiting portion of this hydroamination reaction.

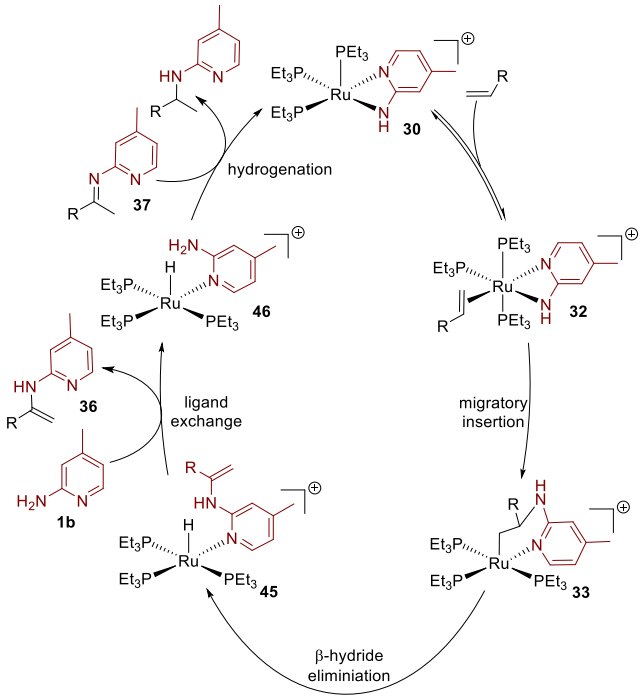


**Figure 2.7.** Proposed Catalytic Cycle for the Ruthenium-Catalyzed Hydroamination of Terminal Alkenes.

The results of our mechanistic investigation are summarized in Figure 7. By this mechanism, the major component of the catalyst resting state, complex **30**, is formed by coordination of the aminopyridine **1b** to the ruthenium precatalyst **Ru-1**, followed by deprotonation of the aminopyridine ligand by another molecule of **1b**. The first step of the catalytic cycle, then, involves reversible coordination of the alkene to **30** to form the alkene complex **32**. Turnover-limiting migratory insertion of the alkene into the Ru-N bond of **32** then affords the Ru-alkyl intermediate **33**, which undergoes *β*-hydride elimination to generate the hydridoruthenium enamine intermediate **45**. Subsequent exchange of the enamine for aminopyridine **1b** in intermediate **45** forms the hydridoruthenium aminopyridine intermediate **46** and free enamine **36**. Eliminated enamine **36** undergoes tautomerization to generate imine **37**, which is computed to be more stable thermodynamically than enamine **36** by 3.3 kcal/mol and would be expected to react with amine-ligated ruthenium hydride complexes by a metal-ligand bifunctional mechanism.[40] Thus, reduction of imine **37** by intermediate **46** affords the final hydroamination product.

The proposed catalytic cycle is supported by a large body of experimental data. The catalyst resting state **30** was identified by $^{31}$P NMR spectroscopy and an independent synthesis. The kinetic measurements support a mechanism by which migratory insertion of the alkene into the Ru-N bond occurs, rather than a potential nucleophilic attack on a coordinated alkene by the amine. Deuterium labeling experiments indicate that the Ru-alkyl complex **33** undergoes *β*-hydride elimination, rather than a potential direct protonation by **1b**, and hydroamination reactions conducted with

added acetone imply the formation of an imine intermediate. Independent studies of the reactivity of the ruthenium-hydride complex resulting from *β*-hydride elimination with the imine resulting from tautomerization of the initially formed enamine show that the reduction of the imine is much faster than the overall catalytic cycle. Finally, DFT calculations indicate that the turnover-limiting step of the reaction is migratory insertion of the alkene into a ruthenium amido complex, rather than β-hydride elimination from a reversibly formed insertion product.

## 2.3 Conclusion

Ruthenium-catalyzed Markovnikov hydroamination of unactivated and activated terminal alkenes occurs with 2-aminopyridine as a surrogate for ammonia with a stoichiometric amount of alkene by an unusual pathway for hydroamination. This process constitutes a rare example of hydroamination of alkenes with ruthenium enabled by a combination of a cationic metal center and a carefully designed aminopyridine as an ammonia surrogate. This combination facilitates the deprotonation of the aminopyridine coordinated to an electron-deficient ruthenium center, the migratory insertion of the alkene into the strained four-member ruthenacycle, and the cooperative reduction of the imine intermediate generated from *β*-hydrogen elimination to lead to an overall redox-neutral addition process. This reaction proceeds with a variety of terminal alkenes to afford the amine products under conditions with the alkene as limiting reagent. A combination of experimental and computational mechanistic studies reveals that this hydroamination reaction occurs by turnover-limiting migratory insertion of the alkene into the Ru–N bond, followed by *β*-hydride elimination to generate an enamine, tautomerization of the enamine to an imine, and reduction of the imine by the hydridoruthenium aminopyridine complex to generate the amine product. This pathway implies that an enantioselective process could be developed if the step involving reduction of the imine intermediate can be rendered enantioselective. Studies to achieve such a process by this mechanism are ongoing.

## 2.4 Experimental

### 2.4.1. General Information

All manipulations were performed in a nitrogen-filled glovebox or on a Schlenk manifold unless otherwise noted. Glassware was dried at 150 °C for at least 4 hours before use. Pentane, $Et_2O$, THF and hexane were collected from a solvent purification system containing a 0.33 m column of activated alumina under nitrogen. Diisopropyl ether, 1,2-dichlorobenzene and olefin substrates were degassed and subjected to 4 Å molecular sieves for at least 12 hours prior to use. Anhydrous methanol was purchased from a commercial source, degassed and stored in the glovebox before use. *cis*-$[Ru(DMSO)_4Cl_2]$[41] and $[Ru_2(PEt_3)_6(OTf)_3](OTf)$[34] were prepared following published procedures. All other reagents were purchased from commercial suppliers, stored in the glove box and used as received.

$^1H$, $^{13}C$, $^{19}F$ and $^{31}P$ NMR spectra were recorded on a Bruker 400, 500 or 600 MHz spectrometer. $^1H$ chemical shifts are reported in parts per million relative residual protiated solvent as a reference ($CHCl_3$ in $CDCl_3$: δ 7.27 ppm; $CH_nD_{2-n}$ in $CDCl_2$: δ 5.32 ppm). $^{13}C$ chemical shifts are reported in parts per million relative to the deuterated solvent as a reference. $^{31}P$ chemical shifts were reported in parts per million relative to an 85% $H_3PO_4$ external standard. $^{19}F$ chemical shifts were reported in parts per million relative to an external standard of $CFCl_3$. Elemental analyses were performed at the Microanalytical Facility at the University of California, Berkeley. X-ray crystal structures were obtained at the Small Molecule X-ray Crystallography Facility at the University of California,

Berkeley. High-resolution mass spectra were obtained on a high-resolution mass spectrometer at the QB3/Chemistry Mass Spectrometry Facility at UC Berkeley and on the Perkin Elmer AxION2 TOF MS operated by the LBNL Catalysis Facility.

### 2.4.2. Procedures for the Synthesis of Ruthenium Complexes

#### *cis*-$Ru(PMe_3)_4Cl_2$

*cis*-$[Ru(DMSO)_4Cl_2]$ (0.24 g, 0.50 mmol), $PMe_3$ (1.0M in toluene, 2.2 mL, 2.2 mmol, 4.4 equiv), and trifluoroethanol (2.0 mL) were combined and heated at 100 ˚C for 2 hours with stirring. Over this period, all the material dissolved, and the supernatant turned bright orange. The reaction was allowed to cool to room temperature, and the solvent was removed under vacuum. The resulting powder was recrystallized using DCM and $^{i}Pr_2O$ to yield light yellow crystals. The resulting crystals were rinsed with $^{i}Pr_2O$ (2 x 5.0 mL) and pentane (5.0 mL) and dried under high vacuum. Yield = 0.21 g (87%). $^1$H NMR (600 MHz, chloroform-*d*) δ 1.56 (t, *J* = 3.2 Hz, 36H), 1.47 (m, 36H). $^{31}$P NMR (243 MHz, chloroform-d) δ 20.05. Anal. Calc'd C:30.26 H:7.62 Found C:30.45 H:7.84.

#### $[Ru_2(PEt_3)_6Cl_3][Cl]$

*cis*-$[Ru(DMSO)_4Cl_2]$ (3.0 g, 6.2 mmol), $PEt_3$ (3.0 mL, 20 mmol, 3.3 equiv), and MeOH (10 mL) were combined and heated at 65 ˚C for 90 minutes with stirring. Over this period, all the material dissolved, and the supernatant turned green and then bright orange. The reaction was allowed to cool to room temperature and the solvent was removed under vacuum. The resulting powder was recrystallized using DCM and $Et_2O$ to yield light yellow crystals. The resulting crystals were rinsed with $Et_2O$ (2 x 10 mL) and pentane (10 mL) and dried under high vacuum. Yield = 2.9 g (88%). $^1$H NMR (400 MHz, chloroform-*d*) δ 1.92 (m, 36H), 1.21 (m, 54H). $^{31}$P NMR (162 MHz, chloroform-*d*) δ 34.06. Anal. Calc'd C:41.07 H:8.62 Found C:41.13 H:8.46.

#### $[Ru_2(P^nPr_3)_6Cl_3][Cl]$

*cis*-$[Ru(DMSO)_4Cl_2]$ (0.24 g, 0.50 mmol), $PPr_3$ (0.31 mL, 0.25 g, 1.6 mmol, 3.1 equiv), and a magnetic stir bar were added to a Schlenk flask in a $N_2$ filled glove box. Outside the glove box, degassed $H_2O$ (0.80 mL) was added via syringe under nitrogen pressure. The Schlenk flask was sealed and heated at 100 ˚C for 2 hours with vigorous stirring. The reaction turned green and the product precipitated as a yellow solid. The reaction was allowed to cool to room temperature, and the yellow precipitation was collected by filtration. The yellow solid was rinsed with $H_2O$ (3 x 5.0 mL) and hexanes (3 x 5.0 mL) and dried under high vacuum. Yield = 0.28 g (86%). $^1$H NMR (600 MHz, chloroform-*d*) δ 1.76 (m, 36H), 1.57 (m, 36H), 0.99 (t, *J* = 7.2 Hz, 54H). $^{31}$P NMR (243 MHz, chloroform-*d*) δ 29.16. Anal. Calc'd C:49.69 H:9.73. Found C:49.87 H:9.60.

#### $[Ru_2(PMePh_2)_6Cl_3][Cl]$

*cis*-[Ru(DMSO)$_4$Cl$_2$] (0.63 g, 1.3 mmol), PPh$_2$Me (0.80 mL, 0.86 g, 4.3 mmol, 3.3 equiv), and MeOH (1.0 mL) were combined and stirred at room temperature for 90 minutes. The mixture was then placed in the freezer (-30 ˚C) overnight and the precipitation was collected by filtration, rinsed with Et$_2$O (2 x 5.0 mL), and dried under vacuum. Combined yield = 0.83 g (83%). $^1$H NMR (600 MHz, chloroform-$d_1$) δ 7.27 (t, J = 7.5 Hz, 12H), 7.07 (m, 24H), 7.02 (m, 24H), 1.82 (m, 18H). $^{13}$C NMR (151 MHz, chloroform-*d*) δ 136.70 (m), 132.93, 129.58, 127.95, 19.88 (m). $^{31}$P NMR (243 MHz, chloroform-*d*) δ 18.93. Anal. Calc'd C:60.63 H:5.09 Found C:60.34 H:5.18.

**_cis_-Ru(Et$_2$P(CH$_2$)$_4$PEt$_2$)$_2$Cl$_2$**

*cis*-[Ru(DMSO)$_4$Cl$_2$] (0.15 g, 0.31 mmol), Et$_2$P(CH$_2$)$_4$PEt$_2$ (0.16 g 0.68 mmol, 2.2 equiv), and MeOH (1.0 mL) were combined and heated at 65 ˚C for 14 hours with stirring. Over this period, all the material dissolved, and the reaction turned bright red and then orange. The mixture was allowed to cool to room temperature and layered with $^i$Pr$_2$O (19 mL) to yield yellow crystals. The crystals were collected by filtration, rinsed with $^i$Pr$_2$O (2 x 5.0 mL) and pentane (1 mL), and dried under high vacuum. Yield = 0.17 g (83%). $^1$H NMR (600 MHz, methylene chloride-$d_2$) δ 2.20-2.75 (m, 8H), 1.45-2.05 (m, 20H), 0.95-1.35 (m, 28H). $^{31}$P NMR (243 MHz, CD$_2$Cl$_2$) δ 32.27 (t, J = 29 Hz), 4.62 (t, J = 29 Hz). Anal. Calc'd C:45.00 H:8.81 Found C:45.33 H:9.05.

**[Ru$_2$(N(CH$_2$PEt$_2$)$_3$)$_2$Cl$_3$][Cl]**

*cis*-[Ru(DMSO)$_4$Cl$_2$] (0.17 g, 0.35 mmol), N(CH$_2$PEt$_2$)$_3$ (0.11 g, 0.35 mmol, 1.0 equiv), MeOH (1 mL), and a magnetic stir bar were combined and heated at 65 ˚C for 5 hours with stirring. The mixture was allowed to cool to room temperature and layered with $^i$Pr$_2$O (12 mL). The yellow microcrystalline precipitation was collected by filtration, rinsed with $^i$Pr$_2$O (2 x 5.0 mL) and dried under high vacuum. Yield = 83 mg (71%). $^1$H NMR (600 MHz, chloroform-*d*) δ 2.87 (s, 12H), 2.19 (h, *J* = 9.8, 9.1 Hz, 12H), 1.80 (dt, *J* = 15.1, 7.5 Hz, 12H), 1.18 (p, *J* = 7.2 Hz, 36H). $^{31}$P NMR (243 MHz, chloroform-*d*) δ 28.08. Anal. Calc'd C:36.37 H:7.33 N:2.83 Found C:36.53 H:7.19 N:2.64.

**Ru(PEt$_3$)$_3$(NTf$_2$)$_2$ (Ru-1)**

[Ru$_2$Cl$_3$(PEt$_3$)$_6$][Cl] (0.38 g, 0.36 mmol), AgNTf$_2$ (0.56 g, 1.4 mmol, 4.0 equiv) and DCM (5.0 mL) were combined and stirred at room temperature for 3 hours. The mixture turned red and orange precipitation was formed during the reaction. The mixture was then filtered, and the solvent was removed under vacuum. The resulting orange solid was recrystallized with DCM and $^i$Pr$_2$O at -35 ˚C, washed with $^i$Pr$_2$O (2 x 5.0 mL) and dried under high vacuum. Yield = 0.65 g (89%). $^1$H NMR (400 MHz, Methylene Chloride-d$_2$) δ 1.91 (m, 18H), 1.24 (m, 27H). $^{31}$P NMR (162 MHz, Methylene Chloride-d$_2$) δ 50.83. Anal. Calc'd C:26.01 H:4.47 N:2.76 Found C:25.91 H:4.49 N:2.70. The identity of the product was confirmed by x-ray crystallography.

### 2.4.3. Development of Reaction Conditions

**Preparation of ruthenium complexes for *in situ* examination of catalytic activity**

The complexes **Ru-1** to **Ru-6** were generated for in situ for the examination of catalytic activity for convenience. To generate the ruthenium triflimide complex from the corresponding ruthenium chloride precursor *in situ*, ruthenium chloride complex (0.020 mmol for dimeric complex or 0.040 mmol for monomeric complex), $AgNTf_2$ (31 mg, 0.080 mmol, 2.0 equiv relative to [Ru]), trifluoroethanol (0.50 mL), and a magnetic stir bar were combined in a 1 dram vial. The vial was capped and heated at 80 ˚C for 2 h with stirring and then allowed to cool to room temperature. The solution was filtered, and the volatile materials were evaporated using high vacuum to form a residue. This residue was then triturated with $^{i}Pr_2O$ and dried. The purity and identity of the ruthenium triflimide complex was verified by NMR spectroscopy.

**Conditions for the examination of catalysts for hydroamination of alkenes**

1-dodecene (0.20 mmol, 44 μL, 34 mg), 2-amino-5-methylpyridine (0.20 mmol, 22 mg), ruthenium complex (0.010 mmol, 5.0 mol % [Ru]), and solvent (60 μL) were combined with a magnetic stir bar in a one-dram vial to form a solution. The vial threads were wrapped with 1 layer of Teflon tape and the resulting mixture was heated at 80 ˚C with stirring for 48 hours. The reaction was allowed to cool to room temperature, and yields were determined by $^1$H NMR spectroscopy using 1,3,5-trimethoxybenzene as the internal standard.

**2.4.4. Procedures for the Catalytic Hydroamination Reactions**

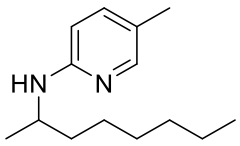


**5-methyl-*N*-(octan-2-yl)pyridine-2-amine (2a)**

1-Octene (31 μL, 23 mg, 0.20 mmol), 2-amino-5-methylpyridine (22 mg, 0.20 mmol), and $Ru(PEt_3)_3(NTf_2)_2$ (10 mg, 0.010 mmol, 5.0 mol%) were combined with DCB (60 μL) and a magnetic stir bar in a one dram vial. The vial threads were wrapped with 1 layer of Teflon tape and the resulting mixture was heated at 80 ˚C with stirring for 48 hours. The reaction was allowed to cool, and all of the volatile materials were evaporated. The crude product was purified by silica gel chromatography, eluting with 15% ethyl acetate in hexanes. Yield = 28 mg (62%). $^1$H NMR (600 MHz, chloroform-*d*) δ 7.88 (s, 1H), 7.23 (dd, J = 8.4, 2.2 Hz, 1H), 6.28 (d, J = 8.4 Hz, 1H), 4.16 (d, J = 8.1 Hz, 1H), 3.67 (m, 1H), 2.16 (s, 3H), 1.57 – 1.24 (m, 10H), 1.17 (d, J = 6.4 Hz, 3H), 0.87 (t, J = 6.9 Hz, 3H). $^{13}$C NMR (126 MHz, chloroform-*d*) δ 156.8, 147.8, 138.58, 121.2, 106.4, 47.5, 37.4, 32.0, 29.5, 26.2, 22.8, 21.1, 17.5, 14.2. GC-MS (EI+): 220 (M), 205 (M-$CH_3$), 135 ([N-ethyl-5-methylpyridin-2-amine]$^{\bullet}$).

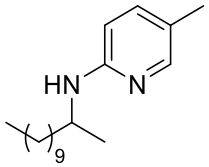


**5-methyl-*N*-(dodecan-2-yl)pyridine-2-amine (3a)**

1-Dodecene (44 μL, 34 mg, 0.20 mmol), 2-amino-5-methylpyridine (22 mg, 0.20 mmol), and $Ru(PEt_3)_3(NTf_2)_2$ (10 mg, 0.010 mmol, 5.0 mol%) were combined with DCB (60 μL) and a magnetic stir bar in a one dram vial. The vial threads were wrapped with 1 layer of Teflon tape and the resulting mixture was heated at 80 ˚C with stirring for 48 hours. The reaction was allowed to cool, and all of the volatile materials were evaporated. The crude product was purified by silica gel chromatography, eluting with 15% ethyl acetate in hexanes. Yield = 35 mg (63%). $^1$H NMR (600 MHz, chloroform-*d*) δ 7.87 (m, 1H), 7.21 (dd, *J* = 8.5, 2.4 Hz, 1H), 6.27 (d, *J* = 8.4 Hz, 1H), 4.21 (d, *J* = 8.6 Hz, 1H), 3.66 (dh, *J* = 8.5, 6.4 Hz, 1H), 2.14 (s, 3H), 1.51 (dddd, *J* = 12.9, 10.0, 6.5, 5.2 Hz, 1H), 1.44 (ddt, *J* = 12.9, 9.5, 6.0 Hz, 1H), 1.39 – 1.31 (m, 2H), 1.30 – 1.22 (m, 14H), 1.16 (d, *J* = 6.4 Hz, 3H), 0.87 (t, *J* = 7.0 Hz, 3H). $^{13}$C NMR (151 MHz, chloroform-*d* ) δ 156.8, 147.9, 138.4, 138.4, 121.0, 106.3, 47.4, 37.4, 32.0, 29.8, 29.7, 29.4, 26.2, 22.8, 21.1, 17.4, 14.2, 14.20. GC-MS (EI+): 276 (M), 261 (M-$CH_3$), 135 ([N-ethyl-5-methylpyridin-2-amine]$^\bullet$).

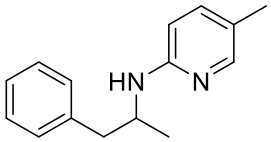


**5-methyl-*N*-(1-phenylpropan-2-yl)pyridine-2-amine (4a)**

Allylbenzene (27 μL, 24 mg, 0.20 mmol), 2-amino-5-methylpyridine (22 mg, 0.20 mmol), and $Ru(PEt_3)_3(NTf_2)_2$ (10 mg, 0.010 mmol, 5.0 mol%) were combined with DCB (60 μL) and a magnetic stir bar in a one dram vial. The vial threads were wrapped with 1 layer of Teflon tape and the resulting mixture was heated at 80 ˚C with stirring for 48 hours. The reaction was allowed to cool, and all of the volatile materials were evaporated. The crude product was purified by silica gel chromatography, eluting with 15% ethyl acetate in hexanes. Yield = 30 mg (66%). $^1$H NMR (600 MHz, chloroform-*d*) δ 7.92 (s, 1H), 7.29 (t, *J* = 7.5 Hz, 2H), 7.24 (dd, *J* = 8.4, 2.4 Hz, 1H), 7.23 – 7.17 (m, 3H), 6.32 (d, *J* = 8.4 Hz, 1H), 4.24 (d, *J* = 8.6 Hz, 1H), 4.03 (dq, *J* = 8.7, 6.7 Hz, 1H), 2.92 (dd, *J* = 13.4, 5.1 Hz, 1H), 2.75 (dd, *J* = 13.4, 7.1 Hz, 1H), 2.17 (s, 3H), 1.16 (d, *J* = 6.5 Hz, 3H). $^{13}$C NMR (151 MHz, chloroform-*d*) δ 156.4, 148.1, 138.7, 138.5, 129.7, 128.4, 126.4, 121.6, 106.9, 48.3, 42.7, 20.3, 17.5. GC-MS (EI+): 226 (M), 211 (M-$CH_3$), 135 ([N-ethyl-5-methylpyridin-2-amine]$^\bullet$).

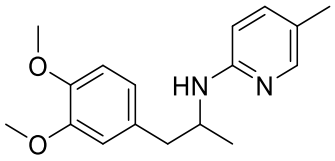


***N*-(1-(3,4-dimethoxyphenyl)propan-2-yl)-5-methylpyridin-2-amine (5a)**

3,4-Dimethoxy-allylbenzene (36 mg, 0.20 mmol), 2-amino-5-methylpyridine (22 mg, 0.20 mmol), and $Ru(PEt_3)_3(NTf_2)_2$ (10 mg, 0.010 mmol, 5.0 mol%) were combined with DCB (60 μL) were combined along with a magnetic stir bar in a one dram vial. The vial threads were wrapped with 1 layer of Teflon tape and the resulting mixture was heated at 80 ˚C with stirring for 48 hours. The reaction was allowed to cool, and all of the volatile materials were evaporated. The crude product was purified by silica gel chromatography, eluting with 40% ethyl acetate in hexanes. Yield = 30 mg (52%). $^1$H NMR (600 MHz, chloroform-*d*) δ 7.91 (d, *J* = 2.3 Hz, 1H), 7.23 (dd, *J* = 8.5, 2.4 Hz, 1H), 6.79 (d, *J* = 8.1 Hz, 1H), 6.72 (dd, *J* = 8.1, 2.0 Hz, 1H), 6.70 (d, *J* = 2.0 Hz, 1H), 6.29 (d, *J* = 8.4 Hz, 1H), 4.23 (d, *J* = 8.6 Hz, 1H), 4.01 (hept, *J* = 6.5 Hz, 1H), 3.85 (d, *J* = 10.2 Hz, 6H), 2.83 (dd, *J* = 13.5, 5.3 Hz, 1H), 2.72 (dd, *J* = 13.6, 6.8 Hz, 1H), 2.17 (s, 3H), 1.16 (d, *J* = 6.5 Hz, 3H). $^{13}$C NMR (151 MHz, chloroform-*d* ) δ 156.5, 148.9, 148.0, 147.7, 138.5, 131.2, 121.7, 121.6, 113.0, 111.3, 107.1, 56.1, 56.0, 48.4, 42.3, 20.5, 17.5. GC-MS (EI+): 286 (M), 135 ([N-ethyl-5-methylpyridin-2-amine]•).

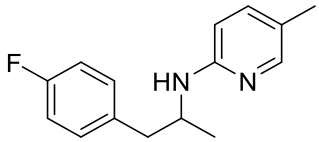


**5-methyl-*N*-(1-(4-fluoro-phenyl)propan-2-yl)pyridine-2-amine (6a)**

*p*-Fluoro-allylbenzene (27 mg, 0.20 mmol), 2-amino-5-methylpyridine (22 mg, 0.20 mmol), and $Ru(PEt_3)_3(NTf_2)_2$ (10 mg, 0.010 mmol, 5.0 mol%) were combined with DCB (60 μL) and a magnetic stir bar in a one dram vial. The vial threads were wrapped with 1 layer of Teflon tape and the resulting mixture was heated at 80 ˚C with stirring for 48 hours. The reaction was allowed to cool, and all of the volatile materials were evaporated. The crude product was purified by silica gel chromatography, eluting with 15% ethyl acetate in hexanes. Yield = 28 mg (56%). $^1$H NMR (600 MHz, chloroform-*d*) δ 7.92 (s, 1H), 7.24 (d, J = 8.4 Hz, 1H), 7.14 (dd, J = 8.0, 5.8 Hz, 2H), 6.96 (t, J = 8.6 Hz, 2H), 6.29 (d, J = 8.4 Hz, 1H), 4.14 (d, J = 7.8 Hz, 1H), 4.01 (m, 1H), 2.87 (dd, J = 13.7, 5.2 Hz, 1H), 2.74 (dd, J = 13.6, 6.9 Hz, 1H), 2.17 (s, 3H), 1.14 (d, J = 6.4 Hz, 3H). 13C NMR (101 MHz, chloroform-*d*) δ 162.9, 160.5, 156.3, 148.0, 138.5, 134.3 (d, *J* = 3.2 Hz), 131.1 (d, *J* = 7.7 Hz), 121.7, 115.2 (d, *J* = 21.1 Hz), 107.0, 48.3, 41.8, 20.3, 17.5. GC-MS (EI+): 244 (M), 229 (M-$CH_3$), 135 ([N-ethyl-5-methylpyridin-2-amine]•).

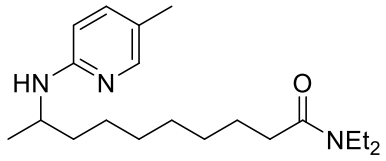


***N,N*-diethyl-9-((5-methylpyridin-2-yl)amino)decanamide (7a)**

9-decenoic acid diethyl amide (45 mg, 0.20 mmol), 2-amino-5-methylpyridine (22 mg, 0.20 mmol), and $Ru(PEt_3)_3(NTf_2)_2$ (10 mg, 0.010 mmol, 5.0 mol%) were combined with DCB (60 μL) and a magnetic stir bar in a one dram vial. The vial threads were wrapped with 1 layer of Teflon tape and the resulting mixture was heated at 80 ˚C with stirring for 48 hours. The reaction was allowed to cool, and all of the volatile materials were evaporated. The crude product was purified by silica gel chromatography, eluting with 40% ethyl acetate in hexanes. Yield = 44 mg (66%). $^1$H NMR (600 MHz, chloroform-d) δ 7.86 (s, 1H), 7.21 (dd, J = 8.4, 2.4 Hz, 1H), 6.27 (d, J = 8.4 Hz, 1H), 4.18 (d, J = 8.6 Hz, 1H), 3.65 (dq, J = 8.3, 6.2 Hz, 1H), 3.34 (q, J = 7.1 Hz, 2H), 3.27 (q, J = 7.1 Hz, 2H), 2.26 (d, J = 8.5 Hz, 1H), 2.24 (d, J = 8.5 Hz, 1H), 2.14 (s, 3H), 1.60 (p, J = 7.5 Hz, 2H), 1.50 (m, 1H), 1.43 (m, 1H), 1.39 – 1.21 (m, 8H), 1.14 (t, J = 6.5 Hz, 6H, 2 methyl groups), 1.08 (t, J = 7.1 Hz, 3H). $^{13}$C NMR (151 MHz, chloroform-*d*) δ 172.4, 156.8, 147.9, 138.5, 121.1, 106.4, 47.5, 42.1, 40.1, 37.3, 33.2, 29.6, 29.5, 29.5, 26.1, 25.6, 21.1, 17.6, 14.5, 13.2. GC-MS (EI+): 333 (M), 318 (M – Me), 135 ([N-ethyl-5-methylpyridin-2-amine]•).

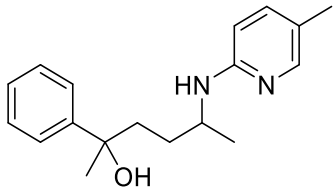


**5-((5-methylpyridin-2-yl)amino)-2-phenylhexan-2-ol (8a)**

2-phenylhex-5-en-2-ol (35 mg, 0.20 mmol), 2-amino-5-methylpyridine (22 mg, 0.20 mmol), and $Ru(PEt_3)_3(NTf_2)_2$ (20 mg, 0.020 mmol, 10 mol%) were combined with DCB (60 μL) and a magnetic stir bar in a one dram vial. The vial threads were wrapped with 1 layer of Teflon tape and the resulting mixture was heated at 80 ˚C with stirring for 48 hours. The reaction was allowed to cool, and all of the volatile materials were evaporated. The crude product was purified by silica gel chromatography, eluting with 40% ethyl acetate in hexanes. Yield = 24 mg (42%, 52:48 dr). The peaks derived from diastereomer 1 are labelled and those derived from diastereomer 2 are given without labels. $^1$H NMR (400 MHz, chloroform-*d*) δ 7.88 (s, 1H), 7.87 (s, 1H, diastereomer 1), 7.47 (d, *J* = 8.1 Hz, 4H, both diastereomers), 7.34 (d, *J* = 7.7 Hz, 2H, diastereomer 1), 7.32 (d, J = 7.7 Hz, 2H), 7.22 (m, 4H, both diastereomers), 6.26 (d, *J* = 8.5 Hz, 2H, both diastereomers), 4.11 (s, 2H, both diastereomers), 3.89 (h, *J* = 6.0 Hz, 2H, both diastereomers), 2.16 (s, 6H, both diastereomers), 1.91 (t, J = 7.5 Hz, 4H, both diastereomers) 1.52 (s, 6H, both diastereomers), 1.50 – 1.38 (m, 4H, both diastereomers), 1.25 (s, 2H, both diastereomers), 1.10 (d, *J* = 6.4 Hz, 6H, both diastereomers). $^{13}$C NMR (101 MHz, chloroform-*d*) δ 156.3 (diastereomer 1), 156.1, 148.8, 148.4 (diastereomer 1), 146.6 (diastereomer 1), 146.6, 139.0 (diastereomer 1), 138.9, 128.2 (diastereomer 1), 128.2, 126.4 (diastereomer 1), 126.4, 125.0, 125.0 (diastereomer 1), 121.35, 121.30 (diastereomer 1), 107.90, 107.71 (diastereomer 1), 74.87, 74.62 (diastereomer 1), 48.1,

47.5 (diastereomer 1), 39.8 (diastereomer 1), 39.7, 32.6 (diastereomer 1), 32.1, 31.4 (diastereomer 1), 31.1, 29.9, 21.7, 21.4 (diastereomer 1), 17.5 (diastereomer 1). GC-MS (EI+): 284 (M), 135 ([N-ethyl-5-methylpyridin-2-amine]•).

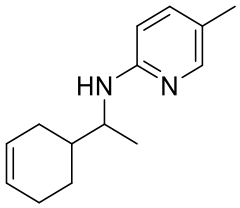


***N*-(1-(cyclohex-3-en-1-yl)ethyl)-5-methylpyridin-2-amine (9a)**

4-ethenyl-cyclohexene (26 µL, 22 mg, 0.20 mmol), 2-amino-5-methylpyridine (22 mg, 0.20 mmol), and $Ru(PEt_3)_3(NTf_2)_2$ (20 mg, 0.020 mmol, 10 mol%) were combined with DCB (60 µL) and a magnetic stir bar in a one dram vial. The vial threads were wrapped with 1 layer of Teflon tape and the resulting mixture was heated at 100 ˚C with stirring for 48 hours. The reaction was allowed to cool, and all of the volatile materials were evaporated. The crude product was purified by silica gel chromatography, eluting with 15% ethyl acetate in hexanes. Yield = 27 mg (61%). $^1$H NMR (600 MHz, chloroform-*d*) δ Major isomer: 7.88 (s, 1H, major), 7.22 (dd, *J* = 8.5, 2.4 Hz, 1H, major), 6.30 (d, *J* = 8.4 Hz, 1H, major), 5.67 (m, 2H, major), 4.19 (d, *J* = 9.3 Hz, 1H, major), 3.67 (h, J = 7 Hz, 1H, major), 2.20 – 1.98 (m, 3H, major), 2.16 (s, 3H, major), 1.88 – 1.83 (m, 2H, major), 1.69 (m, 1H, major), 1.28 (m, 1H, major), 1.16 (t, *J* = 6.4 Hz, 3H, major). Minor isomer: 7.88 (s, 1H), 7.22 (dd, *J* = 8.5, 2.4 Hz, 1H), 6.29 (d, *J* = 8.4 Hz, 1H), 5.67 (m, 2H), 4.24 (d, *J* = 9.3 Hz, 1H), 3.67 (h, J = 7 Hz, 1H), 2.20 – 1.98 (m, 3H), 2.16 (s, 3H), 1.90 (m, 1H), 1.78 (m, 1H), 1.71 (m, 1H), 1.36 (m, 1H), 1.16 (t, *J* = 6.4 Hz, 3H). $^{13}$C NMR (151 MHz, chloroform-*d*) δ 157.0, 156.9 (major), 147.8 (major), 147.8, 138.5 (major), 138.5, 127.2, 127.1 (major), 126.4 (major), 126.4, 121.1, 121.1 (major), 106.5, 106.4 (major), 51.3, 51.1 (major), 39.7, 39.5 (major), 28.3 (major), 28.0, 25.8, 25.5 (major), 25.4, 25.0 (major), 18.1, 18.0 (major), 17.4, 17.4(major). GC-MS (EI+): 216 (M), 201 (M – Me), 135 ([N-ethyl-5-methylpyridin-2-amine]•).

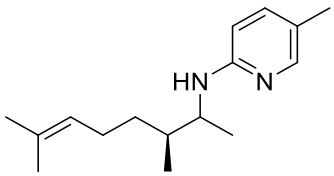


***N*-((*3S*)-3,7-dimethyloct-6-en-2-yl)-5-methylpyridin-2-amine (10a)**

(+)-β-Citronellene (28 mg, 0.20 mmol), 2-amino-5-methylpyridine (22 mg, 0.20 mmol), and $Ru(PEt_3)_3(NTf_2)_2$ (20 mg, 0.020 mmol, 10 mol%) were combined with DCB (60 µL) and a magnetic stir bar in a one dram vial. The vial threads were wrapped with 1 layer of Teflon tape and the resulting mixture was heated at 100 ˚C with stirring for 48 hours. The reaction was allowed to cool, and all of the volatile materials were evaporated. The crude product was purified by silica gel chromatography, eluting with 20% ethyl acetate in hexanes. Yield = 27 mg (54%, 7:4 dr). $^1$H

NMR (600 MHz, chloroform-*d*) $^{1}$H NMR (600 MHz, Chloroform-*d*) δ 7.87 (s, 1H, major), 7.87 (s, 1H, minor), 7.22 (d, *J* = 8.2 Hz, 1H, major), 7.22 (d, *J* = 8.2 Hz, 1H, minor), 6.28 (d, *J* = 8.5 Hz, 1H, major), 6.27 (d, J = 8.4 Hz, 1H, minor), 5.10 (ddt, *J* = 7.1, 5.7, 1.5 Hz, 1H, minor), 5.05 (tt, *J* = 7.2, 1.5 Hz, 1H, major), 4.31 (d, *J* = 9.1 Hz, 1H, minor), 4.27 (d, *J* = 9.1 Hz, 1H, major), 3.68 (dtd, *J* = 13.1, 6.6, 3.2 Hz, 1H, major), 3.63 (ddd, *J* = 8.9, 6.8, 5.0 Hz, 1H, minor), 2.15 (s, 3H, major), 2.15 (s, 3H, minor), 2.06 (m, 1H, minor), 2.04 (m, 1H, major), 1.96 (m, 1H, minor), 1.92 (m, 1H, major), 1.68 (s, 3H, minor), 1.67 (m, 1H, minor), 1.65 (m, 1H, major), 1.65 (s, 3H, major), 1.60 (s, 3H, minor), 1.57 (s, 3H, major), 1.48 (m, 1H, minor), 1.46 (m, 1H, major), 1.19 (m, 1H, minor), 1.18 (m, 1H, major), 1.12 (d, *J* = 6.6 Hz, 3H, major), 1.09 (d, *J* = 6.6 Hz, 3H, minor), 0.95 (d, *J* = 6.9 Hz, 3H, major), 0.89 (d, *J* = 6.8 Hz, 3H, minor). $^{13}$C NMR (151 MHz, chloroform-*d*) δ 157.0 (major), 156.8 (minor), 148.0 (minor), 147.9 (major), 138.5 (minor), 138.5 (major), 131.6 (minor), 131.5 (major), 124.8 (major), 124.7 (minor), 121.1 (minor), 121.1 (major), 106.3 (major), 106.3 (minor), 51.2 (minor), 51.1 (major), 37.5 (major), 36.9 (minor), 33.8 (minor), 32.8 (major), 26.0 (minor), 26.0 (major), 25.8 (minor), 25.8 (major), 17.8 (major), 17.8 (minor), 17.5 (major), 16.4 (minor), 15.5 (major), 14.5 (minor). GC-MS (EI+): 246 (M), 135 ([N-ethyl-5-methylpyridin-2-amine]•).

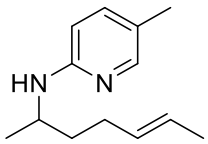


**(*E*)-*N*-(hept-5-en-2-yl)-5-methylpyridin-2-amine (11a)**

1,5-heptadiene (19 mg, 0.20 mmol), 2-amino-5-methylpyridine (22 mg, 0.20 mmol), and $Ru(PEt_3)_3(NTf_2)_2$ (10 mg, 0.010 mmol, 5.0 mol%) were combined with DCB (60 μL) and a magnetic stir bar in a one dram vial. The vial threads were wrapped with 1 layer of Teflon tape and the resulting mixture was heated at 80 ˚C with stirring for 48 hours. The reaction was allowed to cool, and all of the volatile materials were evaporated. The crude product was purified by silica gel chromatography, eluting with 15% ethyl acetate in hexanes. Yield = 27 mg (67%). $^{1}$H NMR (600 MHz, chloroform-*d*) δ 7.88 (s, 1H), 7.23 (d, J = 8.5 Hz, 1H), 6.28 (d, J = 8.3 Hz, 1H), 5.50 – 5.30 (m, 2H), 4.19 (bs, 1H), 3.69 (dt, J = 13.8, 7.0 Hz, 1H), 2.16 (s, 3H), 2.14 – 2.00 (m, 2H), 1.71 – 1.43 (m, 5H), 1.18 (d, J = 6.4 Hz, 3H). $^{13}$C NMR (151 MHz, chloroform-*d*) δ 156.6, 147.7, 138.3, 130.6, 125.2, 121.0, 106.2, 46.9, 37.0, 29.1, 20.8, 17.8, 17.3. GC-MS (EI+): 204 (M), 149 (M-butene), 135 ([N-ethyl-5-methylpyridin-2-amine]•).

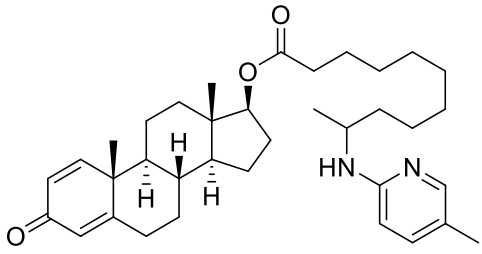


**Aminopyridyl boldenone undecylenate (12a)**

Boldenone undecylenate (91 mg, 0.20 mmol), 2-amino-5-methylpyridine (22 mg, 0.20 mmol), and $Ru(PEt_3)_3(NTf_2)_2$ (30 mg, 0.030 mmol, 15 mol%) were combined with DCB (60 μL) and a magnetic stir bar in a one dram vial. The vial threads were wrapped with 1 layer of Teflon tape and the resulting mixture was heated at 80 ˚C with stirring for 48 hours. The reaction was allowed to cool, and all of the volatile materials were evaporated. The crude product was purified by silica gel chromatography, eluting with a gradient of 20% to 60% ethyl acetate in hexanes. Yield = 38 mg (34%). Both diastereomers gave identical NMR and mass spectra. $^1$H NMR (500 MHz, chloroform-*d*) δ 7.87 (s, 1H), 7.23 (dd, 1H), 7.03 (d, *J* = 10.2 Hz, 1H), 6.28 (d, *J* = 8.5 Hz, 1H), 6.22 (dd, *J* = 10.1, 1.5 Hz, 1H), 6.06 (s, 1H), 4.58 (t, *J* = 8.5 Hz, 1H), 4.18 (d, *J* = 8.4 Hz, 1H), 3.66 (hept, *J* = 6.6 Hz, 1H), 2.46 (td, *J* = 13.4, 4.7 Hz, 1H), 2.36 (d, *J* = 12.6 Hz, 1H), 2.27 (t, *J* = 7.5 Hz, 2H), 2.15 (s, 3H), 1.94 (d, *J* = 14.2 Hz, 2H), 1.86 – 1.54 (m, 9H), 1.54 – 1.41 (m, 4H), 1.38-1.32 (m, 2H), 1.31 – 1.24 (m, 6H), 1.22 (s, 3H), 1.16 (d, *J* = 6.3 Hz, 3H), 1.10 – 0.98 (m, 4H), 0.85 (s, 3H). $^{13}$C NMR (151 MHz, chloroform-*d*) δ 186.4, 173.9, 168.9, 156.2, 155.8, 146.5, 139.3, 127.6, 124.0, 121.2, 106.8, 82.1, 52.3, 50.0, 47.6, 43.6, 42.8, 37.2, 36.6, 35.4, 34.6, 33.1, 32.8, 29.6, 29.4, 29.2, 29.2, 27.5, 26.1, 25.1, 23.8, 22.4, 20.9, 18.8, 17.4, 12.2. ESI-MS (+): Calc. for $C_{36}H_{53}O_3N_2$: 561.4051. Found: 563.4048.

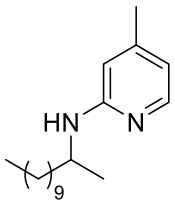


**4-methyl-*N*-(dodecan-2-yl)pyridine-2-amine (13a)**

1-Dodecene (44 μL, 34 mg, 0.20 mmol), 2-amino-4-methylpyridine (22 mg, 0.20 mmol), and $Ru(PEt_3)_3(NTf_2)_2$ (10 mg, 0.010 mmol, 5.0 mol%) were combined with DCB (60 μL) and a magnetic stir bar in a one dram vial. The vial threads were wrapped with 1 layer of Teflon tape and the resulting mixture was heated at 80 ˚C with stirring for 48 hours. The reaction was allowed to cool, and all of the volatile materials were evaporated. The crude product was purified by silica gel chromatography, eluting with 15% ethyl acetate in hexanes. Yield = 35 mg (63%). $^1$H NMR (500 MHz, Chloroform-*d*) δ 7.94 (d, *J* = 5.2 Hz, 1H), 6.39 (d, *J* = 5.2 Hz, 1H), 6.18 (s, 1H), 4.29 (d, *J* = 8.5 Hz, 1H), 3.72 (dq, *J* = 8.4, 6.3 Hz, 1H), 2.24 (s, 3H), 1.60 – 1.50 (m, 1H), 1.51 – 1.43 (m, 1H), 1.43 – 1.35 (m, 2H), 1.20-1.30 (m, 14H), 1.20 (d, *J* = 6.3 Hz, 3H), 0.90 (t, *J* = 6.9 Hz, 3H). $^{13}$C NMR (126 MHz, Chloroform-*d*) δ 158.6, 148.2, 147.9, 113.9, 106.7, 47.1, 37.3, 31.9, 29.6, 29.6, 29.3, 26.0, 22.7, 21.2, 21.0, 14.1. GC-MS (EI+): 276 (M), 261 (M-$CH_3$), 135 ([N-ethyl-5-methylpyridin-2-amine]•).

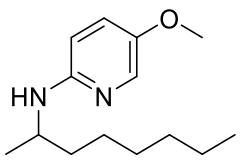


**5-methoxy-*N*-(octan-2-yl)pyridin-2-amine (14a)**

1-octene (31 μL, 23 mg, 0.20 mmol), 5-methoxypyridin-2-amine (25 mg, 0.20 mmol), and $Ru(PEt_3)_3(NTf_2)_2$ (10 mg, 0.010 mmol, 5.0 mol%) were combined with DCB (60 μL) and a magnetic stir bar in a one dram vial. The vial threads were wrapped with 1 layer of Teflon tape and the resulting mixture was heated at 80 ˚C with stirring for 48 hours. The reaction was allowed to cool, and all of the volatile materials were evaporated. The crude product was purified by silica gel chromatography, eluting with 25% ethyl acetate in hexanes. Yield = 32 mg (68%). $^1$H NMR (600 MHz, chloroform-*d*) δ 7.80 (d, *J* = 3.0 Hz, 1H), 7.09 (dd, *J* = 8.9, 3.0 Hz, 1H), 6.33 (d, *J* = 9.0 Hz, 1H), 4.05 (s, 1H), 3.77 (s, 3H), 3.64 (dt, *J* = 11.2, 5.1 Hz, 2H), 1.53 (dddd, *J* = 12.8, 9.9, 6.3, 5.1 Hz, 1H), 1.49 – 1.40 (m, 1H), 1.41 – 1.31 (m, 2H), 1.33 – 1.21 (m, 6H), 1.17 (d, *J* = 6.4 Hz, 3H), 0.87 (t, *J* = 7.0 Hz, 3H). $^{13}$C NMR (151 MHz, chloroform-*d*) δ 153.8, 148.5, 133.8, 125.8, 107.3, 56.7, 48.0, 37.4, 31.9, 29.5, 26.2, 22.7, 21.1, 14.2. GC-MS (EI+): 236 (M), 221 (M-$CH_3$), 151 ([N-ethyl-5-methoxypyridin-2-amine]•).

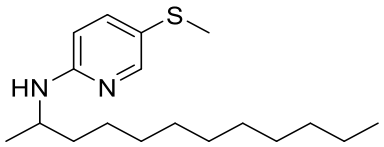


***N*-(dodecan-2-yl)-5-(methylthio)pyridin-2-amine (15a)**

1-dodecene (34 mg, 0.20 mmol), 5-(methylthio)pyridin-2-amine (28 mg, 0.20 mmol), and $Ru(PEt_3)_3(NTf_2)_2$ (10 mg, 0.010 mmol, 5.0 mol%) were combined with DCB (60 μL) and a magnetic stir bar in a one dram vial. The vial threads were wrapped with 1 layer of Teflon tape and the resulting mixture was heated at 100 ˚C with stirring for 48 hours. The reaction was allowed to cool, and all of the volatile materials were evaporated. The crude product was purified by silica gel chromatography, eluting with 40% ethyl acetate in hexanes. Yield = 26 mg (42%). $^1$H NMR (600 MHz, chloroform-*d*) δ 8.12 (d, *J* = 2.2 Hz, 1H), 7.47 (dd, *J* = 8.7, 2.4 Hz, 1H), 6.29 (d, *J* = 8.7 Hz, 1H), 4.44 (d, *J* = 8.3 Hz, 1H), 3.73 – 3.66 (m, 1H), 2.35 (s, 3H), 1.49 (dtdd, *J* = 25.4, 13.2, 9.7, 5.9 Hz, 2H), 1.34 (dtt, *J* = 18.8, 8.4, 4.9 Hz, 2H), 1.29 – 1.22 (m, 14H), 1.17 (d, *J* = 6.4 Hz, 3H), 0.87 (t, *J* = 7.0 Hz, 3H). $^{13}$C NMR (151 MHz, chloroform-*d*) δ 157.6, 151.4, 141.3, 119.9, 106.9, 47.4, 37.3, 32.0, 29.7, 29.7, 29.7, 29.4, 26.1, 22.7, 21.0, 20.4, 14.2. GC-MS (EI+): 308 (M), 292 (M-$CH_4$), 167 ([N-ethyl-5-(methylthio)pyridin-2-amine]•).

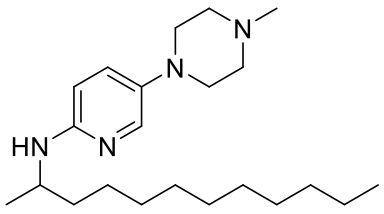


***N*-(dodecan-2-yl)-5-(4-methylpiperazin-1-yl)pyridin-2-amine (16a)**

1-dodecene (34 mg, 0.20 mmol), 5-(4-methylpiperazin-1-yl)pyridin-2-amine (39 mg, 0.20 mmol), and $Ru(PEt_3)_3(NTf_2)_2$ (10 mg, 0.010 mmol, 5.0 mol%) were combined with DCB (60 μL) and a magnetic stir bar in a one dram vial. The vial threads were wrapped with 1 layer of Teflon tape and the resulting mixture was heated at 100 ˚C with stirring for 48 hours. The reaction was allowed

to cool, and all of the volatile materials were evaporated. The crude product was purified by silica gel chromatography, eluting with 5% MeOH in DCM. Yield = 34 mg (47%). $^{1}$H NMR (600 MHz, chloroform-*d*) δ 7.78 (d, *J* = 2.8 Hz, 1H), 7.18 (dd, *J* = 9.0, 2.9 Hz, 1H), 6.33 (d, *J* = 8.9 Hz, 1H), 4.18 (s, 1H), 3.63 (h, *J* = 6.4 Hz, 1H), 3.06 – 3.01 (m, 4H), 2.60 – 2.55 (m, 4H), 2.35 (s, 3H), 1.52 (ddd, *J* = 16.1, 12.2, 5.7 Hz, 1H), 1.44 (ddd, *J* = 13.0, 6.4, 4.2 Hz, 1H), 1.41 – 1.31 (m, 2H), 1.30 – 1.23 (m, 14H), 1.16 (d, *J* = 6.3 Hz, 3H), 0.87 (t, *J* = 7.0 Hz, 3H). $^{13}$C NMR (151 MHz, chloroform-*d* ) δ 153.9, 139.4, 137.5, 129.3, 107.1, 55.3, 51.1, 47.8, 46.2, 37.4, 32.0, 29.8, 29.7, 29.4, 26.2, 22.8, 21.1, 14.2. GC-MS (EI+): 360 (M), 345 (M-$CH_3$), 219 ([N-ethyl-5-(4-methylpiperazin-1-yl)pyridin-2-amine]•).

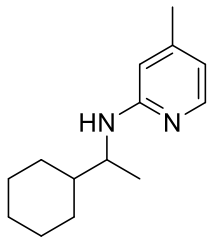


**_N_-(1-cyclohexylethyl)-4-methylpyridin-2-amine (17a)**

Vinylcyclohexane (27 µL, 22 mg, 0.20 mmol), 2-amino-4-methylpyridine (22 mg, 0.20 mmol), $Ru(PEt_3)_3(NTf_2)_2$ (20 mg, 0.010 mmol, 10 mol%), 1,2-DCB (60 µL) and a magnetic stir bar were combined in a one dram vial. The vial threads were wrapped with 1 layer of Teflon tape and the resulting mixture was heated at 100 ˚C with stirring for 48 hours. The mixture was allowed to cool, and all of the volatile materials were removed. The crude product was purified by silica gel chromatography, eluting with 20% ethyl acetate in hexanes. Yield = 28 mg (63%). $^{1}$H NMR (500 MHz, Chloroform-*d*) δ 7.96 (d, *J* = 5.2 Hz, 1H), 6.40 (dd, *J* = 5.2, 1.4 Hz, 1H), 6.20 (s, 1H), 4.38 (d, *J* = 9.1 Hz, 1H), 3.64 (dt, *J* = 9.1, 6.3 Hz, 1H), 2.27 (s, 3H), 1.95 – 1.65 (m, 5H), 1.46 (ddp, *J* = 14.6, 8.6, 3.0 Hz, 1H), 1.35 – 0.99 (m, 9H).$^{13}$C NMR (126 MHz, Chloroform-*d*) δ 159.2, 148.6, 148.2, 114.2, 107.1, 51.9, 43.8, 29.9, 29.2, 26.9, 26.8, 26.7, 21.67, 18.2. GC-MS (EI+): 218 (M), 203 (M-$CH_3$).

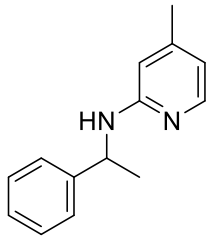


**4-methyl-_N_-(1-phenylethyl)pyridin-2-amine (18a)**

Styrene (23 µL, 21 mg, 0.20 mmol), 2-amino-4-methylpyridine (22 mg, 0.20 mmol), $Ru(PEt_3)_3(NTf_2)_2$ (20 mg, 0.010 mmol, 10 mol%), 1,2-DCB (60 µL) and a magnetic stir bar were combined in a one dram vial. The vial threads were wrapped with 1 layer of Teflon tape and the

resulting mixture was heated at 100 ˚C with stirring for 48 hours. The mixture was allowed to cool, and all of the volatile materials were removed. The crude product was purified by silica gel chromatography, eluting with 30% ethyl acetate in hexanes. Yield = 27 mg (62%). $^{1}$H NMR (600 MHz, Chloroform-*d*) δ 7.93 (dd, *J* = 5.2, 0.8 Hz, 1H), 7.40 – 7.36 (m, 2H), 7.32 (m, *J* = 8.5, 6.9 Hz, 2H), 7.25 – 7.21 (m, 1H), 6.39 (ddd, *J* = 5.1, 1.4, 0.7 Hz, 1H), 6.03 (dt, *J* = 1.6, 0.8 Hz, 1H), 4.92 (d, *J* = 6.4 Hz, 1H), 4.74 (p, *J* = 6.71 Hz, 1H), 2.13 (d, *J* = 0.7 Hz, 3H), 1.54 (d, *J* = 6.8 Hz, 3H). $^{13}$C NMR (151 MHz, $CDCl_3$) δ 158.3, 148.5, 147.9, 144.9, 128.75, 127.0, 125.9, 114.7, 107.1, 51.9, 24.4, 21.3. GC-MS (EI+): 212 (M), 197 (M-$CH_3$).

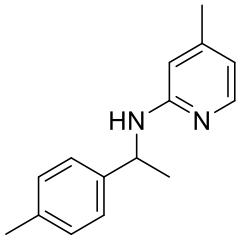


**4-methyl-N-(1-(p-tolyl)ethyl)pyridin-2-amine (19a)**

4-Methylstyrene (26 µL, 24 mg, 0.20 mmol), 2-amino-4-methylpyridine (22 mg, 0.20 mmol), $Ru(PEt_3)_3(NTf_2)_2$ (20 mg, 0.010 mmol, 10 mol%), 1,2-DCB (60 µL) and a magnetic stir bar were combined in a one dram vial. The vial threads were wrapped with 1 layer of Teflon tape and the resulting mixture was heated at 100 ˚C with stirring for 48 hours. The mixture was allowed to cool, and all of the volatile materials were removed. The crude product was purified by silica gel chromatography, eluting with 30% ethyl acetate in hexanes. Yield = 27 mg (59%). $^{1}$H NMR (600 MHz, Chloroform-*d*) δ 7.94 (d, *J* = 5.2 Hz, 1H), 7.28 (d, *J* = 8.0 Hz, 2H), 7.14 (d, *J* = 7.8 Hz, 2H), 6.39 (dd, *J* = 5.2, 1.4 Hz, 1H), 6.05 (s, 1H), 5.07 (d, *J* = 6.5 Hz, 1H), 4.72 (p, *J* = 6.6 Hz, 1H), 2.33 (s, 3H), 2.14 (s, 3H), 1.53 (d, *J* = 6.8 Hz, 3H). $^{13}$C NMR (126 MHz, $CDCl_3$) δ 158.3, 148.7, 147.7, 141.9, 136.6, 129.4, 125.9, 114.7, 107.1, 51.6, 24.5, 21.4, 21.1. GC-MS (EI+): 226 (M), 211 (M-$CH_3$).

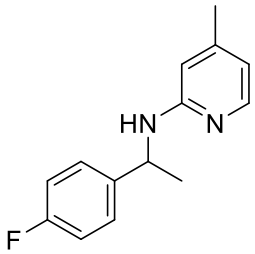


**N-(1-(4-fluorophenyl)ethyl)-4-methylpyridin-2-amine (20a)**

4-Fluorostyrene (24 µL, 25 mg, 0.20 mmol), 2-amino-4-methylpyridine (22 mg, 0.20 mmol), $Ru(PEt_3)_3(NTf_2)_2$ (20 mg, 0.010 mmol, 10 mol%), 1,2-DCB (60 µL) and a magnetic stir bar were combined in a one dram vial. The vial threads were wrapped with 1 layer of Teflon tape and the resulting mixture was heated at 120 ˚C with stirring for 48 hours. The mixture was allowed to cool, and all of the volatile materials were removed. The crude product was purified by silica gel

chromatography, eluting with 30% ethyl acetate in hexanes. Yield = 26 mg (57%). $^{1}$H NMR (600 MHz, Chloroform-*d*) δ 7.92 (dd, *J* = 5.1, 0.7 Hz, 1H), 7.36 – 7.30 (m, 2H), 7.03 – 6.95 (m, 2H), 6.40 (ddd, *J* = 5.2, 1.4, 0.7 Hz, 1H), 6.00 (dt, *J* = 1.6, 0.8 Hz, 1H), 4.91 (d, *J* = 6.4 Hz, 1H), 4.73 (p, *J* = 6.7 Hz, 1H), 2.14 (s, 3H), 1.51 (d, *J* = 6.8 Hz, 3H). $^{13}$C NMR (151 MHz, $CDCl_3$) δ 162.7, 161.1, 158.2, 148.6, 148.0, 140.7 (d, *J* = 3.0 Hz), 127.4 (d, *J* = 7.9 Hz), 115.5 (d, *J* = 21.4 Hz), 114.9, 107.1, 51.2, 24.5, 21.3. $^{19}$F NMR (565 MHz, $CDCl_3$) δ -116.18. GC-MS (EI+): 230 (M), 215 (M-$CH_3$).

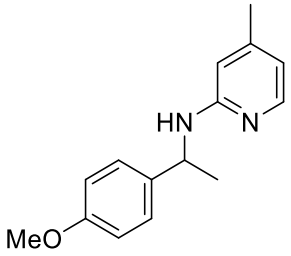


**N-(1-(4-methoxyphenyl)ethyl)-4-methylpyridin-2-amine (21a)**

4-Methoxystyrene (27 µL, 27 mg, 0.20 mmol), 2-amino-4-methylpyridine (22 mg, 0.20 mmol), $Ru(PEt_3)_3(NTf_2)_2$ (20 mg, 0.010 mmol, 10 mol%), 1,2-DCB (60 µL) and a magnetic stir bar were combined in a one dram vial. The vial threads were wrapped with 1 layer of Teflon tape and the resulting mixture was heated at 100 ˚C with stirring for 48 hours. The mixture was allowed to cool, and all of the volatile materials were removed. The crude product was purified by silica gel chromatography, eluting with 30% ethyl acetate in hexanes. Yield = 30 mg (61%). $^{1}$H NMR (600 MHz, Chloroform-*d*) δ 7.93 (dd, *J* = 5.1, 0.8 Hz, 1H), 7.32 – 7.27 (m, 2H), 6.88 – 6.82 (m, 2H), 6.38 (ddd, *J* = 5.2, 1.5, 0.7 Hz, 1H), 6.03 (dt, *J* = 1.6, 0.8 Hz, 1H), 4.91 (d, *J* = 6.5 Hz, 1H), 4.69 (p, *J* = 6.7 Hz, 1H), 3.78 (s, 3H), 2.14 (d, *J* = 0.7 Hz, 3H), 1.51 (d, *J* = 6.7 Hz, 3H).$^{13}$C NMR (151 MHz, $CDCl_3$) δ 158.6, 158.4, 148.5, 147.9, 137.0, 127.0, 114.6, 114.0, 107.1, 55.3, 51.3, 24.4, 21.3. GC-MS (EI+): 242 (M), 227 (M-$CH_3$).

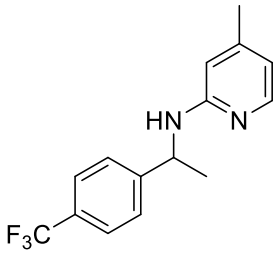


**4-methyl-N-(1-(4-(trifluoromethyl)phenyl)ethyl)pyridin-2-amine (22a)**

4-Trifluoromethylstyrene (30 µL, 34 mg, 0.20 mmol), 2-amino-4-methylpyridine (22 mg, 0.20 mmol), $Ru(PEt_3)_3(NTf_2)_2$ (20 mg, 0.010 mmol, 10 mol%), 1,2-DCB (60 µL) and a magnetic stir bar were combined in a one dram vial. The vial threads were wrapped with 1 layer of Teflon tape and the resulting mixture was heated at 120 ˚C with stirring for 48 hours. The mixture was allowed

to cool, and all of the volatile materials were removed. The crude product was purified by silica gel chromatography, eluting with 30% ethyl acetate in hexanes. Yield = 33 mg (60%). $^{1}$H NMR (600 MHz, Chloroform-*d*) δ 7.93 (d, *J* = 5.2 Hz, 1H), 7.57 (d, *J* = 8.1 Hz, 2H), 7.49 (d, *J* = 8.1 Hz, 2H), 6.44 – 6.37 (m, 1H), 4.95 (b, 1H), 4.88 – 4.77 (p, *J* = 6.8 Hz, 1H), 2.14 (s, 3H), 1.54 (d, *J* = 6.8 Hz, 3H). $^{13}$C NMR (151 MHz, $CDCl_3$) δ 158.0, 149.3, 148.7, 148.0, 129.3 (q, *J* = 32.1 Hz), 124.3 (q, *J* = 272.0 Hz), 126.3, 125.7, 115.1, 107.2, 51.5, 24.4, 21.3. $^{19}$F NMR (565 MHz, $CDCl_3$) δ -62.37. GC-MS (EI+): 280 (M), 265 (M-$CH_3$).

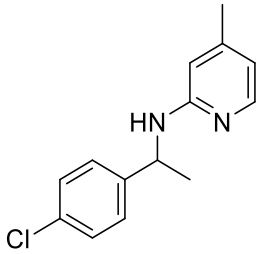


**N-(1-(4-chlorophenyl)ethyl)-4-methylpyridin-2-amine (23a)**

4-Chlorostyrene (24 µL, 28 mg, 0.20 mmol), 2-amino-4-methylpyridine (22 mg, 0.20 mmol), $Ru(PEt_3)_3(NTf_2)_2$ (20 mg, 0.010 mmol, 10 mol%), 1,2-DCB (60 µL) and a magnetic stir bar were combined in a one dram vial. The vial threads were wrapped with 1 layer of Teflon tape and the resulting mixture was heated at 120 ˚C with stirring for 48 hours. The mixture was allowed to cool, and all of the volatile materials were removed. The crude product was purified by silica gel chromatography, eluting with 30% ethyl acetate in hexanes. Yield = 24 mg (49%). $^{1}$H NMR (600 MHz, Chloroform-*d*) δ 7.92 (d, *J* = 5.2 Hz, 1H), 7.35 – 7.21 (m, 4H), 6.39 (dd, *J* = 5.2, 1.4 Hz, 1H), 5.99 (s, 1H), 4.99 (d, *J* = 6.4 Hz, 1H), 4.72 (p, *J* = 6.7 Hz, 1H), 2.13 (s, 3H), 1.50 (d, *J* = 6.8 Hz, 3H). $^{13}$C NMR (151 MHz, $CDCl_3$) δ 158.1, 148.6, 147.9, 143.6, 132.6, 128.8, 127.3, 114.9, 107.1, 51.3, 24.4, 21.3. GC-MS (EI+): 248 (M+2), 246 (M), 231 (M-$CH_3$).

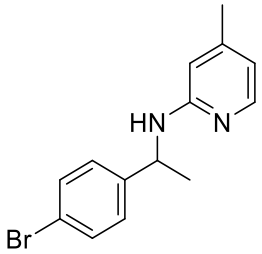


**N-(1-(4-bromophenyl)ethyl)-4-methylpyridin-2-amine (24a)**

4-Bromostyrene (26 µL, 37 mg, 0.20 mmol), 2-amino-4-methylpyridine (22 mg, 0.20 mmol), $Ru(PEt_3)_3(NTf_2)_2$ (20 mg, 0.010 mmol, 10 mol%), 1,2-DCB (60 µL) and a magnetic stir bar were combined in a one dram vial. The vial threads were wrapped with 1 layer of Teflon tape and the resulting mixture was heated at 120 ˚C with stirring for 48 hours. The mixture was allowed to cool, and all of the volatile materials were removed. The crude product was purified by silica gel

chromatography, eluting with 20% ethyl acetate in hexanes. Yield = 27 mg (46%). $^{1}$H NMR (500 MHz, Chloroform-*d*) δ 7.92 (d, *J* = 5.2 Hz, 1H), 7.47 – 7.40 (m, 2H), 7.30 – 7.19 (m, 2H), 6.41 (dd, *J* = 5.2, 1.4 Hz, 1H), 5.99 (s, 1H), 4.89 (d, *J* = 6.2 Hz, 1H), 4.70 (p, *J* = 6.7 Hz, 1H), 2.14 (s, 3H), 1.51 (d, *J* = 6.8 Hz, 3H). $^{13}$C NMR (151 MHz, $CDCl_3$) δ 158.1, 148.6, 148.0, 144.1, 131.8, 127.7, 120.7, 115.0, 107.1, 51.4, 24.4, 21.3. GC-MS (EI+): 292 (M+2), 290 (M), 275 (M-$CH_3$).

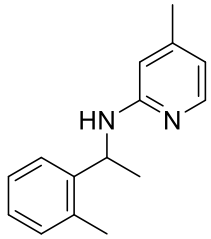


**4-methyl-N-(1-(o-tolyl)ethyl)pyridin-2-amine (25a)**

2-Methylstyrene (26 µL, 24 mg, 0.20 mmol), 2-amino-4-methylpyridine (22 mg, 0.20 mmol), $Ru(PEt_3)_3(NTf_2)_2$ (20 mg, 0.010 mmol, 10 mol%), 1,2-DCB (60 µL) and a magnetic stir bar were combined in a one dram vial. The vial threads were wrapped with 1 layer of Teflon tape and the resulting mixture was heated at 120 ˚C with stirring for 48 hours. The mixture was allowed to cool, and all of the volatile materials were removed. The crude product was purified by silica gel chromatography, eluting with 30% ethyl acetate in hexanes. Yield = 18 mg (40%). $^{1}$H NMR (600 MHz, Chloroform-*d*) δ 7.93 (d, *J* = 5.1 Hz, 1H), 7.42 – 7.38 (m, 1H), 7.20 – 7.11 (m, 3H), 6.38 (dd, *J* = 5.2, 1.4 Hz, 1H), 5.92 (d, *J* = 1.5 Hz, 1H), 4.97 – 4.89 (m, 1H), 4.82 (d, *J* = 6.5 Hz, 1H), 2.44 (s, 3H), 2.13 (s, 3H), 1.50 (d, *J* = 6.6 Hz, 3H).$^{13}$C NMR (151 MHz, $CDCl_3$) δ 158.3, 148.5, 148.0, 142.6, 135.0, 130.7, 126.9, 126.6, 124.8, 114.7, 106.8, 48.3, 22.6, 21.4, 19.2. GC-MS (EI+): 226 (M), 211 (M-$CH_3$).

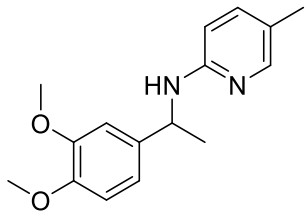


***N*-(1-(3,4-dimethoxyphenyl)ethyl)-5-methylpyridine-2-amine (26a)**

3,4-dimethoxy-vinylbenzene (33 mg, 0.20 mmol), 2-amino-5-methylpyridine (22 mg, 0.20 mmol), $Ru(PEt_3)_3(NTf_2)_2$ (20 mg, 0.010 mmol, 10 mol%), 1,2-DCB (60 µL) and a magnetic stir bar were combined in a one dram vial. The vial threads were wrapped with 1 layer of Teflon tape and the resulting mixture was heated at 100 ˚C with stirring for 48 hours. The reaction was allowed to cool, and all of the volatile materials were evaporated. The crude product was purified by silica gel chromatography, eluting with 30% ethyl acetate in hexanes. Yield = 35 mg (64%). $^{1}$H NMR (600 MHz, chloroform-*d*) δ 7.90 (s, 1H), 7.16 (d, J = 10.0 Hz, 1H), 6.90 (d, J = 10.7 Hz, 2H), 6.81 (d, J = 8.1 Hz, 1H), 6.14 (d, J = 8.4 Hz, 1H), 4.76 (d, J = 5.5 Hz, 1H), 4.61 (p, J = 6.5 Hz, 1H), 3.85 (s,

6H), 2.14 (s, 3H), 1.52 (d, J = 6.7 Hz, 3H). $^{13}$C NMR (151 MHz, chloroform-*d*) δ 156.1, 149.1, 147.8, 147.4, 138.5, 137.4, 121.8, 117.7, 111.1, 109.0, 106.4, 55.8, 55.8, 51.9, 24.4, 17.3. GC-MS (EI+): 272 (M), 267 (M-$CH_3$), 165 (M-[p-Me-aminopyridine]$^{\bullet}$).

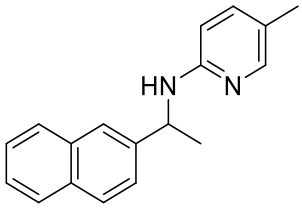


***N*-(ethyl-naphthalene-2-yl)-5-methylpyridin-2-amine (27a)**

Vinyl naphthalene (31 mg, 0.20 mmol), 2-amino-5-methylpyridine (22 mg, 0.20 mmol), $Ru(PEt_3)_3(NTf_2)_2$ (20 mg, 0.010 mmol, 10 mol%), 1,2-DCB (60 μL) and a magnetic stir bar were combined in a one dram vial. The vial threads were wrapped with 1 layer of Teflon tape and the resulting mixture was heated at 100 ˚C with stirring for 48 hours. The reaction was allowed to cool, and all of the volatile materials were evaporated. The crude product was purified by silica gel chromatography, eluting with 40% ethyl acetate in hexanes. Yield = 34 mg (65%). $^1$H NMR (600 MHz, chloroform-*d*) δ 7.93 – 7.90 (m, 1H), 7.84 – 7.77 (m, 4H), 7.50 (dd, *J* = 8.5, 1.7 Hz, 1H), 7.45 (pd, *J* = 6.8, 1.5 Hz, 2H), 7.11 (dd, *J* = 8.4, 2.4 Hz, 1H), 6.16 (d, *J* = 8.5 Hz, 1H), 4.95 (d, *J* = 5.9 Hz, 1H), 4.83 (p, *J* = 6.6 Hz, 1H), 2.12 (s, 3H), 1.61 (d, *J* = 6.8 Hz, 3H). $^{13}$C NMR (151 MHz, chloroform-*d* ) δ 156.4, 148.0, 142.5, 138.5, 133.6, 132.8, 128.6, 127.9, 127.7, 126.1, 125.6, 124.5, 124.3, 122.0, 106.5, 52.4, 24.6, 17.4. GC-MS (EI+): 262 (M), 155 (M-[p-Me-aminopyridine]$^{\bullet}$).

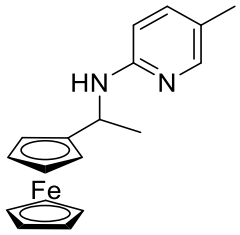


**N-(ethylferrocene-2-yl)-5-methylpyridin-2-amine (28a)**

Vinyl ferrocene (42 mg, 0.20 mmol), 2-amino-5-methylpyridine (22 mg, 0.20 mmol), $Ru(PEt_3)_3(NTf_2)_2$ (20 mg, 0.010 mmol, 10 mol%), 1,2-DCB (60 μL) and a magnetic stir bar were combined in a one dram vial. The vial threads were wrapped with 1 layer of Teflon tape and the resulting mixture was heated at 100 ˚C with stirring for 48 hours. The reaction was allowed to cool, and all of the volatile materials were evaporated. The crude product was purified by silica gel chromatography, eluting with 40% ethyl acetate in hexanes. Yield = 39 mg (61%). $^1$H NMR (600 MHz, chloroform-*d*) δ 7.95 (s, 1H), 7.27 – 7.24 (m, *J* = 2.0 Hz, 1H), 6.34 (d, *J* = 8.4 Hz, 1H), 4.66 (m, 1H), 4.55 (d, *J* = 8.2 Hz, 1H), 4.20 (s, 5H), 4.18 (m, 2H), 4.13 (dt, *J* = 7.7, 1.7 Hz, 2H), 2.18 (s, 3H), 1.52 (d, *J* = 6.5 Hz, 3H). $^{13}$C NMR (151 MHz, chloroform-*d*) δ 156.4, 147.9, 138.5, 121.5, 107.0, 93.3, 68.5, 67.8, 67.6, 67.0, 66.1, 45.7, 21.3, 17.5. GCMS: (EI+): 320 (M), 305 (M-$CH_3$), 213 (M-[p-Me-aminopyridine]$^{\bullet}$).

### 2.4.5. Removal of Pyridyl Group from the Hydroamination Product

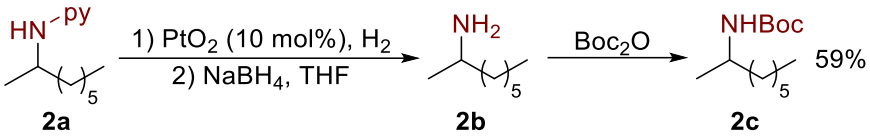


5-methyl-*N*-(octan-2-yl)pyridine-2-amine **2a** (44 mg, 0.20 mmol), HCl in dioxane (4.0 M, 0.10 mL, 2.0 equiv), ethanol (2.0 mL) and a stir bar were combined in a reaction tube. The tube was capped with a septum-cap and stirred for 15 minutes. $PtO_2$ (4.6 mg, 10 mol%) was added to the tube and the tube was capped and sealed. The tube was purged with $H_2$ for 10 minutes using a hydrogen balloon and placed in a cold bath set at 0 ℃. After 15 hours, the mixture was filtered through celite and the solvent was removed *in vacuo*. The residue was dissolved in 1.0 mL of THF and 0.2 mL of EtOH and placed in in a cold bath set at 0 ℃. Sodium borohydride (76 mg, 2.0 mmol, 10 equiv) was added to the mixture and the mixture was allowed to stir for 2 hours. Water (10 mL) was added to the mixture and the mixture was extracted with DCM (10 mL) three times. The combined organic layer was dried over anhydrous $Na_2SO_4$. The solvent was then removed *in vacuo* and the residue was dissolved in 2.0 mL of THF. $Boc_2O$ (87 mg, 0.40 mmol, 2.0 equiv) and 4-Dimethylaminopyridine (2.4 mg, 0.020 mmol, 0.10 equiv) was added to the mixture and the mixture was stirred overnight. The solvent was removed and the crude Boc-protected amine product **2c** was purified by column chromatography, eluting with 10% ethyl acetate in hexanes. Yield = 27 mg (59%). $^1$H NMR (600 MHz, $CDCl_3$) δ 4.32 (s, 1H), 3.64 (s, 1H), 1.46 (s, 9H), 1.37-1.42 (m, 2H), 1.35 – 1.23 (m, 8H), 1.11 (d, *J* = 6.6 Hz, 3H), 0.89 (t, *J* = 6.8 Hz, 3H).

### 2.4.6. Determination of the Catalyst Resting State

#### Initial Investigation of the Catalyst Resting State

$Ru(PEt_3)_3(NTf_2)_2$ (**Ru-1**) (10 mg, 0.010 mmol) were combined with $D_4$-DCB (0.50 mL) and appropriate amount of 2-amino-4-methylpyridine **(1b)** and dodecane in a J-young tube. The tube was heated at 80 ˚C for 4 hours and a $^{31}$P NMR spectrum of the mixture was taken at 80 ˚C.

#### Independent Synthesis of the Catalyst Resting State

**$Ru(PEt_3)_3$(amine)$(NTf_2)_2$ (29)**

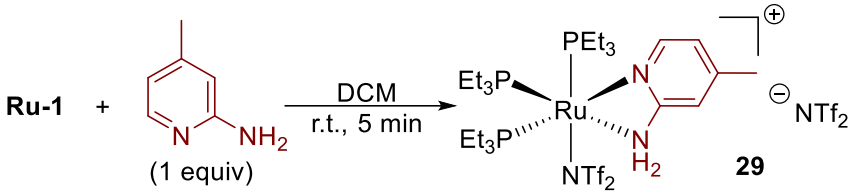


$Ru(PEt_3)_3(NTf_2)_2$ (**Ru-1**) (51 mg, 0.050 mmol), 2-amino-5-methylpyridine (5.4 mg, 0.050 mmol) and DCM (2.0 mL) were combined in a 20-mL vial and stirred at room temperature for 5 minutes. The mixture turned bright yellow. The solvent was removed under vacuum and the resulting yellow solid was washed with cold diethyl ether three times. Single crystals suitable for x-ray crystallography analysis was obtained by cooling a DCM/$^{i}Pr_2O$ saturated solution of $Ru(PEt_3)_3$(amine)$(NTf_2)_2$ (**29**). Yield = 46 mg (82%). $^{1}$H NMR (600 MHz, Methylene Chloride-$d_2$) δ 8.16 (s, 1H), 7.84 (d, $J$ = 8.2 Hz, 1H), 7.28 (d, $J$ = 8.2 Hz, 1H), 5.14 (s, 2H), 2.44 (s, 3H), 2.00 – 1.80 (m, 18H), 1.15 (m, 24H). $^{31}$P NMR (162 MHz, Methylene Chloride-$d_2$) δ 38.33. $^{19}$F NMR (376 MHz, Methylene Chloride-$d_2$) δ -78.19. The identity of the product was confirmed by x-ray crystallography. Anal. Calc'd C:28.64 H:4.44 N:4.99 Found C:28.51 H:4.46 N:4.61.

**$Ru(PEt_3)_3$(amido)$(NTf_2)$ (30)**

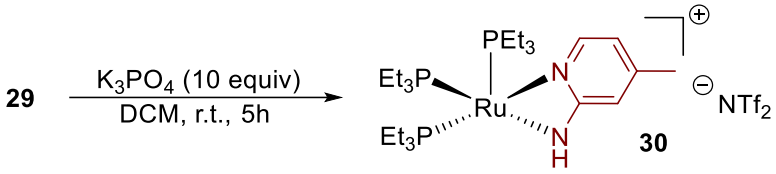


$Ru(PEt_3)_3$(amine)$(NTf_2)_2$ (**29**) (56 mg, 0.050 mmol), anhydrous $K_3PO_4$ (0.11 g, 0.50 mmol, 10 equiv) and DCM (3.0 mL) were combined in a 20-mL vial and stirred at room temperature for 5 hours. The black mixture was then filtered, and the solvent was removed under vacuum. The resulting black oil was triturated with cold $^{i}Pr_2O$ three times to afford black powder. Single crystals suitable for x-ray crystallography analysis was obtained by cooling a DCM/$^{i}Pr_2O$ saturated solution of $Ru(PEt_3)_3$(amido)$(NTf_2)$ (**30**). Yield = 36 mg (85%). $^{1}$H NMR (600 MHz, Methylene Chloride-$d_2$) δ 7.34 (d, $J$ = 5.6 Hz, 1H), 6.06 (d, $J$ = 5.6 Hz, 1H), 5.56 (s, 1H), 4.64 (s, 1H), 2.05 (s, 3H), 1.79 (m, 18H), 1.17 (m, 24H). $^{31}$P NMR (243 MHz, Methylene Chloride-$d_2$) δ 51.95. $^{19}$F NMR (376 MHz, Methylene Chloride-$d_2$) δ -78.76. The identity of the product was confirmed by x-ray crystallography. Anal. Calc'd C:36.60 H:5.94 N:5.09 Found C:36.87 H:6.11 N:5.03.

**Examination of the kinetic Competence of $Ru(PEt_3)_3$(amido)$(NTf_2)$**

1-Dodecene (44 µL, 34 mg, 0.20 mmol), 2-amino-4-methylpyridine (22 mg, 0.20 mmol), and $Ru(PEt_3)_3$(amido)$(NTf_2)$ (**30**) (8.4 mg, 0.010 mmol, 5.0 mol%) were combined with DCB (60 µL) and a magnetic stir bar in a one dram vial. The vial was capped, and the resulting mixture was heated at 80 ˚C with stirring for 48 hours. The mixture was allowed to cool to room temperature and an NMR yield (65%) of this reaction was obtained using 1,3,5-trimethoxybenzene as the internal standard.

**Variable Temperature NMR Spectroscopy Analysis of the Mixture of $Ru(PEt_3)_3$(amido)$(NTf_2)$ and 2-amino-4-methylpyridine**

$Ru(PEt_3)_3$(amido)$(NTf_2)$ (**30**) (8.4 mg, 0.010 mmol) and 2-amino-4-methylpyridine (22 mg, 0.20 mmol) and were combined with $D_4$-DCB (0.50 mL) in a J-young tube. The mixture turned black and $^1H$ (Figure S1) and $^{31}P$ NMR spectra of the mixture were taken at 80 ˚C, 60 ˚C, 40 ˚C and 25 ˚C. $Ru(PEt_3)_3$(amido)$(NTf_2)$ (**30**) (8.4 mg, 0.010 mmol) and 2-amino-4-methylpyridine (22 mg, 0.20 mmol) and were combined with $D_2$-DCM (0.50 mL) in a J-young tube. The mixture turned black and $^{31}P$ NMR spectra of the mixture was taken at 0 ˚C, -20 ˚C, and -40 ˚C (Figure 2.8).

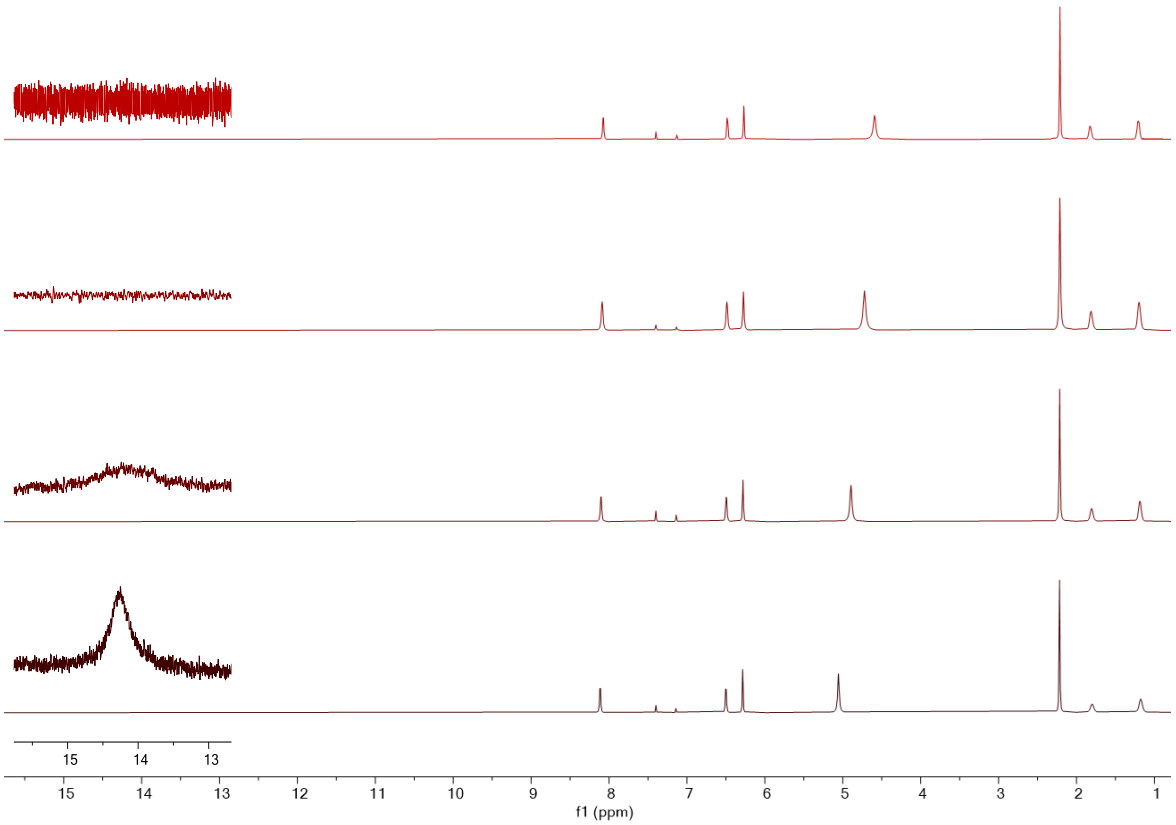


**Figure 2.8.** $^1H$ NMR spectra of the mixture of complex **30** and aminopyridine **1b** (20 equiv) at 80 ˚C, 60 ˚C, 40 ˚C and 25 ˚C (from top to bottom).

### 2.4.7. Kinetic Studies of Catalytic Hydroamination

All samples for kinetic experiments were prepared and analyzed according to the following procedures. In a nitrogen-filled glovebox, an appropriate amount of vinylcyclohexane, 2-amino-4-methylpyridine, $Ru(PEt_3)_3(NTf_2)_2$ and 1,3,5-trimethoxybenzene (internal standard) were mixed in a 1.0 mL volumetric flask. Then, 1,2-dichlorobenzene was added to prepare a 1.0 mL solution.

The mixture was then transferred into a Schlenk tube equipped with a magnetic stir bar. A $t_0$ aliquot was then taken and the tube was sealed and heated in an oil bath at 120 ˚C outside the glovebox. The Schlenk tube was removed from the oil bath after a certain amount of time of heating and rapidly cooled. The mixture was then taken into the glovebox, and a 50 µL aliquot was removed from the mixture. The tube was resealed and returned to the oil bath. The aliquots were analyzed by $^1$H NMR spectroscopy and concentrations were determined by integration relative to the 1,3,5-trimethoxybenzene internal standard. Initial reaction rates were subsequently determined by measuring product formation at low conversion (<10%).

**Order in vinylcyclohexane (Figure 2.9-2.12)**

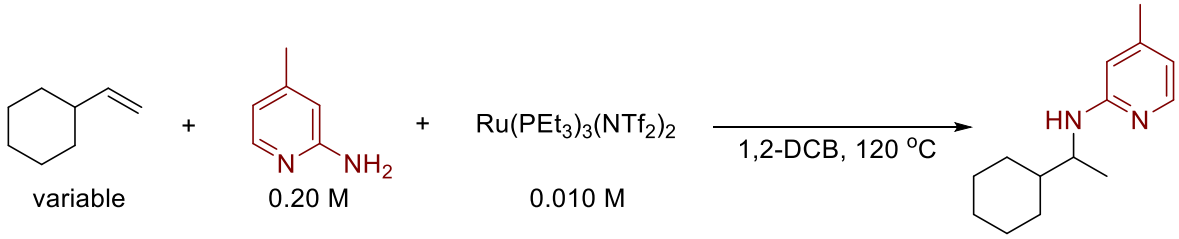


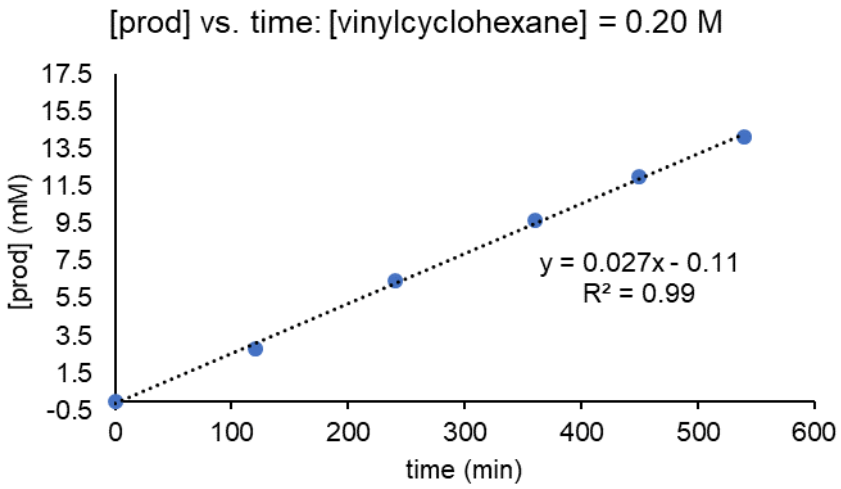


**Figure 2.9.** Rate of product formation as a function of time when [vinylcyclohexane] = 0.20 M.

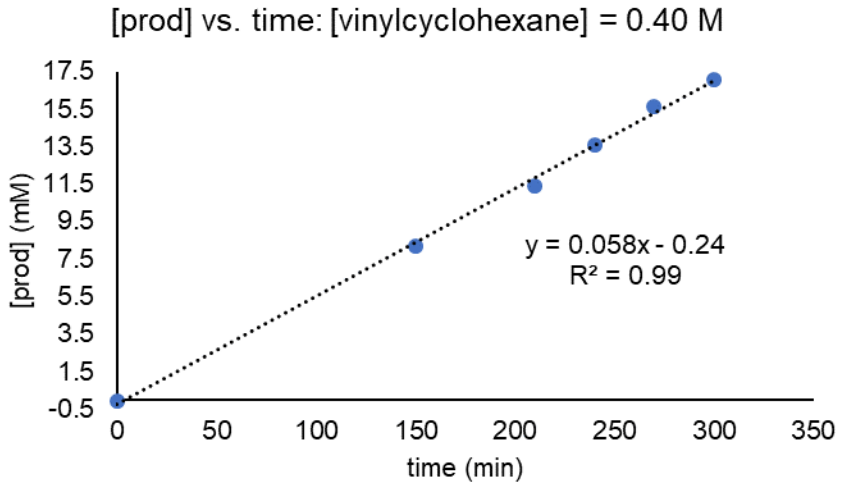


**Figure 2.10.** Rate of product formation as a function of time when [vinylcyclohexane] = 0.40 M.

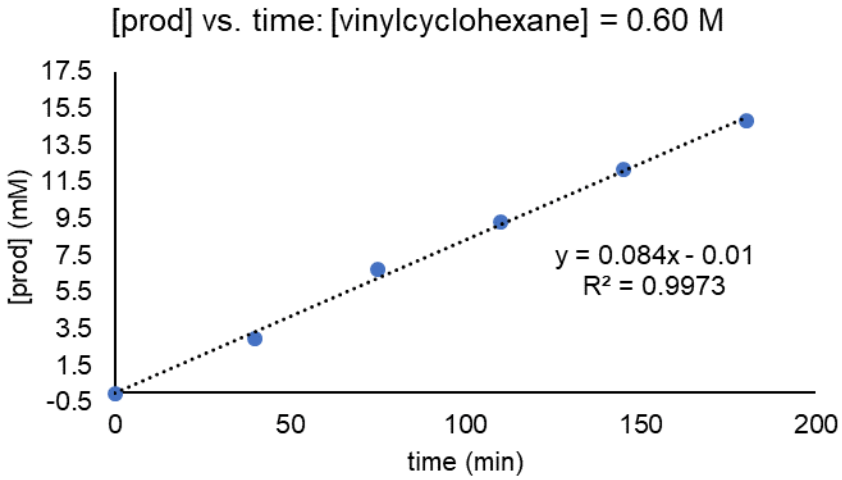


**Figure 2.11.** Rate of product formation as a function of time when [vinylcyclohexane] = 0.60 M.

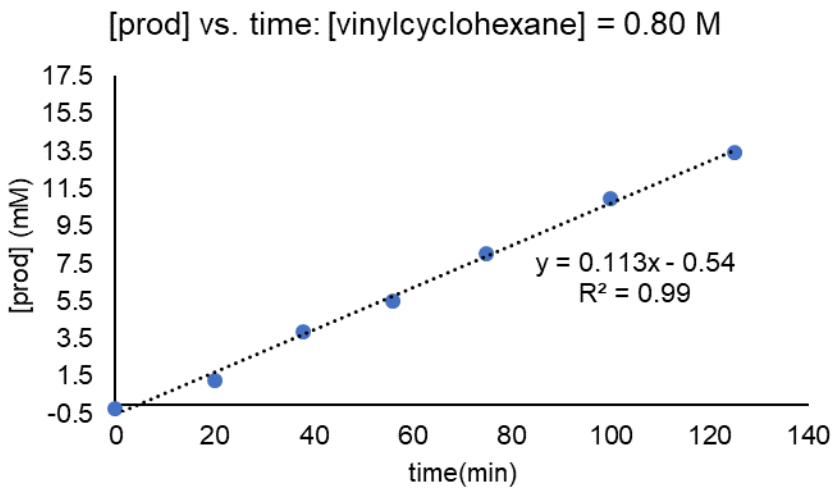


**Figure 2.12.** Rate of product formation as a function of time when [vinylcyclohexane] = 0.80 M.

**Order in 2-amino-4-methylpyridine (1b) (Figure 2.13-2.16)**

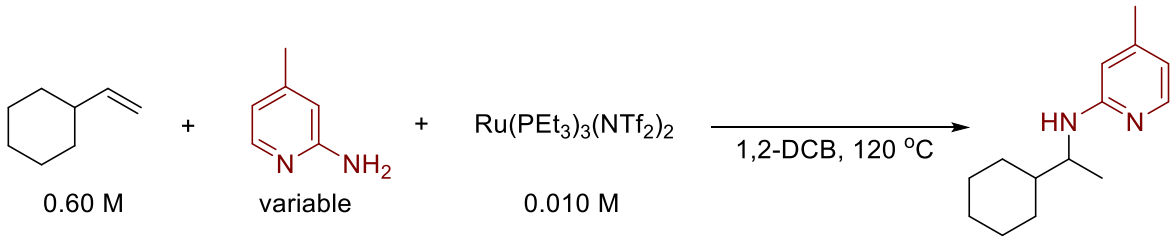


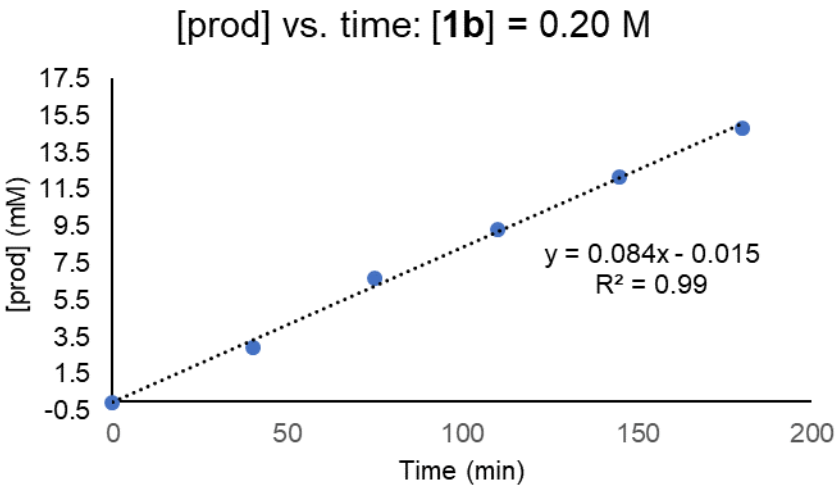


**Figure 2.13.** Rate of product formation as a function of time when [**1b**] = 0.20 M.

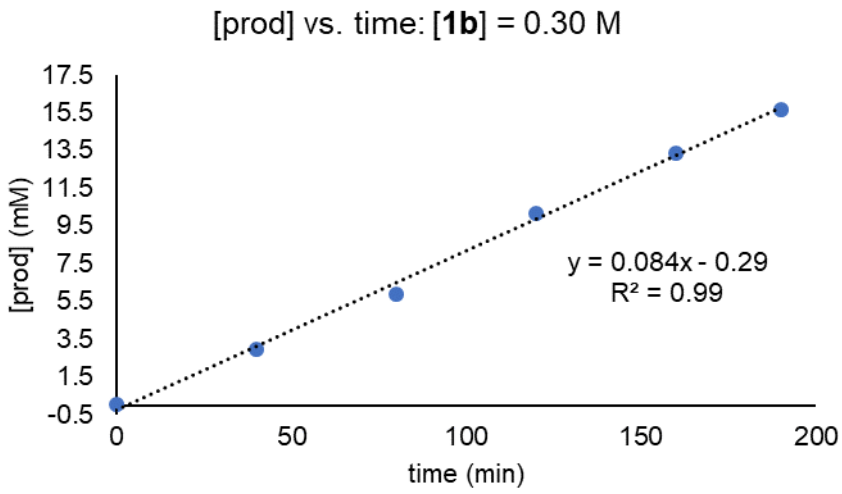


**Figure 2.14.** Rate of product formation as a function of time when [**1b**] = 0.30 M.

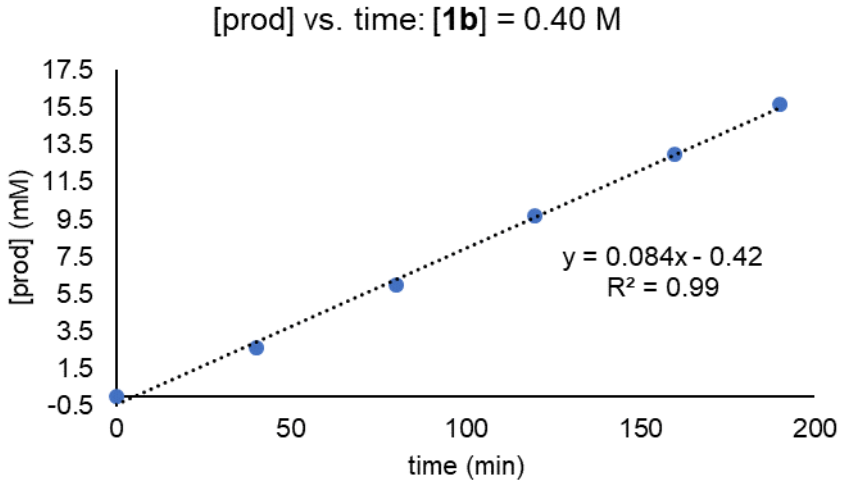


**Figure 2.15.** Rate of product formation as a function of time when [**1b**] = 0.40 M.

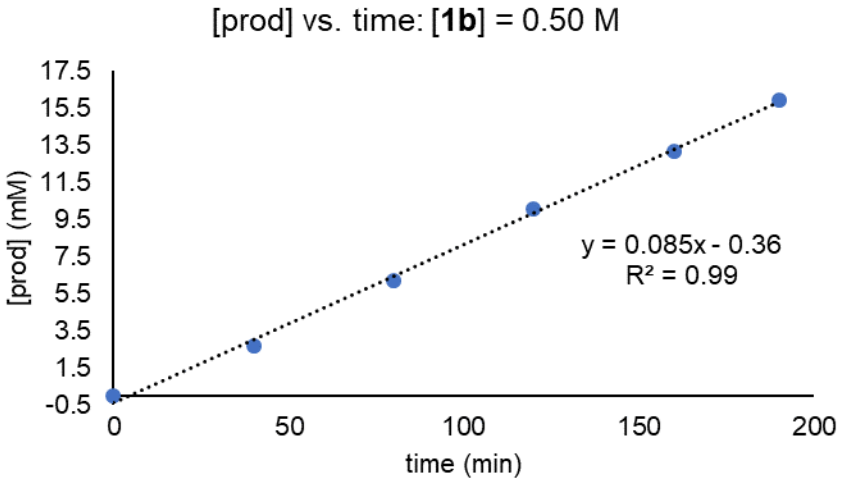


**Figure 2.16.** Rate of product formation as a function of time when [**1b**] = 0.50 M.

**Order in $Ru(PEt_3)_3(NTf_2)_2$ (Ru-1) (Figure 2.17-2.20)**

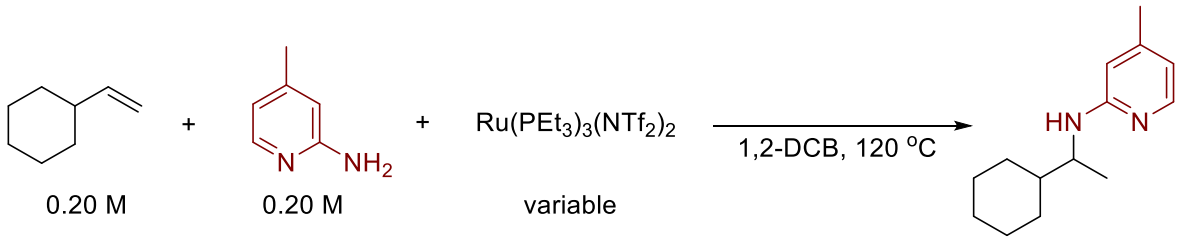


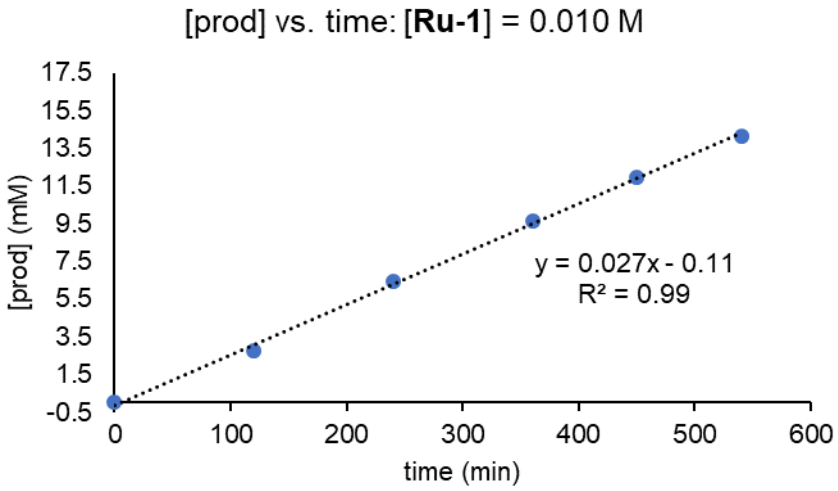


**Figure 2.17.** Rate of product formation as a function of time when [**Ru-1**] = 0.010 M.

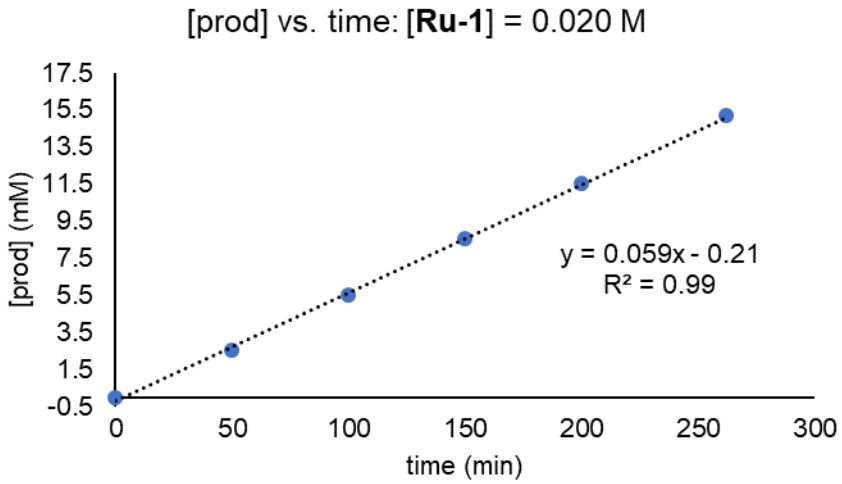


**Figure 2.18.** Rate of product formation as a function of time when [**Ru-1**] = 0.020 M.

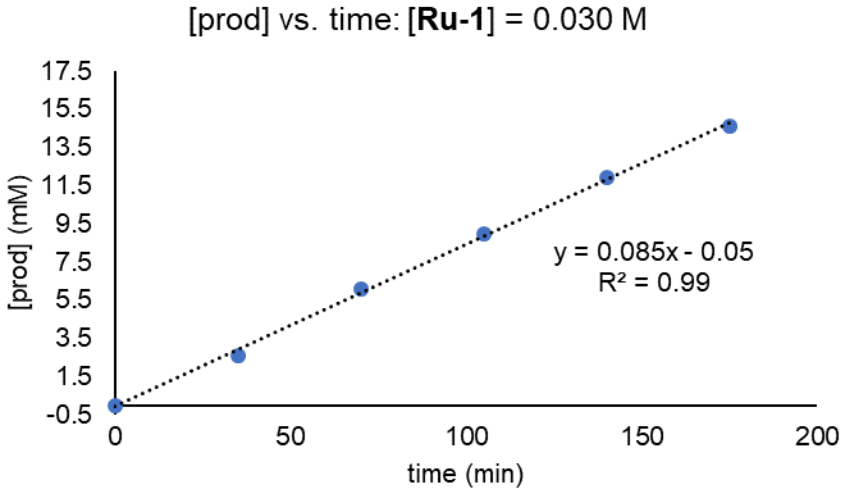


**Figure 2.19.** Rate of product formation as a function of time when [**Ru-1**] = 0.030 M.

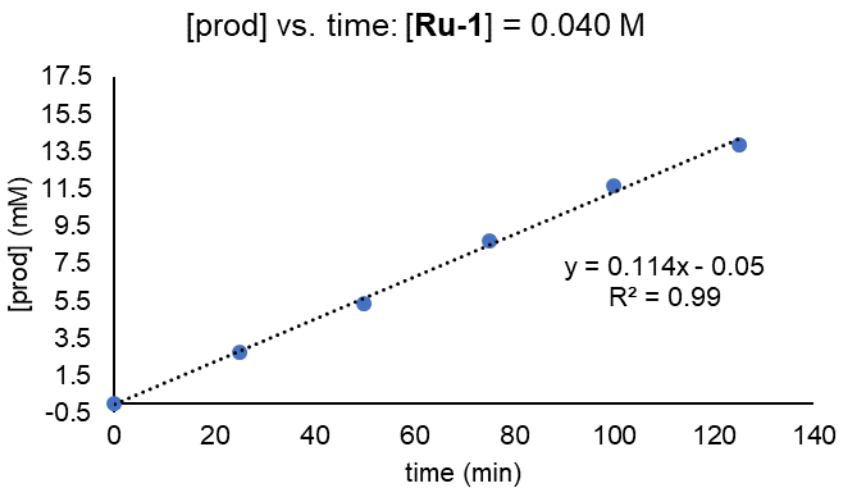


**Figure 2.20.** Rate of product formation as a function of time when [**Ru-1**] = 0.040 M.

**Order in $PEt_3$ (Figure 2.21-2.24)**

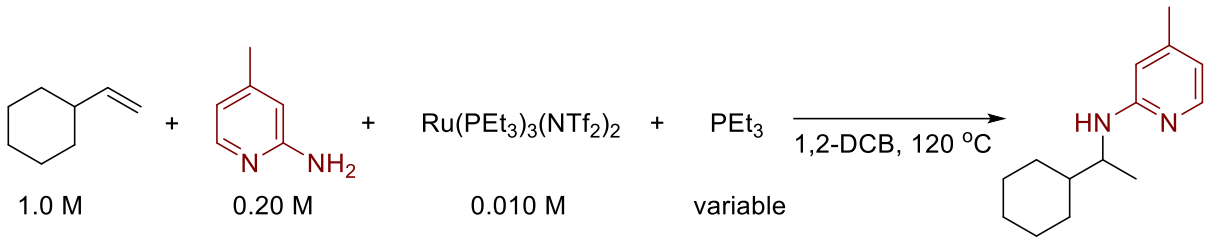


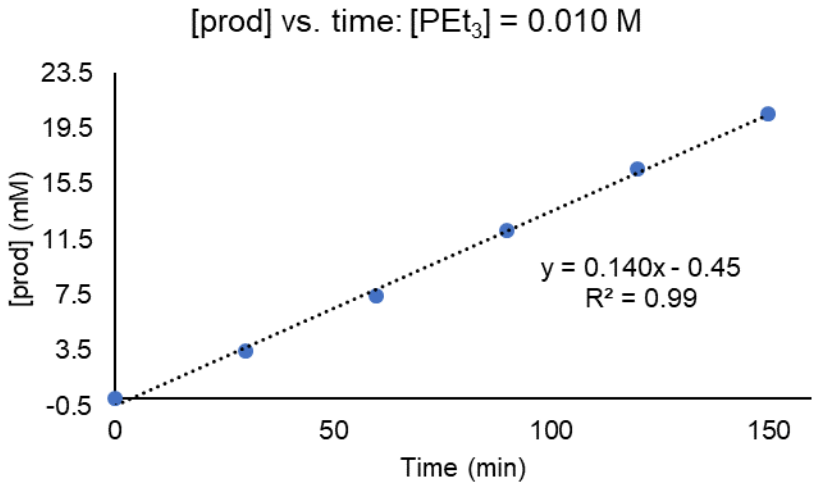


**Figure 2.21.** Rate of product formation as a function of time when [$PEt_3$] = 0.010 M.

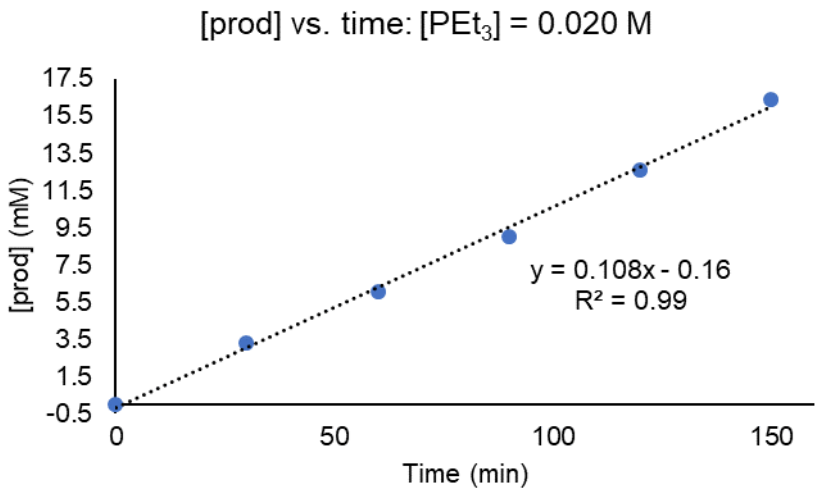


**Figure 2.22.** Rate of product formation as a function of time when [$PEt_3$] = 0.020 M.

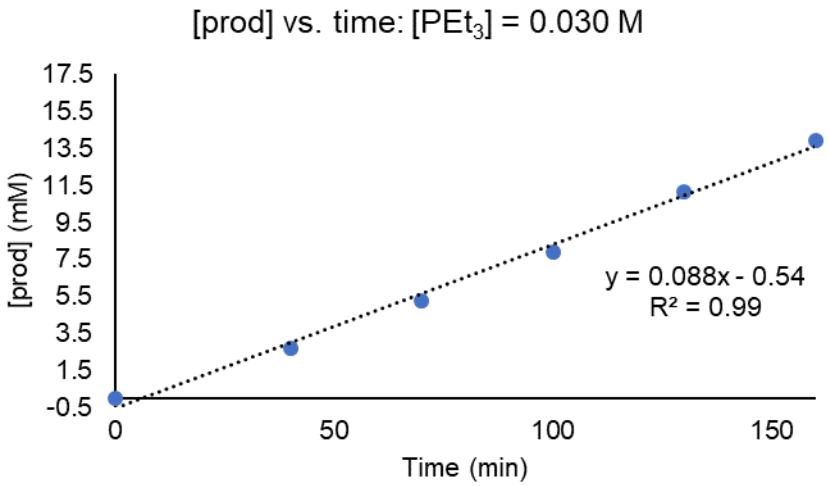


**Figure 2.23.** Rate of product formation as a function of time when [$PEt_3$] = 0.030 M.

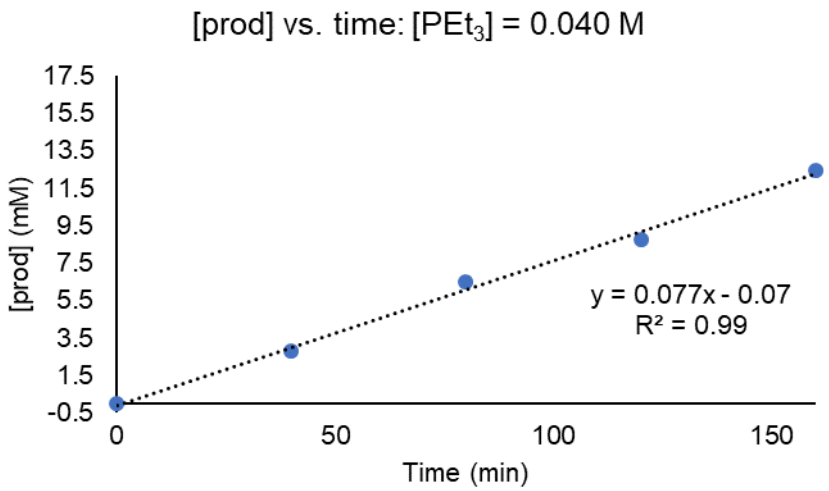


**Figure 2.24.** Rate of product formation as a function of time when [$PEt_3$] = 0.040 M.

### 2.4.8. Studies on the Origin of $PEt_3$ Inhibition

**Low Temperature NMR Spectroscopy**

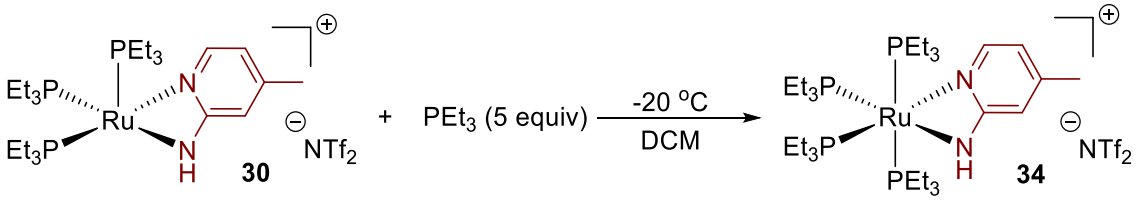


$Ru(PEt_3)_3$(amido)($NTf_2$) (**30**) (8.4 mg, 0.010 mmol), $PEt_3$ (5.9 mg, 7.4 µL, 0.050 mmol) were combined with $CD_2Cl_2$ (0.50 mL) in a J-young tube and $^{31}P$ NMR spectrum of this mixture was acquired at -20 ˚C (Figure S18).

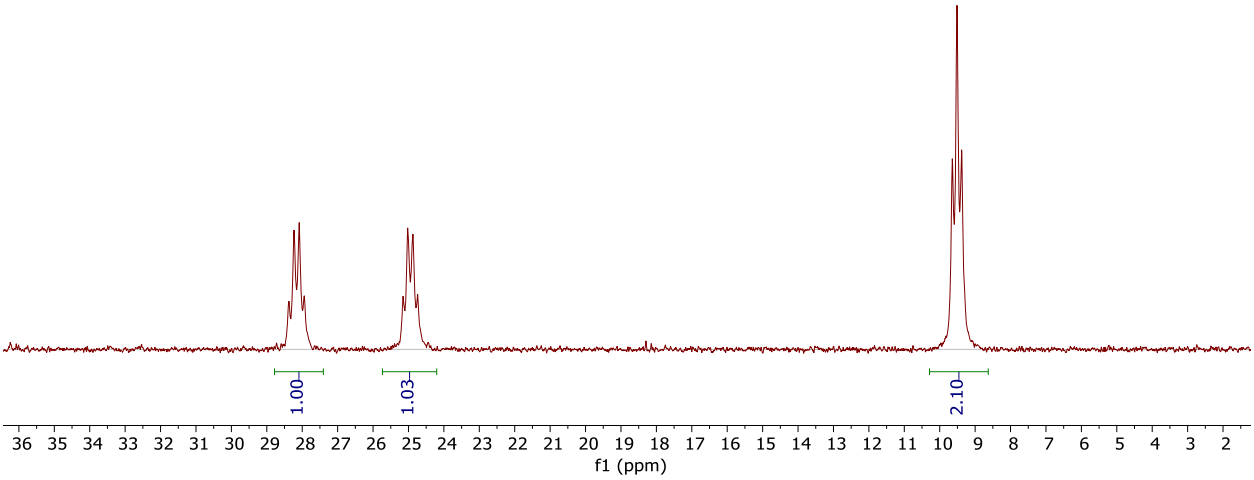


**Figure 2.25.** Low T NMR spectrum of Ru-amido complex with excess $PEt_3$ (the $PEt_3$ peak is not shown for clarity).

### 2.4.9. Deuterium Labelling Experiment

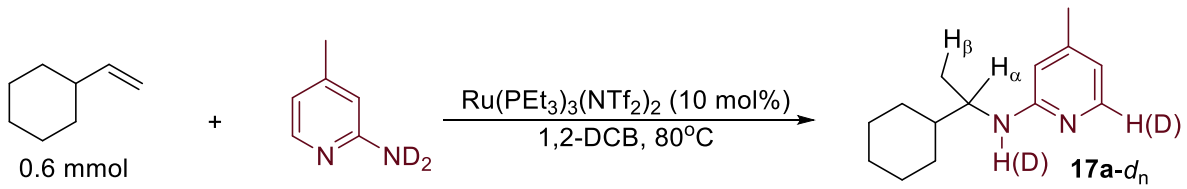


In a nitrogen-filled glovebox, vinylcyclohexane (66 µL, 53 mg, 0.48 mmol), 2-amino-4-methylpyridine-$d_2$ (66 mg, 0.60 mmol, 80% deuteration), $Ru(PEt_3)_3(NTf_2)_2$ (49 mg, 0.050 mmol, 10 mol%), 1,3,5-trimethoxybenzene (11 mg, 0.060 mmol) and DCB-$d_4$ (11 mg, 0.070 mmol) were dissolved in DCB (0.32 mL) in a 4 mL vial. After all the solid material was dissolved, the mixture was evenly distributed into 4 vials equipped with a stir bar. The mixture in each vial was heated at 80 ˚C for 0, 24, 36 and 48 hours respectively and analyzed by $^1H$ and $^2H$ NMR spectroscopy (Table 2.5).

| Reaction Time | % Yield | %D at $H_\alpha$ position | %D at $H_\beta$ position |
|---|---|---|---|
| 24h | 13% | 29% | 29% |
| 36h | 18% | 31% | 32% |
| 48h | 25% | 29% | 28% |

**Table 2.5.** % Yield and % D incorporation at $H_\alpha$ and $H_\beta$ position at 24, 36 and 48h of the reaction between vinylcyclohexane and 2-amino-4-methylpyridine-$D_2$.

### 2.4.10. Catalytic Hydroamination with Acetone as an Additive

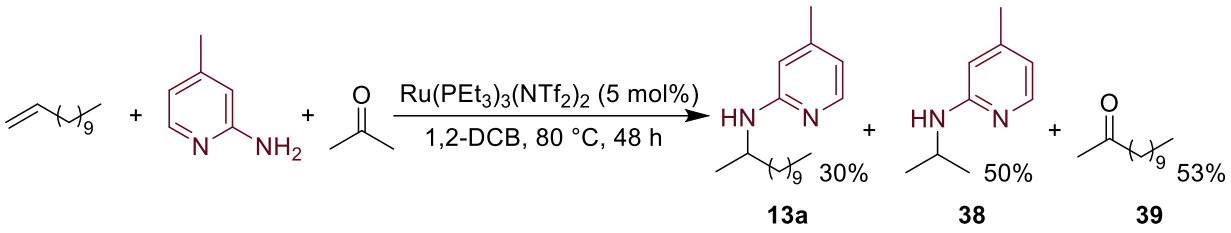


1-Dodecene (44 µL, 34 mg, 0.20 mmol), 2-amino-4-methylpyridine (22 mg, 0.20 mmol), acetone (15 µL, 0.20 mmol) and $Ru(PEt_3)_3(NTf_2)_2$ (10 mg, 0.010 mmol, 5.0 mol%) were combined with DCB (60 µL) and a magnetic stir bar in a one dram vial. The vial was capped, and the resulting mixture was heated at 80 ˚C with stirring for 48 hours. The mixture was allowed to cool and analyzed by $^1$H NMR spectroscopy using 1,3,5-trimethoxybenzene as the internal standard and gas chromatography.

### 2.4.11. Synthesis, Characterization, and Reactivity of the Hydridoruthenium Intermediate

#### Catalytic Imine Hydrogenation with $Ru(PEt_3)_3(NTf_2)_2$

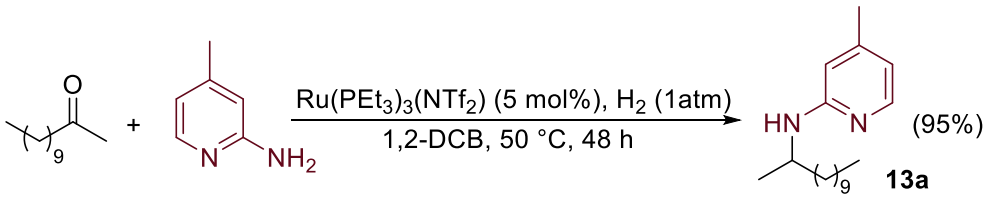


2-dodecanone (37 mg, 0.20 mmol), 2-amino-4-methylpyridine (22 mg, 0.20 mmol), $Ru(PEt_3)_3(amido)(NTf_2)$ (8.4 mg, 0.010 mmol, 5.0 mol%), 1,2-DCB (0.20 mL) and a magnetic stir bar were combined in a sealed tube equipped with a $H_2$ balloon. The flask was heated at 50 ˚C with stirring for 48 hours. The mixture was allowed to cool and analyzed by $^1$H NMR spectroscopy using 1,3,5-trimethoxybenzene as the internal standard.

#### Synthesis of the Potential Intermediate for Imine Hydrogenation

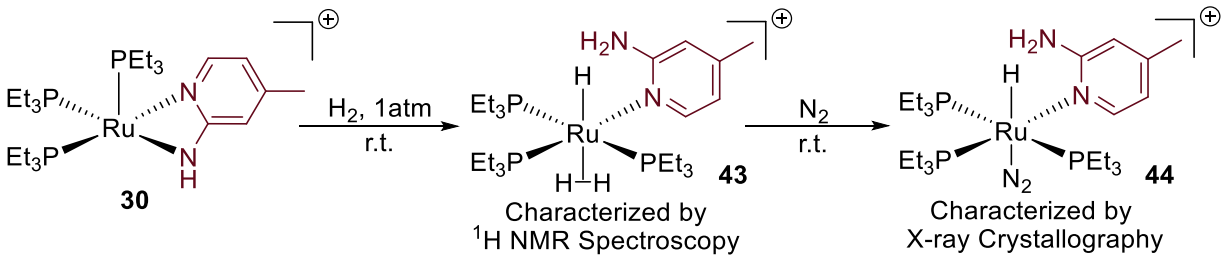

$Ru(PEt_3)_3(amido)(NTf_2)_2$ (**30**) (17 mg, 0.020 mmol) was dissolved in DCB-$D_4$ (0.50 mL) in a J-young tube. The tube was then sealed and connected to a Schlenk manifold and the $N_2$ atmosphere in the tube was removed by freeze-pump-thaw. $H_2$ (1.0 atm) was added to the tube and the mixture was allowed to warm to room temperature. The mixture turned yellow, and was analyzed by NMR spectroscopy (88% NMR yield before crystallization). $^1$H NMR (400 MHz, $CD_2Cl_2$) δ 7.67 (d, *J* = 5.5 Hz, 1H), 6.38 (s, 1H), 6.20 (d, *J* = 5.5 Hz, 1H), 5.91-6.68 (s, 2H), 2.19 (s, 3H), 1.55 – 1.21 (m, 18H), 1.02 (dp, *J* = 22.2, 7.7 Hz, 27H), -2.98 (s, 2H), -9.22 (q, *J* = 21.7 Hz, 1H). $^{31}$P NMR (162 MHz, $CD_2Cl_2$) δ 39.45, 28.16. Single crystals suitable for x-ray crystallography analysis was obtained by layering $^{i}Pr_2O$ and pentane onto the mixture. Due to the instability of this hydridoruthenium aminopyridyl complex **44**, we were unable to obtain high quality NMR spectroscopic data.

### 2.4.12. DFT Computational Studies

Initial conformational search and preoptimization of all reported structures were conducted using the (Geometry, Frequency, Noncovalent, eXtended Tight Binding") GFN-xTB method to account for the conformational flexibility of the triethylphosphine ligands.[42] The GFN2-xTB implementation of DFT tight binding was used and CREST was used for conformational search.[43-45] The ten GFN2-xTB optimized structures that was found by CREST with the lowest energies were then used as inputs for subsequent DFT optimization.

All DFT calculations were performed with the Gaussian 16 software package. Geometry optimization for all reported structures were performed in the gas-phase using the B3LYP-D3BJ /[6-31G+(d) + Lanl2dz (for Ru)] level of theory with the corresponding Hay-Wadt effective core potential for Ru and Grimme's empirical dispersion correction with Becke-Johnson damping for B3LYP.[46] Frequency calculations were performed on all reported structures to ensure that each minimum-energy structure has no imaginary frequencies and each transition state (TS) structure has precisely one imaginary frequency. Thermal corrections for Gibbs free energy (G) and enthalpy (H) were calculated at the same level of theory and the free energies were corrected at 353.15 K.[47] The electronic energy of every optimized structure was further recalculated under the B3LYP-D3BJ/[6-311+G(d,p) + SDD (for Ru)] level of theory. Bulk solvent effects were taken into consideration for single point energy calculations using the self-consistent reaction field SMD model (IEF-SMD) with chlorobenzene as the solvent.[48] The thermal corrections were applied to the recalculated electronic energies to give the final Gibbs free energy and enthalpy values.

### Energy Data for all Reported Structures

| Structures | E (Hartree) | ZPE (Hartree) | H (Hartree) | qh-G (Hartree) | Imaginary Frequency ($cm^{-1}$) |
|---|---|---|---|---|---|
| **Propene** | -117.954319 | -117.839391 | -117.834906 | -117.9012 | - |

| | | | | | |
|---|---|---|---|---|---|
| **1b** | -343.108724 | -342.876285 | -342.867932 | -343.01048 | - |
| **Enamine** | -459.863233 | -459.541634 | -459.529619 | -459.70979 | - |
| **Imine** | -459.866639 | -459.551747 | -459.539461 | -459.71122 | - |
| **Product** | -461.093957 | -460.749437 | -460.736895 | -460.91768 | - |
| **30** | -2175.003901 | -2172.772013 | -2172.728276 | -2174.3525 | - |
| **32** | -2292.961218 | -2290.616426 | -2290.569029 | -2292.2278 | - |
| **TS1** | -2292.941595 | -2290.601895 | -2290.555350 | -2292.2079 | -317.14 |
| **33** | -2292.97462 | -2290.634056 | -2290.586816 | -2292.2408 | - |
| **TS2** | -2292.954251 | -2290.611982 | -2290.565490 | -2292.2229 | -675.89 |
| **45** | -2292.971315 | -2290.629788 | -2290.581564 | -2292.2443 | - |
| **46** | -2176.216361 | -2173.964766 | -2173.920112 | -2175.5462 | - |

**Table 2.6**. Electronic energies (E), zero-point energy corrections (ZPE), enthalpies (H), quasi-harmonic Gibbs free energies calculated at T = 353.15 K (qh-G), and imaginary frequencies of all reported structures.

**Cartesian Coordinates (Å) of Optimized Structures**

**Propene**

| | | | |
|---|---|---|---|
| C | -1.28406500 | -0.22563000 | -0.00001400 |
| H | -1.29932000 | -1.31508800 | -0.00005000 |
| H | -2.24911000 | 0.27458000 | -0.00000100 |
| C | -0.13787900 | 0.46174400 | 0.00001200 |
| H | -0.18438100 | 1.55116000 | 0.00004700 |
| C | 1.24131500 | -0.15856800 | 0.00000200 |
| H | 1.39546000 | -0.79065500 | -0.88371300 |

| | | | |
|---|---|---|---|
| H | 2.02560000 | 0.60527300 | -0.00007300 |
| H | 1.39552300 | -0.79054300 | 0.88378700 |

**2-amino-4-methylpyridine (1b)**

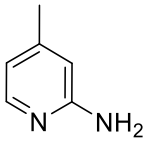

| | | | |
|---|---|---|---|
| C | -0.17223800 | 1.73587100 | 0.00297100 |
| C | 1.09708300 | 1.17006600 | 0.00476600 |
| C | 1.20812700 | -0.23240400 | 0.00135600 |
| C | 0.03309600 | -0.97481300 | -0.00708600 |
| C | -1.20890700 | -0.30551500 | -0.00701700 |
| N | -1.31276700 | 1.03013600 | 0.00176900 |
| H | -0.29218300 | 2.81770900 | 0.00712400 |
| H | 1.98143600 | 1.80094200 | 0.01027000 |
| H | 0.06601300 | -2.06170800 | -0.02373000 |
| C | 2.55914800 | -0.90161200 | 0.00244200 |
| H | 3.14255100 | -0.60542100 | -0.87791900 |
| H | 3.13889600 | -0.61176000 | 0.88735800 |
| H | 2.46819300 | -1.99236300 | -0.00197500 |
| N | -2.39959600 | -1.01293700 | -0.06880600 |
| H | -2.39936500 | -1.95095600 | 0.30905100 |
| H | -3.21685800 | -0.46639700 | 0.17449100 |

**4-methyl-N-(prop-1-en-2-yl)pyridin-2-amine (Enamine)**

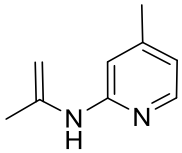

| | | | |
|---|---|---|---|
| C | -1.31701700 | 1.76455800 | 0.00032300 |
| C | -2.47834100 | 1.00608800 | 0.00021900 |

| | | | |
|---|---|---|---|
| C | -2.36369200 | -0.39833300 | -0.00004200 |
| C | -1.08688600 | -0.93843700 | -0.00015200 |
| C | 0.03903700 | -0.07882700 | 0.00003500 |
| N | -0.07482100 | 1.25303200 | 0.00023400 |
| H | -1.37078300 | 2.85180200 | 0.00049800 |
| H | -3.45221200 | 1.48742200 | 0.00032900 |
| H | -0.94829400 | -2.01788400 | -0.00037900 |
| C | -3.58991100 | -1.27504800 | -0.00021900 |
| H | -4.21077900 | -1.07872500 | 0.88247000 |
| H | -4.21078700 | -1.07835500 | -0.88281900 |
| H | -3.32600300 | -2.33732800 | -0.00044100 |
| N | 1.29728200 | -0.65695000 | -0.00001000 |
| H | 1.28553800 | -1.66711800 | -0.00023400 |
| C | 3.65415200 | -1.14870100 | 0.00048500 |
| H | 3.57812200 | -1.79252000 | 0.88800200 |
| H | 3.57739500 | -1.79446100 | -0.88556300 |
| H | 4.64614600 | -0.69188700 | -0.00045300 |
| C | 2.58059300 | -0.08624500 | -0.00018500 |
| C | 2.87098200 | 1.22688700 | -0.00068100 |
| H | 3.91408700 | 1.52592400 | -0.00070000 |
| H | 2.10682700 | 1.98890700 | -0.00097200 |

**N-(4-methylpyridin-2-yl)propan-2-imine (Imine)**

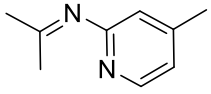


| | | | |
|---|---|---|---|
| C | 1.30737900 | 1.72942400 | -0.35818100 |
| C | 2.43384200 | 0.96695000 | -0.06674200 |
| C | 2.29078100 | -0.42129900 | 0.09666500 |
| C | 1.01288100 | -0.95302300 | -0.05259100 |
| C | -0.07222300 | -0.09889500 | -0.32239300 |

| | | | |
|---|---|---|---|
| N | 0.06926500 | 1.22692900 | -0.47834600 |
| H | 1.39457600 | 2.80504200 | -0.50226900 |
| H | 3.40777800 | 1.44135100 | 0.02130600 |
| H | 0.83258200 | -2.02055900 | 0.03121100 |
| C | 3.47926900 | -1.29552200 | 0.40695100 |
| H | 4.25717500 | -1.18688700 | -0.35849700 |
| H | 3.92940400 | -1.01784700 | 1.36815500 |
| H | 3.19671200 | -2.35149100 | 0.45757600 |
| N | -1.33190100 | -0.67931200 | -0.52111800 |
| C | -2.38935000 | -0.23799400 | 0.05165900 |
| C | -2.45443800 | 0.86636500 | 1.08272200 |
| H | -2.71942100 | 1.81184000 | 0.59377000 |
| H | -3.23148900 | 0.64401900 | 1.82310300 |
| H | -1.49839200 | 1.02015900 | 1.58632400 |
| C | -3.70625600 | -0.87301100 | -0.31167900 |
| H | -4.15272500 | -1.35941500 | 0.56611700 |
| H | -4.41859900 | -0.10609900 | -0.64435400 |
| H | -3.57046300 | -1.61140600 | -1.10465500 |

**N-isopropyl-4-methylpyridin-2-amine (Product)**

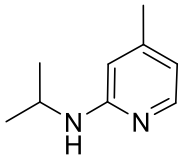


| | | | |
|---|---|---|---|
| C | -1.33402500 | 1.73458400 | -0.33785000 |
| N | -0.10699300 | 1.18980700 | -0.34158200 |
| C | -0.02051100 | -0.13596000 | -0.15371300 |
| C | -1.16241100 | -0.94645300 | 0.05939100 |
| C | -2.42310000 | -0.36896500 | 0.06477400 |
| C | -2.50921900 | 1.02225700 | -0.14348200 |

| | | | |
|---|---|---|---|
| H | -3.47003100 | 1.52914900 | -0.14836500 |
| C | -3.66508200 | -1.19486700 | 0.28513400 |
| H | -4.34070200 | -1.12157400 | -0.57600000 |
| H | -4.22013300 | -0.84082400 | 1.16257500 |
| H | -3.42427900 | -2.25159000 | 0.43862500 |
| H | -1.04569600 | -2.01795300 | 0.20846400 |
| N | 1.23087000 | -0.71107000 | -0.20851600 |
| H | 1.29215000 | -1.65358500 | 0.15618800 |
| C | 2.46694200 | 0.07156600 | -0.14800300 |
| C | 3.62131000 | -0.79669400 | -0.65042400 |
| H | 3.43224100 | -1.14890200 | -1.67011600 |
| H | 4.55785600 | -0.22862000 | -0.64535400 |
| H | 3.76503800 | -1.67395500 | -0.00382500 |
| C | 2.73107900 | 0.62250700 | 1.26008400 |
| H | 2.87374300 | -0.19747100 | 1.97648700 |
| H | 1.88853300 | 1.23588200 | 1.59269900 |
| H | 3.63476700 | 1.24436700 | 1.27044800 |
| H | 2.32448800 | 0.91477800 | -0.82956400 |
| H | -1.36500900 | 2.81128900 | -0.49703200 |

**Ru-amido Complex (30)**

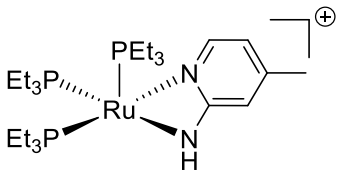


| | | | |
|---|---|---|---|
| Ru | -0.07138200 | 0.15865700 | 0.25365000 |
| P | 1.98491600 | 1.10000900 | 0.74982600 |
| P | 0.06219400 | 0.43212600 | -1.97919300 |
| P | 0.59690500 | -2.09083500 | 0.32812900 |
| N | -2.30716200 | -0.03759400 | 0.32122600 |

| | | | |
|---|---|---|---|
| N | -1.19644900 | 1.81014100 | 0.84771500 |
| C | -3.40275800 | -0.80707600 | 0.24402200 |
| H | -3.25958800 | -1.82580600 | -0.10167300 |
| C | -4.66839200 | -0.34715600 | 0.56838200 |
| H | -5.52607900 | -1.00511300 | 0.47486200 |
| C | -4.82074300 | 0.98579600 | 1.01532000 |
| C | -6.18543300 | 1.51572100 | 1.36788700 |
| H | -6.14284100 | 2.55854800 | 1.69446900 |
| H | -6.63535500 | 0.92221500 | 2.17290200 |
| H | -6.86085300 | 1.45308800 | 0.50617800 |
| C | -3.68656100 | 1.78263100 | 1.12576900 |
| H | -3.75561500 | 2.80651500 | 1.48236400 |
| C | -2.42582100 | 1.24841800 | 0.78415900 |
| C | 1.85185800 | 2.95274800 | 0.81181500 |
| H | 1.37312100 | 3.27062500 | -0.11753700 |
| H | 1.12405000 | 3.15638900 | 1.60473900 |
| C | 3.12965100 | 3.76459900 | 1.04886000 |
| H | 3.83682200 | 3.66077800 | 0.22013400 |
| H | 3.64075300 | 3.47471900 | 1.97256300 |
| H | 2.88075500 | 4.82822500 | 1.13390200 |
| C | 3.49644800 | 0.75593000 | -0.28248800 |
| H | 3.36091100 | -0.24614700 | -0.69719800 |
| H | 3.45010500 | 1.44548400 | -1.13476000 |
| C | 4.87038700 | 0.84545400 | 0.39631100 |
| H | 5.65711900 | 0.62630800 | -0.33408300 |
| H | 4.96765100 | 0.11902000 | 1.20848300 |
| H | 5.06823500 | 1.83647000 | 0.80968400 |
| C | 2.48158000 | 0.69129400 | 2.49267300 |
| H | 2.82067300 | -0.34844900 | 2.50967800 |
| H | 3.34343700 | 1.30625900 | 2.77322900 |

| | | | |
|---|---|---|---|
| C | 1.33609000 | 0.88399200 | 3.49491900 |
| H | 0.46736200 | 0.26785900 | 3.24188300 |
| H | 0.99603100 | 1.92316900 | 3.53242000 |
| H | 1.66340500 | 0.60520900 | 4.50214000 |
| C | -1.57702100 | 0.28434100 | -2.83364900 |
| H | -2.28935500 | 0.85432500 | -2.23045300 |
| H | -1.48349900 | 0.79978500 | -3.79764600 |
| C | -2.08652200 | -1.14206500 | -3.04341500 |
| H | -3.06975100 | -1.12097300 | -3.52497200 |
| H | -2.19214700 | -1.66588100 | -2.09412700 |
| H | -1.41850800 | -1.72796100 | -3.68334500 |
| C | 1.18345400 | -0.67504600 | -2.95880100 |
| H | 2.18532800 | -0.55966800 | -2.53337900 |
| H | 0.87098500 | -1.70015100 | -2.73657800 |
| C | 1.22678700 | -0.46051400 | -4.47787300 |
| H | 0.23218200 | -0.51685200 | -4.93073900 |
| H | 1.84419200 | -1.23693400 | -4.94285300 |
| H | 1.66546400 | 0.50554700 | -4.74341700 |
| C | 0.58785300 | 2.12797300 | -2.52011200 |
| H | 1.56785700 | 2.33153500 | -2.07709000 |
| H | 0.73954000 | 2.09036100 | -3.60438700 |
| C | -0.41249600 | 3.23728600 | -2.17602200 |
| H | -1.32876000 | 3.13993300 | -2.76651200 |
| H | 0.01916500 | 4.21909300 | -2.39872200 |
| H | -0.69621500 | 3.20554400 | -1.12150900 |
| C | 0.46357700 | -2.60157700 | 2.11116900 |
| H | 0.72642800 | -3.66162900 | 2.20326100 |
| H | 1.21979600 | -2.04182600 | 2.67072200 |
| C | -0.92834400 | -2.33698000 | 2.70077400 |
| H | -1.70538600 | -2.90472400 | 2.17900000 |

| | | | |
|---|---|---|---|
| H | -1.20563400 | -1.27971000 | 2.63500300 |
| H | -0.95596400 | -2.62690000 | 3.75636100 |
| C | -0.56504800 | -3.27557500 | -0.51754600 |
| H | -1.57074300 | -2.87376500 | -0.37813200 |
| H | -0.35702100 | -3.20289100 | -1.59132500 |
| C | -0.52743500 | -4.74107300 | -0.06890900 |
| H | -1.19845200 | -5.33883500 | -0.69560500 |
| H | -0.85861400 | -4.85590300 | 0.96749700 |
| H | 0.47169500 | -5.18095400 | -0.15240500 |
| C | 2.24590900 | -2.79891200 | -0.19589900 |
| H | 2.08068300 | -3.84668400 | -0.46823100 |
| H | 2.53686700 | -2.28657400 | -1.11736100 |
| C | 3.38012600 | -2.72495700 | 0.83144400 |
| H | 4.30324500 | -3.12556100 | 0.39868000 |
| H | 3.15448200 | -3.31224900 | 1.72627700 |
| H | 3.58649600 | -1.70035800 | 1.14627200 |
| H | -1.14145300 | 2.78574500 | 1.11397100 |

**Ru-alkene Complex (32)**

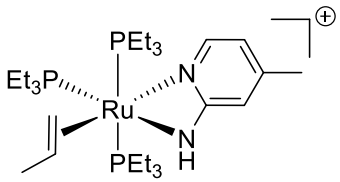


| | | | |
|---|---|---|---|
| Ru | 0.03345800 | -0.16157800 | -0.56441800 |
| P | 0.93189200 | -1.76775000 | 0.97999000 |
| C | 0.80642200 | -1.05241600 | 2.70460900 |
| H | 0.82384500 | 0.03041200 | 2.57591500 |
| H | -0.20198900 | -1.30384400 | 3.05533000 |
| C | 1.83758200 | -1.44061300 | 3.77176400 |
| H | 2.84033200 | -1.08519400 | 3.51377200 |

| | | | |
|---|---|---|---|
| H | 1.56426300 | -0.97334000 | 4.72460400 |
| H | 1.89510500 | -2.51904700 | 3.93814100 |
| C | 2.72086500 | -2.30283700 | 0.89214000 |
| C | 3.08841300 | -3.40476000 | -0.11041300 |
| H | 4.14571600 | -3.66428600 | 0.01183600 |
| H | 2.94408300 | -3.10608400 | -1.14926600 |
| H | 2.50989700 | -4.31826800 | 0.05564100 |
| H | 3.32876500 | -1.41333400 | 0.71201200 |
| H | 2.98832600 | -2.65075200 | 1.89337100 |
| C | 0.07681900 | -3.41260100 | 1.12765800 |
| H | -0.98904500 | -3.20076200 | 1.23277700 |
| C | 0.51892200 | -4.34463500 | 2.26244600 |
| H | 1.59181000 | -4.55695900 | 2.23770600 |
| H | 0.27927500 | -3.92272600 | 3.24280800 |
| H | -0.00711900 | -5.30243400 | 2.18180700 |
| H | 0.19593100 | -3.91114200 | 0.15911600 |
| P | 2.16788100 | 1.05852300 | -0.50793600 |
| C | 2.85823100 | 1.47733700 | 1.17506600 |
| H | 2.88794500 | 0.55595700 | 1.76384100 |
| C | 2.09630500 | 2.56778300 | 1.93711100 |
| H | 2.16364800 | 3.53364900 | 1.42749600 |
| H | 1.03883200 | 2.33275000 | 2.05520500 |
| H | 2.53180400 | 2.69404700 | 2.93463800 |
| H | 3.89823800 | 1.78956700 | 1.04881900 |
| C | 2.06992900 | 2.73492800 | -1.29989300 |
| C | 3.36654700 | 3.55074200 | -1.35020200 |
| H | 4.13187200 | 3.06352600 | -1.96235900 |
| H | 3.78855700 | 3.72167700 | -0.35468900 |
| H | 3.17055800 | 4.53273900 | -1.79528800 |
| H | 1.68512100 | 2.57466800 | -2.31158800 |

| | | | |
|---|---|---|---|
| H | 1.28815900 | 3.28362600 | -0.76636000 |
| C | 3.63582500 | 0.28098600 | -1.38988300 |
| C | 5.03623600 | 0.44380000 | -0.78508100 |
| H | 5.33047100 | 1.49204200 | -0.68675100 |
| H | 5.11341200 | -0.02068000 | 0.20348400 |
| H | 5.77098100 | -0.04585700 | -1.43413600 |
| H | 3.42403400 | -0.78398000 | -1.50376700 |
| H | 3.62981000 | 0.69626400 | -2.40392800 |
| H | 0.30984700 | 1.18484700 | -3.72579500 |
| C | 0.79240500 | 0.20400600 | -3.68911200 |
| H | 0.74440600 | -0.21331200 | -4.70466700 |
| H | 1.84606900 | 0.34180900 | -3.44213900 |
| C | 0.10289500 | -0.74398100 | -2.74602800 |
| C | 0.76610000 | -1.73052400 | -2.02403300 |
| H | 0.27610800 | -2.67133500 | -1.80016100 |
| H | 1.84480500 | -1.77723500 | -2.08220900 |
| H | -0.93848700 | -0.91231400 | -2.99641600 |
| P | -2.20956300 | -1.06475400 | -0.51818800 |
| C | -3.50243900 | 0.02594800 | -1.28522100 |
| C | -3.40586100 | 0.17850700 | -2.80617000 |
| H | -3.47232500 | -0.78430900 | -3.32482600 |
| H | -4.23260400 | 0.79947700 | -3.16845600 |
| H | -2.47172100 | 0.66350500 | -3.09518000 |
| H | -4.48199700 | -0.38038000 | -1.01711300 |
| H | -3.42417500 | 1.00543000 | -0.80707000 |
| C | -2.85809800 | -1.36855300 | 1.21672000 |
| H | -2.03233500 | -1.14307500 | 1.89403400 |
| C | -4.09547100 | -0.57790200 | 1.65888800 |
| H | -3.94397500 | 0.50076500 | 1.56206900 |
| H | -4.98582500 | -0.85362700 | 1.08665900 |

| | | | |
|---|---|---|---|
| H | -4.30531600 | -0.78912500 | 2.71356000 |
| H | -3.05791100 | -2.44199800 | 1.31269300 |
| C | -2.51903900 | -2.69652600 | -1.35932900 |
| H | -1.89288300 | -3.43620400 | -0.85041600 |
| C | -3.97759900 | -3.17096300 | -1.38448400 |
| H | -4.03999000 | -4.17218800 | -1.82480800 |
| H | -4.60993800 | -2.50912700 | -1.98332700 |
| H | -4.40824400 | -3.22734000 | -0.37884500 |
| H | -2.13241400 | -2.62632100 | -2.38210000 |
| N | -0.81091400 | 1.64388600 | -1.33611100 |
| C | -1.18931700 | 2.18079200 | -0.18090000 |
| N | -0.89783500 | 1.29122200 | 0.82957600 |
| C | -1.31052900 | 1.56712400 | 2.08141800 |
| C | -1.96149900 | 2.73931100 | 2.41214700 |
| C | -2.20860600 | 3.70651300 | 1.40269200 |
| C | -1.81777500 | 3.42140800 | 0.10541800 |
| H | -2.00414000 | 4.12127700 | -0.70470800 |
| C | -2.88990900 | 5.00335200 | 1.75178400 |
| H | -3.02393500 | 5.63952300 | 0.87229000 |
| H | -2.30499100 | 5.56157500 | 2.49287300 |
| H | -3.87594800 | 4.81813300 | 2.19483700 |
| H | -2.26864200 | 2.91562700 | 3.43772800 |
| H | -1.10002500 | 0.82331500 | 2.84033200 |
| H | -0.86423100 | 2.19640300 | -2.18154000 |

**Migratory Insertion TS (TS1)**

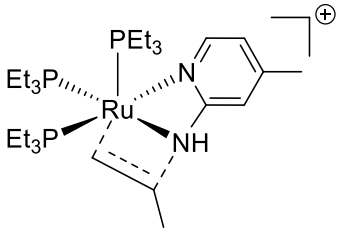


| | | | |
|---|---|---|---|
| Ru | 0.07116900 | -0.06715500 | -0.42929400 |
| P | 2.10440500 | -1.22477700 | -0.37085200 |
| P | -0.40697100 | -0.31733700 | 1.88365700 |
| P | 1.06451100 | 2.02978400 | -0.25046100 |
| N | -2.08425100 | 0.42635200 | -0.56575500 |
| C | -3.02086100 | 1.35290600 | -0.29386700 |
| H | -2.66261700 | 2.34916900 | -0.06291100 |
| C | -4.37639600 | 1.07204700 | -0.29752600 |
| H | -5.09022000 | 1.85805900 | -0.07232000 |
| C | -4.81601900 | -0.23693300 | -0.60005800 |
| C | -6.28529800 | -0.56622200 | -0.61237800 |
| H | -6.81155000 | 0.03630000 | -1.36250400 |
| H | -6.74350900 | -0.34315300 | 0.35851900 |
| H | -6.46066800 | -1.62163700 | -0.83912400 |
| C | -3.85276300 | -1.19640400 | -0.88905100 |
| H | -4.13505000 | -2.21900700 | -1.12437900 |
| C | -2.48787200 | -0.84481200 | -0.85848000 |
| C | 1.94797900 | -3.01170800 | 0.12987500 |
| H | 2.94391000 | -3.40725700 | 0.34768000 |
| H | 1.38729000 | -3.03706600 | 1.06751000 |
| C | 1.26266500 | -3.90138500 | -0.91226100 |
| H | 1.11096300 | -4.90847200 | -0.50901600 |
| H | 1.86657200 | -4.00034200 | -1.81988000 |
| H | 0.28790000 | -3.50382700 | -1.19988700 |
| C | 3.45059300 | -0.56455500 | 0.75369300 |

| | | | |
|---|---|---|---|
| H | 4.07090400 | 0.08985800 | 0.12822800 |
| H | 2.95889400 | 0.08744800 | 1.47332600 |
| C | 4.34040800 | -1.55722800 | 1.51182600 |
| H | 4.88097900 | -2.23468300 | 0.84595200 |
| H | 3.75824500 | -2.16613400 | 2.21086500 |
| H | 5.08528200 | -1.00797500 | 2.09896000 |
| C | 3.01724600 | -1.38264300 | -1.98981900 |
| H | 2.32574900 | -1.84420900 | -2.70300100 |
| H | 3.19058800 | -0.36436700 | -2.35448000 |
| C | 4.34263600 | -2.15315500 | -1.97630500 |
| H | 4.74922000 | -2.21199900 | -2.99216200 |
| H | 4.22296300 | -3.17826800 | -1.61162100 |
| H | 5.09337600 | -1.65805700 | -1.35326500 |
| C | -1.09741400 | 1.26029900 | 2.63491800 |
| H | -0.30572600 | 1.69137300 | 3.25889000 |
| H | -1.23990600 | 1.95333800 | 1.80365600 |
| C | -2.40075500 | 1.17045100 | 3.43727800 |
| H | -2.29942400 | 0.54080900 | 4.32600300 |
| H | -3.21940700 | 0.77263700 | 2.82973500 |
| H | -2.69487500 | 2.17095800 | 3.77494900 |
| C | 0.89535800 | -0.78892600 | 3.13278200 |
| H | 1.37590300 | -1.70643900 | 2.77857400 |
| H | 1.66750900 | -0.01399300 | 3.09516200 |
| C | 0.42259900 | -0.96696400 | 4.58038500 |
| H | -0.04524200 | -0.05703000 | 4.96964400 |
| H | 1.27538800 | -1.19985400 | 5.22789300 |
| H | -0.29712200 | -1.78503700 | 4.67900100 |
| C | -1.72364000 | -1.58381000 | 2.23271000 |
| H | -2.06467300 | -1.46117400 | 3.26437300 |
| H | -2.57866500 | -1.34964100 | 1.59380200 |

| | | | |
|---|---|---|---|
| C | -1.27273300 | -3.02936500 | 2.00277800 |
| H | -2.11286800 | -3.71592300 | 2.15575000 |
| H | -0.48185600 | -3.32428800 | 2.70117300 |
| H | -0.89835600 | -3.17167000 | 0.98711400 |
| C | 2.37092400 | 2.38142400 | -1.52967000 |
| H | 3.16228200 | 1.64173300 | -1.36515100 |
| H | 1.93415000 | 2.14667100 | -2.50525300 |
| C | 2.97551000 | 3.78980400 | -1.54563000 |
| H | 2.22291400 | 4.55634100 | -1.75499500 |
| H | 3.73910300 | 3.86024400 | -2.32834300 |
| H | 3.45816100 | 4.03917700 | -0.59534300 |
| C | -0.11628400 | 3.44494200 | -0.51994200 |
| H | -0.87698400 | 3.38953600 | 0.26571900 |
| H | 0.42676600 | 4.37755900 | -0.34403600 |
| C | -0.77461100 | 3.48867800 | -1.90170600 |
| H | -1.37222200 | 2.59612400 | -2.09330200 |
| H | -0.02986500 | 3.57481900 | -2.69984700 |
| H | -1.43380000 | 4.36086500 | -1.97474300 |
| C | 1.94799800 | 2.52821100 | 1.33238100 |
| H | 1.65517900 | 1.80497700 | 2.09476100 |
| H | 3.01682800 | 2.36451800 | 1.15398700 |
| C | 1.72785300 | 3.94222500 | 1.88412400 |
| H | 0.67506900 | 4.12754900 | 2.11974600 |
| H | 2.05926900 | 4.71837900 | 1.18873200 |
| H | 2.29924300 | 4.06643100 | 2.81110000 |
| N | -1.40232200 | -1.62694800 | -1.08694300 |
| H | -1.59325100 | -2.62208600 | -1.14613900 |
| C | -0.62186800 | -1.09985600 | -2.97141800 |
| H | -0.05967200 | -2.03090300 | -3.00551600 |
| C | -1.90563100 | -1.09516400 | -3.74469200 |

| | | | |
|---|---|---|---|
| H | -1.65290100 | -1.02124800 | -4.81230900 |
| H | -2.49452900 | -2.00559500 | -3.60005500 |
| H | -2.52120600 | -0.22588100 | -3.49453800 |
| C | 0.10438200 | 0.08363800 | -2.72471100 |
| H | -0.37249300 | 1.00741000 | -3.04066500 |
| H | 1.16942500 | 0.04592000 | -2.91475700 |

**Ru-alkyl Complex (33)**

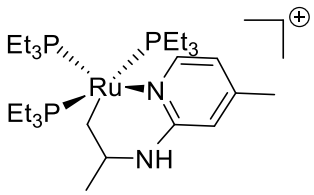


| | | | |
|---|---|---|---|
| Ru | -0.16285900 | -0.00105500 | -0.04158900 |
| P | -2.46903900 | -0.38545800 | 0.09894800 |
| C | -3.29195100 | -1.05758100 | -1.42954300 |
| H | -2.74728800 | -1.95730000 | -1.72806300 |
| H | -4.31167300 | -1.37352300 | -1.19057500 |
| C | -3.30924400 | -0.05599400 | -2.58955500 |
| H | -3.92349100 | 0.82018800 | -2.35673100 |
| H | -2.30305700 | 0.29543100 | -2.83407500 |
| H | -3.72810700 | -0.51959400 | -3.48916000 |
| C | -3.57810800 | 1.05471200 | 0.51273400 |
| C | -5.08651700 | 0.79451700 | 0.58975000 |
| H | -5.61454000 | 1.72700200 | 0.81949900 |
| H | -5.33580500 | 0.07742900 | 1.37718500 |
| H | -5.48920500 | 0.41492700 | -0.35467700 |
| H | -3.22447400 | 1.43039400 | 1.47829600 |
| H | -3.37644800 | 1.84729800 | -0.21197800 |
| C | -2.94885300 | -1.56512000 | 1.47711400 |
| H | -2.03854300 | -2.08514600 | 1.77909300 |

| | | | |
|---|---|---|---|
| C | -4.06499700 | -2.58193100 | 1.21203700 |
| H | -3.80844400 | -3.26548800 | 0.39688000 |
| H | -4.23279300 | -3.18960100 | 2.10870100 |
| H | -5.01446100 | -2.10356700 | 0.95735000 |
| H | -3.21830700 | -0.92979600 | 2.32970800 |
| P | -0.32990300 | 2.37791200 | -0.13988600 |
| C | -1.18071600 | 2.97795700 | -1.68285600 |
| H | -2.19794200 | 2.57853100 | -1.68319300 |
| C | -0.44788900 | 2.51699200 | -2.94865100 |
| H | 0.54313400 | 2.97435400 | -3.03361800 |
| H | -0.31554700 | 1.42881700 | -2.96024000 |
| H | -1.01602200 | 2.78884400 | -3.84445100 |
| H | -1.26795300 | 4.06830600 | -1.67221600 |
| C | 1.31088500 | 3.25686700 | -0.26642100 |
| C | 1.26560300 | 4.78004700 | -0.42772600 |
| H | 0.75155200 | 5.08054400 | -1.34654700 |
| H | 2.28439400 | 5.18074000 | -0.47864900 |
| H | 0.76504100 | 5.26945100 | 0.41363500 |
| H | 1.87343900 | 2.99002300 | 0.63519500 |
| H | 1.86376600 | 2.81085000 | -1.09741400 |
| C | -1.11192700 | 3.31414400 | 1.28381800 |
| C | -2.09051700 | 4.44375900 | 0.94269200 |
| H | -1.61619400 | 5.23736600 | 0.35836000 |
| H | -2.95088900 | 4.07795100 | 0.37346100 |
| H | -2.47412200 | 4.89574900 | 1.86435600 |
| H | -1.60491200 | 2.57796200 | 1.92209400 |
| H | -0.27919400 | 3.71055900 | 1.87720900 |
| P | 0.37256900 | -2.35707800 | -0.32009900 |
| C | 1.85535800 | -3.06468900 | 0.55141100 |
| C | 1.63734600 | -3.39135100 | 2.03201800 |

| | | | |
|---|---|---|---|
| H | 0.84006200 | -4.12887500 | 2.17521200 |
| H | 2.55190900 | -3.81284000 | 2.46415300 |
| H | 1.38435600 | -2.49351600 | 2.60020400 |
| H | 2.16275800 | -3.96426700 | 0.00467300 |
| H | 2.66739300 | -2.34140200 | 0.43945500 |
| C | 0.93363300 | -2.53177300 | -2.08519500 |
| H | 1.11802400 | -3.58741800 | -2.31079900 |
| C | -0.04263900 | -1.92333600 | -3.09568700 |
| H | -0.25572900 | -0.87265500 | -2.86260900 |
| H | 0.36561600 | -1.96376700 | -4.11144000 |
| H | -1.00082100 | -2.45267500 | -3.10386900 |
| H | 1.90479000 | -2.02988100 | -2.14769800 |
| C | -0.86658900 | -3.73750800 | -0.13460400 |
| H | -1.75851900 | -3.44342800 | -0.69506100 |
| C | -0.42615400 | -5.14346900 | -0.55729500 |
| H | -1.23831300 | -5.85658900 | -0.37651200 |
| H | 0.44375600 | -5.48920200 | 0.00948500 |
| H | -0.17907100 | -5.19558600 | -1.62212600 |
| H | -1.16736000 | -3.74883800 | 0.91761800 |
| C | -0.10531400 | 0.01980300 | 2.04238500 |
| C | 1.13555600 | 0.68159500 | 2.62198000 |
| N | 2.38522400 | 0.05751200 | 2.14725700 |
| C | 2.86555400 | 0.15030400 | 0.86849500 |
| N | 1.99995800 | 0.24902900 | -0.16238400 |
| C | 2.51364300 | 0.35490700 | -1.41239400 |
| C | 3.85893300 | 0.31742400 | -1.70363200 |
| C | 4.77981700 | 0.16680500 | -0.64124400 |
| C | 4.26299800 | 0.09309300 | 0.64037200 |
| H | 4.92842800 | 0.00072000 | 1.49478800 |
| C | 6.26004300 | 0.11230900 | -0.90520000 |

| | | | |
|---|---|---|---|
| H | 6.83216400 | -0.00138800 | 0.01970800 |
| H | 6.59871800 | 1.02608800 | -1.40790700 |
| H | 6.50509000 | -0.72815700 | -1.56555400 |
| H | 4.19610000 | 0.40229500 | -2.73165700 |
| H | 1.77880300 | 0.46647400 | -2.20407300 |
| H | 3.12004300 | 0.04430900 | 2.84364900 |
| C | 1.14652200 | 0.61529100 | 4.15416900 |
| H | 2.01591400 | 1.13562600 | 4.57740200 |
| H | 0.24706700 | 1.09171600 | 4.55463300 |
| H | 1.16026200 | -0.42600900 | 4.49675700 |
| H | 1.14603400 | 1.74182900 | 2.33102000 |
| H | -0.97364500 | 0.55971500 | 2.44181200 |
| H | -0.16747600 | -1.00764200 | 2.41685600 |

**BHE TS (TS2)**

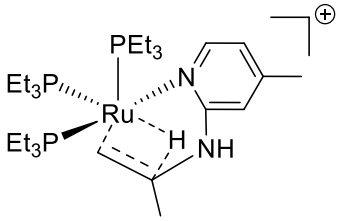


| | | | |
|---|---|---|---|
| Ru | -0.04283900 | -0.19725900 | -0.40840600 |
| P | -2.37676400 | -0.46095000 | -0.62340700 |
| C | -3.45019900 | 0.61561200 | 0.47526300 |
| H | -2.82962200 | 0.89899600 | 1.32412900 |
| H | -3.63449200 | 1.53796900 | -0.08743000 |
| C | -4.78164200 | 0.06026900 | 0.99828400 |
| H | -5.46137400 | -0.23732300 | 0.19635500 |
| H | -4.63326800 | -0.80658900 | 1.64963300 |
| H | -5.28815200 | 0.82992900 | 1.59186000 |
| C | -3.06148300 | -2.16056300 | -0.27319600 |

| | | | |
|---|---|---|---|
| C | -2.54040500 | -3.29246400 | -1.15790500 |
| H | -2.81281200 | -3.14754300 | -2.20810200 |
| H | -2.97472500 | -4.24596200 | -0.83767500 |
| H | -1.45289600 | -3.37986200 | -1.09532100 |
| H | -2.84022500 | -2.38831800 | 0.77320900 |
| H | -4.15115100 | -2.10741700 | -0.34854300 |
| C | -3.07519100 | -0.10674900 | -2.31508300 |
| H | -2.72251800 | 0.89308100 | -2.58826500 |
| C | -4.59486400 | -0.18890700 | -2.49603300 |
| H | -5.11786700 | 0.55796700 | -1.89159100 |
| H | -4.85382000 | 0.00032500 | -3.54386400 |
| H | -4.99039700 | -1.17577000 | -2.23533900 |
| H | -2.58632500 | -0.79296800 | -3.01246300 |
| P | -0.08552100 | -1.16270200 | 1.80376900 |
| C | -1.56384900 | -0.93556000 | 2.92723400 |
| H | -1.65139200 | 0.14160000 | 3.10565200 |
| C | -1.57269400 | -1.68221100 | 4.26647400 |
| H | -0.71708800 | -1.41814400 | 4.89532200 |
| H | -2.47965800 | -1.42746700 | 4.82658200 |
| H | -1.56843200 | -2.76779300 | 4.13026200 |
| H | -2.45345200 | -1.21047600 | 2.35652700 |
| C | 1.28919800 | -0.79646600 | 3.01130100 |
| C | 1.23778500 | 0.59570400 | 3.64858900 |
| H | 2.12829600 | 0.77152300 | 4.26217300 |
| H | 0.36482400 | 0.71054200 | 4.29919800 |
| H | 1.18605900 | 1.39215500 | 2.89961600 |
| H | 1.25120400 | -1.56331800 | 3.79354100 |
| H | 2.23744400 | -0.94533700 | 2.48943400 |
| C | 0.06648800 | -3.01826400 | 1.73356200 |
| C | 1.33528700 | -3.50693300 | 1.02626600 |

| | | | |
|---|---|---|---|
| H | 1.38485800 | -3.13578500 | -0.00174800 |
| H | 2.24137000 | -3.17767200 | 1.54654800 |
| H | 1.35339400 | -4.60192900 | 0.99482600 |
| H | 0.03695300 | -3.41284500 | 2.75501600 |
| H | -0.81920800 | -3.39886800 | 1.21363200 |
| P | -0.20971700 | 2.17516200 | 0.00797900 |
| C | 1.35118500 | 3.19768800 | -0.07717000 |
| C | 2.12310200 | 3.10371600 | -1.39641800 |
| H | 2.98172800 | 3.78396100 | -1.37386400 |
| H | 2.50141400 | 2.09555900 | -1.57390900 |
| H | 1.50127500 | 3.38942300 | -2.25134800 |
| H | 1.06586100 | 4.23713300 | 0.10512900 |
| H | 2.00003100 | 2.91964700 | 0.75706500 |
| C | -1.00558300 | 2.80422500 | 1.59463500 |
| H | -1.01141800 | 1.96042600 | 2.28825100 |
| C | -0.39757800 | 4.02420000 | 2.29776300 |
| H | -0.42718300 | 4.92222100 | 1.67434400 |
| H | -0.96280800 | 4.23965200 | 3.21178100 |
| H | 0.64338500 | 3.85330200 | 2.59016800 |
| H | -2.05489300 | 3.00879800 | 1.35517800 |
| C | -1.23168300 | 3.03163800 | -1.29668900 |
| H | -2.22418200 | 2.57443500 | -1.25420000 |
| C | -1.36877100 | 4.55520200 | -1.21190400 |
| H | -2.02843200 | 4.91626200 | -2.00921800 |
| H | -0.40708300 | 5.06322900 | -1.33195700 |
| H | -1.80401200 | 4.87388000 | -0.25909800 |
| H | -0.80862000 | 2.73753300 | -2.26263300 |
| C | 0.29958000 | 0.17391400 | -2.53473100 |
| C | 0.62381800 | -1.21707400 | -2.37592000 |
| N | 2.00440800 | -1.55489300 | -2.17529000 |

| | | | |
|---|---|---|---|
| C | 2.80333100 | -0.89572100 | -1.28831600 |
| N | 2.17150700 | -0.18181100 | -0.32771800 |
| C | 2.95217000 | 0.44243900 | 0.58070700 |
| C | 4.33048600 | 0.38530800 | 0.58971600 |
| C | 4.99583900 | -0.35585900 | -0.40956700 |
| C | 4.20785400 | -0.99329600 | -1.35555200 |
| H | 4.66141500 | -1.56560800 | -2.15977800 |
| C | 6.49769800 | -0.43431800 | -0.44556600 |
| H | 6.88478800 | -0.86976800 | 0.48335000 |
| H | 6.93618000 | 0.56620700 | -0.54008800 |
| H | 6.85142200 | -1.04331400 | -1.28202100 |
| H | 4.88595000 | 0.91169200 | 1.35932100 |
| H | 2.42146300 | 1.00515300 | 1.33114000 |
| H | 2.44341800 | -2.15323200 | -2.86168900 |
| C | -0.04331200 | -2.26792400 | -3.24159300 |
| H | -1.10670400 | -2.06929800 | -3.35508900 |
| H | 0.40555100 | -2.22625700 | -4.24297200 |
| H | 0.08457600 | -3.27729000 | -2.84022500 |
| H | 0.04674800 | -1.77551600 | -0.98211200 |
| H | -0.58020900 | 0.41081900 | -3.12265700 |
| H | 1.12895800 | 0.85633100 | -2.68515100 |

**Ru-hydridoenamine Complex (45)**

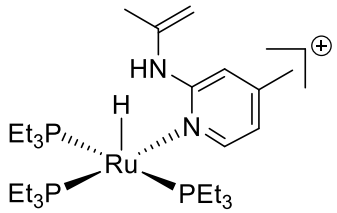


| | | | |
|---|---|---|---|
| Ru | -0.48232700 | -0.02642500 | -0.21907300 |
| P | -0.59065900 | 2.35840000 | -0.04750700 |
| P | -2.77935100 | -0.37103300 | 0.05581000 |

| | | | |
|---|---|---|---|
| P | 0.00787000 | -2.37610100 | -0.20840600 |
| N | 1.63747200 | 0.26047800 | -0.69989000 |
| N | 2.27938600 | 0.27130500 | 1.49540600 |
| C | 1.90065100 | 0.37413000 | -2.01666600 |
| H | 1.03749900 | 0.29927000 | -2.67331200 |
| C | 3.16450900 | 0.57046600 | -2.53365800 |
| H | 3.31140700 | 0.64422400 | -3.60609700 |
| C | 4.24510800 | 0.69038600 | -1.63496300 |
| C | 5.64122700 | 0.93542800 | -2.14112500 |
| H | 5.97154800 | 0.10761000 | -2.78014300 |
| H | 6.35667100 | 1.03920300 | -1.32074900 |
| H | 5.68069100 | 1.84687800 | -2.74913000 |
| C | 3.97867800 | 0.59310200 | -0.27566700 |
| H | 4.78319100 | 0.72463700 | 0.43188300 |
| C | 2.66522900 | 0.35953300 | 0.18405000 |
| C | 1.07467700 | 3.19457000 | -0.13034400 |
| H | 1.69965500 | 2.72338200 | 0.63321400 |
| H | 1.51844000 | 2.92269600 | -1.09397100 |
| C | 1.10185000 | 4.71676300 | 0.04813800 |
| H | 2.13371600 | 5.07788500 | -0.02878900 |
| H | 0.72197600 | 5.02480300 | 1.02711600 |
| H | 0.51975900 | 5.23866400 | -0.71773900 |
| C | -1.51029800 | 3.22325400 | -1.41393700 |
| H | -2.57671200 | 3.20128300 | -1.17732800 |
| H | -1.22012600 | 4.27860300 | -1.43848600 |
| C | -1.25098100 | 2.55837800 | -2.77098200 |
| H | -1.55900500 | 1.50483100 | -2.75656900 |
| H | -0.18878300 | 2.59394600 | -3.03899500 |
| H | -1.80863200 | 3.05978400 | -3.56935300 |
| C | -1.30533000 | 3.09866800 | 1.49655300 |

| | | | |
|---|---|---|---|
| H | -1.42335600 | 4.17857800 | 1.34886500 |
| H | -2.30897100 | 2.68568600 | 1.62819300 |
| C | -0.46281000 | 2.81333900 | 2.74474400 |
| H | 0.52744500 | 3.27526200 | 2.68452400 |
| H | -0.31851100 | 1.73804300 | 2.88571600 |
| H | -0.95857800 | 3.20586500 | 3.63881500 |
| C | -3.93662600 | 1.04112500 | -0.32438700 |
| H | -3.64099400 | 1.87864600 | 0.31221600 |
| H | -3.71521300 | 1.34720500 | -1.35206500 |
| C | -5.44008500 | 0.78638900 | -0.16779900 |
| H | -5.79758000 | -0.00344900 | -0.83536700 |
| H | -5.99816100 | 1.69669900 | -0.41408500 |
| H | -5.70497300 | 0.50929800 | 0.85730500 |
| C | -3.38128500 | -0.92819900 | 1.72111200 |
| H | -4.43890200 | -1.20045200 | 1.63079500 |
| H | -2.84193900 | -1.84521200 | 1.96825300 |
| C | -3.18448800 | 0.10317700 | 2.83497900 |
| H | -2.13181000 | 0.38384700 | 2.92815700 |
| H | -3.51282400 | -0.30554000 | 3.79657400 |
| H | -3.76393300 | 1.01476200 | 2.65200500 |
| C | -3.49070000 | -1.68795200 | -1.04657900 |
| H | -3.01409800 | -2.63448900 | -0.77634000 |
| H | -4.55627100 | -1.80903100 | -0.82408900 |
| C | -3.28201300 | -1.38549400 | -2.53420100 |
| H | -2.22686600 | -1.19019100 | -2.75682200 |
| H | -3.85565400 | -0.50729500 | -2.84874800 |
| H | -3.60468000 | -2.22754200 | -3.15602000 |
| C | -0.79213900 | -3.44213100 | 1.08242000 |
| H | -1.87487500 | -3.39551500 | 0.92960300 |
| H | -0.50383300 | -4.48392600 | 0.90233600 |

| | | | |
|---|---|---|---|
| C | -0.43092500 | -3.02435300 | 2.51239200 |
| H | 0.63713800 | -3.15624200 | 2.71262800 |
| H | -0.98176800 | -3.62871600 | 3.24124600 |
| H | -0.66810400 | -1.97109700 | 2.69126600 |
| C | 1.81346700 | -2.74110400 | 0.07689700 |
| H | 2.36842000 | -2.23567200 | -0.71887500 |
| H | 2.08592700 | -2.23301700 | 1.00632800 |
| C | 2.22675200 | -4.21491000 | 0.14682100 |
| H | 2.00450100 | -4.75291400 | -0.78012200 |
| H | 1.73711700 | -4.74320300 | 0.97076100 |
| H | 3.30778200 | -4.28757700 | 0.31203100 |
| C | -0.33119000 | -3.34674300 | -1.76064100 |
| H | -0.00860100 | -4.38190800 | -1.60298300 |
| H | -1.41423000 | -3.37931300 | -1.90776700 |
| C | 0.34621500 | -2.75820800 | -3.00240500 |
| H | 0.12654000 | -3.36616200 | -3.88642100 |
| H | 1.43480600 | -2.71346800 | -2.89160600 |
| H | -0.00972200 | -1.74194300 | -3.20428300 |
| H | -0.44356700 | -0.08614500 | 1.34867700 |
| H | 1.25988300 | 0.21067400 | 1.55972600 |
| C | 2.94979200 | -0.10148300 | 2.67664900 |
| C | 2.21842300 | -0.26464100 | 3.79445700 |
| H | 1.14462800 | -0.10110000 | 3.80858400 |
| H | 2.68881000 | -0.55967400 | 4.72420000 |
| C | 4.43569700 | -0.33238700 | 2.65878400 |
| H | 4.72873000 | -1.04329900 | 1.87792400 |
| H | 4.99444500 | 0.59722300 | 2.49910600 |
| H | 4.74659200 | -0.74079100 | 3.62251300 |

**Ru-hydrido-aminopyridine Complex (46)**

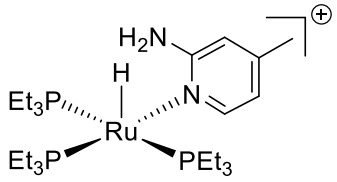


| | | | |
|---|---|---|---|
| Ru | -0.23966100 | -0.03393300 | -0.03616000 |
| P | -0.40299400 | 2.35215300 | -0.04174200 |
| P | -2.54745000 | -0.41287700 | -0.15369000 |
| P | 0.26743400 | -2.37265400 | 0.14498100 |
| N | 1.92490100 | 0.26871300 | -0.07798900 |
| N | 2.15029200 | 0.53993700 | 2.21423600 |
| C | 2.48350400 | 0.25037500 | -1.30965200 |
| H | 1.78861400 | 0.11302500 | -2.13348800 |
| C | 3.83504900 | 0.38499200 | -1.54246400 |
| H | 4.21831900 | 0.35573300 | -2.55716900 |
| C | 4.70180300 | 0.55831400 | -0.43907500 |
| C | 6.18536100 | 0.70502600 | -0.64273100 |
| H | 6.59548300 | -0.17395500 | -1.15410300 |
| H | 6.71415500 | 0.82671100 | 0.30652700 |
| H | 6.40559800 | 1.57561400 | -1.27196800 |
| C | 4.13233500 | 0.59361300 | 0.82376200 |
| H | 4.75188800 | 0.73815300 | 1.70427100 |
| C | 2.73694600 | 0.45172900 | 0.98436600 |
| C | 1.23728500 | 3.22465000 | 0.11283100 |
| H | 1.71213500 | 2.83446100 | 1.01691800 |
| H | 1.85559600 | 2.88614500 | -0.72564200 |
| C | 1.21038400 | 4.75666900 | 0.15942600 |
| H | 2.23372800 | 5.14074400 | 0.23936100 |
| H | 0.65343600 | 5.13406500 | 1.02262800 |
| H | 0.77093900 | 5.19587500 | -0.74166200 |
| C | -1.05465300 | 3.06352400 | -1.63246800 |

| | | | |
|---|---|---|---|
| H | -2.14639200 | 3.03735800 | -1.60039500 |
| H | -0.77134700 | 4.11828900 | -1.70850000 |
| C | -0.53707600 | 2.27432500 | -2.84126300 |
| H | -0.83296700 | 1.21892300 | -2.77502500 |
| H | 0.55633900 | 2.31293800 | -2.90719200 |
| H | -0.93776900 | 2.67595500 | -3.77827600 |
| C | -1.40756200 | 3.19932800 | 1.26799900 |
| H | -1.50838100 | 4.25925300 | 1.00649000 |
| H | -2.41281400 | 2.77040900 | 1.24478100 |
| C | -0.81372000 | 3.04345700 | 2.67244100 |
| H | 0.15960000 | 3.53603500 | 2.75960000 |
| H | -0.67556700 | 1.98782900 | 2.92586600 |
| H | -1.47993300 | 3.48648100 | 3.42028100 |
| C | -3.64321900 | 0.94749400 | -0.80864700 |
| H | -3.46181700 | 1.83215000 | -0.19375000 |
| H | -3.26385900 | 1.18884300 | -1.80708800 |
| C | -5.14972800 | 0.67222700 | -0.87520200 |
| H | -5.38857700 | -0.16641600 | -1.53616100 |
| H | -5.67088900 | 1.55287400 | -1.26720600 |
| H | -5.57139800 | 0.45655000 | 0.11144000 |
| C | -3.40624900 | -0.88096500 | 1.42471700 |
| H | -4.42775500 | -1.19564000 | 1.18297400 |
| H | -2.89184900 | -1.76007100 | 1.82024000 |
| C | -3.41986500 | 0.22722600 | 2.48062400 |
| H | -2.40340700 | 0.54828800 | 2.72376000 |
| H | -3.89362100 | -0.12809400 | 3.40201500 |
| H | -3.98130300 | 1.10477400 | 2.14171400 |
| C | -3.06276200 | -1.80748100 | -1.27036300 |
| H | -2.62134000 | -2.72554800 | -0.87338400 |
| H | -4.14807400 | -1.93916700 | -1.20475100 |

| | | | |
|---|---|---|---|
| C | -2.63492800 | -1.58976800 | -2.72539600 |
| H | -1.56221500 | -1.37917600 | -2.79860800 |
| H | -3.16973600 | -0.74845900 | -3.17843300 |
| H | -2.84427000 | -2.47641000 | -3.33362900 |
| C | -0.71641300 | -3.40542900 | 1.33292100 |
| H | -1.76236000 | -3.37498900 | 1.01250900 |
| H | -0.39768800 | -4.44959200 | 1.23766600 |
| C | -0.58831900 | -2.93534400 | 2.78612700 |
| H | 0.43452300 | -3.06065900 | 3.15728200 |
| H | -1.24829500 | -3.51577300 | 3.43982100 |
| H | -0.85206700 | -1.87743300 | 2.88589100 |
| C | 2.01140800 | -2.69463400 | 0.72209100 |
| H | 2.67804000 | -2.23535900 | -0.01373900 |
| H | 2.14345300 | -2.12016800 | 1.64436700 |
| C | 2.41562600 | -4.15491500 | 0.95081200 |
| H | 2.32977300 | -4.75547700 | 0.03973000 |
| H | 1.81425100 | -4.63488200 | 1.72912300 |
| H | 3.46223100 | -4.20301600 | 1.27242000 |
| C | 0.19094300 | -3.40979000 | -1.40026300 |
| H | 0.50573700 | -4.42971900 | -1.15286900 |
| H | -0.85571000 | -3.47576600 | -1.70930700 |
| C | 1.03868600 | -2.85259800 | -2.54839200 |
| H | 0.96202600 | -3.49577800 | -3.43144200 |
| H | 2.09774100 | -2.78411800 | -2.27826000 |
| H | 0.70313100 | -1.85111800 | -2.84027100 |
| H | -0.46250300 | -0.01980400 | 1.51787900 |
| H | 1.17339600 | 0.26374500 | 2.26636400 |
| H | 2.71861200 | 0.42639100 | 3.04126600 |

### 2.4.13. X-ray Structure of Ruthenium Complexes

**$Ru(PEt_3)_3(NTf_2)_2$**

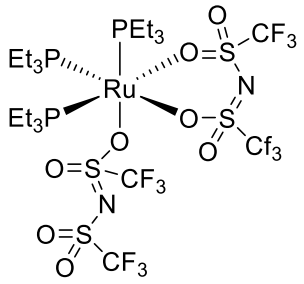

A yellow prism 0.060 x 0.050 x 0.050 mm in size was mounted on a Cryoloop with Paratone oil. Data were collected in a nitrogen gas stream at 100(2) K using and scans. Crystal-to-detector distance was 50 mm and exposure time was 10 seconds per frame using a scan width of 1.0°. Data collection was 100.0% complete to 25.000° in □. A total of 122543 reflections were collected covering the indices, -13<=*h*<=13, -22<=*k*<=22, -21<=*l*<=21. 7199 reflections were found to be symmetry independent, with an $R_{int}$ of 0.0671. Indexing and unit cell refinement indicated a primitive, monoclinic lattice. The space group was found to be P 21/c (No. 14). The data were integrated using the Bruker SAINT software program and scaled using the SADABS software program. Solution by iterative methods (SHELXT-2014) produced a complete heavy-atom phasing model consistent with the proposed structure. All non-hydrogen atoms were refined anisotropically by full-matrix least-squares (SHELXL-2016). All hydrogen atoms were placed using a riding model. Their positions were constrained relative to their parent atom using the appropriate HFIX command in SHELXL-2016.

Table 1. Crystal data and structure refinement for $Ru(PEt_3)_3(NTf_2)_2$.

Empirical formula C22 H45.25 F12 N2 O8.25 P3 Ru S4

Formula weight 1020.14

Temperature 100(2) K

Wavelength 0.71073 Å

Crystal system Monoclinic

Space group P 21/c

Unit cell dimensions a = 11.433(3) Å □□= 90°.

b = 18.944(5) Å β = 91.423(5)°.

c = 18.126(5) Å γ = 90°.

Volume 3924.6(18) Å3

Z 4

Density (calculated) 1.727 Mg/m3

Absorption coefficient 0.836 mm-1

F(000) 2073

Crystal size 0.060 x 0.050 x 0.050 mm3

Theta range for data collection 1.555 to 25.384°.

Index ranges -13<=h<=13, -22<=k<=22, -21<=l<=21

Reflections collected 122543

Independent reflections 7199 [R(int) = 0.0671]

Completeness to theta = 25.000° 100.0 %

Absorption correction Semi-empirical from equivalents

Max. and min. transmission 0.928 and 0.836

Refinement method Full-matrix least-squares on F2

Data / restraints / parameters 7199 / 4 / 468

Goodness-of-fit on F2 1.092

Final R indices [I>2sigma(I)] R1 = 0.0419, wR2 = 0.0933

R indices (all data) R1 = 0.0468, wR2 = 0.0965

Extinction coefficient n/a

Largest diff. peak and hole 1.150 and -0.993 e.Å-3

**$Ru(PEt_3)_3(Amine)(NTf_2)_2$ (29)**

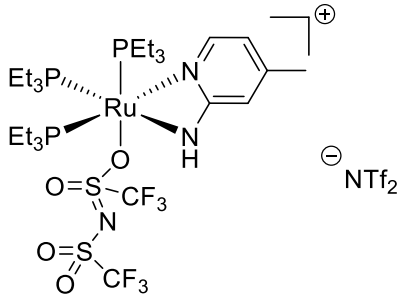


A yellow block 0.24 x 0.10 x 0.09 mm in size was mounted on a Cryoloop with Paratone oil. Data were collected in a nitrogen gas stream at 100(2) K using omega scans. Crystal-to-detector distance was 35 mm and exposure time was 6.00 seconds per frame using a scan width of 0.5°. Data collection was 100% complete to 26.372° in θ. A total of 72140 reflections were collected covering the indices -13<=h<=13, -22<=k<=23, -28<=l<=30. 9834 reflections were founded to be symmetry independent, with an $R_{int}$ of 0.0536. Indexing and unit cell refinement indicated a primitive, monoclinic lattice. The space group was found to be P 21/c (No. 14). The data were integrated using the CrysAlis$^{Pro}$ 1.171.40.44a software program and scaled using the SCALE3

ABSPACK scaling algorithm. Solution by intrinsic phasing (SHELXT-2015) produced a heavy-atom phasing model consistent with the proposed structure. All non-hydrogen atoms were refined anisotropically by full-matrix least-squares (SHELXL-2014). All hydrogen atoms were placed using a riding model. Their positions were constrained relative to their parent atom using the appropriate HFIX command in SHELXL-2014.

Table 2.7. Crystal data and structure refinement for $Ru(PEt_3)_3(Amine)(NTf_2)_2$.

| | |
|---|---|
| Empirical formula | C29 H55 Cl2 F12 N4 O8 P3 Ru S4 |
| Formula weight | 1208.89 |
| Temperature | 100(2) K |
| Wavelength | 0.71073 Å |
| Crystal system | Monoclinic |
| Space group | P 21/c |
| Unit cell dimensions | a = 10.5702(2) Å α = 90°. |
| | b = 18.7348(4) Å β = 92.934(2)°. |
| | c = 24.3472(5) Å γ = 90°. |
| Volume | 4815.17(17) Å3 |
| Z | 4 |
| Density (calculated) | 1.668 Mg/m3 |
| Absorption coefficient | 0.804 mm-1 |
| F(000) | 2464 |
| Crystal size | 0.240 x 0.100 x 0.090 mm3 |
| Theta range for data collection | 2.738 to 26.372°. |
| Index ranges | -13<=h<=13, -22<=k<=23, -28<=l<=30 |
| Reflections collected | 72140 |
| Independent reflections | 9834 [R(int) = 0.0536] |
| Completeness to theta = 26.372° | 99.8 % |
| Absorption correction | Semi-empirical from equivalents |
| Max. and min. transmission | 1.00000 and 0.55675 |
| Refinement method | Full-matrix least-squares on F2 |
| Data / restraints / parameters | 9834 / 2 / 632 |

Goodness-of-fit on F2 1.029

Final R indices [I>2sigma(I)] R1 = 0.0316, wR2 = 0.0730

R indices (all data) R1 = 0.0378, wR2 = 0.0754

Extinction coefficient n/a

Largest diff. peak and hole 0.617 and -1.025 e.Å-3

**$Ru(PEt_3)_3$(Amido)$(NTf_2)$ (30)**

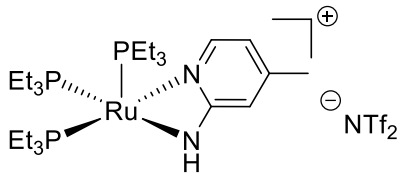


A red block 0.25 x 0.11 x 0.09 mm in size was mounted on a Cryoloop with Paratone oil. Data were collected in a nitrogen gas stream at 100(2) K using omega scans. Crystal-to-detector distance was 35 mm and exposure time was 2.00 seconds per frame using a scan width of 0.5°. Data collection was 100% complete to 26.369° in θ. A total of 49254 reflections were collected covering the indices -15<=h<=15, -17<=k<=17, -25<=l<=25. 7366 reflections were founded to be symmetry independent, with an $R_{int}$ of 0.0659. Indexing and unit cell refinement indicated a primitive, monoclinic lattice. The space group was found to be P 21/n (No. 14). The data were integrated using the CrysAlis$^{Pro}$ 1.171.40.44a software program and scaled using the SCALE3 ABSPACK scaling algorithm. Solution by intrinsic phasing (SHELXT-2015) produced a heavy-atom phasing model consistent with the proposed structure. All non-hydrogen atoms were refined anisotropically by full-matrix least-squares (SHELXL-2014). All hydrogen atoms were placed using a riding model. Their positions were constrained relative to their parent atom using the appropriate HFIX command in SHELXL-2014.

Table 2.7. Crystal data and structure refinement for $Ru(PEt_3)_3$(Amido)$(NTf_2)$.

Empirical formula C26 H52 F6 N3 O4 P3 Ru S2

Formula weight 842.80

Temperature 100(2) K

Wavelength 0.71073 Å

Crystal system Monoclinic

Space group P 21/n

Unit cell dimensions a = 12.6581(4) Å α = 90°.

b = 14.3288(4) Å β = 106.345(3)°.

c = 20.7537(6) Å γ = 90°.

Volume 3612.08(19) Å3

Z 4

Density (calculated) 1.550 Mg/m3

Absorption coefficient 0.749 mm-1

F(000) 1744

Crystal size 0.250 x 0.110 x 0.090 mm3

Theta range for data collection 2.843 to 26.369°.

Index ranges -15<=h<=15, -17<=k<=17, -25<=l<=25

Reflections collected 49254

Independent reflections 7366 [R(int) = 0.0659]

Completeness to theta = 26.369° 99.9 %

Absorption correction Semi-empirical from equivalents

Max. and min. transmission 1.00000 and 0.28562

Refinement method Full-matrix least-squares on F2

Data / restraints / parameters 7366 / 6 / 440

Goodness-of-fit on F2 1.033

Final R indices [I>2sigma(I)] R1 = 0.0335, wR2 = 0.0794

R indices (all data) R1 = 0.0401, wR2 = 0.0819

Extinction coefficient n/a

Largest diff. peak and hole 0.719 and -0.511 e.Å-3

**Ru(H)(PEt$_3$)$_3$(Amine)(NTf$_2$)$_2$ (44)**

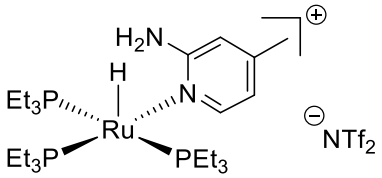


A colorless block 0.31 x 0.17 x 0.10 mm in size was mounted on a Cryoloop with Paratone oil. Data were collected in a nitrogen gas stream at 100(2) K using omega scans. Crystal-to-detector distance was 33.00 mm and exposure time was 4.00 seconds per frame using a scan width of 0.5°. Data collection was 100% complete to 30.500° in θ. A total of 60357 reflections were collected covering the indices -14<=h<=14, -16<=k<=16, -23<=l<=23. 11552 reflections were found to be symmetry independent, with an $R_{int}$ of 0.0955. Indexing and unit cell refinement indicated a

primitive, triclinic lattice. The space group was found to be P -1 (No. 2). The data were integrated using the CrysAlis$^{Pro}$ 1.171.40.54a software program and scaled using the SCALE3 ABSPACK scaling algorithm. Solution by intrinsic phasing (SHELXT-2015) produced a heavy-atom phasing model consistent with the proposed structure. All non-hydrogen atoms were refined anisotropically by full-matrix least-squares (SHELXL-2014). All hydrogen atoms were placed using a riding model. Their positions were constrained relative to their parent atom using the appropriate HFIX command in SHELXL-2014.

Table 2.8. Crystal data and structure refinement for $Ru(H)(PEt_3)_3(Amine)(NTf_2)_2$.

| | |
|---|---|
| Empirical formula | C26 H54 F6 N3.80 O4 P3 Ru S2 |
| Formula weight | 856.03 |
| Temperature | 100(2) K |
| Wavelength | 0.71073 Å |
| Crystal system | Triclinic |
| Space group | P -1 |
| Unit cell dimensions | a = 10.2586(2) Å α = 79.6870(10)°. |
| | b = 11.4779(2) Å β = 82.7900(10)°. |
| | c = 16.7535(2) Å γ = 78.3830(10)°. |
| Volume | 1892.84(6) Å3 |
| Z | 2 |
| Density (calculated) | 1.502 Mg/m3 |
| Absorption coefficient | 0.716 mm-1 |
| F(000) | 887 |
| Crystal size | 0.310 x 0.170 x 0.100 mm3 |
| Theta range for data collection | 2.979 to 30.508°. |
| Index ranges | -14<=h<=14, -16<=k<=16, -23<=l<=23 |
| Reflections collected | 60357 |
| Independent reflections | 11552 [R(int) = 0.0955] |
| Completeness to theta = 30.500° | 99.9 % |
| Absorption correction | Semi-empirical from equivalents |
| Max. and min. transmission | 1.00000 and 0.78072 |
| Refinement method | Full-matrix least-squares on F2 |

Data / restraints / parameters 11552 / 1 / 555

Goodness-of-fit on F2 1.055

Final R indices [I>2sigma(I)] R1 = 0.0310, wR2 = 0.0736

R indices (all data) R1 = 0.0392, wR2 = 0.0765

Extinction coefficient n/a

Largest diff. peak and hole 0.684 and -0.750 e.Å-3

## 2.5 References

Parts of this chapter were reprinted with permission from:

"Ruthenium-Catalyzed Hydroamination of Unactivated Terminal Alkenes with Stoichiometric Amounts of Alkene and an Ammonia Surrogate by Sequential Oxidation and Reduction"

Ma, S.; Hill, C. K.; Olen, C. L.; Hartwig, J. F. *J. Am. Chem. Soc.* **2021**, *143*, 359-368.


(1) Bagley, M. C.; Dale, J. W.; Merritt, E. A.; Xiong, X. Thiopeptide Antibiotics. *Chem. Rev.* **2005,** *105*, 685-714.

(2) Nugent, T. C. *Chiral amine synthesis: methods, developments and applications*. Wiley-VCH: Weinheim, 2010.

(3) Wang, C.; Bai, X.; Wang, R.; Zheng, X.; Ma, X.; Chen, H.; Ai, Y.; Bai, Y.; Liu, Y. Synthesis of Imatinib by C–N Coupling Reaction of Primary Amide and Bromo-Substituted Pyrimidine Amine. *Org. Process Res. Dev.* **2019,** *23*, 1918-1925.

(4) Shen, Q.; Hartwig, J. F. [(CyPF-$^t$Bu)PdCl$_2$]: An Air-Stable, One-Component, Highly Efficient Catalyst for Amination of Heteroaryl and Aryl Halides. *Org. Lett.* **2008,** *10*, 4109-4112.

(5) Afanasyev, O. I.; Kuchuk, E.; Usanov, D. L.; Chusov, D. Reductive Amination in the Synthesis of Pharmaceuticals. *Chem. Rev.* **2019,** *119*, 11857-11911.

(6) Tripathi, R. P.; Verma, S. S.; Pandey, J.; Tiwari, V. K. Recent Development on Catalytic Reductive Amination and Applications. *Curr. Org. Chem.* **2008,** *12*, 1093-1115.

(7) Müller, T. E.; Beller, M. Metal-Initiated Amination of Alkenes and Alkynes. *Chem. Rev.* **1998,** *98*, 675-704.

(8) Müller, T. E.; Hultzsch, K. C.; Yus, M.; Foubelo, F.; Tada, M. Hydroamination: Direct Addition of Amines to Alkenes and Alkynes. *Chem. Rev.* **2008,** *108*, 3795-3892.

(9) Huang, L.; Arndt, M.; Gooßen, K.; Heydt, H.; Gooßen, L. J. Late Transition Metal-Catalyzed Hydroamination and Hydroamidation. *Chem. Rev.* **2015,** *115*, 2596-2697.

(10) Pawlas, J.; Nakao, Y.; Kawatsura, M.; Hartwig, J. F. A General Nickel-Catalyzed Hydroamination of 1,3-Dienes by Alkylamines: Catalyst Selection, Scope, and Mechanism. *J. Am. Chem. Soc.* **2002,** *124*, 3669-3679.

(11) Yang, X.-H.; Lu, A.; Dong, V. M. Intermolecular Hydroamination of 1,3-Dienes to Generate Homoallylic Amines. *J. Am. Chem. Soc.* **2017,** *139*, 14049-14052.

(12) Utsunomiya, M.; Hartwig, J. F. Intermolecular, Markovnikov Hydroamination of Vinylarenes with Alkylamines. *J. Am. Chem. Soc.* **2003,** *125*, 14286-14287.

(13) Utsunomiya, M.; Hartwig, J. F. Ruthenium-Catalyzed Anti-Markovnikov Hydroamination of Vinylarenes. *J. Am. Chem. Soc.* **2004,** *126*, 2702-2703.

(14) Zhou, J.; Hartwig, J. F. Intermolecular, Catalytic Asymmetric Hydroamination of Bicyclic Alkenes and Dienes in High Yield and Enantioselectivity. *J. Am. Chem. Soc.* **2008,** *130*, 12220-12221.

(15) Dorta, R.; Egli, P.; Zürcher, F.; Togni, A. The $[IrCl(Diphosphine)]_2$/Fluoride System. Developing Catalytic Asymmetric Olefin Hydroamination. *J. Am. Chem. Soc.* **1997,** *119*, 10857-10858.

(16) Teng, H.-L.; Luo, Y.; Nishiura, M.; Hou, Z. Diastereodivergent Asymmetric Carboamination/Annulation of Cyclopropenes with Aminoalkenes by Chiral Lanthanum Catalysts. *J. Am. Chem. Soc.* **2017,** *139*, 16506-16509.

(17) Teng, H.-L.; Luo, Y.; Wang, B.; Zhang, L.; Nishiura, M.; Hou, Z. Synthesis of Chiral Aminocyclopropanes by Rare-Earth-Metal-Catalyzed Cyclopropene Hydroamination. *Angew. Chem., Int. Ed.* **2016,** *55*, 15406-15410.

(18) Sevov, C. S.; Zhou, J.; Hartwig, J. F. Iridium-Catalyzed Intermolecular Hydroamination of Unactivated Aliphatic Alkenes with Amides and Sulfonamides. *J. Am. Chem. Soc.* **2012,** *134*, 11960-11963.

(19) Sevov, C. S.; Zhou, J.; Hartwig, J. F. Iridium-Catalyzed, Intermolecular Hydroamination of Unactivated Alkenes with Indoles. *J. Am. Chem. Soc.* **2014,** *136*, 3200-3207.

(20) Nguyen, H. N.; Lee, H.; Audörsch, S.; Reznichenko, A. L.; Nawara-Hultzsch, A. J.; Schmidt, B.; Hultzsch, K. C. Asymmetric Intra- and Intermolecular Hydroamination Catalyzed by 3,3'-Bis(trisarylsilyl)- and 3,3'-Bis(arylalkylsilyl)-Substituted Binaphtholate Rare-Earth-Metal Complexes. *Organometallics* **2018,** *37*, 4358-4379.

(21) Miller, D. C.; Ganley, J. M.; Musacchio, A. J.; Sherwood, T. C.; Ewing, W. R.; Knowles, R. R. Anti-Markovnikov Hydroamination of Unactivated Alkenes with Primary Alkyl Amines. *J. Am. Chem. Soc.* **2019,** *141*, 16590-16594.

(22) Zhang, Z.; Lee, S. D.; Widenhoefer, R. A. Intermolecular Hydroamination of Ethylene and 1-Alkenes with Cyclic Ureas Catalyzed by Achiral and Chiral Gold(I) Complexes. *J. Am. Chem. Soc.* **2009,** *131*, 5372-5373.

(23) Musacchio, A. J.; Lainhart, B. C.; Zhang, X.; Naguib, S. G.; Sherwood, T. C.; Knowles, R. R. Catalytic intermolecular hydroaminations of unactivated olefins with secondary alkyl amines. *Science* **2017,** *355*, 727.

(24) Xi, Y.; Ma, S.; Hartwig, J. F. Catalytic asymmetric addition of an amine N–H bond across internal alkenes. *Nature* (2020). https://doi.org/10.1038/s41586-020-2919-z.

(25) Zhang, J.; Yang, C.; He, C. Gold(I)-Catalyzed Intra- and Intermolecular Hydroamination of Unactivated Olefins. *J. Am. Chem.Soc.* **2006,** *128*, 1798−1799.

(26) Reznichenko, A. L.; Nguyen, H. N.; Hultzsch, K. C. Asymmetric Intermolecular Hydroamination of Unactivated Alkenes with Simple Amines. *Angew. Chem., Int. Ed.* **2010,** *49*, 8984-8987.

(27) Gurak, J. A.; Yang, K. S.; Liu, Z.; Engle, K. M. Directed, Regiocontrolled Hydroamination of Unactivated Alkenes via Protodepalladation. *J. Am. Chem. Soc.* **2016,** *138*, 5805-5808.

(28) Vanable, E. P.; Kennemur, J. L.; Joyce, L. A.; Ruck, R. T.; Schultz, D. M.; Hull, K. L. Rhodium-Catalyzed Asymmetric Hydroamination of Allyl Amines. *J. Am. Chem. Soc.* **2019,** *141*, 739-742.

(29) Zhu, S.; Buchwald, S. L. Enantioselective CuH-Catalyzed Anti-Markovnikov Hydroamination of 1,1-Disubstituted Alkenes. *J. Am. Chem. Soc.* **2014,** *136*, 15913-15916.

(30) Guo, S.; Yang, J. C.; Buchwald, S. L. A Practical Electrophilic Nitrogen Source for the Synthesis of Chiral Primary Amines by Copper-Catalyzed Hydroamination. *J. Am. Chem. Soc.* **2018,** *140*, 15976-15984.

(31) Liu, Z.; Yamamichi, H.; Madrahimov, S. T.; Hartwig, J. F. Rhodium Phosphine−π-Arene Intermediates in the Hydroamination of Alkenes. *J. Am. Chem. Soc.* **2011,** *133*, 2772-2782.

(32) Cheung, H. W.; So, C. M.; Pun, K. H.; Zhou, Z.; Lau, C. P. Hydro(trispyrazolyl)borato-Ruthenium(II) Diphosphinoamino Complex-Catalyzed Addition of β-Diketones to 1-Alkynes and Anti-Markovnikov Addition of Secondary Amines to Aromatic 1-Alkynes. *Adv. Synth. Catal.* **2011,** *353*, 411-425.

(33) Johns, A. M.; Sakai, N.; Ridder, A.; Hartwig, J. F. Direct Measurement of the Thermodynamics of Vinylarene Hydroamination. *J. Am. Chem. Soc.* **2006,** *128*, 9306-9307.

(34) Hill, C. K.; Hartwig, J. F. Site-selective oxidation, amination and epimerization reactions of complex polyols enabled by transfer hydrogenation. *Nat. Chem.* **2017,** *9*, 1213-1221.

(35) McBee, J. L.; Bell, A. T.; Tilley, T. D. Mechanistic Studies of the Hydroamination of Norbornene with Electrophilic Platinum Complexes: The Role of Proton Transfer. *J. Am. Chem. Soc.* **2008,** *130*, 16562-16571.

(36) Smout, V.; Peschiulli, A.; Verbeeck, S.; Mitchell, E. A.; Herrebout, W.; Bultinck, P.; Vande Velde, C. M. L.; Berthelot, D.; Meerpoel, L.; Maes, B. U. W. Removal of the Pyridine Directing Group from α-Substituted N-(Pyridin-2-yl)piperidines Obtained via Directed Ru-Catalyzed sp3 C–H Functionalization. *J. Org. Chem.* **2013,** *78*, 9803-9814.

(37) Ronson, T. O.; Renders, E.; Van Steijvoort, B. F.; Wang, X.; Wybon, C. C. D.; Prokopcová, H.; Meerpoel, L.; Maes, B. U. W. Ruthenium-Catalyzed Reductive Arylation of N-(2-Pyridinyl)amides with Isopropanol and Arylboronate Esters. *Angew. Chem. Int. Ed.* **2019,** *58*, 482-487.

(38) Pan, S.; Endo, K.; Shibata, T. Ir(I)-Catalyzed Enantioselective Secondary sp3 C–H Bond Activation of 2-(Alkylamino)pyridines with Alkenes. *Org. Lett.* **2011,** *13*, 4692-4695.

(39) Bruneau, C.; Dixneuf, P. H. Metal Vinylidenes and Allenylidenes in Catalysis: Applications in Anti-Markovnikov Additions to Terminal Alkynes and Alkene Metathesis. *Angew. Chem. Int. Ed.* **2006,** *45*, 2176-2203.

(40) Cobley, C. J.; Henschke, J. P. Enantioselective Hydrogenation of Imines Using a Diverse Library of Ruthenium Dichloride(diphosphine)(diamine) Precatalysts. *Adv. Synth. Catal.* **2003,** *345*, 195-201.

(41) Evans, I. P.; Spencer, A.; Wilkinson, G., Dichlorotetrakis(dimethyl sulphoxide)ruthenium(II) and its use as a source material for some new ruthenium(II) complexes. *J. Chem. Soc., Dalton Trans.* **1973,** (2), 204-209.

(42) Bannwarth, C.; Ehlert, S.; Grimme, S., GFN2-xTB—An Accurate and Broadly Parametrized Self-Consistent Tight-Binding Quantum Chemical Method with Multipole Electrostatics and Density-Dependent Dispersion Contributions. *J. Chem. Theory Comput.* **2019,** *15* (3), 1652-1671.

(43) Bursch, M.; Neugebauer, H.; Grimme, S., Structure Optimisation of Large Transition-Metal Complexes with Extended Tight-Binding Methods. *Angew. Chem. Int. Ed.* **2019,** *58* (32), 11078-11087.

(44) Meta-Dynamics Simulations Based on Tight-Binding Quantum Chemical Calculations. *J. Chem. Theory Comput.* **2019,** *15* (5), 2847-2862.

(45) Grimme, S. grimme-lab / xtb. https://github.com/grimme-lab/xtb/releases.

(46) M. J. Frisch, G. W. T., H. B. Schlegel, G. E. Scuseria, M. A.; Robb, J. R. C., G. Scalmani, V. Barone, G. A. Petersson, H. Nakatsuji, X. Li, M.; Caricato, A. V. M., J. Bloino, B. G. Janesko, R. Gomperts, B. Mennucci, H. P. Hratchian,; J. V. Ortiz, A. F. I., J. L. Sonnenberg, D. Williams-Young, F. Ding, F. Lipparini, F. Egidi, J.; Goings, B. P., A. Petrone, T. Henderson, D. Ranasinghe, V. G. Zakrzewski, J. Gao, N. Rega,; G. Zheng, W. L., M. Hada, M. Ehara, K. Toyota, R. Fukuda, J. Hasegawa, M. Ishida, T.; Nakajima, Y. H., O. Kitao, H. Nakai, T. Vreven, K. Throssell, J. A. Montgomery, Jr., J. E.; Peralta, F. O., M. J. Bearpark, J. J. Heyd, E. N. Brothers, K. N. Kudin, V. N. Staroverov, T.; A. Keith, R. K., J. Normand, K. Raghavachari, A. P. Rendell, J. C. Burant, S. S. Iyengar,; J. Tomasi, M. C., J. M. Millam, M. Klene, C. Adamo, R. Cammi, J. W. Ochterski, R. L.; Martin, K. M., O. Farkas, J. B. Foresman, D. J. Fox, Gaussian 16, Revision A.03. **2016**.

(47) Paton, R. S. GoodVibes v3.0.1 2019. https://github.com/bobbypaton/GoodVibes.

(48) Marenich, A. V.; Cramer, C. J.; Truhlar, D. G., Universal Solvation Model Based on Solute Electron Density and on a Continuum Model of the Solvent Defined by the Bulk Dielectric Constant and Atomic Surface Tensions. *J. Phys. Chem. B* **2009,** *113* (18), 6378-6396.

# CHAPTER 3
# Enantioselective Hydroamination of Unactivated Terminal Alkenes

## 3.1 Introduction

Catalytic, asymmetric hydrofunctionalization of alkenes can provide direct access to an array of chiral building blocks containing stereogenic centers from simple chemical feedstocks.[1-4] The hydrofunctionalization of terminal alkenes is particularly valuable for converting feedstocks to structurally diverse compounds and for the late-stage derivatization of medicinally relevant molecules because terminal alkenes are broadly accessible and possess orthogonal reactivity to common polar functional groups, such as ketones, halides, and alcohols.[5] However, hydrofunctionalizations that proceed with high Markovnikov selectivity, excellent enantioselectivity, and a high degree of generality are rare.[6]

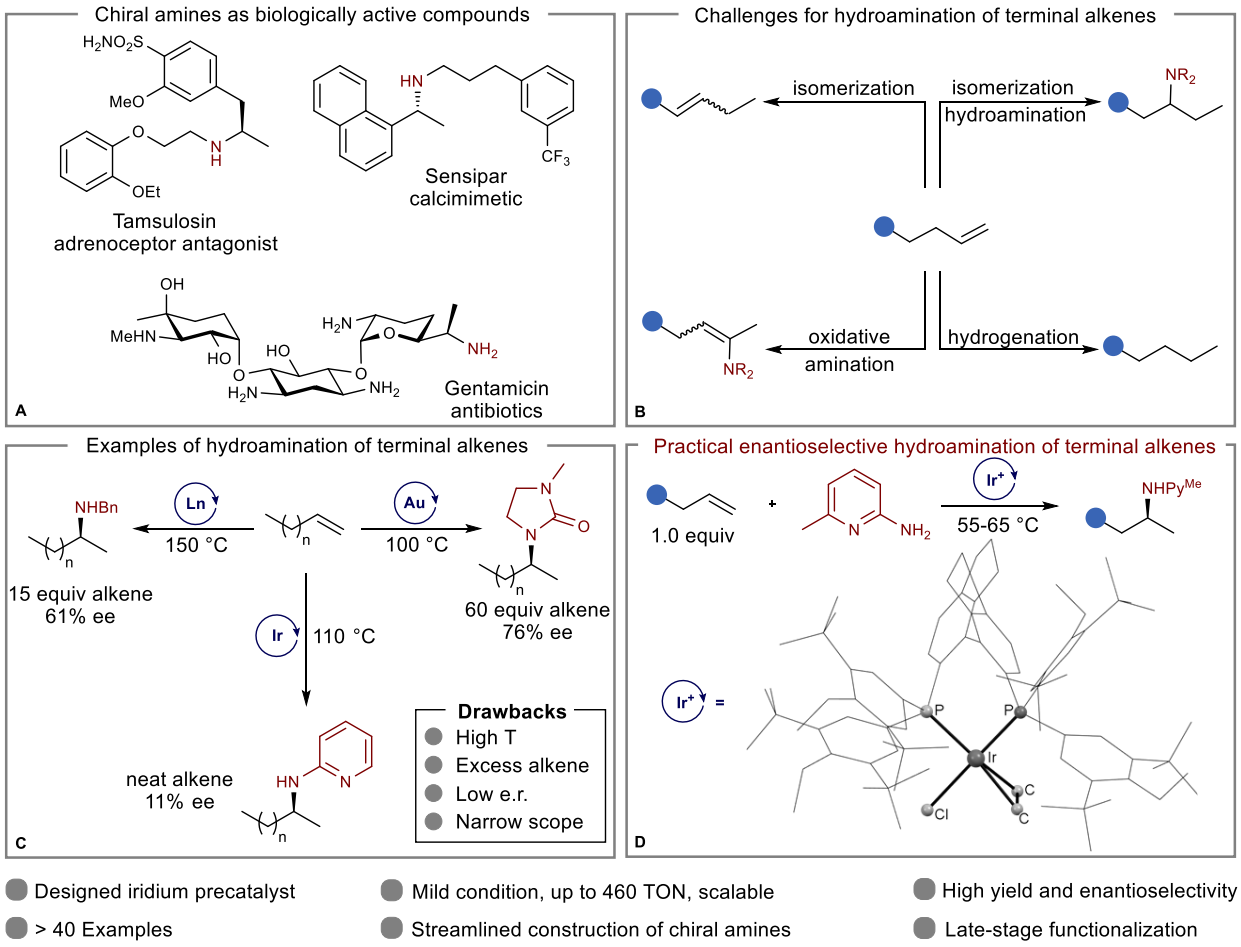


**Figure 3.1. Amines as biologically active compounds and catalytic hydroamination of terminal alkenes.** (A) Biologically active compounds containing chiral alkyl methyl amines. (B) Major challenges for the enantioselective hydroamination of terminal alkenes. (C) Representative examples of enantioselective hydroamination of terminal alkenes and their limitations. (D) This work: Practical hydroamination of terminal alkenes.

Among potential enantioselective hydrofunctionalizations, the asymmetric Markovnikov hydroamination of a terminal alkene is particularly valuable because it produces chiral amines bearing an α-"alkyl-methyl" stereocenter, which is found in a wide range of pharmaceuticals and agrochemicals (Fig. 3.1A).[7] These amines are commonly prepared by enantioselective reductive amination[8-12] and hydrogenation of enamides and imines,[10,13] enzymatic amination of alcohols,[14]

and the addition of an organometallic reagent to an imine bearing a chiral auxiliary.[15] Although valuable, these approaches have limited compatibility with functional groups, high dependence of the yield and enantioselectivity on the structure of the substrate, and a need to install a reactive functional group into feedstock hydrocarbons before the amination reaction.

Although the addition of an N–H bond to an alkene has long been envisioned as a route to chiral amines from abundant alkene feedstocks, intermolecular additions of an amine to unactivated alkenes that occur in high enantiomeric excess are rare, and very few have been reported to occur with unactivated terminal alkenes with high e.e.[16-20] Despite decades of effort toward the development of efficient catalytic hydroamination, current methods suffer from competing side reactions, such as the isomerization,[21] oxidative amination,[22] and hydrogenation of the alkenes (Fig. 3.1B).[22] Consequently, they often occur only with alkenes that lack additional functional groups, and they occur at relatively high temperatures, in moderate yields, and with modest enantioselectivity (Fig. 3.1C). Moreover, no asymmetric hydroamination has been reported in which the amine adds to the alkene lacking a directing group with nearly equal amounts of the alkene and amine, even though this stoichiometry is needed for the reaction to be practical. Emerging, alternative strategies, such as formal hydroamination form linear amines exclusively, precluding the formation of α-chiral amines from terminal alkenes.[23-27] We report a system for the catalytic hydroamination to form chiral amines bearing an α-"alkyl-methyl" stereocenter by an operationally simple, highly enantioselective hydroamination of structurally diverse, unactivated terminal alkenes under mild conditions (Fig. 3.1D). Suppression of a series of side reactions and promotion of the N–H addition process were essential to achieving the high efficiency and high stereoselectivity of this hydroamination.

### 3.2 Results and Discussion

**Development of the reaction and mechanistic investigation** We recently reported that the combination of a cationic iridium catalyst, [(*R*)-TMS-SYNPHOSIr(COD)]$NTf_2$, and a carefully designed amine, 2-amino-6-methylpyridine, enabled the direct asymmetric addition of an N-H bond across unactivated internal alkenes.[16] Although the components of this catalyst and the accompanying reagent significantly enhanced the rate of hydroamination over that of prior hydroaminations, excess alkene (i.e. 10 equivalents) was required for the hydroamination to occur with high regioselectivity, and the compatibility of this reaction with functional groups was limited by the harsh reaction conditions (120 °C). Therefore, we sought to address these limitations by developing a highly active system that would catalyze enantioselective hydroamination of unconjugated, unstrained terminal alkenes with a 1:1 ratio of alkene and amine under mild conditions.

At the outset of our study, we selected allylbenzene (**2a**) as the model alkene because its propensity to undergo isomerization to form a thermodynamically stable, conjugated alkene, β-methylstyrene. This alkene would be a stringent test of a new system to resist isomerization. In the presence of [(*R*)-TMS-SYNPHOSIr(COD)]$NTf_2$ (**Ir-0**) as the catalyst, the equimolar reaction of allylbenzene and 6-methyl-2-aminopyridine (**1a**) at 120 °C afforded the desired amine (**2b**) in only 42% yield with a modest 71:29 enantiomeric ratio (e.r.) after 35 h, along with β-methylstyrene (**2c**) in 58% yield (Fig. 3.2A, entry 1).

To understand the low selectivity towards hydroamination, we monitored the progress of this reaction by $^1$H NMR spectroscopy and found that the ratio of amine **2b** to β-methylstyrene **2c** decreased throughout the reaction. Moreover, this ratio decreased further, even after >95%

conversion of allylbenzene was observed (see supporting information for details). This result and the knowledge that hydroamination is close to ergoneutral[28] led us to consider that retrohydroamination (Fig. 3.2C, pathway i), the reverse of hydroamination, could be occurring. To probe whether retrohydroamination is occurring, we subjected amine **2b** to **Ir-0** at 120 °C for 24 hours and observed the formation of β-methylstyrene **2c** and the starting amine **1a** in 19% and 22% yield, respectively (Fig. 3.2B, reaction i). Furthermore, when a mixture of *cis*- and *trans*-**2c** was heated at 120 °C in the presence of **Ir-0** and amine **1a** for 24 hours, we did not observe the formation of either allylbenzene or amine **2b** in significant amounts (<5%) (Fig. 3.2B, reaction ii). These results implied that amine **2b** formed in the catalytic reaction underwent retrohydroamination to form β-methylstyrene directly or underwent retrohydroamination to form allylbenzene, which isomerized to β-methylstyrene irreversibly (Fig. 3.2C, pathway ii). Therefore, a catalyst that promotes the N–H addition at sufficiently low temperatures is required for the hydroamination to be favored over retrohydroamination and isomerization of the alkene.

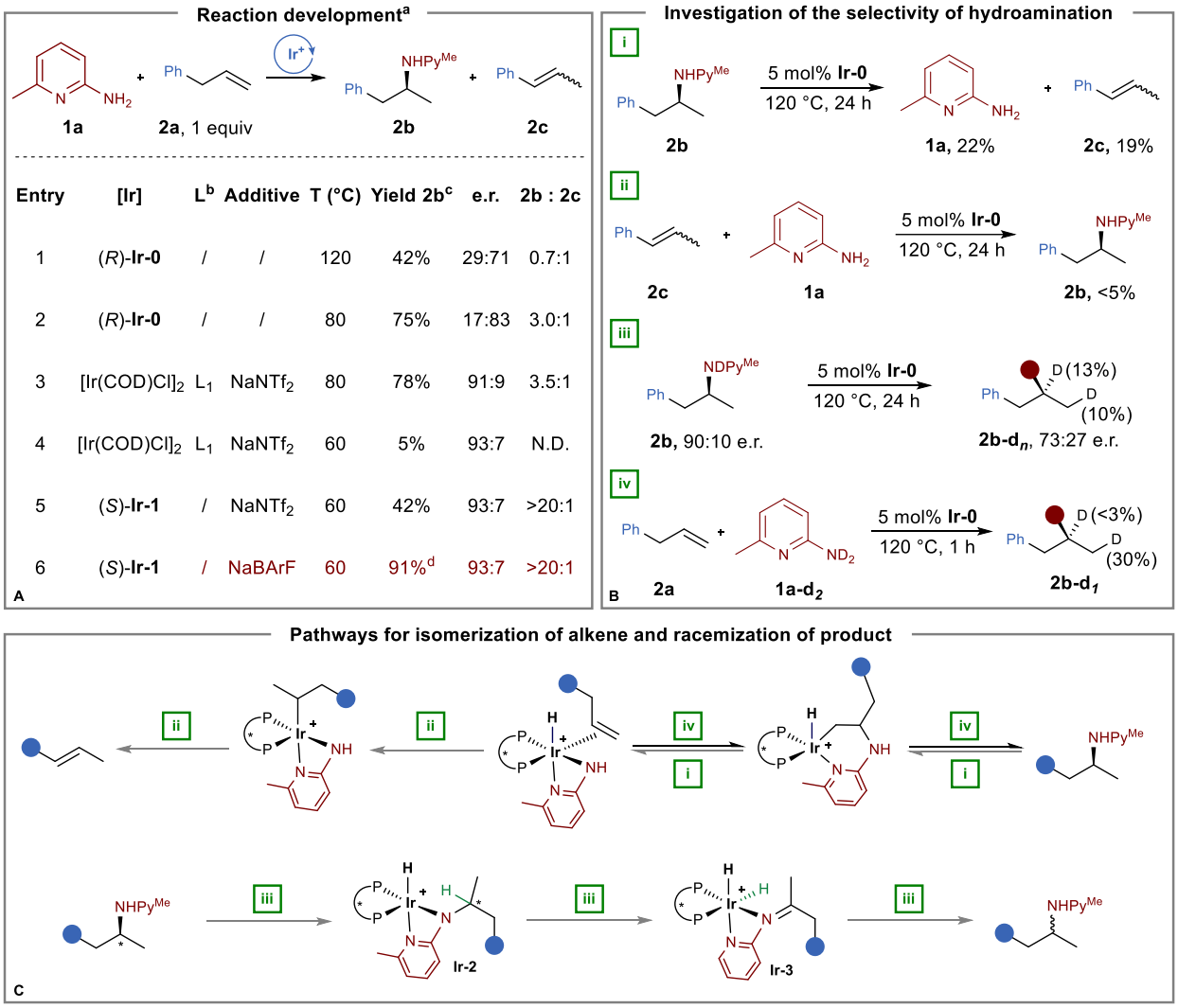


**Figure 3.2. Reaction development and mechanistic investigation.** (A) Development of the reaction condition for the hydroamination of allylbenzene. [a]Conditions: **1a** (0.1 mmol), **2a** (0.1 mmol), [Ir] (5 mol% by Ir), ligand (5 mol%), additive (6 mol%), dioxane (200 μL). [b]L1 = (*S*)-

DTBM-SEGPHOS. [c]Determined by $^1$H NMR spectroscopy with 1,3,5-trimethoxybenzene as the internal standard. [d]Isolated yield. (B) Investigation on the selectivity of the hydroamination of allylbenzene. (C) Pathways for the isomerization of the alkene and the racemization of the product of hydroamination.

To probe the origin of the low enantioselectivity, we monitored the change in the enantiomeric ratio of *N*-deuterated amine **2b** when it was subjected to **Ir-0** at 120 °C. We observed a decrease of the e.r. from 90:10 to 73:27 after 24 hours, a 13% decrease in the intensity of the $^1$H NMR signal for the α-position of amine **2b** (Fig. 3.2B, reaction iii), and a $^2$H signal corresponding to this α-position, indicating that the N–H proton exchanges with the α-C–H proton (see supporting information for more details). In contrast, the reaction of allylbenzene with *N*,*N*-dideuterio-6-methyl-2-aminopyridine (**1a-*d*$_2$**) and **Ir-0** at 120 °C for 1 hour, led to less than 3% incorporation of deuterium at the α-position of amine **2b** (Fig. 3.2B, reaction iv), as determined by $^2$H NMR spectroscopy and comparison of integrations in the $^1$H NMR spectra of **2b** from reaction with **1a** and **1a-*d*$_2$**. These results imply that deuterium at the α-position of amine **2b** observed after heating *N*-deuterated amine **2b** with catalyst **Ir-0** did not result from the reversibility of the hydroamination process that forms amine **2b** (Fig. 3.2C, pathway iv). Instead, it was most likely incorporated by a separate pathway (Fig. 3.2C, pathway iii) that also leads to racemization and that occurs by oxidative addition of the N-D bond of amine **2b** to form intermediate **Ir-2**, subsequent *β*-hydrogen elimination of **Ir-2** to generate intermediate **Ir-3**, site exchange between the hydride and the deuteride, and addition of deuteride to the imine to form the amine **2b** with incorporation of deuterium at the α-position. The above pathway, together with the retrohydroamination of amine **2b**, would then contribute to the erosion of the enantiopurity of amine **2b**, and a catalyst that undergoes this competing *β*-hydrogen elimination more slowly is needed to suppress the racemization of the enantioenriched amine product.[21]

As a consequence of these detrimental processes, a highly chemo- and enantioselective hydroamination of terminal alkenes without the use of an excess amount of alkene would require a catalytic system that promotes the pathway for hydroamination (Fig. 3.2C, pathway iv) over the three undesired pathways of retrohydroamination (Fig. 2C, pathway i), alkene isomerization (Fig. 3.2C, pathway ii), and reversible dehydrogenation of the product amine to form the imine (Fig. 3.2C, pathway iii). To identify such a system, we first attempted to conduct the reaction at temperatures lower than 120 °C. We observed that the ratio between amine **2b** and β-methylstyrene **2c** increased from 0.7 to 3.0 and the e.r. of product **2b** increased from 71:29 to 83:17 when the reaction was conducted at 80 °C (Fig. 3.2A, entry 2). The ratio between **2b** and **2c** and the e.r. further increased to 3.5 and 91:9 by replacing **Ir-0** with a combination of $[Ir(COD)Cl]_2$, (*S*)-DTBM-SEGPHOS ((*S*)-$L_1$) and $NaNTf_2$ (Fig. 3.2A, entry 3). We were unable to increase the selectivity of the reaction further by conducting the reaction at temperatures lower than 80 °C because **2b** was formed in only 5% yield when the reaction was conducted at 60 °C, due to the low conversion of allylbenzene (Fig. 3.2A, entry 4). Therefore, the development of a more active catalyst that could promote the reaction below 80 °C was required to enhance the selectivity of the reaction further.

To achieve this goal, we first sought to understand the large decrease in catalytic activity at 60 °C. The $^{31}$P NMR spectrum of the reaction catalyzed by the mixture of $[Ir(COD)Cl]_2$, (*S*)-DTBM-SEGPHOS and $NaNTf_2$ at 60 °C contained two resonances that correspond to [Ir[(*S*)-DTBM-SEGPHOS](COD)]$NTf_2$ and free DTBM-SEGPHOS. This result suggests that cyclooctadiene

(COD) coordinated more strongly to iridium than did (*S*)-DTBM-SEGPHOS and aminopyridine at 60 °C, forming off-cycle intermediates that did not catalyze the desired hydroamination.

We hypothesized that initiation of the hydroamination with an iridium precursor containing a monodentate, unstrained and volatile alkene would suppress the formation of off-cycle intermediates, leading to an increase in the rate of the catalytic reaction. Thus, we prepared [Ir[(*S*)-DTBM-SEGPHOS](ethylene)(Cl)] ([(*S*)-**Ir-1**])[29], which contains ethylene as the ancillary ligand in place of COD, and examined the hydroamination of allylbenzene with (*S*)-**Ir-1** as the precatalyst. The reaction catalyzed by the combination of (*S*)-**Ir-1** and $NaNTf_2$ at 60 °C was significantly faster than that catalyzed by the combination of an iridium precursor containing COD as the ligand, affording **2b** in 42% yield with 93:7 e.r. (Fig. 3.2A, entry 5). The yield of **2b** increased to 91% when NaBArF was used instead of $NaNTf_2$ (Fig. 3.2A, entry 6). Side products, such as β-methylstyrene, were not observed under these conditions, indicating that the catalyst formed from (*S*)-**Ir-1** was selective for hydroamination, even with an alkene that is prone to isomerization. In addition, the $^{31}P$ NMR spectrum of the reaction catalyzed by the combination of (*S*)-**Ir-1** and NaBArF did not contain a resonance corresponding to free DTBM-SEGPHOS. This observation supported our hypothesis that the reaction with an iridium precursor containing a monodentate, unstrained and volatile alkene suppressed the formation of unligated, off-cycle intermediates and led to higher catalytic activity for hydroamination. Finally, heating *N*-deuterated amine **2b** with (*S*)-**Ir-1** and NaBArF at 60 °C for 24 hours to probe for reversible hydroamination did not lead to the incorporation of deuterium into the positions α or β to the nitrogen, and only minimum erosion of the enantiomeric excess (1%) of amine **2b** was observed (see supporting information for more details). These results imply that the catalyst formed from (*S*)-**Ir-1** leads to less racemization of the enantioenriched product via retrohydroamination (Fig. 3.2c, pathway i) and the formation of an imine intermediate (Fig. 3.2c, pathway iii) than the catalyst we reported previously for the hydroamination of internal alkenes[16].

**Investigation of the scope of the reaction** Having established suitable conditions for the enantioselective hydroamination of the model alkene, we examined the scope of hydroaminations with amine **1a** catalyzed by (*S*)-**Ir-1** (Fig. 3.3, 3.4). The scope of the asymmetric hydrogenation is remarkably broad. Both simple (**2b**-**5b**) and functionalized terminal alkenes (**6b**-**34b**) underwent hydroamination in high yields and with good to excellent enantioselectivity. The asymmetric hydroamination tolerates a wide range of functional groups, including phenols (**8b**, **9b**), ethers (**10b**), internal alkenes (**11b**), silyl-protected and free alcohols (**12b**, **13b**), phosphates (**14b**), esters (**15b**-**17b**), amides (**18b**), protected amines (**19b**-**21b**), ketals (**22b**), acetals (**23b**), and cyclopropanes (**24b**). Nitro- (**25b**) and haloarenes (**26b**), which are often sensitive to reductive and nucleophilic conditions, were also compatible with the conditions of this hydroamination. Furthermore, hydroamination of alkenes in substrates containing medicinally privileged motifs, such as trifluoromethyl (**27b**, **28b**), furyl (**29b**), thienyl (**30b**), pyridyl (**31b**), indolyl (**33b**), and carbazolyl (**34b**) groups, furnished products in high yields and with excellent enantioselectivity.

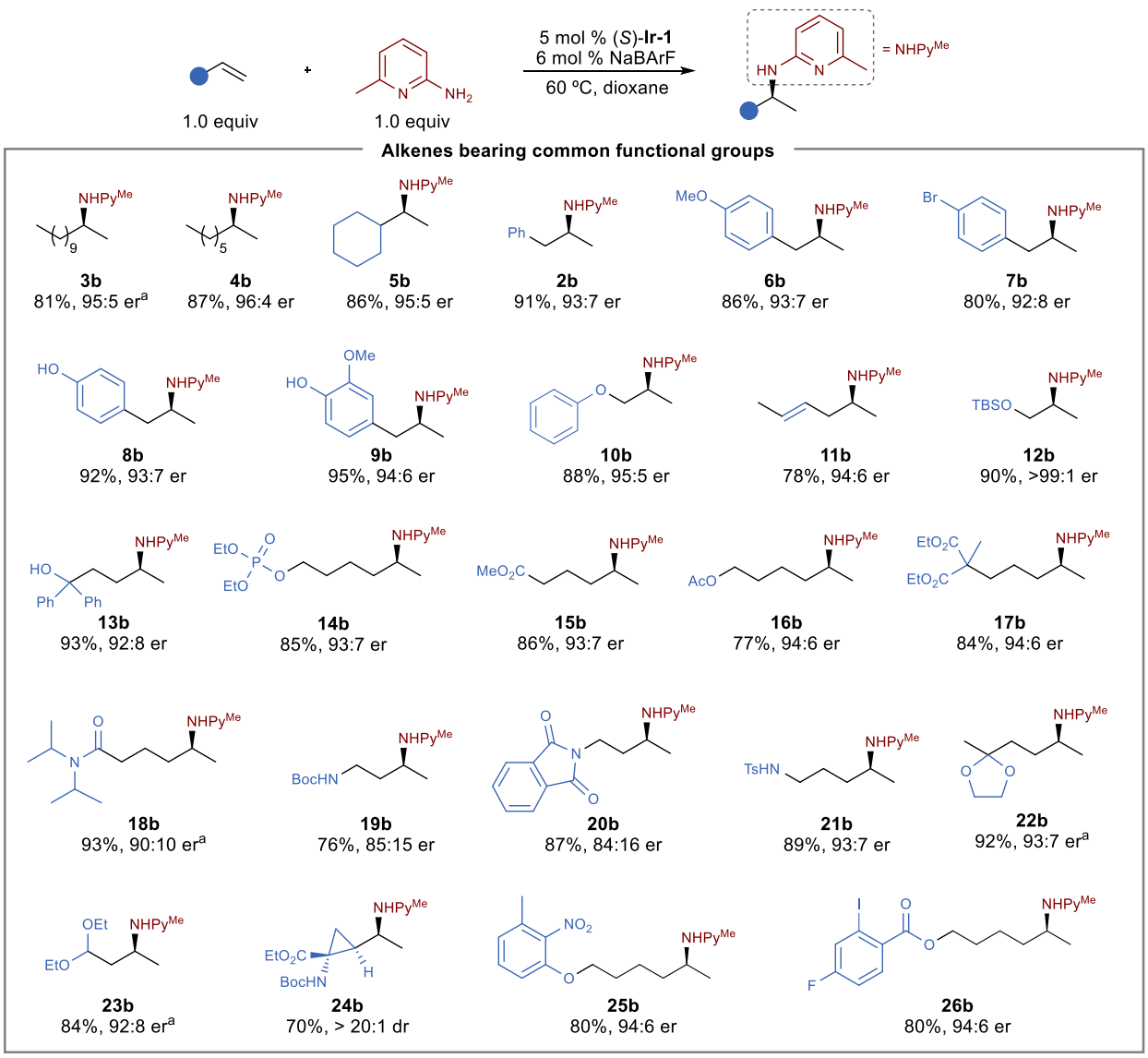


**Figure 3.3. Scope of the hydroamination of unactivated alkenes with common functional groups.** [a]The reaction was performed at 55 °C.

To explore the possibility of late-stage functionalization of bioactive and drug-like molecules with this hydroamination process, we conducted the hydroamination of alkenes that are tethered to the bioactive cores of natural products and active pharmaceutical ingredients (Fig. 3.4). Substrates derived from natural products containing alcohol, ester, α,β-unsaturated carbonyl, and hemiacetal groups (**35b**-**38b**) underwent hydroamination in high yields and with high diastereo- or enantioselectivity. The hydroamination of steroids with different levels of oxidation (**39b**-**43b**) also proceeded smoothly to afford the corresponding chiral amines. Moreover, alkenes derived from pharmaceuticals that contain allylic alcohols, heterocycles, aryl halides and sulfonamides (**43b**-**46b**) underwent hydroamination in high yield and with high enantioselectivity. The absolute configuration of product **4b** was determined to be *S* at the nitrogen-bound stereocenter by comparison of the chiral HPLC traces of the standard sample *ent*-***4b*** prepared by corss-coupling.[16]

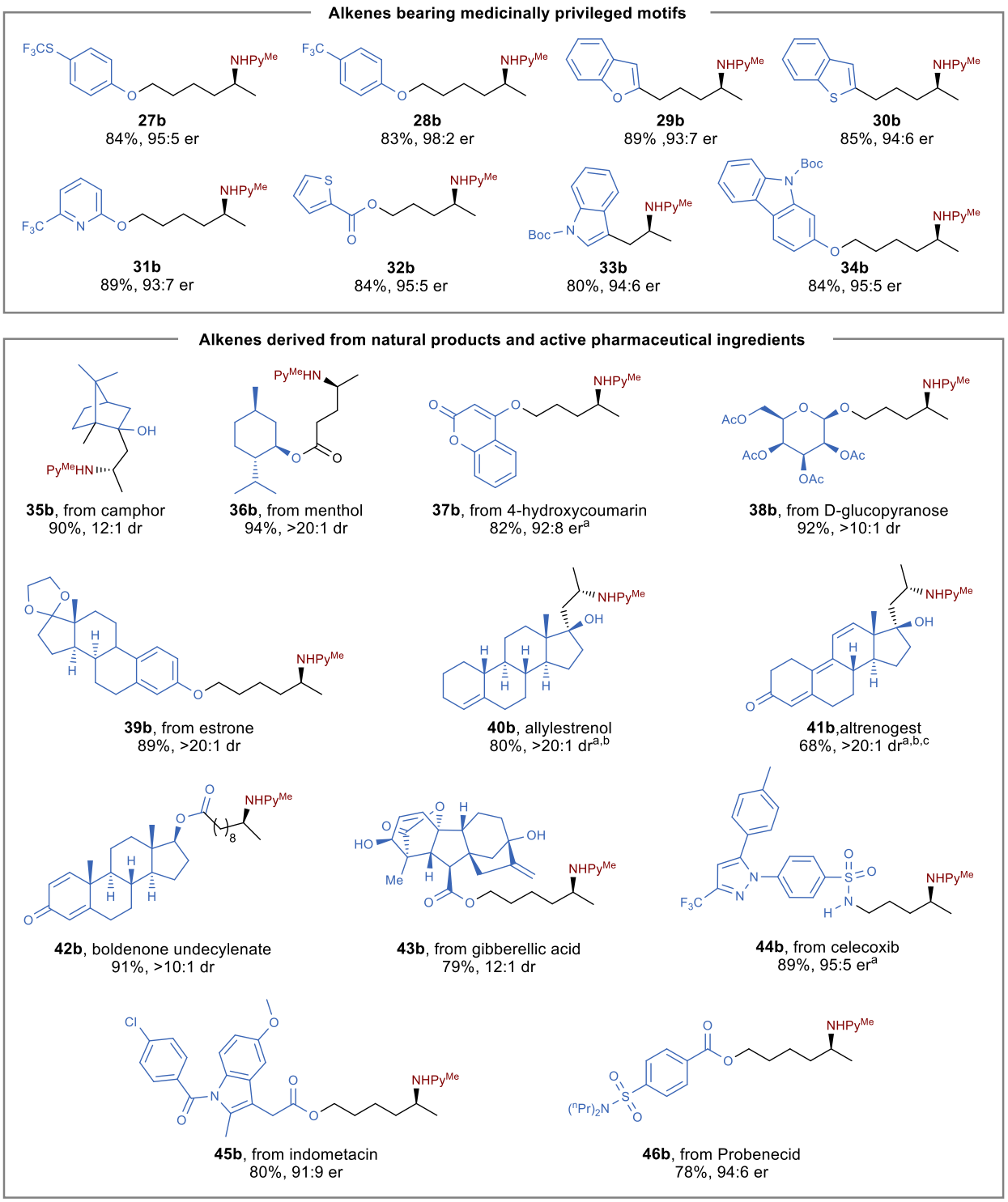


**Figure 3.4. Scope of alkenes bearing medicinally privileged motifs and alkenes derived from natural products and pharmaceuticals.** [a]The reaction was performed at 65 °C. [b]The reaction was performed with (*R*)-**Ir-1**. [c]The reaction was performed with 7.5 mol% (*R*)-**Ir-1**.

The absolute configurations of the other products were assigned by analogy. In all of the above cases, we did not observe the formation of side products from the isomerization or oxidative

amination during the hydroamination, and the mass balance corresponded to the unreacted terminal alkene. The successful incorporation of amines into complex molecules containing a variety of functional groups demonstrated a high level of both chemoselectivity and stereoselectivity of our method.

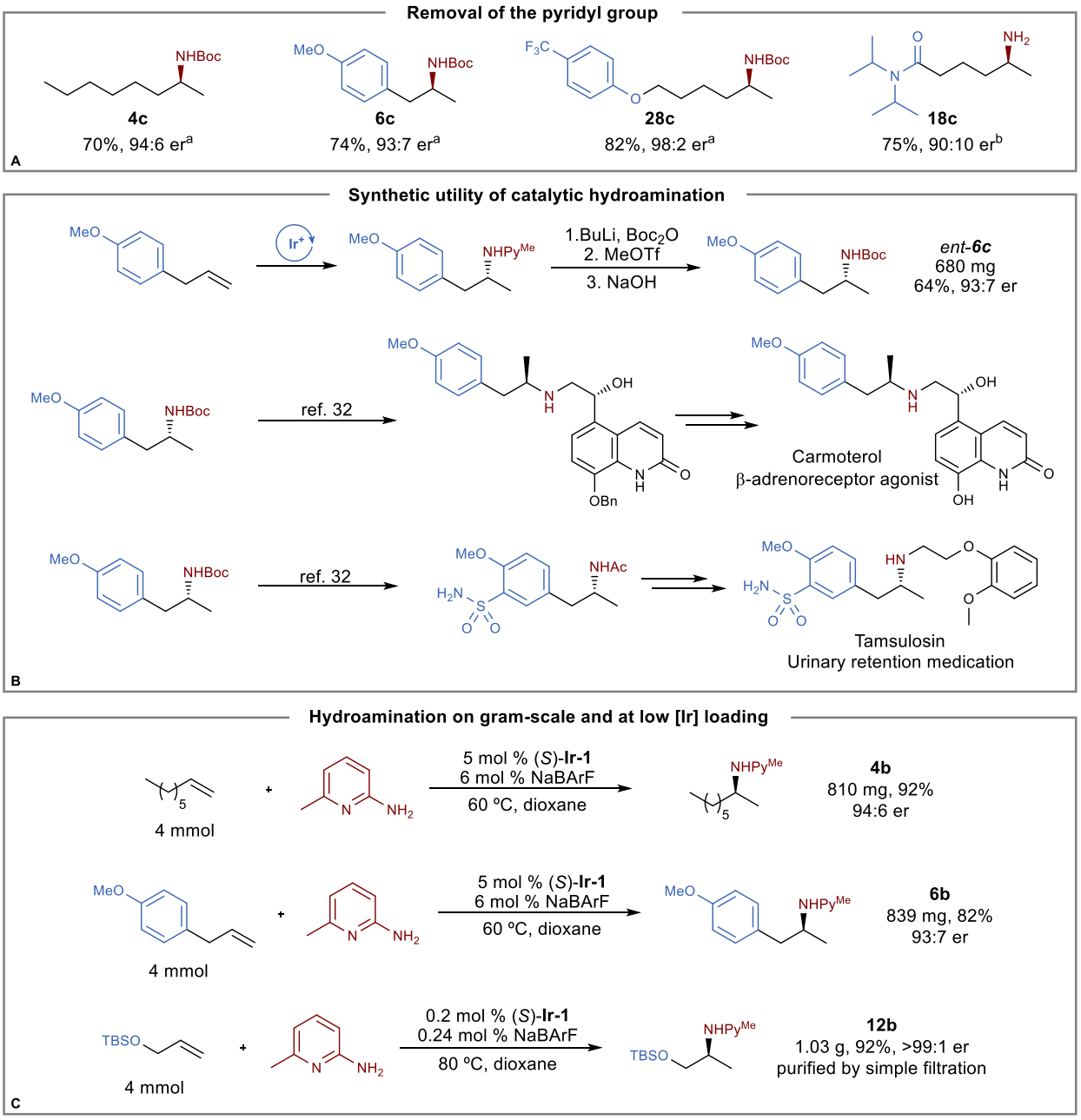


**Figure 3.5. Synthetic applications.** (A) Removal of the pyridyl group from the hydroamination products. [a]Conditions: n-BuLi, $Boc_2O$, THF; MeOTf, DCM; NaOH, EtOH, reflux. [b]Conditions: $PtO_2$, HCl, $H_2$ (1 atm); $NaBH_4$, EtOH. (B) Synthetic utility of the catalytic enantioselective hydroamination. (C) Hydroamination on gram-scale and at low [Ir] loading.

**Synthetic applications** The pyridyl group of the hydroamination products can be removed by a short sequence of reactions (Fig. 3.5A). Acylation, *N*-methylation at the pyridine nitrogen, and nucleophilic aromatic substitution converted pyridylamines **4b**, **6b**, and **28b** into the corresponding Boc-protected amines (**4c**, **6c**, and **28c**) in 70-82% yield with no erosion of enantiopurity.[30] The corresponding primary amine (**18c**) was obtained by successive hydrogenation and reduction of amine **18b** in high yield and without racemization.[31] Amine *ent*-**6c** is a key intermediate for the synthesis of the biologically active molecules, carmoterol and tamsulosin (Fig. 3.5B), demonstrating the value of this method for the preparation of pharmaceutically relevant chiral amines.[32]

Our catalytic hydroamination is easily scalable and operationally simple. The hydroaminations of 1-octene and of 4-methoxyallylbenzene at 4 mmol scale afforded the corresponding products in yields and with enantioselectivity that were comparable to those conducted at 0.1 mmol scale (Fig. 3.5C). In contrast to prior hydroaminations of unactivated alkenes, even those with achiral catalysts or catalysts forming products with low enantioselectivity,[17-19,21,22] our current catalyst enabled the reaction to occur with a high turnover number (TON = 460). The hydroamination of silyl-protected 2-propen-1-ol reached >95% conversion with 0.2 mol% loading of (*S*)-**Ir-1**, and over 1g of the pure chiral amine **12b** was isolated by a simple filtration in 92% yield. The high TON suggests that our new iridium precursor forms a highly active, yet robust catalyst.

## 3.3 Conclusion

The combination of high activity, broad scope, and high enantioselectivity show that the often-stated potential of hydroamination to convert commodity alkenes to chiral amines enantioselectively can be a reality. We show that recognition of and implementation of strategies to overcome the competing side reactions, including the isomerization of the alkene, retrohydroamination of the product amine, and dehydrogenation of the amine to form the imine, which diminished the chemo- and enantioselectivity of this transformation, can lead to a catalyst that bypasses these processes and enables the addition of amine to a structurally diverse set of alkenes with a 1:1 ratio of the two reactants. Detailed mechanistic investigation of this Ir-catalyzed hydroamination is currently ongoing in our laboratory. We anticipate that this discovery will inspire the future development of more active and selective catalysts for the hydrofunctionalization of alkenes and that reactions with additional nitrogen-based reagents that possess the properties of our 2-aminopyridine can lead to discovery of processes to form a variety of products containing stereogenic centers alpha to nitrogen derived from simple alkene feedstocks.

## 3.4 Experimental

### 3.4.1 General Experimental Procedures

All manipulations were performed in a nitrogen-filled glovebox or on a Schlenk manifold unless otherwise noted. Glassware was dried at 150 °C for at least 4 hours before use. All liquid alkenes were stored over 4 Å molecular sieves for at least 12 hours prior to use. All solid alkenes were used as received or isolated without further purification. All catalytic reactions were assembled in a nitrogen-filled glovebox with oven-dried glassware and were stirred with Teflon-coated magnetic stirring bars.

### 3.4.2 Reagents and Solvents

Pentane, $Et_2O$, THF, benzene, and hexanes were collected from a solvent purification system containing a 0.33 m column of activated alumina under nitrogen and stored over 4 Å molecular sieves for at least 12 hours prior to use. Anhydrous 1,4-dioxane was purchased from Acros, stored in a glovebox, and stored over 4 Å molecular sieves for at least 12 hours prior to use. (*S*)-DTBM-SEGPHOS and (*R*)-DTBM-SEGPHOS were used as received from Takasago. 2-Amino-6-methylpyridine was purchased from Aldrich, recrystallized from a mixture of dichloromethane and hexanes, and stored in a glovebox. NaBArF was used as received from Ambeed. $[Ir(coe)_2Cl]_2$ and $[Ir(cod)Cl]_2$ were used as received from Strem. Ir[(*R*)-DTBM-SEGPHOS](COD)$NTf_2$ and $Ru(PEt_3)_3(NTf_2)_2$ was prepared according to literature procedures[33-34].

### 3.4.3 Chromatography and Data Analysis

**Flash column chromatography** was carried out with a Teledyne Isco CombiFlash Rf system using RediSep Rf Gold columns or with Fisher silica gel Grade 60 (230-400 mesh).

**$^1$H, $^{13}$C and $^{31}$P NMR** were recorded on a Bruker 400, 500 or 600 MHz spectrometer. $^1$H chemical shifts are reported in parts per million relative residual protiated solvent as a reference. $^{13}$C chemical shifts are reported in parts per million relative to the deuterated solvent as a reference. $^{31}$P chemical shifts were reported in parts per million relative to an 85% $H_3PO_4$ external standard. $^{19}$F chemical shifts were reported in parts per million relative to an external standard of $CFCl_3$.

**High-resolution mass spectral (HRMS)** data were obtained with PerkinElmer AxION 2 TOF (ESI and APCI), Thermo LTQ-FTICR (ESI) and Waters Autospec Premier (EI) mass spectrometers at the QB3/Chemistry Mass Spectrometry Facility at UC Berkeley at the LBNL Catalysis Facility.

**Optical rotation** ($[\alpha]_D^T$) was measured on a PerkinElmer 241 Polarimeter.

**Gas Chromatography (GC)** was performed on an Agilent 7890 GC with an FID detector.

**Chiral high-performance liquid chromatography (HPLC)** separations were performed on a Waters e2695 separations module equipped with a 2998 PDA detector. The racemic samples were obtained with racemic DTBM-SEGPHOS as the ligand, which was prepared by mixing equal amounts of (*S*)-DTBM-SEGPHOS and (*R*)-DTBM-SEGPHOS.

### 3.4.4 Naming of Compounds

Compound names are those generated by ChemDraw 16.0 software (PerkinElmer), following the IUPAC nomenclature.

### 3.4.5. General Procedures for the Hydroamination of Terminal Alkenes

**Condition A: Hydroamination at 0.1 mmol Scale**

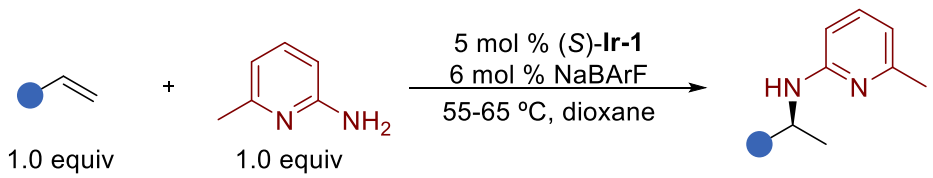


**Condition A:** In a nitrogen-filled glovebox, a 1-dram vial was charged sequentially with Ir[(*S*)-DTBM-SEGPHOS](ethylene)(Cl) [(*S*)-**Ir-1**] (7.2 mg, 5.0 mol%), 2-amino-6-methylpyridine (11

mg, 0.10 mmol, 1.0 equiv), sodium tetrakis[3,5-bis(trifluoromethyl)phenyl]borate(5.4 mg, 6.0 mol%), 1,4-dioxane (0.2 mL), the corresponding alkene (1.0 equiv), and a magnetic stir bar. The vial was capped and removed from the glovebox. The reaction was heated at 55 to 65 °C in an aluminium heating block. The ratio between the product and 2-amino-6-methylpyridine was monitored by $^1$H NMR spectroscopy periodically, and the reaction was diluted with 1 mL of DCM after this ratio was great than 5:1. The crude material was concentrated in vacuo and purified by flash column chromatography to afford the pure product (Note: prolonged reaction time will result in racemization of products in some cases).

**Condition B: Hydroamination at 4 mmol Scale**

**Condition B:** In a nitrogen-filled glovebox, a 20-mL vial was charged sequentially with Ir[(*S*)-DTBM-SEGPHOS](ethylene)(Cl) [(*S*)-**Ir-1**] (0.29 g, 5.0 mol%), 2-amino-6-methylpyridine (0.43 g, 4.0 mmol, 1.0 equiv), sodium tetrakis[3,5-bis(trifluoromethyl)phenyl]borate(0.21 g, 6.0 mol%), 1,4-dioxane (8 mL), the corresponding alkene (1.0 equiv), and a magnetic stir bar. The vial was capped and removed from the glovebox. The reaction was heated at 60 °C in an oil bath. The ratio between the product and 2-amino-6-methylpyridine was monitored by $^1$H NMR spectroscopy periodically, and the reaction was diluted with 5 mL of DCM after this ratio was great than 5:1. The crude material was concentrated in vacuo and purified by flash column chromatography to afford the pure product.

**Condition C: Hydroamination with 0.2 mol % Catalyst Loading**

**Condition C:** In a nitrogen-filled glovebox, a 1-dram vial was charged sequentially with Ir[(*S*)-DTBM-SEGPHOS](ethylene)(Cl) [(*S*)-**Ir-1**] (11.5 mg, 0.200 mol%), 2-amino-6-methylpyridine (0.43 g, 4.0 mmol, 1.0 equiv), sodium tetrakis[3,5-bis(trifluoromethyl)phenyl]borate(8.6 mg, 0.24 mol%), 1,4-dioxane (8 mL), the corresponding alkene (1 equiv), and a magnetic stir bar. The vial was capped, sealed with electrical tape, and removed from the glovebox. The reaction was heated at 80 °C in an aluminium heating block. The ratio between the product and 2-amino-6-methylpyridine was monitored by $^1$H NMR spectroscopy periodically, and the reaction was diluted with 5 mL of DCM after this ratio was great than 20:1. The crude material filtered through celite and concentrated in vacuo to afford the pure product.

**3.4.6. Evaluation of Conditions for the Hydroamination of Terminal Alkenes**

In a nitrogen-filled glovebox, a 1-dram vial was charged sequentially with Ir complex (5.0 mol% by Ir), ligand (5.0 mol%), additive (6 mol%), allylbenzene (12 mg, 0.10 mmol), 2-amino-6-methylpyridine (11 mg, 0.10 mmol), 1,3,5-trimethoxybenzene (5.6 mg, 0.033 mmol), 1,4-dioxane (0.2 mL) and a magnetic stir bar. The vial was capped and removed from the glovebox. The reaction was heated at the designated temperature in an aluminium heating block for 35 hours. An aliquot (5 μL) was then taken from the reaction and analyzed by $^1$H NMR spectroscopy and HPLC.

**Reaction development**

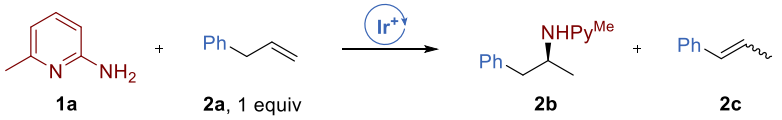


**1a** **2a**, 1 equiv **2b** **2c**

| Entry | [Ir][a] | Ligand | Additive | solvent | T (°C) | Conversion of 2a (%) | Yield 2b (%) | e.r. | 2b : 2c |
|---|---|---|---|---|---|---|---|---|---|
| 1 | (*R*)-**Ir-0** | / | / | dioxane | 120 | >95% | 42% | 29:71 | 0.7:1 |
| 2 | (*R*)-**Ir-0** | / | / | dioxane | 100 | >95% | 60% | 23:77 | 1.5:1 |
| 3 | (*R*)-**Ir-0** | / | / | dioxane | 80 | >95% | 75% | 17:83 | 3.0:1 |
| 4 | $[Ir(COD)Cl]_2$ | (*R*)-TMS-SYNPHOS | $NaNTf_2$ | dioxane | 80 | >95% | 73% | 17:83 | 3.0:1 |
| 5 | $[Ir(COD)Cl]_2$ | (*S*)-DTBM-SEGPHOS | $NaNTf_2$ | dioxane | 80 | >95% | 78% | 91:9 | 3.5:1 |
| 6 | $[Ir(COD)Cl]_2$ | (*S*)-SEGPHOS | $NaNTf_2$ | dioxane | 80 | >95% | 59% | 73:27 | 3.3:1 |
| 7 | $[Ir(COD)Cl]_2$ | (*S*)-DM-SEGPHOS | $NaNTf_2$ | dioxane | 80 | >95% | 57% | 64:36 | 1.8:1 |
| 8 | $[Ir(COD)Cl]_2$ | (*S*)-DTBM-SEGPHOS | $NaNTf_2$ | dioxane | 60 | >95% | 5% | N.D. | >20:1 |
| 9 | $[Ir(COD)Cl]_2$ | (*S*)-DTBM-SEGPHOS | $NaNTf_2$ | DCM | 80 | >95% | 90% | 89:11 | >20:1 |
| 10 | $[Ir(COD)Cl]_2$ | (*S*)-DTBM-SEGPHOS | $NaNTf_2$ | THF | 80 | 85% | 76% | 90:10 | 3.4:1 |
| 11 | $[Ir(COD)Cl]_2$ | (*S*)-DTBM-SEGPHOS | $NaNTf_2$ | PhF | 80 | >95% | 95% | 89:11 | >20:1 |
| 12 | $[Ir(COD)Cl]_2$ | (*S*)-DTBM-SEGPHOS | $NaNTf_2$ | toluene | 80 | 78% | 74% | 93:7 | >20:1 |
| 13 | $[Ir(COD)Cl]_2$ | (*S*)-DTBM-SEGPHOS | $NaNTf_2$ | MeCN | 80 | 0% | 0% | N.D. | N.D. |
| 14 | (*S*)-**Ir-1** | / | $NaNTf_2$ | dioxane | 60 | >95% | 42% | 93:7 | >20:1 |
| 15 | (*S*)-**Ir-1** | / | NaOTf | dioxane | 60 | >95% | 12% | 93:7 | >20:1 |
| 16 | (*S*)-**Ir-1** | / | NaBArF | dioxane | 60 | >95% | 97% (91%)[b] | 93:7 | >20:1 |

**Figure 3.6.** Development of the reaction condition for the hydroamination of allylbenzene. [a](*R*)-**Ir-0** = Ir[(*R*)-TMS-SYNPHOS](COD)$NTf_2$, (*S*)-**Ir-1** = Ir[(*S*)-DTBM-SEGPHOS](ethylene)(Cl). [b]Isolated yield.

### 3.4.7. Time Course of the Hydroamination of Allylbenzene at 120 °C

In a nitrogen-filled glovebox, a 1-dram vial was charged sequentially with Ir[(*R*)-TMS-SYNPHOS](COD)$NTf_2$ (9.0 mg, 5.0 μmol, 5.0 mol%), allylbenzene (12 mg, 0.10 mmol), 2-amino-6-methylpyridine (11 mg, 0.10 mmol), 1,3,5-trimethoxybenzene (5.6 mg, 0.033 mmol), 1,4-dioxane (0.2 mL) and a magnetic stir bar. The vial was capped and removed from the glovebox. The reaction was heated at 120 °C in an aluminium heating block. The reaction was removed from the heating block after a certain amount of time of heating and rapidly cooled to room temperature. The reaction was then taken into the glovebox, and a 5 μL aliquot was taken. The above process was repeated until a total reaction time of 35 h was reached. The aliquots were analyzed by $^1$H NMR spectroscopy.

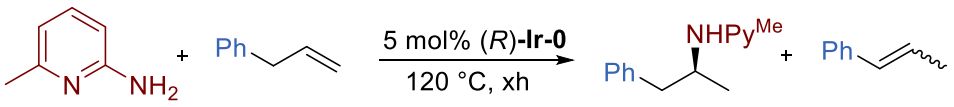


**1a** **2a**, 1 equiv **2b** **2c**

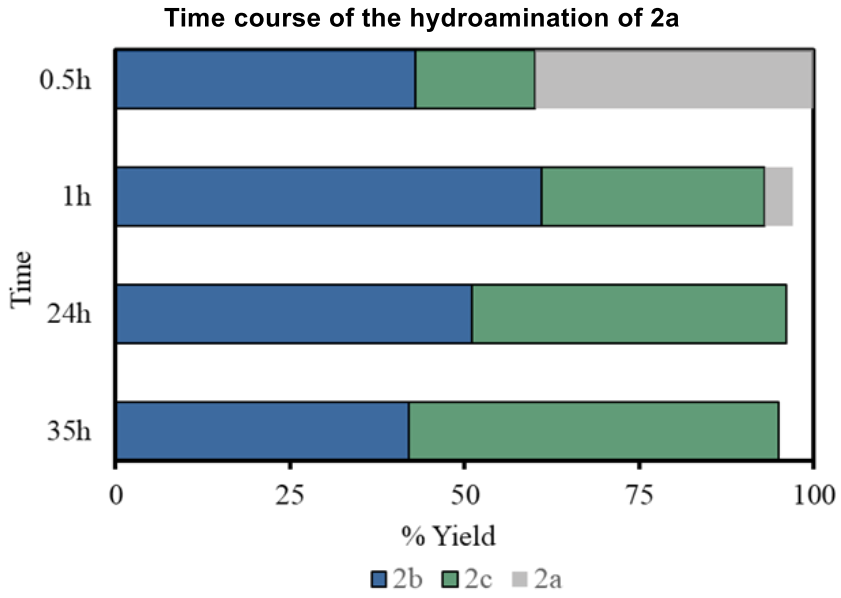


**Figure 3.7.** Time course of the hydroamination of allylbenzene at 120 °C.

### 3.4.8. Investigation on the Selectivity of the Hydroamination of Allylbenzene

#### Investigation of the reversibility of hydroamination

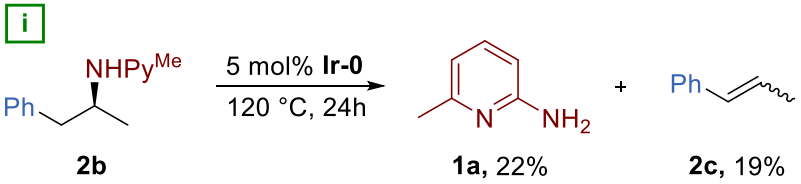


In a nitrogen-filled glovebox, a 1-dram vial was charged sequentially with Ir[(*R*)-TMS-SYNPHOS](COD)$NTf_2$ (9.0 mg, 5.0 μmol, 5.0 mol%), amine **2b** (23 mg, 0.10 mmol), 1,3,5-trimethoxybenzene (5.6 mg, 0.033 mmol), 1,4-dioxane (0.2 mL) and a magnetic stir bar. The vial was capped and removed from the glovebox. The reaction was heated at 120 °C in an aluminium heating block for the 24 hours. An aliquot (5 μL) was then taken from the reaction and analyzed by $^1$H NMR spectroscopy.

#### Hydroamination with β-methylstyrene as the substrate

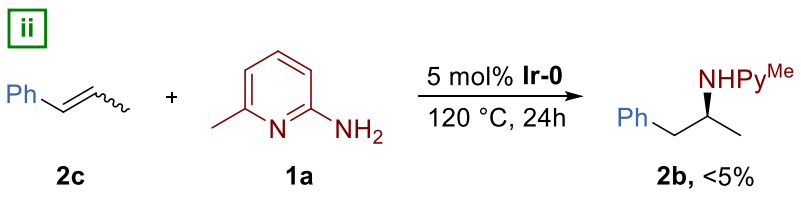

In a nitrogen-filled glovebox, a 1-dram vial was charged sequentially with Ir[(*R*)-TMS-SYNPHOS](COD)$NTf_2$ (9.0 mg, 5.0 μmol, 5.0 mol%), β-methylstyrene (12 mg, 0.10 mmol), 2-amino-6-methylpyridine (11 mg, 0.10 mmol), 1,3,5-trimethoxybenzene (5.6 mg, 0.033 mmol), 1,4-dioxane (0.2 mL) and a magnetic stir bar. The vial was capped and removed from the glovebox. The reaction was heated at 120 °C in an aluminium heating block for the 24 hours. An aliquot (5 μL) was then taken from the reaction and analyzed by $^1$H NMR spectroscopy.

**Retrohydroamination of *N*-deuterated amine 2b in the presence of (*R*)-Ir-0**

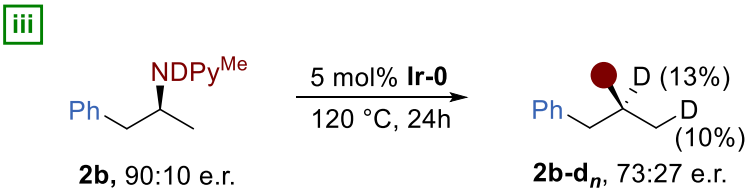


In a nitrogen-filled glovebox, a 1-dram vial was charged sequentially with Ir[(*R*)-TMS-SYNPHOS](COD)$NTf_2$ (9.0 mg, 5.0 μmol, 5.0 mol%), N-deuterated amine **2b** (23 mg, 0.10 mmol), 1,4-dioxane (0.2 mL) and a magnetic stir bar. The vial was capped and removed from the glovebox. The reaction was heated at 120 °C in an aluminium heating block for the 24 hours. The reaction was diluted with 1 mL of DCM, and the crude material was concentrated in vacuo and purified by flash column chromatography ($SiO_2$; 75:25 hexanes:EA) to afford compound **2b-d*n*** which was analyzed by $^1$H and $^2$H NMR spectroscopy.

**Hydroamination of allylbenzene with *N,N*-dideuterio-6-methyl-2-aminopyridine in the presence of (*R*)-Ir-0**

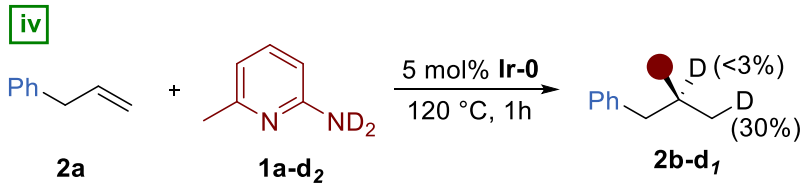


In a nitrogen-filled glovebox, a 1-dram vial was charged sequentially with Ir[(*R*)-TMS-SYNPHOS](COD)$NTf_2$ (9.0 mg, 5.0 μmol, 5.0 mol%), allylbenzene (12 mg, 0.10 mmol), *N,N*-dideuterio-6-methy-2aminolpyridine (11 mg, 0.10 mmol), 1,4-dioxane (0.2 mL) and a magnetic stir bar. The vial was capped and removed from the glovebox. The reaction was heated at 120 °C in an aluminium heating block for the 24 hours. The reaction was diluted with 1 mL of DCM, and the crude material was concentrated in vacuo and purified by flash column chromatography ($SiO_2$; 75:25 hexanes:EA) to afford compound **2b-d*1*** (12 mg, 55%) which was analyzed by $^1$H and $^2$H NMR spectroscopy.

**Retrohydroamination of *N*-deuterated amine 2b in the presence of (*S*)-Ir-1**

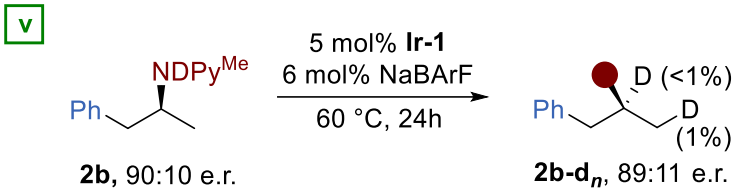


In a nitrogen-filled glovebox, a 1-dram vial was charged sequentially with Ir[(*S*)-DTBM-SEGPHOS](ethylene)Cl (7.2 mg, 5.0 µmol, 5.0 mol%), sodium tetrakis[3,5-bis(trifluoromethyl)phenyl]borate(5.4 mg, 6 µmol, 6.0 mol%), N-deuterated amine **2b** (23 mg, 0.10 mmol), 1,4-dioxane (0.2 mL) and a magnetic stir bar. The vial was capped and removed from the glovebox. The reaction was heated at 120 °C in an aluminium heating block for the 24 hours. The reaction was diluted with 1 mL of DCM, and the crude material was concentrated in vacuo and purified by flash column chromatography ($SiO_2$; 75:25 hexanes:EA) to afford compound **2b-d*n*** which was analyzed by $^1H$ and $^2H$ NMR spectroscopy.

**Hydroamination of allylbenzene with *N,N*-dideuterio-6-methyl-2-aminopyridine in the presence of (*S*)-Ir-1**

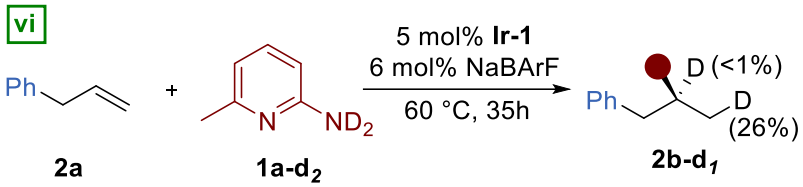


In a nitrogen-filled glovebox, a 1-dram vial was charged sequentially with Ir[(*S*)-DTBM-SEGPHOS](ethylene)Cl (7.2 mg, 5.0 µmol, 5.0 mol%), sodium tetrakis[3,5-bis(trifluoromethyl)phenyl]borate(5.4 mg, 6 µmol, 6.0 mol%), allylbenzene (12 mg, 0.10 mmol), *N,N*-dideuterio-6-methyl-2aminopyridine (11 mg, 0.10 mmol), 1,4-dioxane (0.2 mL) and a magnetic stir bar. The vial was capped and removed from the glovebox. The reaction was heated at 120 °C in an aluminium heating block for the 24 hours. The reaction was diluted with 1 mL of DCM, and the crude material was concentrated in vacuo and purified by flash column chromatography ($SiO_2$; 75:25 hexanes:EA) to afford compound **2b-d*1*** (10 mg, 44%) which was analyzed by $^1H$ and $^2H$ NMR spectroscopy.

### 3.4.9 $^{31}P$ NMR analysis of the hydroamination of allylbenzene with a combination of $[Ir(COD)Cl]_2$, (*S*)-DTBM-SEGPHOS, and $NaNTf_2$ at 60 °C.

In a nitrogen-filled glovebox, a 1-dram vial was charged sequentially with $[Ir(COD)Cl]_2$ (5.0 mg, 7.5 µmol, 2.5 mol%), (*S*)-DTBM-SEGPHOS (18 mg, 15 µmol, 5 mol%), $NaNTf_2$ (5.5 mg, 18 µmol, 6.0 mol%), allylbenzene (36 mg, 0.30 mmol), 2-amino-6-methylpyridine (33 mg, 0.30 mmol), 1,4-dioxane (0.6 mL) and a magnetic stir bar. The vial was capped and removed from the glovebox. The reaction was heated at 60 °C for 4 hours in an aluminium heating block. The reaction was removed from the heating block and transferred into a J-Young tube in the glovebox for NMR analysis.

### 3.4.10 $^{31}$P NMR analysis of the hydroamination of allylbenzene with (*S*)-Ir-1 at 60 °C.

In a nitrogen-filled glovebox, a 1-dram vial was charged sequentially with Ir[(*S*)-DTBM-SEGPHOS](ethylene)(Cl) (21 mg, 15 μmol, 5.0 mol%), allylbenzene (36 mg, 0.30 mmol), 2-amino-6-methylpyridine (33 mg, 0.30 mmol), sodium tetrakis[3,5-bis(trifluoromethyl)phenyl]borate(15 mg, 18 μmol, 6.0 mol%), 1,4-dioxane (0.6 mL) and a magnetic stir bar. The vial was capped and removed from the glovebox. The reaction was heated at 60 °C for 4 hours in an aluminium heating block. The reaction was removed from the heating block and transferred into a J-Young tube in the glovebox for NMR analysis.

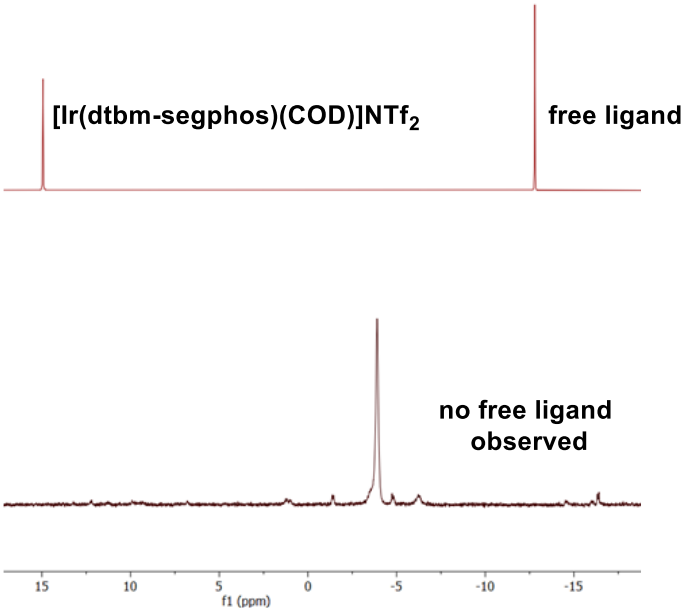


**Figure 3.8.** $^{31}$P NMR spectra of the hydroamination of allylbenzene with a combination of $[Ir(COD)Cl]_2$, (*S*)-DTBM-SEGPHOS , and $NaNTf_2$ (top) and with (*S*)-**Ir-1** and NaBArF (bottom) at 60 °C.

### 3.4.11. Synthesis of Substrates and Iridium Complexes

**Ir[(*S*)-DTBM-SEGPHOS](ethylene)(Cl) [(*S*)-Ir-1]**

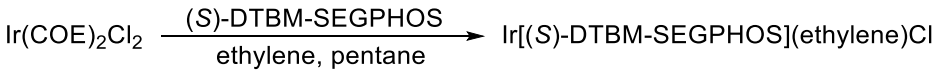


Ir[(*S*)-DTBM-SEGPHOS](ethylene)(Cl)was synthesized according to the following procedure. In a nitrogen-filled glovebox, a 25-mL Schlenk flask was charged with $[Ir(COE)_2Cl]_2$ (0.13 g, 0.15 mmol), (*S*)-DTBM-SEGPHOS (0.35 mg, 0.30 mmol, 2 equiv) pentane (5 mL), and a magnetic stir bar. The flask was capped with rubber septum and removed from the glovebox. The flask was degassed once by the standard freeze-pump-thaw procedure and ethylene was condensed into the flask using a balloon. The flask was slowly warmed to room and stirred until the mixture turned white (presumably Ir[(*S*)-DTBM-SEGPHOS](ethylene)$_2$Cl). (Note: Do not detach the balloon

from the Schlenk flask when the flask is still warming up as it would result in a build-up of pressure in the flask). The balloon was then removed, and the flask was transferred back into the glovebox. The white slurry mixture was diluted with cold pentane (5 mL) and filtered through a fine frit. (Note during the filtration, the color of the solid gradually changed from white to brick red as the bis-ethylene complex gradually turned into the mono-ethylene complex.) The resulting solid was washed with cold pentane (5 mL) three times and lyophilized with benzene to yield Ir[(*S*)-DTBM-SEGPHOS](ethylene)(Cl) (304 mg, 70%) as a brick red solid. Single crystals suitable for x-ray crystallography analysis was obtained by cooling a ether/pentane saturated solution of Ir[(*S*)-DTBM-SEGPHOS](ethylene)(Cl) to -30°C for two weeks. The $^{1}$H NMR spectrum and x-ray structure of (*S*)-**Ir-1** matched that reported in the literature[35].

**$^{31}$P NMR** (243 MHz, $C_6D6$) δ 21.09 (d, J = 25.3 Hz), 12.2 (d, J = 24.9 Hz).

### Ir[(*R*)-DTBM-SEGPHOS](ethylene)Cl ((*R*)-Ir-1)

**[(*R*)-DTBM-SEGPHOSIr(ethylene)]Cl** was prepared using the above procedure using (*R*)-DTBM-SEGPHOS.

### Alkene Substrates

Substrates **2a-13a**, **15a-16a**, **19a-24a**, **40a-42a** are available commercially. Compounds **14a**, **17a**, **18a**, **28a**, **29a**, **30a**, **32a**, **33a**, **35a**, **36a**, **37a**, **38a**, **45a**, and **46a**[36-48] are synthesized according to literature procedures. Compounds **25a**, **26a**, **27a**, **31a**, **34a**, **39a**, **43a**, and **44a** are synthesized according to the procedures in the sections below.

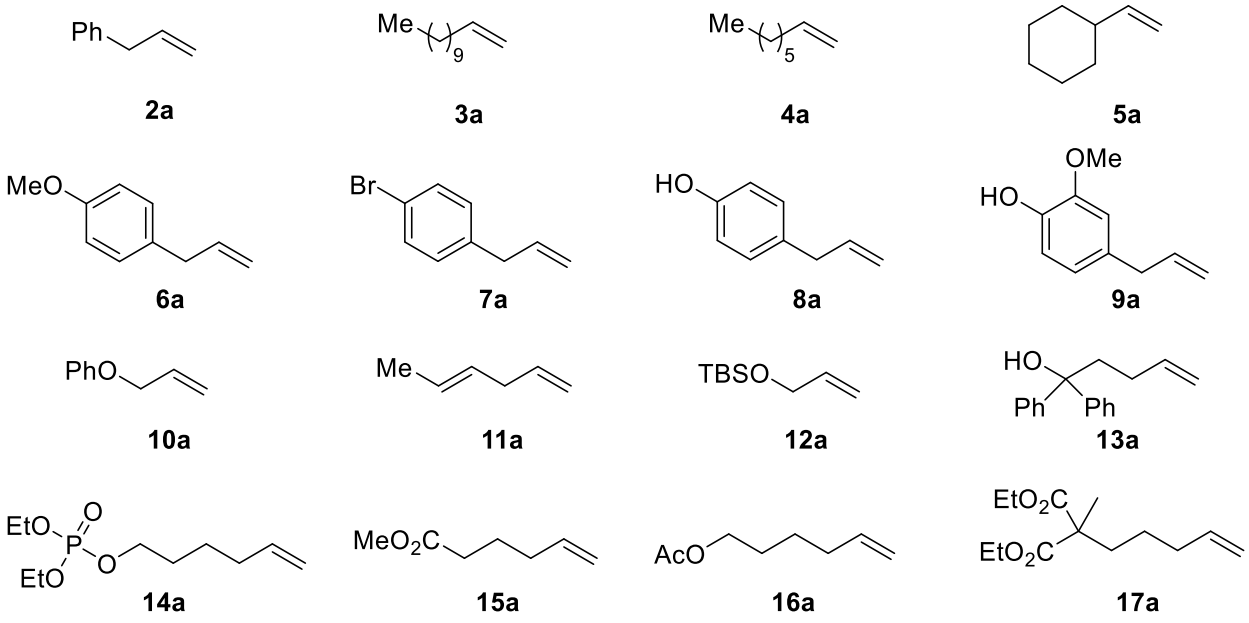


**Figure 3.9.** Alkene substrates for hydroamination, part 1.

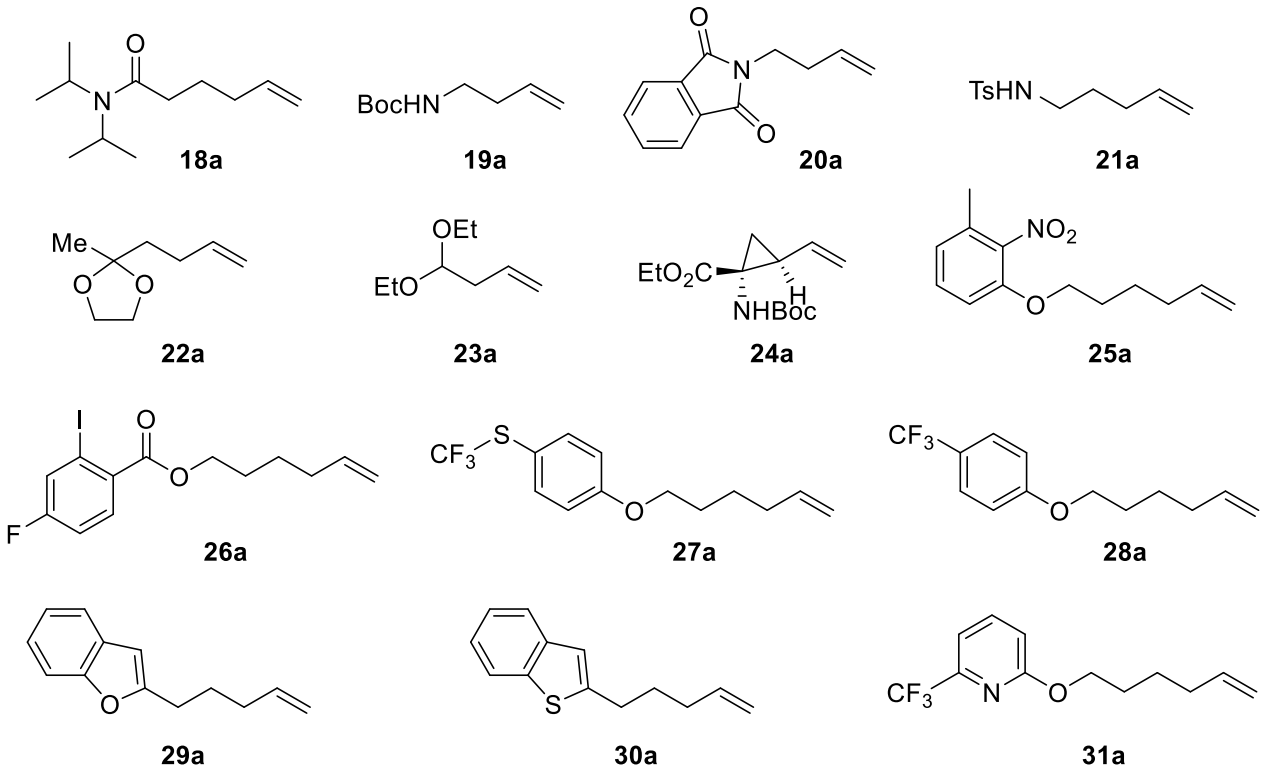


**Figure 3.10.** Alkene substrates for hydroamination, part 2.

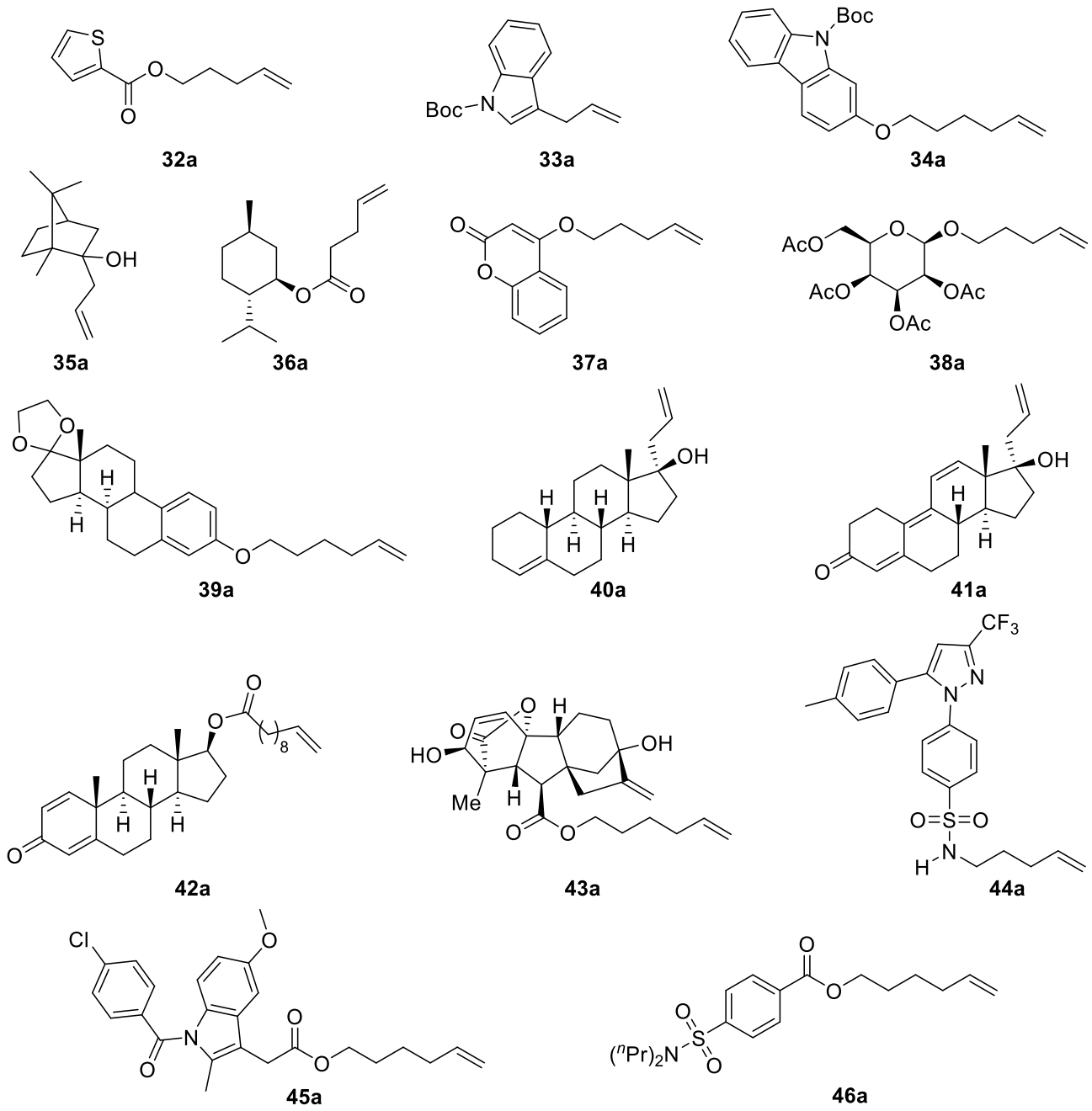


**Figure 3.11.** Alkene substrates for hydroamination, part 3.

**Condition D:** An oven-dried flask was charged with dry DCM (15 mL), carboxylic acid (1.0 equiv), 4-dimethylamino pyridine (0.10 equiv), hex-5-en-1-ol (1.0 equiv), *N*,*N*'-diisopropylcarbodiimide (DIC) (1.0 equiv) and a magnetic stir bar. The reaction mixture was allowed to stir at room temperature for 24h, before filtering and concentrating under reduced pressure. The crude residue was directly purified by flash column chromatography to yield pure ester. **Notes:** No attempts were made to optimize for yield.

**Condition E:** An oven-dried flask was charged with hex-5-en-1-ol (1.0 equiv), triphenylphosphine (1.3 equiv), phenol (1.3 equiv), 15 mL of dry THF, and a magnetic stir bar. The solution was cooled to 0 °C, and diisopropyl azodicarboxylate (DIAD) (1.3 equiv) was added dropwise. The resulting mixture was warmed to rt. After stirring for 24h, the reaction was concentrated in vacuo. The crude material was purified by flash column chromatography or preparative TLC to yield pure ether. **Notes:** No attempts were made to optimize for yield.

**Compound 25a**

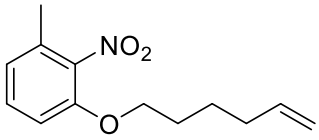


According to **Condition E**, hex-5-en-1-ol (0.30 g, 3.0 mmol) and 3-methyl-2-nitrophenol (0.55 g, 3.0 mmol) were coupled, and the product was purified by preparative TLC ($SiO_2$; 96:4 Hexanes:EA) to afford the corresponding ether **25a** (0.43 g, 60%) as a yellow oil.

**$^1$H NMR** (500 MHz, Chloroform-d) δ 7.30 – 7.19 (m, 1H), 6.91 – 6.74 (m, 2H), 5.80 (ddt, J = 16.9, 10.2, 6.7 Hz, 1H), 5.02 (dq, J = 17.1, 1.7 Hz, 1H), 4.97 (ddt, J = 10.2, 2.2, 1.3 Hz, 1H), 4.04 (t, J = 6.4 Hz, 2H), 2.29 (s, 3H), 2.13 – 2.05 (m, 2H), 1.84 – 1.70 (m, 2H), 1.60 – 1.46 (m, 2H).

**$^{13}$C NMR** (126 MHz, Chloroform-d) δ 150.42, 142.46, 138.49, 131.03, 130.66, 122.51, 115.02, 111.05, 69.34, 33.39, 28.44, 25.16, 17.08.

**HRMS (*m/z*):** (EI) calc'd $[M]^+$: 235.1208, found: 235.1210.

**Compound 26a**

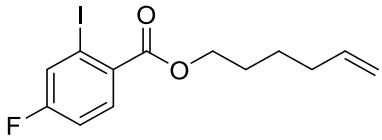


According to **Condition D**, hex-5-en-1-ol (0.30 g, 3.0 mmol) and 4-fluoro-2-iodobenzoic acid (0.80 g, 3.0 mmol) were coupled, and the product was purified by flash column chromatography ($SiO_2$; 98:2 Hexanes:EA) to afford the corresponding ester **26a** (0.21 g, 20%) as a colorless oil.

**$^1$H NMR** (500 MHz, Chloroform-d) δ 7.85 (dd, J = 8.7, 5.9 Hz, 1H), 7.72 (dd, J = 8.2, 2.6 Hz, 1H), 7.12 (ddd, J = 8.7, 7.7, 2.6 Hz, 1H), 5.81 (ddt, J = 16.9, 10.1, 6.6 Hz, 1H), 5.03 (dq, J = 17.1, 1.7 Hz, 1H), 4.98 (ddt, J = 10.1, 2.2, 1.3 Hz, 1H), 4.33 (t, J = 6.7 Hz, 2H), 2.17 – 2.08 (m, 2H), 1.79 (dt, J = 15.3, 6.8 Hz, 2H), 1.55 (dq, J = 10.0, 7.6 Hz, 2H).

**$^{13}$C NMR** (126 MHz, Chloroform-d) δ 165.64, 163.54 (d, J = 257.4 Hz), 138.38, 132.78 (d, J = 9.0 Hz), 131.24, 128.77 (d, J = 23.9 Hz), 115.29 (d, J = 21.2 Hz), 115.12, 94.67 (d, J = 8.4 Hz), 65.87, 33.41, 28.15, 25.45.

**HRMS (*m/z*):** (APCI) calc'd $[M+H]^+$: 349.0096, found: 349.0110.

**Compound 27a**

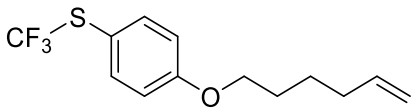

According to **Condition E**, hex-5-en-1-ol (0.30 g, 3.0 mmol) and 4-((trifluoromethyl)thio)phenol (0.70 g, 3.0 mmol) were coupled, and the product was purified by flash column chromatography ($SiO_2$; 95:5 Hexanes:EA) to afford the corresponding ether **27a** (0.59 g, 71%) as a colorless oil.

**$^1$H NMR** (500 MHz, Chloroform-d) δ 7.60 – 7.44 (m, 2H), 7.02 – 6.78 (m, 2H), 5.83 (ddt, J = 17.0, 10.2, 6.6 Hz, 1H), 5.04 (dq, J = 17.1, 1.7 Hz, 1H), 4.98 (ddt, J = 10.2, 2.2, 1.3 Hz, 1H), 3.98 (t, J = 6.4 Hz, 2H), 2.20 – 2.06 (m, 2H), 1.90 – 1.73 (m, 2H), 1.67 – 1.49 (m, 2H).

**$^{13}$C NMR** (151 MHz, Chloroform-d) (126 MHz, Chloroform-d) δ 161.53, 138.52, 138.42, 129.77 (q, J = 308.2 Hz), 115.60, 115.02, 114.69 (d, J = 2.4 Hz), 68.15, 33.51, 28.67, 25.39.

**HRMS (*m/z*):** (EI) calc'd $[M]^+$: 276.0796, found: 276.0794.

**Compound 31a**

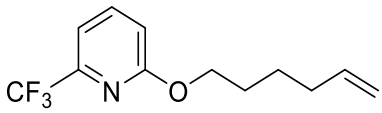

According to **Condition E**, hex-5-en-1-ol (0.30 g, 3.0 mmol) and 6-(trifluoromethyl)pyridin-2-ol (0.59 g, 3.0 mmol) were coupled, and the product was purified by preparative flash column chromatography ($SiO_2$; 100% Hexanes) to afford the corresponding ether **31a** (0.62 g, 85%) as a colorless oil.

**$^1$H NMR** (500 MHz, Chloroform-d) δ 7.68 (t, J = 7.8 Hz, 1H), 7.22 (d, J = 7.2 Hz, 1H), 6.88 (d, J = 8.4 Hz, 1H), 5.83 (ddt, J = 16.9, 10.2, 6.7 Hz, 1H), 5.03 (dq, J = 17.2, 1.7 Hz, 1H), 4.97 (dq, J = 10.2, 1.5 Hz, 1H), 4.36 (t, J = 6.6 Hz, 2H), 2.13 (q, J = 7.2 Hz, 2H), 1.88 – 1.71 (m, 2H), 1.56 (tt, J = 9.7, 6.5 Hz, 2H).

**$^{13}$C NMR** (126 MHz, Chloroform-d) δ 164.11, 145.65 (q, J = 34.6 Hz), 139.33, 138.70, 121.55 (q, J = 273.6 Hz), 114.84, 114.72, 113.06, 66.50, 33.56, 28.44, 25.44.

**HRMS (*m/z*):** (APCI) calc'd $[M+H]^+$: 246.1100, found: 246.1101.

**Compound 34a**

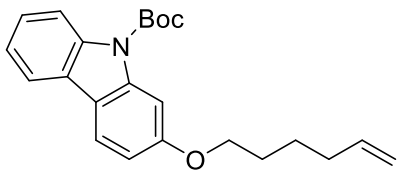

According to **Condition E**, hex-5-en-1-ol (0.15 g, 1.5 mmol) and tert-butyl 2-hydroxy-9H-carbazole-9-carboxylate (0.34 g, 1.2 mmol) were coupled, and the product was purified by flash column chromatography ($SiO_2$; 97:3 Hexanes:EA) to afford the corresponding ether **34a** (0.34 g, 77%) as a colorless oil.

**$^1$H NMR** (500 MHz, Chloroform-d) δ 8.24 (d, J = 8.3 Hz, 1H), 7.91 (d, J = 2.3 Hz, 1H), 7.87 (dt, J = 7.6, 1.0 Hz, 1H), 7.83 (d, J = 8.5 Hz, 1H), 7.38 (ddd, J = 8.5, 7.3, 1.4 Hz, 1H), 7.32 (td, J = 7.4, 1.1 Hz, 1H), 6.95 (dd, J = 8.5, 2.3 Hz, 1H), 5.86 (ddt, J = 16.9, 10.1, 6.6 Hz, 1H), 5.06 (dq, J = 17.1, 1.7 Hz, 1H), 4.99 (ddt, J = 10.2, 2.3, 1.2 Hz, 1H), 4.09 (t, J = 6.4 Hz, 2H), 2.25 – 2.07 (m, 2H), 1.95 – 1.82 (m, 2H), 1.77 (s, 9H), 1.63 (tt, J = 9.9, 6.4 Hz, 2H).

**$^{13}$C NMR** (126 MHz, Chloroform-d) δ 159.28, 151.30, 139.98, 138.73, 138.54, 126.11, 125.76, 123.17, 120.21, 119.23, 118.87, 116.30, 114.89, 112.08, 101.74, 83.94, 68.34, 33.62, 28.95, 28.54, 25.55.

**HRMS (*m/z*):** (APCI) calc'd for $[M+H]^+$: 366.2064, found: 366.2068.

**Compound 39a**

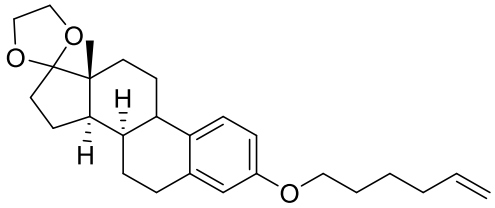

According to **Condition E**, hex-5-en-1-ol (0.25 g, 2.5 mmol) and (8R,13R,14R)-13-methyl-6,7,8,9,11,12,13,14,15,16-decahydrospiro[cyclopenta[a]phenanthrene-17,2'-[1,3]dioxolan]-3-ol (0.63 g, 2.0 mmol) were coupled, and the product was purified by flash column chromatography ($SiO_2$; 95:5 Hexanes:EA) to afford the corresponding ether **39a** (0.42 g, 52%) as a colorless oil.

**$^1$H NMR** (600 MHz, Chloroform-d) δ 7.19 (dd, J = 8.7, 1.1 Hz, 1H), 6.69 (dd, J = 8.6, 2.8 Hz, 1H), 6.62 (d, J = 2.7 Hz, 1H), 5.83 (ddt, J = 17.0, 10.2, 6.7 Hz, 1H), 5.03 (dq, J = 17.1, 1.7 Hz, 1H), 4.97 (ddt, J = 10.2, 2.3, 1.2 Hz, 1H), 4.00 – 3.86 (m, 6H), 2.90 – 2.77 (m, 2H), 2.32 (dtd, J = 13.3, 4.3, 2.6 Hz, 1H), 2.26 – 2.19 (m, 1H), 2.15 – 2.09 (m, 2H), 2.03 (ddd, J = 14.3, 11.6, 3.0 Hz, 1H), 1.92 – 1.86 (m, 1H), 1.86 – 1.81 (m, 1H), 1.82 – 1.73 (m, 4H), 1.64 (ddd, J = 12.1, 10.6, 7.1 Hz, 1H), 1.59 – 1.51 (m, 3H), 1.51 – 1.42 (m, 1H), 1.42 – 1.30 (m, 3H), 0.88 (s, 3H).

**$^{13}$C NMR** (151 MHz, Chloroform-d) δ 157.10, 138.76, 138.12, 132.73, 126.42, 119.60, 114.81, 114.61, 112.16, 67.81, 65.40, 64.74, 49.52, 46.33, 43.79, 39.24, 34.40, 33.59, 30.90, 29.96, 28.95, 27.17, 26.31, 25.51, 22.52, 14.49.

**HRMS (*m/z*):** (APCI) calc'd for $[M+H]^+$: 397.2737, found: 397.2747.

**Compound 43a**

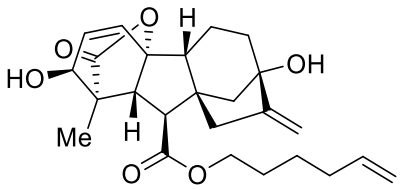

According to **Condition D**, hex-5-en-1-ol (0.30 g, 3.0 mmol) and gibberellic acid (1.0 g, 3.0 mmol) were coupled, and the product was purified by flash column chromatography ($SiO_2$; 60:40 Hexanes:EA) to afford the corresponding ester **43a** (0.95 g, 74%) as a white solid.

**$^1$H NMR** (500 MHz, Chloroform-d) δ 6.32 (dd, J = 9.3, 0.9 Hz, 1H), 5.91 (dd, J = 9.3, 3.7 Hz, 1H), 5.78 (ddt, J = 16.9, 10.1, 6.6 Hz, 1H), 5.28 (t, J = 2.4 Hz, 1H), 5.05 – 4.90 (m, 3H), 4.23 – 4.02 (m, 3H), 3.20 (d, J = 10.7 Hz, 1H), 2.78 (d, J = 10.8 Hz, 1H), 2.24 – 2.15 (m, 2H), 2.12 – 2.02 (m, 4H), 1.98 – 1.87 (m, 2H), 1.85 – 1.76 (m, 1H), 1.74 – 1.63 (m, 4H), 1.46 (p, J = 7.4 Hz, 2H), 1.25 (s, 3H).

**$^{13}$C NMR** (151 MHz, Chloroform-d) δ 178.49, 172.23, 157.13, 138.29, 133.18, 132.51, 115.17, 107.70, 90.51, 78.33, 69.98, 65.16, 53.63, 52.98, 51.32, 50.94, 50.60, 45.09, 43.23, 38.35, 33.27, 28.16, 25.29, 17.16, 14.57.

HRMS (*m/z*): (ESI) calc'd for $[M-H]^-$: 427.2126, found: 427.2123.

**Compound 44a**

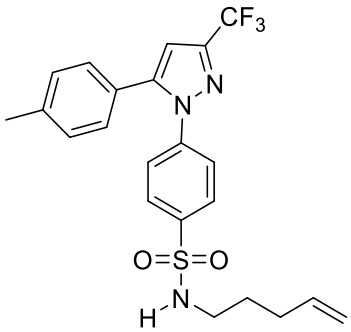

According to a literature procedure, an oven-dried 20-mL vial was charged with 5-bromopent-1-ene (0.67 g, 4.5 mmol), Celecoxib (1.0 g, 3.0 mmol), potassium carbonate (0.83 g, 6.0 mmol), potassium iodide (0.50 g, 0.3 mmol), 7.5 mL of dry acetone, and a magnetic stir bar. The reaction was heated at 65 °C for 12h and filtered. The product was purified by flash column chromatography ($SiO_2$; 85:15 Hexanes:EA) to afford the corresponding compound **44a** (818 mg, 61%) as a white solid.

**$^1$H NMR** (500 MHz, Chloroform-d) δ 7.97 – 7.70 (m, 2H), 7.57 – 7.34 (m, 2H), 7.17 (d, J = 7.8 Hz, 2H), 7.13 – 7.06 (m, 2H), 6.74 (s, 1H), 5.71 (ddt, J = 17.0, 10.2, 6.7 Hz, 1H), 5.05 – 4.93 (m, 2H), 4.48 (t, J = 6.3 Hz, 1H), 2.97 (q, J = 6.8 Hz, 2H), 2.38 (s, 3H), 2.09 – 1.99 (m, 2H), 1.57 (p, J = 7.2 Hz, 2H).

**$^{13}$C NMR** (151 MHz, Chloroform-d) δ 145.28, 144.10 (q, J = 38.6 Hz), 142.49, 139.81, 139.54, 137.03, 129.75, 128.72, 128.07, 125.70, 125.59, 121.07 (q, J = 269.2 Hz), 115.81, 106.28 (d, J = 2.1 Hz), 42.70, 30.61, 28.65, 21.31.

**HRMS (*m/z*):** (EI) calc'd for $[M]^+$: 450.1458, found: 450.1451.

### 3.4.12. Scope of Hydroamination

#### Small Organic Molecules

#### Compound 3b

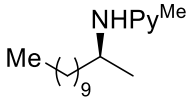


According to **Condition A** at 55 °C for 55 h, compound **3a** (17 mg, 0.10 mmol) was allowed to react, and the product was purified by flash column chromatography ($SiO_2$; 75:25 hexanes:EA) to afford amine **3b** (22 mg, 81%) as a yellow oil.

**$^{1}$H NMR** (500 MHz, Chloroform-d) δ 7.32 (dd, J = 8.3, 7.3 Hz, 1H), 6.40 (d, J = 7.3 Hz, 1H), 6.16 (d, J = 8.3 Hz, 1H), 4.39 (d, J = 8.6 Hz, 1H), 3.57 (dq, J = 8.5, 6.3 Hz, 1H), 2.35 (s, 3H), 1.58 – 1.49 (m, 1H), 1.49 – 1.42 (m, 1H), 1.41 – 1.32 (m, 2H), 1.32 – 1.21 (m, 15H), 1.18 (d, J = 6.4 Hz, 3H), 0.88 (t, J = 6.9 Hz, 3H).

**$^{13}$C NMR** (151 MHz, Chloroform-d) δ 158.16, 157.17, 138.06, 111.84, 102.55, 47.58, 37.41, 32.05, 29.79, 29.75, 29.74, 29.47, 26.20, 24.42, 22.82, 20.99, 14.25.

**HPLC:** (IF, 99:1:0.1 hexanes/IPA/DEA, 1.0 mL/min, 300 nm) indicated 96:4 er: $t_R$ (major) = 4.4 min, $t_R$ (minor) = 6.0 min.

**$[\alpha]_D^{25}$:** □21.3 (*c* = 1.4, $CH_2Cl_2$).

**HRMS (*m/z*):** (ESI) calc'd $[M+H]^+$: 277.2639, found: 277.2638.

#### Compound 4b

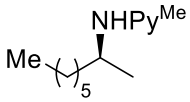


According to **Condition A** at 60 °C for 21h, compound **4a** (11 mg, 0.10 mmol) was allowed to react, and the product was purified by flash column chromatography ($SiO_2$; 75:25 hexanes:EA) to afford compound **4b** (19 mg, 87%) as a yellow oil.

Large Scale Reaction: According to **Condition B** at 60 °C for 30 h, compound **4a** (449 mg, 4.00 mmol) was allowed to react, and the product was purified by flash column chromatography ($SiO_2$; 75:25 hexanes:EA) to afford compound **4b** (810 mg, 92%) as a yellow oil.

**$^{1}$H NMR** (500 MHz, Chloroform-d) δ 7.31 (dd, J = 8.3, 7.2 Hz, 1H), 6.39 (d, J = 7.2 Hz, 1H), 6.16 (d, J = 8.3 Hz, 1H), 4.39 (d, J = 8.5 Hz, 1H), 3.57 (dq, J = 8.5, 6.4 Hz, 1H), 2.34 (s, 3H), 1.57 - 1.50 (m, 1H), 1.49 – 1.41 (m, 1H), 1.40 – 1.33 (m, 2H), 1.32 – 1.22 (m, 6H), 1.17 (d, J = 6.3 Hz, 3H), 0.91 – 0.85 (t, H = 6.8 Hz, 3H).

**$^{13}$C NMR** (151 MHz, Chloroform-d) δ 158.16, 157.17, 138.05, 111.83, 102.54, 47.58, 37.41, 31.94, 29.45, 26.17, 24.40, 22.74, 20.98, 14.20.

**HPLC:** (IF, 99:1:0.1 hexanes/IPA/DEA, 1.0 mL/min, 300 nm) indicated 95:5 er: $t_R$ (major) = 5.1 min, $t_R$ (minor) = 6.2 min.

**$[\alpha]_D^{25}$:** □23.5 (*c* = 0.9, $CH_2Cl_2$).

**HRMS (*m/z*):** (ESI) calc'd $[M+H]^+$: 221.2012, found: 221.2022.

**Compound 5b**

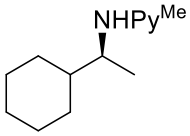


According to **Condition A** at 60 °C for 55.5h, compound **5a** (11 mg, 0.10 mmol) was allowed to react, and the product was purified by flash column chromatography ($SiO_2$; 75:25 hexanes:EA) to afford compound **5b** (19 mg, 86%) as a yellow oil.

**$^{1}$H NMR** (500 MHz, Chloroform-d) δ 7.31 (dd, J = 8.4, 7.2 Hz, 1H), 6.38 (d, J = 7.3 Hz, 1H), 6.16 (d, J = 8.4 Hz, 1H), 4.64 (s, 1H), 3.50 – 3.36 (m, 1H), 2.34 (s, 3H), 1.87 – 1.60 (m, 5H), 1.41 (ttd, J = 11.7, 5.8, 3.2 Hz, 1H), 1.27 – 1.15 (m, 2H), 1.15 – 1.10 (m, 4H), 1.10 – 0.97 (m, 2H).

**$^{13}$C NMR** (151 MHz, Chloroform-d) δ 158.27, 156.92, 138.19, 111.62, 102.46, 52.12, 43.50, 29.58, 28.86, 26.69, 26.55, 26.45, 24.25, 17.78.

**HPLC:** (IE, 99:1:0.1 hexanes/IPA/DEA, 1.0 mL/min, 300 nm) indicated 95:5 er: $t_R$ (major) = 9.3 min, $t_R$ (minor) = 8.4 min.

**$[\alpha]_D^{25}$:** □□□□□ (*c* = 1.2, $CH_2Cl_2$).

**HRMS (*m/z*):** (ESI) calc'd $[M+H]^+$: 219.1856, found: 219.1891.

**Compound 2b**

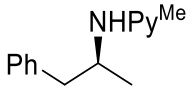


According to **Condition A** at 60 °C for 35h, compound **2a** (12 mg, 0.10 mmol) was allowed to react, and the product was purified by flash column chromatography ($SiO_2$; 75:25 hexanes:EA) to afford compound **2b** (21 mg, 91%) as a yellow oil.

**$^1$H NMR** (500 MHz, Chloroform-d) δ 7.35 – 7.27 (m, 3H), 7.22 (ddt, J = 7.4, 3.5, 2.0 Hz, 3H), 6.43 (d, J = 7.2 Hz, 1H), 6.20 (d, J = 8.3 Hz, 1H), 4.44 (d, J = 8.6 Hz, 1H), 4.06 – 3.81 (m, 1H), 2.97 (dd, J = 13.3, 5.0 Hz, 1H), 2.69 (dd, J = 13.4, 7.5 Hz, 1H), 2.38 (s, 3H), 1.17 (d, J = 6.5 Hz, 3H).

**$^{13}$C NMR** (151 MHz, Chloroform-d) δ 157.75, 157.23, 138.76, 137.99, 129.62, 128.46, 126.39, 112.15, 103.23, 48.68, 42.95, 24.46, 20.27.

**HPLC:** (IF, 99:1:0.1 hexanes/IPA/DEA, 1.0 mL/min, 300 nm) indicated 93:7 er: $t_R$ (major) = 6.7 min, $t_R$ (minor) = 7.3 min.

**$[\alpha]_D^{25}$:** □□□□□ (*c* = 1.4, $CH_2Cl_2$).

**HRMS (*m/z*):** (ESI) calc'd $[M+H]^+$: 227.1543, found: 227.1538.

**Compound 6b**

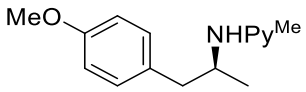


According to **Condition A** at 60 °C for 19h, compound **6a** (15 mg, 0.10 mmol) was allowed to react, and the product was purified by flash column chromatography ($SiO_2$; 70:30 hexanes:EA) to afford compound **6b** (22 mg, 86%) as a yellow oil.

**$^1$H NMR** (600 MHz, Chloroform-d) δ 7.45 (t, J = 7.8 Hz, 1H), 7.29 – 7.15 (m, 2H), 7.04 – 6.89 (m, 2H), 6.55 (d, J = 7.2 Hz, 1H), 6.32 (d, J = 8.3 Hz, 1H), 4.56 (d, J = 8.5 Hz, 1H), 4.02 (p, J = 6.9 Hz, 1H), 3.91 (s, 3H), 3.02 (dd, J = 13.5, 5.0 Hz, 1H), 2.77 (dd, J = 13.5, 7.4 Hz, 1H), 2.50 (s, 3H), 1.28 (d, J = 6.4 Hz, 3H).

**$^{13}$C NMR** (151 MHz, Chloroform-d) δ 158.26, 157.79, 157.19, 137.97, 130.75, 130.52, 113.89, 112.09, 103.20, 55.35, 48.76, 41.96, 24.44, 20.20.

**HPLC:** (IF, 99:1:0.1 hexanes/IPA/DEA, 1.0 mL/min, 300 nm) indicated 93:7 er: $t_R$ (major) = 9.7 min, $t_R$ (minor) = 12.2 min.

**$[\alpha]_D^{25}$:** □□□□□ (*c* = 1.4, $CH_2Cl_2$).

**HRMS (*m/z*):** (ESI) calc'd $[M+H]^+$: 257.1649, found: 257.1656.

Large Scale Reaction for the synthesis of ***ent*-6b**: According to **Condition B** at 60 °C for 23 h, except with Ir[(*R*)-DTBM-SEGPHOS(ethylene)]Cl as the catalyst instead of Ir[(*S*)-DTBM-SEGPHOS(ethylene)]Cl, compound **6a** (593 mg, 4.00 mmol) was allowed to react, and the product was purified by flash column chromatography ($SiO_2$; 70:30 hexanes:EA) to afford compound ***ent*-6b** (838.5 mg, 82%) as a yellow oil.

**Compound 7b**

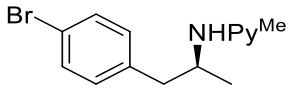


According to **Condition A** at 60 °C for 61.5 h, compound **7a** (20 mg, 0.10 mmol) was allowed to react, and the product was purified by flash column chromatography ($SiO_2$; 70:30 hexanes:EA) to afford compound **7b** (24 mg, 80%) as a yellow oil. (Note: The product decomposed slightly on silica gel.)

**$^1$H NMR** (600 MHz, Methylene Chloride-$d_2$) δ 7.45 – 7.38 (m, 2H), 7.30 (dd, J = 8.3, 7.2 Hz, 1H), 7.16 – 7.07 (m, 2H), 6.41 (dt, J = 7.3, 0.7 Hz, 1H), 6.17 (d, J = 8.3 Hz, 1H), 4.37 (d, J = 8.5 Hz, 1H), 4.01 (dtd, J = 8.5, 6.8, 5.5 Hz, 1H), 2.89 (dd, J = 13.4, 5.5 Hz, 1H), 2.68 (dd, J = 13.5, 7.1 Hz, 1H), 2.33 (s, 3H), 1.15 (d, J = 6.5 Hz, 3H).

**$^{13}$C NMR** (151 MHz, Methylene Chloride-$d_2$) δ 157.97, 157.42, 138.62, 137.98, 131.70, 131.63, 120.27, 112.17, 48.55, 42.42, 24.46, 20.34.

**HPLC:** (IF, 99:1:0.1 hexanes/IPA/DEA, 1.0 mL/min, 300 nm) indicated 92:8 er: $t_R$ (major) = 7.3 min, $t_R$ (minor) = 8.6 min.

$[\boldsymbol{\alpha}]_{\boldsymbol{D}}^{\boldsymbol{25}}$**:** □□□□□ (*c* = 1.5, $CH_2Cl_2$).

**HRMS (*m/z*):** (ESI) calc'd $[M+H]^+$: 305.0648, found: 305.0635.

**Compound 8b**

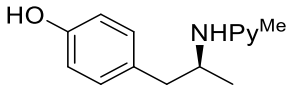


According to **Condition A** at 60 °C for 18h, compound **8a** (13 mg, 0.10 mmol) was allowed to react, and the product was purified by flash column chromatography ($SiO_2$; 50:50 hexanes:EA) to afford compound **8b** (22 mg, 92%) as a yellow solid.

**$^1$H NMR** (600 MHz, Chloroform-d) δ 7.39 (dd, J = 8.4, 7.3 Hz, 1H), 6.95 – 6.84 (m, 2H), 6.67 – 6.61 (m, 2H), 6.41 (d, J = 7.3 Hz, 1H), 6.27 (d, J = 8.4 Hz, 1H), 4.92 (d, J = 7.9 Hz, 1H), 3.80 (hept, J = 6.3 Hz, 1H), 2.85 (dd, J = 13.9, 5.2 Hz, 1H), 2.63 (dd, J = 13.9, 6.4 Hz, 1H), 2.33 (s, 3H), 1.18 (d, J = 6.4 Hz, 3H).

**$^{13}$C NMR** (151 MHz, Chloroform-d) δ 157.37, 156.35, 155.76, 139.12, 130.59, 128.25, 115.76, 112.14, 103.11, 48.39, 41.14, 23.22, 20.33.

**HPLC:** (ODH, 97:3:0.1 hexanes/IPA/DEA, 1.0 mL/min, 300 nm) indicated 93:7 er: $t_R$ (major) = 29.2 min, $t_R$ (minor) = 26.1 min.

$[\boldsymbol{\alpha}]_{\boldsymbol{D}}^{\boldsymbol{25}}$**:** □□□□□ (*c* = 1.7, $CH_2Cl_2$).

**HRMS (*m/z*):** (ESI) calc'd $[M+H]^+$: 243.1492, found: 243.1495.

**Compound 9b**

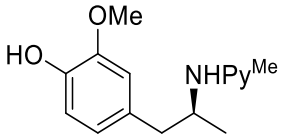


According to **Condition A** at 60 °C for 18h, compound **9a** (16 mg, 0.10 mmol) was allowed to react, and the product was purified by flash column chromatography ($SiO_2$; 50:50 hexanes:EA) to afford compound **9b** (26 mg, 95%) as a yellow solid.

**$^1$H NMR** (600 MHz, Chloroform-d) δ 7.32 (dd, J = 8.4, 7.2 Hz, 1H), 6.80 (d, J = 7.8 Hz, 1H), 6.70 – 6.64 (m, 2H), 6.40 (d, J = 7.2 Hz, 1H), 6.18 (d, J = 8.3 Hz, 1H), 5.38 (s, 1H), 5.07 (d, J = 62.8 Hz, 1H), 3.90 – 3.84 (m, 1H), 3.82 (s, 3H), 2.84 (dd, J = 13.6, 5.4 Hz, 1H), 2.66 (dd, J = 13.6, 7.0 Hz, 1H), 2.36 (s, 3H), 1.17 (d, J = 6.4 Hz, 3H).

**$^{13}$C NMR** 13C NMR (151 MHz, Chloroform-d) δ 157.62, 156.56, 146.65, 144.38, 138.40, 130.39, 122.21, 114.49, 112.35, 111.93, 103.44, 55.95, 48.91, 42.44, 23.88, 20.32.

**HPLC:** (IF, 97:3:0.1 hexanes/IPA/DEA, 1.0 mL/min, 300 nm) indicated 94:6 er: $t_R$ (major) = 18.5 min, $t_R$ (minor) = 21.4 min.

**$[\alpha]_D^{25}$:** □□□□□ (*c* = 1.8, $CH_2Cl_2$).

**HRMS (*m/z*):** (ESI) calc'd $[M+H]^+$: 273.1598, found: 273.1604.

**Compound 10b**

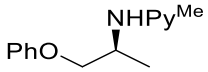


According to **Condition A** at 60 °C for 19h, compound **10a** (13 mg, 0.10 mmol) was allowed to react, and the product was purified by flash column chromatography ($SiO_2$; 70:30 hexanes:EA) to afford compound **10b** (21 mg, 88%) as a yellow oil.

**$^1$H NMR** (600 MHz, Chloroform-d) δ 7.32 (dd, J = 8.3, 7.3 Hz, 1H), 7.28 (dt, J = 9.3, 6.9 Hz, 2H), 6.97 – 6.95 (m, 3H), 6.45 (dt, J = 7.3, 0.7 Hz, 1H), 6.25 (d, J = 8.3 Hz, 1H), 4.62 (d, J = 8.3 Hz, 1H), 4.25 – 4.17 (m, 1H), 4.09 (dd, J = 9.1, 3.9 Hz, 1H), 3.92 (dd, J = 9.1, 5.8 Hz, 1H), 2.39 (s, 3H), 1.38 (d, J = 6.6 Hz, 3H).

**$^{13}$C NMR** (151 MHz, Chloroform-d) δ 158.98, 157.66, 157.20, 137.94, 120.96, 114.71, 112.39, 103.76, 71.08, 46.58, 24.48, 18.24.

**HPLC:** (ODH, 98:2:0.1 hexanes/IPA/DEA, 1.0 mL/min, 300 nm) indicated 95:5 er: $t_R$ (major) = 10.7 min, $t_R$ (minor) = 8.9 min.

**$[\alpha]_D^{25}$:** □□□□□ (*c* = 1.5, $CH_2Cl_2$).

**HRMS (*m/z*):** (ESI) calc'd $[M+H]^+$: 243.1492, found: 243.1496.

**Compound 11b**

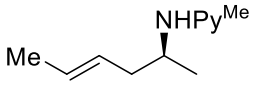


According to **Condition A** at 60 °C for 20h, compound **11a** (8.2 mg, 0.10 mmol) was allowed to react, and the product was purified by flash column chromatography ($SiO_2$;75:25 hexanes:EA) to afford compound **11b** (15 mg, 78%) as a yellow oil.

**$^1$H NMR** (500 MHz, Chloroform-d) δ 7.33 (t, J = 7.8 Hz, 1H), 6.39 (d, J = 7.2 Hz, 1H), 6.19 (d, J = 8.4 Hz, 1H), 5.52 (dq, J = 12.4, 6.1 Hz, 1H), 5.48 – 5.39 (m, 1H), 5.07 (s, 1H), 3.61 (q, J = 6.4 Hz, 1H), 2.35 (s, 3H), 2.31 – 2.23 (m, 1H), 2.17 (dt, J = 13.9, 6.9 Hz, 1H), 1.70 – 1.62 (m, 3H), 1.19 (d, J = 6.4 Hz, 3H).

**$^{13}$C NMR** (151 MHz, Chloroform-d) δ 157.74, 156.59, 138.42, 128.44, 127.17, 111.83, 103.10, 47.62, 39.88, 23.93, 20.31, 18.18.

**HPLC:** (IF, 99:1:0.1 hexanes/IPA/DEA, 1.0 mL/min, 300 nm) indicated 94:6 er: $t_R$ (major) = 5.6 min, $t_R$ (minor) = 6.4 min.

**$[\alpha]_D^{25}$:** +14.5 (*c* = 1.0, $CH_2Cl_2$).

**HRMS (*m/z*):** (ESI) calc'd $[M+H]^+$: 191.1543, found: 191.1544.

**Compound 12b**

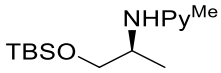


According to **Condition A** at 60 °C for 19h, compound **12a** (17 mg, 0.10 mmol) was allowed to react, and the product was purified by flash column chromatography ($SiO_2$; 75:25 hexanes:EA) to afford compound **12b** (25 mg, 90%) as a yellow oil.

Hydroamination with 0.2 mol% catalyst loading: According to **Condition C** at 80 °C for 44h, compound **12a** (0.69 g, 4.00 mmol) was allowed to react, and the product was purified by filtration to afford compound **12b** (1.03 g, 92%) as a yellow oil.

**$^1$H NMR** (500 MHz, Chloroform-d) δ 7.30 (dd, J = 8.3, 7.2 Hz, 1H), 6.41 (d, J = 7.3 Hz, 1H), 6.20 (d, J = 8.3 Hz, 1H), 4.58 (d, J = 8.6 Hz, 1H), 3.85 – 3.74 (m, 1H), 3.66 (dd, J = 9.8, 3.9 Hz, 1H), 3.57 (dd, J = 9.8, 5.4 Hz, 1H), 2.35 (s, 3H), 1.22 (d, J = 6.5 Hz, 3H), 0.89 (s, 9H), 0.04 (d, J = 3.0 Hz, 6H).

**$^{13}$C NMR** (151 MHz, Chloroform-d) δ 158.05, 157.10, 137.88, 48.79, 24.44, 18.48, 17.81.

**HPLC:** (ODH, 99:1:0.1 hexanes/IPA/DEA, 1.0 mL/min, 300 nm) indicated >99:1 er: $t_R$ (major) = 4.2 min, $t_R$ (minor) = 3.4 min.

**$[\alpha]_D^{25}$:** -13.4 (*c* = 1.8, $CH_2Cl_2$).

**HRMS (*m/z*):** (ESI) calc'd $[M+H]^+$: 281.2044, found: 281.2041.

**Compound 13b**

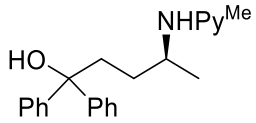


According to **Condition A** at 60 °C for 24.5h, compound **13a** (24 mg, 0.10 mmol) was allowed to react, and the product was purified by flash column chromatography ($SiO_2$; 65:35 hexanes:EA) to afford compound **13b** (32 mg, 93%) as a yellow solid. (Note: The product decomposed slightly on silica gel.)

**$^1$H NMR** (600 MHz, Methylene Chloride-$d_2$) δ 7.36 (tt, J = 8.2, 1.3 Hz, 4H), 7.23 – 7.12 (m, 5H), 7.11 – 7.02 (m, 2H), 6.24 (d, J = 7.2 Hz, 1H), 6.05 (d, J = 8.3 Hz, 1H), 4.33 – 4.29 (m, 1H), 4.02 – 3.94 (m, 1H), 2.35 (ddd, J = 14.2, 7.6, 6.5 Hz, 1H), 2.24 (dt, J = 14.4, 6.2 Hz, 1H), 2.19 (s, 3H), 1.44 (qd, J = 6.4, 3.0 Hz, 2H), 1.06 (d, J = 6.5 Hz, 3H).

**$^{13}$C NMR** (151 MHz, Methylene Chloride-d2) δ 158.30, 156.75, 149.13, 148.39, 138.12, 128.34, 128.33, 126.78, 126.65, 126.47, 126.23, 111.82, 105.44, 78.51, 47.77, 37.34, 33.13, 23.89, 21.85.

**HPLC:** (IF, 97:3:0.1 hexanes/IPA/DEA, 1.0 mL/min, 300 nm) indicated 92:8 er: $t_R$ (major) = 18.6 min, $t_R$ (minor) = 13.6 min.

**$[\alpha]_D^{25}$:** +51.1 (*c* = 2.0, $CH_2Cl_2$).

**HRMS (*m/z*):** (ESI) calc'd $[M+H]^+$: 347.2118, found: 347.2121.

**Compound 14b**

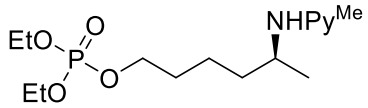


According to **Condition A** at 60 °C for 38.5h, compound **14a** (24 mg, 0.10 mmol) was allowed to react, and the product was purified by preparative TLC ($SiO_2$; 50:50 hexanes:acetone) to afford compound **14b** (29 mg, 85%) as a yellow oil.

**$^1$H NMR** (600 MHz, Chloroform-d) δ 7.30 (d, J = 7.8 Hz, 1H), 6.38 (d, J = 7.2 Hz, 1H), 6.14 (d, J = 8.3 Hz, 1H), 4.41 (d, J = 8.1 Hz, 1H), 4.08 (pd, J = 7.2, 3.1 Hz, 4H), 4.01 (q, J = 6.7 Hz, 2H), 3.62 (dq, J = 12.0, 6.3 Hz, 1H), 2.32 (s, 3H), 1.74 – 1.62 (m, 2H), 1.60 – 1.39 (m, 4H), 1.34 – 1.28 (m, 6H), 1.17 (d, J = 6.4 Hz, 3H).

**$^{13}$C NMR** (126 MHz, Chloroform-d) δ 157.97, 157.05, 138.09, 111.92, 102.73, 67.49, 63.78, 47.27, 36.76, 30.33 (d, J = 6.9 Hz), 24.30, 22.13, 20.99, 16.24.

**HPLC:** (IF, 93:7:0.1 hexanes/IPA/DEA, 1.0 mL/min, 300 nm) indicated 93:7 er: $t_R$ (major) = 17.8 min, $t_R$ (minor) = 19.9 min.

**$[\alpha]_D^{25}$:** +15.9 (*c* = 2.0, $CH_2Cl_2$).

**HRMS (*m/z*):** (ESI) calc'd $[M+H]^+$: 345.1938, found: 345.1927.

**Compound 15b**

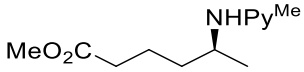


According to **Condition A** at 60 °C for 42.5h, compound **15a** (13 mg, 0.10 mmol) was allowed to react, and the product was purified by flash column chromatography ($SiO_2$; 65:35 hexanes:EA) to afford compound **15b** (20 mg, 86%) as a yellow oil.

**$^1$H NMR** (500 MHz, Chloroform-d) δ 7.31 (dd, J = 8.3, 7.3 Hz, 1H), 6.40 (d, J = 7.3 Hz, 1H), 6.15 (d, J = 8.3 Hz, 1H), 4.44 (d, J = 7.8 Hz, 1H), 3.65 (s, 4H), 2.36 – 2.27 (m, 5H), 1.79 – 1.62 (m, 2H), 1.53 (qdt, J = 13.4, 10.0, 6.4 Hz, 2H), 1.19 (d, J = 6.4 Hz, 3H).

**$^{13}$C NMR** (151 MHz, Chloroform-d) δ 174.03, 157.93, 157.06, 138.12, 111.99, 102.84, 51.63, 47.19, 36.66, 34.02, 24.32, 21.64, 20.99.

**HPLC:** (IF, 98:2:0.1 hexanes/IPA/DEA, 1.0 mL/min, 300 nm) indicated 93:7 er: $t_R$ (major) = 13.4 min, $t_R$ (minor) = 28.8 min.

**$[\alpha]_D^{25}$:** +13.7 (*c* = 1.3, $CH_2Cl_2$).

**HRMS (*m/z*):** (ESI) calc'd $[M+H]^+$: 237.1598, found: 237.1590.

**Compound 16b**

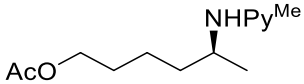


According to **Condition A** at 60 °C for 64h, compound **16a** (14 mg, 0.10 mmol) was allowed to react, and the product was purified by flash column chromatography ($SiO_2$; 65:35 hexanes:EA) to afford compound **16b** (19 mg, 77%) as a yellow oil.

**$^1$H NMR** (500 MHz, Chloroform-d) δ 7.31 (dd, J = 8.2, 7.3 Hz, 1H), 6.40 (d, J = 7.2 Hz, 1H), 6.15 (d, J = 8.3 Hz, 1H), 4.38 (d, J = 8.6 Hz, 1H), 4.04 (t, J = 6.6 Hz, 2H), 3.62 (dq, J = 8.6, 6.2 Hz, 1H), 2.34 (s, 3H), 2.03 (s, 3H), 1.64 (qd, J = 7.9, 7.3, 5.9 Hz, 2H), 1.59 – 1.34 (m, 4H), 1.18 (d, J = 6.4 Hz, 3H).

**$^{13}$C NMR** (151 MHz, Chloroform-d) δ 171.32, 158.03, 157.15, 138.10, 111.98, 102.70, 64.49, 47.34, 36.94, 28.72, 24.37, 22.62, 21.12, 21.01.

**HPLC:** (IF, 98:2:0.1 hexanes/IPA/DEA, 1.0 mL/min, 300 nm) indicated 94:6 er: $t_R$ (major) = 13.3 min, $t_R$ (minor) = 21.1 min.

**$[\alpha]_D^{25}$:** +21.2 (*c* = 1.3, $CH_2Cl_2$).

**HRMS (*m/z*):** (ESI) calc'd $[M+H]^+$: 251.1754, found: 251.1746.

**Compound 17b**

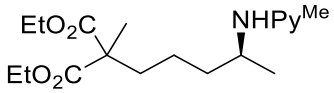


According to **Condition A** at 60 °C for 77h, compound **17a** (24 mg, 0.10 mmol) was allowed to react, and the product was purified by flash column chromatography ($SiO_2$; 65:35 hexanes:EA) to afford compound **17b** (29 mg, 84%) as a yellow oil.

**$^1$H NMR** (600 MHz, Chloroform-d) δ 7.31 (dd, J = 8.3, 7.3 Hz, 1H), 6.39 (d, J = 7.2 Hz, 1H), 6.14 (d, J = 8.3 Hz, 1H), 4.43 (s, 1H), 4.15 (dq, J = 9.1, 7.1 Hz, 4H), 3.62 (dq, J = 8.1, 6.2 Hz, 1H), 2.34 (s, 3H), 1.86 (dd, J = 9.2, 7.7 Hz, 2H), 1.60 – 1.52 (m, 1H), 1.48 (ddt, J = 13.5, 9.4, 6.2 Hz, 1H), 1.38 (s, 3H), 1.36 – 1.27 (m, 2H), 1.22 (dt, J = 10.8, 7.1 Hz, 6H), 1.17 (d, J = 6.4 Hz, 3H).

**$^{13}$C NMR** (151 MHz, Chloroform-d) δ 172.48, 157.95, 157.00, 138.15, 111.95, 102.78, 61.28, 61.27, 53.76, 47.23, 37.53, 35.57, 24.28, 21.01, 20.91, 19.96, 14.18, 14.15.

**HPLC:** (IF, 98:2:0.1 hexanes/IPA/DEA, 1.0 mL/min, 300 nm) indicated 94:6 er: $t_R$ (major) = 12.5 min, $t_R$ (minor) = 14.1 min.

**$[\alpha]_D^{25}$:** +14.5 (*c* = 2.0, $CH_2Cl_2$).

**HRMS (*m/z*):** (ESI) calc'd $[M+H]^+$: 351.2279, found: 351.2274.

**Compound 18b**

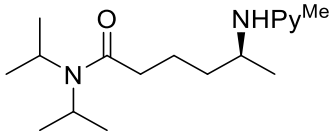


According to **Condition A** at 55 °C for 22.5h, compound **18a** (20 mg, 0.10 mmol) was allowed to react, and the product was purified by flash column chromatography ($SiO_2$; 70:30 hexanes:acetone) to afford compound **18b** (28 mg, 93%) as a yellow oil.

**$^1$H NMR** δ 7.29 (t, J = 7.8 Hz, 1H), 6.37 (d, J = 7.2 Hz, 1H), 6.16 (d, J = 8.3 Hz, 1H), 4.66 (s, 1H), 3.91 (p, J = 6.8 Hz, 1H), 3.65 (h, J = 6.1, 5.1 Hz, 1H), 3.44 (s, 1H), 2.32 (s, 3H), 2.27 (t, J = 7.5 Hz, 2H), 1.69 (tq, J = 13.3, 6.7 Hz, 2H), 1.54 (dddd, J = 25.7, 16.1, 13.3, 6.5 Hz, 2H), 1.35 (d, J = 6.8 Hz, 6H), 1.19 (d, J = 6.4 Hz, 3H), 1.16 – 1.09 (m, 6H).

**$^{13}$C NMR** (151 MHz, Chloroform-d) δ 171.62, 157.93, 156.79, 138.15, 111.74, 102.96, 48.35, 47.35, 45.65, 36.80, 35.16, 24.17, 22.01, 21.08, 20.96, 20.82.

**HPLC:** (ODH, 97.5:2.5:0.1 hexanes/IPA/DEA, 1.0 mL/min, 300 nm) indicated 90:10 er: $t_R$ (major) = 11.8 min, $t_R$ (minor) = 10.5 min.

**$[\alpha]_D^{25}$:** +3.9 (*c* = 2.0, $CH_2Cl_2$).

**HRMS (*m/z*):** (ESI) calc'd $[M+H]^+$: 306.2540, found: 306.2533.

**Compound 19b**

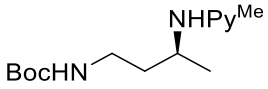


According to **Condition A** at 60 °C for 51h, compound **19a** (17 mg, 0.10 mmol) was allowed to react, and the product was purified by flash column chromatography ($SiO_2$; 65:35 hexanes:EA) to afford compound **19b** (21 mg, 76%) as a yellow oil.

**$^1$H NMR** (600 MHz, Chloroform-d) δ 7.35 – 7.17 (m, 1H), 6.39 (d, J = 7.2 Hz, 1H), 6.15 (d, J = 8.3 Hz, 1H), 6.09 (s, 1H), 4.13 (s, 1H), 4.05 (s, 0H), 3.36 (dd, J = 14.3, 7.8 Hz, 1H), 3.06 – 2.88 (m, 1H), 2.38 (s, 3H), 1.73 (ddt, J = 13.5, 9.0, 4.6 Hz, 1H), 1.50 (tt, J = 8.7, 4.5 Hz, 1H), 1.44 (s, 9H), 1.22 (d, J = 6.5 Hz, 3H).

**$^{13}$C NMR** (151 MHz, Chloroform-d) δ 158.00, 156.79, 156.32, 137.89, 111.84, 104.77, 78.81, 44.35, 38.24, 37.40, 28.62, 24.21, 22.11.

**HPLC:** (IF, 98:2:0.1 hexanes/IPA/DEA, 1.0 mL/min, 300 nm) indicated 85:15 er: $t_R$ (major) = 13.7 min, $t_R$ (minor) = 17.1 min.

**$[\alpha]_D^{25}$:** +73.1 (*c* = 1.5, $CH_2Cl_2$).

**HRMS (*m/z*):** (ESI) calc'd $[M+H]^+$: 280.2020, found: 280.2021.

**Compound 20b**

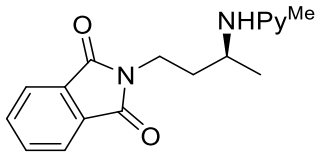


According to **Condition A** at 60 °C for 66h, compound **20a** (20 mg, 0.10 mmol) was allowed to react, and the product was purified by flash column chromatography ($SiO_2$; 60:40 hexanes:EA) to afford compound **20b** (27 mg, 87%) as a yellow solid.

**$^1$H NMR** (500 MHz, Chloroform-d) δ 7.75 (dd, J = 5.4, 3.0 Hz, 2H), 7.62 (dd, J = 5.5, 3.0 Hz, 2H), 7.21 (t, J = 8.0 Hz, 1H), 6.30 (d, J = 7.2 Hz, 1H), 6.09 (d, J = 8.3 Hz, 1H), 4.64 (d, J = 8.9 Hz, 1H), 3.82 – 3.67 (m, 3H), 2.21 (s, 3H), 1.93 – 1.74 (m, 2H), 1.19 (t, J = 4.9 Hz, 3H).

**$^{13}$C NMR** (151 MHz, Chloroform-d) δ 168.42, 157.62, 156.76, 138.14, 133.97, 132.28, 123.29, 112.08, 103.43, 45.64, 35.66, 35.55, 24.08, 21.07.

**HPLC:** (ODH, 97:3:0.1 hexanes/IPA/DEA, 1.0 mL/min, 300 nm) indicated 84:16 er: $t_R$ (major) = 21.6 min, $t_R$ (minor) = 19.1 min.

**$[\alpha]_D^{25}$:** -5.3 (*c* = 1.6, $CH_2Cl_2$).

**HRMS (*m/z*):** (ESI) calc'd $[M+H]^+$: 310.1550, found: 310.1563.

**Compound 21b**

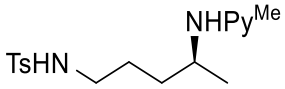


According to **Condition A** at 60 °C for 34.5 h, compound **21a** (24 mg, 0.10 mmol) was allowed to react, and the product was purified by flash column chromatography ($SiO_2$; 75:25 hexanes:acetone) to afford compound **21b** (31 mg, 89%) as white solid.

**$^1$H NMR** (600 MHz, Chloroform-d) δ 7.72 (d, J = 8.0 Hz, 2H), 7.31 – 7.25 (m, 3H), 6.38 (d, J = 7.2 Hz, 1H), 6.12 (d, J = 8.3 Hz, 1H), 5.55 – 5.26 (m, 1H), 4.76 – 4.46 (m, 1H), 3.63 (h, J = 6.4 Hz, 1H), 2.96 (q, J = 5.8 Hz, 2H), 2.40 (s, 3H), 2.33 (s, 3H), 1.61 – 1.39 (m, 4H), 1.10 (d, J = 6.4 Hz, 3H).

**$^{13}$C NMR** (151 MHz, Chloroform-d) δ 157.79, 156.68, 143.29, 138.29, 137.36, 129.75, 127.16, 111.92, 103.48, 46.73, 43.19, 34.17, 25.92, 24.06, 21.60, 21.06.

**HPLC:** (ODH, 90:10:0.1 hexanes/IPA/DEA, 1.0 mL/min, 300 nm) indicated 93:7 er: $t_R$ (major) = 32.1 min, $t_R$ (minor) = 16.0 min.

**$[\alpha]_D^{25}$:** +6.2 (*c* = 2.1, $CH_2Cl_2$).

**HRMS (*m/z*):** (ESI) calc'd $[M+H]^+$: 348.1740, found: 348.1729.

**Compound 22b**

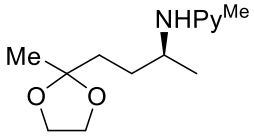


According to **Condition A** at 55 °C for 41.5h, compound **22a** (14 mg, 0.10 mmol) was allowed to react, and the product was purified by flash column chromatography ($SiO_2$; 70:30 hexanes:EA) to afford compound **22b** (23 mg, 92%) as a yellow oil.

**$^1$H NMR** (500 MHz, Chloroform-d) δ 7.30 (dd, J = 8.3, 7.3 Hz, 1H), 6.39 (d, J = 7.2 Hz, 1H), 6.16 (d, J = 8.3 Hz, 1H), 4.47 (d, J = 8.7 Hz, 1H), 3.98 – 3.82 (m, 4H), 3.62 (dq, J = 8.1, 6.1 Hz, 1H), 2.34 (s, 3H), 1.86 – 1.51 (m, 4H), 1.30 (s, 3H), 1.18 (d, J = 6.3 Hz, 3H).

**$^{13}$C NMR** (151 MHz, Chloroform-d) δ 158.05, 157.04, 138.09, 111.89, 110.03, 102.74, 64.77, 47.62, 35.71, 31.55, 24.32, 24.02, 21.14.

**HPLC:** (ODH, 99:1:0.1 hexanes/IPA/DEA, 1.0 mL/min, 300 nm) indicated 93:7 er: $t_R$ (major) = 14.9 min, $t_R$ (minor) = 13.7 min.

**$[\alpha]_D^{25}$:** +21.4 (*c* = 1.8, $CH_2Cl_2$).

**HRMS (*m/z*):** (ESI) calc'd $[M+H]^+$: 251.1754, found: 251.1759.

**Compound 23b**

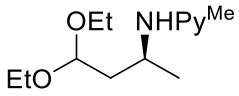


According to **Condition A** at 55 °C for 32h, compound **23a** (14 mg, 0.10 mmol) was allowed to react, and the product was purified by flash column chromatography ($SiO_2$;65:35 hexanes:EA) to afford compound **23b** (21 mg, 84%) as a yellow oil.

**$^1$H NMR** (500 MHz, Chloroform-d) δ 7.31 (dd, J = 8.3, 7.3 Hz, 1H), 6.40 (d, J = 7.3 Hz, 1H), 6.21 (d, J = 8.3 Hz, 1H), 4.63 (dd, J = 6.5, 5.0 Hz, 1H), 4.52 (d, J = 8.8 Hz, 1H), 3.91 – 3.75 (m, 1H), 3.71 – 3.58 (m, 2H), 3.47 (ddq, J = 14.0, 9.4, 7.0 Hz, 2H), 2.34 (s, 3H), 1.81 (qdd, J = 14.1, 7.0, 5.3 Hz, 2H), 1.26 – 1.13 (m, 9H).

**$^{13}$C NMR** (151 MHz, Chloroform-d) δ 157.99, 157.07, 138.03, 112.04, 102.95, 101.20, 61.98, 61.47, 44.54, 41.51, 24.37, 21.48, 15.51, 15.48.

**HPLC:** (IF, 99:1:0.1 hexanes/IPA/DEA, 1.0 mL/min, 300 nm) indicated 92:8 er: $t_R$ (major) = 8.4 min, $t_R$ (minor) = 13.1 min.

**$[\alpha]_D^{25}$:** +19.3 (*c* = 1.5, $CH_2Cl_2$).

**HRMS (*m/z*):** (ESI) calc'd $[M+H]^+$: 253.1911, found: 253.1916.

**Compound 24b**

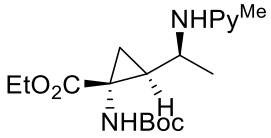


According to **Condition A** at 60 °C for 23.5h, compound **24a** (26 mg, 0.10 mmol) was allowed to react, and the product was purified by flash column chromatography ($SiO_2$; 65:35 hexanes:EA) to afford compound **24b** (25 mg, 70%) as a yellow oil. The dr was determined to be >20:1 by $^1$H NMR spectroscopy. (Note: The product decomposed slightly on silica gel.)

**$^1$H NMR** (600 MHz, Methylene Chloride-d2) δ 7.25 (t, J = 7.8 Hz, 1H), 6.34 (d, J = 7.2 Hz, 1H), 6.10 (d, J = 8.3 Hz, 1H), 6.06 (s, 1H), 5.45 (s, 1H), 3.91 – 3.71 (m, 2H), 3.62 (dp, J = 11.9, 6.1 Hz, 1H), 2.30 (s, 3H), 1.73 (q, J = 9.3 Hz, 1H), 1.65 (dd, J = 8.1, 5.0 Hz, 1H), 1.47 (s, 9H), 1.39 – 1.33 (m, 4H), 1.03 (t, J = 7.1 Hz, 3H).

**$^{13}$C NMR** 13C NMR (151 MHz, Methylene Chloride-d2) δ 171.60, 158.11, 156.96, 156.65, 137.92, 111.40, 103.93, 80.24, 61.77, 47.15, 38.17, 30.10, 28.49, 24.09, 22.69, 20.88, 14.12.

**$[\alpha]_D^{25}$:** +41.5 (*c* = 1.7, $CH_2Cl_2$).

**HRMS (*m/z*):** (ESI) calc'd $[M+H]^+$: 364.2231, found: 364.2247.

**Compound 25b**

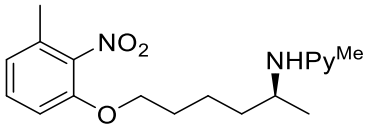


According to **Condition A** at 60 °C for 18h, compound **25a** (24 mg, 0.10 mmol) was allowed to react, and the product was purified by flash column chromatography ($SiO_2$; 65:35 hexanes:EA) to afford compound **25b** (27 mg, 80%) as a white solid.

**$^1$H NMR** (600 MHz, Chloroform-d) δ 7.30 (dd, J = 8.3, 7.3 Hz, 1H), 7.25 (t, J = 8.5 Hz, 1H), 6.81 (d, J = 8.1 Hz, 2H), 6.39 (d, J = 7.2 Hz, 1H), 6.16 (d, J = 8.3 Hz, 1H), 4.45 (d, J = 8.7 Hz, 1H), 4.01 (t, J = 6.4 Hz, 2H), 3.63 (ddd, J = 11.7, 6.9, 3.3 Hz, 1H), 2.33 (s, 3H), 2.28 (s, 3H), 1.77 (pd, J = 6.7, 6.2, 2.4 Hz, 2H), 1.62 – 1.45 (m, 4H), 1.19 (d, J = 6.4 Hz, 3H).

**$^{13}$C NMR** (151 MHz, Chloroform-d) δ 158.01, 156.98, 150.32, 142.44, 138.10, 130.97, 130.64, 122.52, 111.87, 111.08, 102.84, 69.26, 47.32, 36.77, 28.89, 24.30, 20.94, 17.02.

**HPLC:** (ODH, 95:5:0.1 hexanes/IPA/DEA, 1.0 mL/min, 300 nm) indicated 94:6 er: $t_R$ (major) = 54.3 min, $t_R$ (minor) = 24.3 min.

**$[\alpha]_D^{25}$:** +22.4 (*c* = 1.9, $CH_2Cl_2$).

**HRMS (*m/z*):** (ESI) calc'd $[M+H]^+$: 344.1969, found: 344.1986.

**Compound 26b**

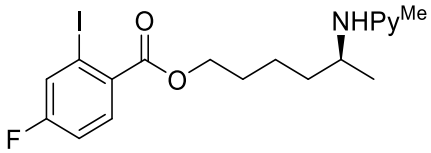


According to **Condition A** at 60 °C for 65h, compound **26a** (35 mg, 0.10 mmol) was allowed to react, and the product was purified by flash column chromatography ($SiO_2$; 65:35 hexanes:EA) to afford compound **26b** (36 mg, 80%) as a yellow oil.

**$^1$H NMR** (600 MHz, Chloroform-d) δ 7.80 (dd, J = 8.7, 5.9 Hz, 1H), 7.70 (dd, J = 8.1, 2.6 Hz, 1H), 7.30 (dd, J = 8.3, 7.3 Hz, 1H), 7.08 (ddd, J = 8.8, 7.7, 2.6 Hz, 1H), 6.39 (d, J = 7.3 Hz, 1H), 6.15 (d, J = 8.3 Hz, 1H), 4.36 (d, J = 8.6 Hz, 1H), 4.31 (t, J = 6.6 Hz, 2H), 3.75 – 3.58 (m, 1H), 2.34 (s, 3H), 1.86 – 1.71 (m, 2H), 1.64 – 1.49 (m, 4H), 1.19 (d, J = 6.4 Hz, 3H).

**$^{13}$C NMR** (151 MHz, Chloroform-d) δ 165.63, 163.48 (d, J = 257.9 Hz), 158.00, 157.15, 138.06, 132.75 (d, J = 9.1 Hz), 131.28 (d, J = 3.3 Hz), 128.68 (d, J = 23.8 Hz), 115.23 (d, J = 21.4 Hz), 111.98, 102.71, 94.63 (d, J = 8.4 Hz), 65.78, 47.23, 36.91, 28.67, 24.40, 22.75, 21.10.

**HPLC:** (IF, 98:2:0.1 hexanes/IPA/DEA, 1.0 mL/min, 300 nm) indicated 94:6 er: $t_R$ (major) = 17.0 min, $t_R$ (minor) = 23.0 min.

**$[\alpha]_D^{25}$:** +9.2 (*c* = 2.3, $CH_2Cl_2$).

**HRMS (*m/z*):** (ESI) calc'd $[M+H]^+$: 457.0783, found: 457.0783.

**Compound 27b**

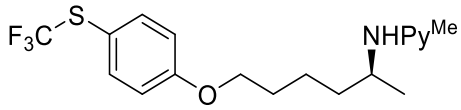


According to **Condition A** at 60 °C for 52h, compound **27a** (28 mg, 0.10 mmol) was allowed to react, and the product was purified by flash column chromatography ($SiO_2$; 65:35 hexanes:EA) to afford compound **27b** (32 mg, 84%) as a yellow oil.

**$^1$H NMR** (600 MHz, Chloroform-d) δ 7.61 – 7.50 (m, 2H), 7.31 (dd, J = 8.3, 7.3 Hz, 1H), 6.93 – 6.79 (m, 2H), 6.41 (d, J = 7.3 Hz, 1H), 6.16 (d, J = 8.3 Hz, 1H), 4.34 (d, J = 8.6 Hz, 1H), 3.96 (t, J = 6.4 Hz, 2H), 3.67 (pd, J = 6.2, 1.9 Hz, 1H), 2.35 (s, 3H), 1.81 (dtd, J = 8.4, 6.6, 3.6 Hz, 2H), 1.67 – 1.50 (m, 4H), 1.20 (d, J = 6.3 Hz, 3H).

**$^{13}$C NMR** (151 MHz, Chloroform-d) δ 161.46, 158.07, 157.25, 138.38, 138.04, 129.76 (q, J = 308.1 Hz), 115.58, 114.71 (q, J = 2.2 Hz), 112.02, 102.68, 68.12, 47.35, 37.01, 29.19, 24.43, 22.70, 21.05.

**HPLC:** (IF, 99:1:0.1 hexanes/IPA/DEA, 1.0 mL/min, 300 nm) indicated 95:5 er: $t_R$ (major) = 9.1 min, $t_R$ (minor) = 11.8 min.

$[\boldsymbol{\alpha}]_{\boldsymbol{D}}^{\mathbf{25}}$**:** +16.9 (*c* = 2.1, $CH_2Cl_2$).

**HRMS (*m/z*):** (ESI) calc'd $[M+H]^+$: 385.1556, found: 385.1552.

**Compound 28b**

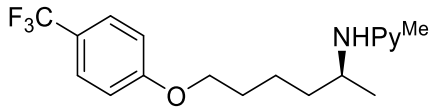


According to **Condition A** at 60 °C for 54h, compound **28a** (24 mg, 0.10 mmol) was allowed to react, and the product was purified by flash column chromatography ($SiO_2$; 65:35 hexanes:EA) to afford compound **28b** (30 mg, 83%) as a yellow oil.

**$^1$H NMR** (500 MHz, Chloroform-d) δ 7.52 (d, J = 8.5 Hz, 2H), 7.31 (t, J = 7.8 Hz, 1H), 6.92 (d, J = 8.4 Hz, 2H), 6.41 (d, J = 7.2 Hz, 1H), 6.16 (d, J = 8.3 Hz, 1H), 4.52 – 4.32 (m, 1H), 3.98 (t, J = 6.4 Hz, 2H), 3.66 (dp, J = 12.6, 6.4 Hz, 1H), 2.35 (s, 3H), 1.82 (dtd, J = 13.9, 7.4, 7.0, 4.2 Hz, 2H), 1.68 – 1.51 (m, 4H), 1.21 (d, J = 6.4 Hz, 3H).

**$^{13}$C NMR** (151 MHz, Chloroform-d) δ 161.62, 158.05, 157.17, 138.06, 126.96 (q, J = 3.7 Hz), 124.62 (q, J = 271.5 Hz), 122.79 (q, J = 32.6 Hz), 114.54, 111.99, 102.70, 68.12, 47.36, 37.00, 29.18, 24.37, 22.70, 21.04.

**HPLC:** (IF, 99:1:0.1 hexanes/IPA/DEA, 1.0 mL/min, 300 nm) indicated 98:2 er: $t_R$ (major) = 9.6 min, $t_R$ (minor) = 10.9 min.

$[\boldsymbol{\alpha}]_{\boldsymbol{D}}^{\mathbf{25}}$**:** +17.1 (*c* = 2.0, $CH_2Cl_2$).

**HRMS (*m/z*):** (ESI) calc'd $[M+H]^+$: 353.1835, found: 353.1846.

**Compound 29b**

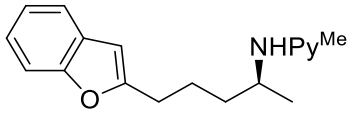


According to **Condition A** at 60 °C for 30.5h, compound **29a** (19 mg, 0.10 mmol) was allowed to react, and the product was purified by flash column chromatography ($SiO_2$; 70:30 hexanes:EA) to afford compound **29b** (26 mg, 89%) as a yellow oil.

**$^1$H NMR** (500 MHz, Chloroform-d) δ 7.52 – 7.44 (m, 1H), 7.41 (dt, J = 7.3, 1.2 Hz, 1H), 7.30 (dd, J = 8.3, 7.3 Hz, 1H), 7.23 – 7.14 (m, 2H), 6.41 (d, J = 7.2 Hz, 1H), 6.37 (d, J = 1.1 Hz, 1H), 6.15 (d, J = 8.3 Hz, 1H), 4.36 (d, J = 8.4 Hz, 1H), 3.70 (dq, J = 8.7, 6.4 Hz, 1H), 2.89 – 2.74 (m, 2H), 2.36 (s, 3H), 1.97 – 1.75 (m, 2H), 1.70 – 1.54 (m, 2H), 1.21 (d, J = 6.4 Hz, 3H).

**$^{13}$C NMR** (151 MHz, Chloroform-d) δ 159.19, 158.02, 157.18, 154.75, 138.02, 129.03, 123.24, 122.52, 120.32, 111.99, 110.84, 102.75, 102.18, 47.23, 36.74, 28.47, 24.41, 24.36, 21.07.

**HPLC:** (IF, 99:1:0.1 hexanes/IPA/DEA, 1.0 mL/min, 300 nm) indicated 93:7 er: $t_R$ (major) = 10.0 min, $t_R$ (minor) = 12.4 min.

**$[\alpha]_D^{25}$:** +16.7 (*c* = 1.9, $CH_2Cl_2$).

**HRMS (*m/z*):** (ESI) calc'd $[M+H]^+$: 295.1805, found:295.1808.

**Compound 30b**

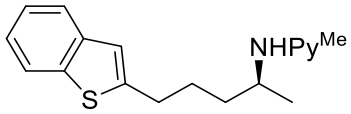


According to **Condition A** at 60 °C for 30.5h, compound **30a** (20 mg, 0.10 mmol) was allowed to react, and the product was purified by flash column chromatography ($SiO_2$; 70:30 hexanes:EA) to afford compound **30b** (26 mg, 85%) as a yellow oil. (Note: The product decomposed slightly on silica gel.)

**$^1$H NMR** (500 MHz, Chloroform-d) δ 7.76 (dq, J = 8.0, 0.9 Hz, 1H), 7.66 (dt, J = 8.0, 1.0 Hz, 1H), 7.35 – 7.21 (m, 3H), 6/99 (s, 1H), 6.41 (d, J = 7.2 Hz, 1H), 6.15 (d, J = 8.3 Hz, 1H), 4.34 (d, J = 7.9 Hz, 1H), 3.69 (dq, J = 8.5, 6.4 Hz, 1H), 2.93 (t, J = 7.4 Hz, 2H), 2.36 (s, 3H), 1.93 – 1.77 (m, 2H), 1.70 – 1.54 (m, 2H), 1.20 (d, J = 6.4 Hz, 3H).

**$^{13}$C NMR** (151 MHz, Methylene Chloride-d2) δ 158.37, 157.22, 146.90, 140.67, 139.71, 138.09, 124.45, 123.78, 123.06, 122.44, 121.01, 111.85, 103.49, 47.29, 36.90, 31.03, 28.03, 24.31, 21.15.

**HPLC:** (IF, 99:1:0.1 hexanes/IPA/DEA, 1.0 mL/min, 300 nm) indicated 94:6 er: $t_R$ (major) = 10.9 min, $t_R$ (minor) = 12.2 min.

$[\boldsymbol{\alpha}]_{\boldsymbol{D}}^{\mathbf{25}}$**:** +13.7 (*c* = 1.8, $CH_2Cl_2$).

**HRMS (*m/z*):** (ESI) calc'd $[M+H]^+$: 311.1577, found: 311.1584.

**Compound 31b**

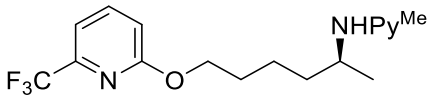


According to **Condition A** at 60 °C for 35.5h, compound **31a** (25 mg, 0.10 mmol) was allowed to react, and the product was purified by flash column chromatography ($SiO_2$; 70:30 hexanes:EA) to afford compound **31b** (31 mg, 89%) as a yellow oil.

**$^1$H NMR** (600 MHz, Chloroform-d) δ 7.66 (t, J = 7.8 Hz, 1H), 7.31 (dd, J = 8.3, 7.3 Hz, 1H), 7.21 (d, J = 7.3 Hz, 1H), 6.86 (d, J = 8.4 Hz, 1H), 6.40 (d, J = 7.2 Hz, 1H), 6.16 (d, J = 8.3 Hz, 1H), 4.38 (d, J = 8.6 Hz, 1H), 4.36 – 4.31 (m, 2H), 3.75 – 3.55 (m, 1H), 2.34 (s, 3H), 1.86 – 1.72 (m, 2H), 1.68 – 1.46 (m, 4H), 1.19 (d, J = 6.4 Hz, 3H).

**$^{13}$C NMR** (151 MHz, Chloroform-d) δ 164.04, 158.08, 157.16, 145.61 (q, J = 34.6 Hz), 139.32, 138.07, 121.52 (q, J = 273.7 Hz), 114.70, 113.10 (q, J = 3.2 Hz), 111.93, 102.65, 66.44, 47.42, 37.04, 28.92, 24.38, 22.74, 20.99.

**HPLC:** (ODH, 99:1:0.1 hexanes/IPA/DEA, 1.0 mL/min, 300 nm) indicated 93:7 er: $t_R$ (major) = 17.1 min, $t_R$ (minor) = 11.8 min.

$[\boldsymbol{\alpha}]_{\boldsymbol{D}}^{\mathbf{25}}$**:** +19.2 (*c* = 2.0, $CH_2Cl_2$).

**HRMS (*m/z*):** (ESI) calc'd $[M+H]^+$: 354.1788, found: 354.1802.

**Compound 32b**

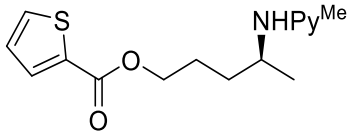


According to **Condition A** at 60 °C for 44h, compound **32a** (20 mg, 0.10 mmol) was allowed to react, and the product was purified by flash column chromatography ($SiO_2$; 65:35 hexanes:EA) to afford compound **32b** (25 mg, 81%) as a yellow oil.

**$^1$H NMR** (600 MHz, Chloroform-d) δ 7.78 (dd, J = 3.7, 1.3 Hz, 1H), 7.54 (dd, J = 5.0, 1.3 Hz, 1H), 7.30 (dd, J = 8.3, 7.3 Hz, 1H), 7.08 (dd, J = 5.0, 3.7 Hz, 1H), 6.40 (d, J = 7.3 Hz, 1H), 6.16 (d, J = 8.3 Hz, 1H), 4.36 (d, J = 8.7 Hz, 1H), 4.30 (td, J = 6.5, 1.9 Hz, 2H), 3.73 (dh, J = 8.3, 6.4 Hz, 1H), 2.34 (s, 3H), 1.94 – 1.77 (m, 2H), 1.72 – 1.59 (m, 2H), 1.22 (d, J = 6.4 Hz, 3H).

**$^{13}$C NMR** (151 MHz, Chloroform-d) δ 162.36, 157.94, 157.18, 138.06, 134.01, 133.45, 132.39, 127.83, 112.09, 102.84, 65.09, 47.06, 33.59, 25.50, 24.39, 21.09.

**HPLC:** (ADH, 98.5:1.5:0.1 hexanes/IPA/DEA, 1.0 mL/min, 300 nm) indicated 94:6 er: $t_R$ (major) = 27.6 min, $t_R$ (minor) = 31.4 min.

$[\boldsymbol{\alpha}]_{\boldsymbol{D}}^{\mathbf{25}}$**:** +13.2 (*c* = 1.7, $CH_2Cl_2$).

**HRMS (*m/z*):** (ESI) calc'd $[M+H]^+$: 305.1318, found: 305.1330.

**Compound 33b**

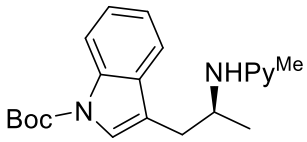


According to **Condition A** at 60 °C for 25h, compound **33a** (26 mg, 0.10 mmol) was allowed to react, and the product was purified by flash column chromatography ($SiO_2$; 70:30 hexanes:EA) to afford compound **33b** (29 mg, 80%) as a yellow oil.

**$^1$H NMR** (600 MHz, Chloroform-d) δ 8.13 (s, 1H), 7.70 (dt, J = 7.8, 1.0 Hz, 1H), 7.41 (s, 1H), 7.34 – 7.28 (m, 2H), 7.27 – 7.22 (m, 1H), 6.44 (d, J = 7.2 Hz, 1H), 6.21 (d, J = 8.2 Hz, 1H), 4.43 (d, J = 8.3 Hz, 1H), 4.21 – 4.12 (m, 1H), 3.08 (ddd, J = 14.3, 4.9, 1.1 Hz, 1H), 2.77 (dd, J = 14.3, 7.7 Hz, 1H), 2.41 (s, 3H), 1.67 (s, 9H), 1.23 (d, J = 6.5 Hz, 3H).

**$^{13}$C NMR** (151 MHz, Chloroform-d) δ 157.79, 157.22, 149.88, 137.86, 131.15, 124.40, 123.88, 122.48, 119.55, 117.72, 115.33, 112.12, 103.76, 83.55, 60.50, 47.14, 32.38, 28.34, 24.47, 20.76.

**HPLC:** (ODH, 99:1:0.1 hexanes/IPA/DEA, 1.0 mL/min, 300 nm) indicated 94:6 er: $t_R$ (major) = 12.6 min, $t_R$ (minor) = 10.1 min.

$[\boldsymbol{\alpha}]_{\boldsymbol{D}}^{\mathbf{25}}$**:** +48.5 (*c* = 2.0, $CH_2Cl_2$).

**HRMS (*m/z*):** (ESI) calc'd $[M+H]^+$: 366.2176, found: 366.2184.

**Compound 34b**

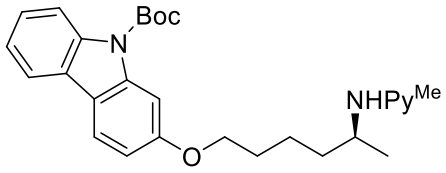


According to **Condition A** at 60 °C for 31h, compound **S34a** (37 mg, 0.10 mmol) was allowed to react, and the product was purified by flash column chromatography ($SiO_2$; 65:35 hexanes:EA) to afford compound **34b** (40 mg, 84%) as a yellow oil.

**$^1$H NMR** (600 MHz, Chloroform-d) δ 8.24 (d, J = 8.3 Hz, 1H), 7.94 – 7.89 (m, 1H), 7.87 (ddd, J = 7.6, 1.4, 0.7 Hz, 1H), 7.82 (d, J = 8.4 Hz, 1H), 7.38 (ddd, J = 8.4, 7.2, 1.4 Hz, 1H), 7.31 (td, J = 7.4, 0.9 Hz, 2H), 6.94 (dd, J = 8.5, 2.3 Hz, 1H), 6.41 (d, J = 7.2 Hz, 1H), 6.18 (d, J = 8.3 Hz, 1H),

4.42 (d, J = 8.6 Hz, 1H), 4.08 (t, J = 6.4 Hz, 2H), 3.68 (dq, J = 8.5, 6.2 Hz, 1H), 2.36 (s, 3H), 1.92 – 1.82 (m, 2H), 1.76 (s, 9H), 1.70 – 1.55 (m, 4H), 1.22 (d, J = 6.4 Hz, 3H).

**$^{13}$C NMR** (151 MHz, Chloroform-d) δ 159.18, 158.06, 157.13, 151.23, 139.93, 138.50, 138.05, 126.06, 125.74, 123.13, 120.17, 119.22, 118.83, 116.25, 112.03, 111.93, 102.69, 101.73, 83.89, 68.29, 47.41, 37.08, 29.43, 28.49, 24.38, 22.83, 21.01.

**HPLC:** (IG, 98.5:1.5:0.1 hexanes/IPA/DEA, 1.0 mL/min, 300 nm) indicated 95:5 er: $t_R$ (major) = 48.2 min, $t_R$ (minor) = 44.3 min.

**$[\alpha]_D^{25}$:** +18.8 (*c* = 2.5, $CH_2Cl_2$).

**HRMS (*m/z*):** (ESI) calc'd $[M+H]^+$: 474.2571, found: 474.2766.

**Natural Product and Drug Derivatives**

**Compound 35b**

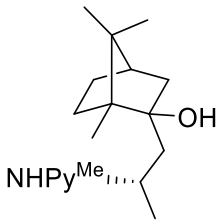


According to **Condition A** at 60 °C for 55h, compound **35a** (19 mg, 0.10 mmol) was allowed to react, and the product was purified by flash column chromatography ($SiO_2$; 65:35 hexanes:EA) to afford compound **35b** (27 mg, 90%) as a white solid. The dr was determined to be 12:1 by $^1$H NMR spectroscopy.

**$^1$H NMR** (600 MHz, Chloroform-d) δ 7.28 (d, J = 7.7 Hz, 1H), 6.41 (d, J = 7.2 Hz, 1H), 6.24 (d, J = 8.3 Hz, 1H), 5.68 – 4.57 (m, 1H), 4.55 – 4.25 (m, 1H), 4.18 – 4.01 (m, 1H), 2.36 (s, 3H), 2.05 (dt, J = 13.0, 3.8 Hz, 1H), 1.91 (dd, J = 14.1, 5.0 Hz, 1H), 1.71 (t, J = 4.7 Hz, 1H), 1.67 (tt, J = 7.1, 3.6 Hz, 1H), 1.56 (dd, J = 14.0, 4.8 Hz, 1H), 1.48 (d, J = 12.9 Hz, 1H), 1.33 (d, J = 7.4 Hz, 2H), 1.31 (d, J = 6.5 Hz, 3H), 1.28 – 1.23 (m, 1H), 1.13 (s, 3H), 0.84 (s, 3H), 0.82 (s, 3H).

**$^{13}$C NMR** (151 MHz, Chloroform-d) δ 157.15, 156.43, 137.99, 112.43, 105.93, 80.27, 52.90, 48.78, 46.29, 45.54, 45.48, 44.88, 30.02, 27.26, 23.74, 21.71, 21.22, 10.57.

**$[\alpha]_D^{25}$:** -34.2 (*c* = 1.5, $CH_2Cl_2$).

**HRMS (*m/z*):** (ESI) calc'd $[M+H]^+$: 303.2431, found: 303.2424.

**Compound 36b**

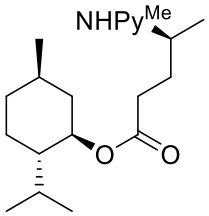


According to **Condition A** at 60 °C for 48h, compound **36a** (24 mg, 0.10 mmol) was allowed to react, and the product was purified by flash column chromatography ($SiO_2$; 65:35 hexanes:EA) to afford compound **36b** (33 mg, 94%) as a yellow oil. The dr was determined to be >20:1 by $^1$H NMR spectroscopy.

**$^1$H NMR** (600 MHz, Methylene Chloride-$d_2$) δ 7.29 (dd, J = 8.3, 7.3 Hz, 1H), 6.39 (d, J = 7.3 Hz, 1H), 6.18 (d, J = 8.4 Hz, 1H), 4.67 (td, J = 10.9, 4.4 Hz, 1H), 4.60 – 4.44 (m, 1H), 3.84 – 3.74 (m, 1H), 2.38 (td, J = 7.4, 2.0 Hz, 2H), 2.30 (s, 3H), 1.95 (dtd, J = 12.0, 4.0, 1.9 Hz, 1H), 1.87 – 1.78 (m, 3H), 1.67 (dtq, J = 13.6, 6.9, 3.4 Hz, 2H), 1.48 (ddtt, J = 16.4, 13.4, 6.7, 3.4 Hz, 1H), 1.36 (ddt, J = 12.4, 10.7, 3.2 Hz, 1H), 1.19 (d, J = 6.4 Hz, 3H), 1.06 (qd, J = 13.4, 12.8, 3.8 Hz, 1H), 0.95 (td, J = 12.3, 11.0 Hz, 1H), 0.91 – 0.83 (m, 8H), 0.74 (dd, J = 7.0, 2.3 Hz, 3H).

**$^{13}$C NMR** (151 MHz, Methylene Chloride-$d_2$) δ 173.34, 158.36, 157.23, 138.12, 112.02, 103.57, 74.38, 47.49, 47.12, 41.37, 34.70, 32.51, 31.83, 31.77, 26.70, 24.32, 23.85, 22.22, 21.12, 20.92, 16.50.

**$[\alpha]_D^{25}$:** -33.0 (*c* = 1.9, $CH_2Cl_2$).

**HRMS (*m/z*):** (ESI) calc'd $[M+H]^+$: 347.2693, found: 347.2696.

**Compound 37b**

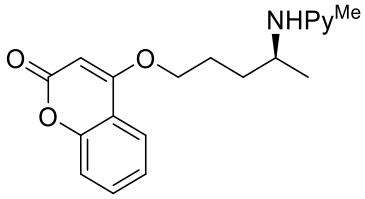


According to **Condition A** at 65 °C for 120h, compound **37a** (23 mg, 0.10 mmol) was allowed to react, and the product was purified by flash column chromatography ($SiO_2$; 45:55 hexanes:EA) to afford compound **37b** (28 mg, 82%) as a yellow solid.

**$^1$H NMR** (600 MHz, Chloroform-d) δ 7.52 (dd, J = 8.0, 1.6 Hz, 1H), 7.28 (ddd, J = 8.6, 7.2, 1.6 Hz, 1H), 7.06 (q, J = 7.9 Hz, 2H), 7.00 (m, 1H), 6.16 (d, J = 7.3 Hz, 1H), 5.94 (d, J = 8.3 Hz, 1H), 5.40 (s, 1H), 4.62 (s, 1H), 3.94 – 3.85 (m, 2H), 3.54 (p, J = 6.4 Hz, 1H), 2.10 (s, 3H), 1.86 – 1.70 (m, 2H), 1.51 (qd, J = 7.5, 6.8, 4.3 Hz, 2H), 1.01 (d, J = 6.4 Hz, 3H).

**$^{13}$C NMR** (151 MHz, Chloroform-d) δ 165.72, 163.04, 157.74, 156.81, 153.45, 138.39, 132.46, 123.97, 123.10, 116.87, 115.84, 112.11, 103.16, 90.57, 69.27, 46.96, 33.41, 25.25, 24.02, 21.12.

**HPLC:** (IF, 95:5:0.1 hexanes/IPA/DEA, 1.0 mL/min, 300 nm) indicated 92:8 er: $t_R$ (major) = 16.9 min, $t_R$ (minor) = 20.8 min.

$[\boldsymbol{\alpha}]_{\boldsymbol{D}}^{\boldsymbol{25}}$**:** -3.5 (*c* = 1.9, $CH_2Cl_2$).

**HRMS (*m/z*):** (ESI) calc'd $[M+H]^+$: 339.1703, found: 339.1714.

**Compound 38b**

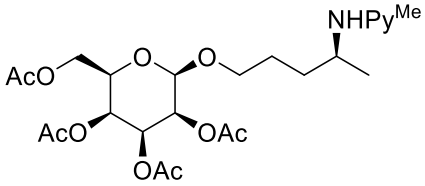


According to **Condition A** at 60 °C for 38h, compound **38a** (42 mg, 0.10 mmol) was allowed to react, and the product was purified by flash column chromatography ($SiO_2$; 40:60 hexanes:EA) to afford compound **38b** (48 mg, 92%) as a yellow oil. The dr was determined to be >10:1 by chiral HPLC because the $^1$H NMR spectra of the two diastereomers were identical.

**$^1$H NMR** (600 MHz, Chloroform-d) δ 7.29 (t, J = 7.8 Hz, 1H), 6.38 (d, J = 7.3 Hz, 1H), 6.13 (dd, J = 8.3, 1.7 Hz, 1H), 5.36 (d, J = 3.4 Hz, 1H), 5.17 (dd, J = 10.5, 7.9 Hz, 1H), 4.98 (ddd, J = 10.5, 3.5, 2.2 Hz, 1H), 4.43 (dd, J = 8.0, 2.3 Hz, 1H), 4.32 (d, J = 8.7 Hz, 1H), 4.19 – 4.05 (m, 2H), 3.94 – 3.82 (m, 2H), 3.65 (dp, J = 14.2, 7.0 Hz, 1H), 3.54 – 3.40 (m, 1H), 2.31 (s, 3H), 2.12 (s, 3H), 2.01 (s, 3H), 2.00 (s, 3H), 1.98 (s, 3H), 1.95 (d, J = 1.0 Hz, 3H), 1.74 – 1.45 (m, 4H), 1.16 (dd, J = 6.4, 1.4 Hz, 3H).

**$^{13}$C NMR** (151 MHz, Chloroform-d) δ 170.45, 170.34, 170.23, 169.42, 157.92, 157.00, 138.06, 111.92, 102.90, 101.37, 71.05, 70.70, 69.96, 68.99, 67.16, 61.36, 46.97, 33.39, 26.09, 24.31, 21.05, 20.78, 20.74, 20.66.

**HPLC:** (ODH, 90:10:0.1 hexanes/IPA/DEA, 1.0 mL/min, 300 nm) indicated 93:7 dr: $t_R$ (major) = 20.8 min, $t_R$ (minor) = 16.7 min.

$[\boldsymbol{\alpha}]_{\boldsymbol{D}}^{\boldsymbol{25}}$**:** -11.0 (*c* = 3.2, $CH_2Cl_2$).

**HRMS (*m/z*):** (ESI) calc'd $[M+H]^+$: 525.2443, found: 525.2426.

**Compound 39b**

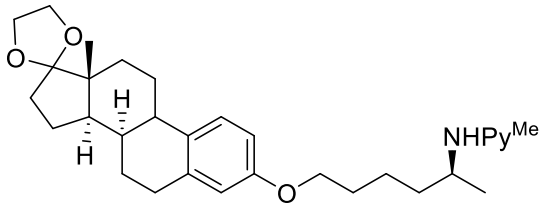


According to **Condition A** at 60 °C for 28.5h, compound **39a** (40 mg, 0.10 mmol) was allowed to react, and the product was purified by flash column chromatography ($SiO_2$; 65:35 hexanes:EA) to afford compound **s9b** (45 mg, 89%) as a yellow oil. The dr was determined to be >20:1 by chiral HPLC because the $^1$H NMR spectra of the two diastereomers were identical.

**$^1$H NMR** (600 MHz, Methylene Chloride-d2) δ 7.30 (t, J = 7.8 Hz, 1H), 7.17 (d, J = 8.5 Hz, 1H), 6.65 (dd, J = 8.6, 2.7 Hz, 1H), 6.59 (d, J = 2.7 Hz, 1H), 6.39 (d, J = 7.2 Hz, 1H), 6.17 (d, J = 8.3 Hz, 1H), 4.45 (d, J = 8.5 Hz, 1H), 3.99 – 3.79 (m, 6H), 3.79 – 3.64 (m, 1H), 2.91 – 2.69 (m, 2H), 2.31 (m, 4H), 2.20 (td, J = 11.0, 10.6, 4.1 Hz, 1H), 2.05 – 1.95 (m, 1H), 1.93 – 1.86 (m, 1H), 1.86 – 1.71 (m, 5H), 1.68 – 1.49 (m, 6H), 1.49 – 1.30 (m, 4H), 1.19 (d, J = 6.4 Hz, 3H), 0.87 (s, 3H).

**$^{13}$C NMR** (151 MHz, Methylene Chloride-d2) δ 171.20, 158.44, 157.33, 138.42, 138.04, 133.08, 126.58, 119.69, 114.73, 112.29, 111.81, 103.36, 68.13, 65.59, 64.97, 60.64, 49.77, 47.47, 46.56, 44.13, 39.58, 37.30, 34.62, 31.21, 30.21, 29.73, 27.47, 26.66, 24.39, 23.08, 22.73, 21.10.

**HPLC:** (ADH, 98.5:1.5:0.25 hexanes/IPA/DEA, 1.0 mL/min, 300 nm) indicated 96:4 dr: $t_R$ (major) = 23.5 min, $t_R$ (minor) = 21.5 min.

**$[\alpha]_D^{25}$:** +29.8 (*c* = 2.8, $CH_2Cl_2$).

**HRMS (*m/z*):** (ESI) calc'd $[M+H]^+$: 505.3425, found: 505.3419.

**Compound 40b**

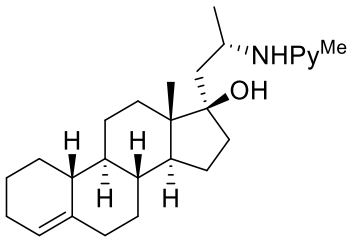


According to **Condition A** at 65 °C for 27h, compound **40a** (30 mg, 0.10 mmol) was allowed to react, and the product was purified by flash column chromatography ($SiO_2$; 65:35 hexanes:EA) to afford compound **40b** (33 mg, 80%) as a white solid. The dr was determined to be >20:1 by $^1$H NMR spectroscopy. Note: Ir[(*R*)-DTBM-SEGPHOS(ethylene)]Cl was used as the catalyst instead of Ir[(*S*)-DTBM-SEGPHOS(ethylene)]Cl.

**$^1$H NMR** (600 MHz, Chloroform-d) δ 7.32 – 7.22 (m, 1H), 6.41 (d, J = 7.2 Hz, 1H), 6.22 (d, J = 8.3 Hz, 1H), 5.68 (s, 1H), 5.37 (q, J = 2.5, 2.1 Hz, 1H), 4.37 (s, 1H), 4.08 (q, J = 5.8 Hz, 1H), 2.36 (s, 3H), 2.19 (ddd, J = 13.6, 4.0, 2.5 Hz, 1H), 1.98 – 1.89 (m, 4H), 1.86 (ddd, J = 14.4, 5.3, 1.9 Hz, 1H), 1.76 (m, 3H), 1.71 – 1.63 (m, 2H), 1.61 – 1.49 (m, 2H), 1.42 (dd, J = 8.4, 2.8 Hz, 1H), 1.38 – 1.32 (m, 2H), 1.30 (d, J = 6.5 Hz, 3H), 1.28 – 1.22 (m, 2H), 1.21 – 1.17 (m, 2H), 1.15 – 1.03 (m, 2H), 0.93 (s, 3H), 0.88 – 0.78 (m, 1H), 0.58 (qd, J = 10.6, 4.3 Hz, 1H).

**$^{13}$C NMR** (151 MHz, Chloroform-d) δ 157.17, 156.50, 140.78, 137.82, 119.88, 112.30, 106.17, 82.58, 50.60, 49.52, 46.65, 44.61, 43.89, 42.16, 42.07, 35.71, 34.40, 32.08, 31.42, 28.98, 26.15, 25.64, 24.26, 23.85, 23.57, 22.24, 14.29.

**$[\alpha]_D^{25}$:** +91.0 (*c* = 2.3, $CH_2Cl_2$).

**HRMS (*m/z*):** (ESI) calc'd $[M+H]^+$: 409.3214, found: 409.3221.

**Compound 41b**

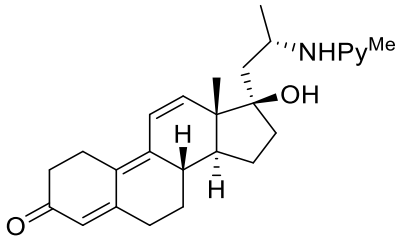


According to **Condition A** at 65 °C for 27h, compound **41a** (31 mg, 0.10 mmol) was allowed to react, and the product was purified by flash column chromatography ($SiO_2$; 50:50 hexanes:EA) to afford compound **41b** (28 mg, 68%) as a yellow solid. The dr was determined to be >20:1 by $^1$H NMR spectroscopy. Note: 7.5 mol% Ir[(*R*)-DTBM-SEGPHOS(ethylene)]Cl was used as the catalyst instead of Ir[(*S*)-DTBM-SEGPHOS(ethylene)]Cl. 1,3,5-Trimethoxybenzene (4mg) was added as the internal standard to monitor the conversion of this reaction. This reaction stopped at about 75% conversion of compound **S40**.

**$^1$H NMR** (600 MHz, Chloroform-d) δ 7.30 (t, J = 7.8 Hz, 1H), 6.43 (d, J = 7.3 Hz, 1H), 6.40 (d, J = 9.9 Hz, 1H), 6.28 (d, J = 9.9 Hz, 1H), 6.25 (d, J = 8.3 Hz, 1H), 5.76 (s, 1H), 4.07 (q, J = 5.6 Hz, 1H), 2.87 – 2.70 (m, 2H), 2.55 (qq, J = 15.7, 4.3 Hz, 2H), 2.45 (t, J = 7.2 Hz, 3H), 2.40 (s, 3H), 2.07 – 2.00 (m, 1H), 1.95 – 1.81 (m, 3H), 1.70 – 1.57 (m, 3H), 1.53 (dt, J = 11.8, 8.0 Hz, 1H), 1.30 (d, J = 5.7 Hz, 3H), 1.27 – 1.22 (m, 3H), 1.04 (s, 3H).

**$^{13}$C NMR** (151 MHz, Chloroform-d) δ 199.32, 156.85, 156.80, 155.95, 142.89, 142.60, 138.29, 126.81, 123.61, 123.54, 112.33, 106.51, 81.23, 49.61, 47.91, 45.33, 44.36, 38.62, 36.83, 34.76, 31.69, 27.27, 24.45, 24.19, 23.46, 23.13, 16.69.

**$[\alpha]_D^{25}$:** +81.3 (*c* = 1.9, $CH_2Cl_2$).

**HRMS (*m/z*):** (ESI) calc'd $[M+H]^+$: 419.2693, found: 419.2690.

**Compound 42b**

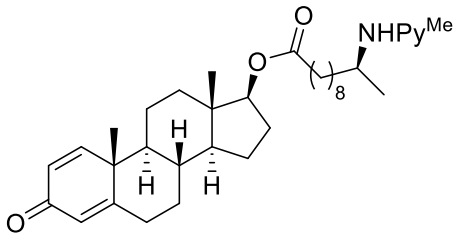


According to **Condition A** at 60 °C for 22.5h, compound **42a** (45 mg, 0.10 mmol) was allowed to react, and the product was purified by flash column chromatography ($SiO_2$; 50:50 hexanes:EA) to afford compound **42b** (51 mg, 91%) as a yellow oil. The dr was determined to be >10:1 by chiral HPLC because the $^1$H NMR spectra of the two diastereomers were identical.

**$^1$H NMR** (600 MHz, Chloroform-d) δ 7.30 (dd, J = 8.3, 7.3 Hz, 1H), 7.02 (d, J = 10.1 Hz, 1H), 6.38 (d, J = 7.2 Hz, 1H), 6.21 (dd, J = 10.1, 1.9 Hz, 1H), 6.14 (d, J = 8.3 Hz, 1H), 6.05 (t, J = 1.7 Hz, 1H), 4.57 (dd, J = 9.2, 7.8 Hz, 1H), 4.55 – 4.48 (m, 1H), 3.56 (p, J = 6.5 Hz, 1H), 2.45 (tdd, J = 13.5, 5.2, 1.6 Hz, 1H), 2.33 (m, 4H), 2.27 (t, J = 7.5 Hz, 2H), 2.15 (dtd, J = 13.7, 9.3, 6.3 Hz,

1H), 1.93 (ddq, J = 12.8, 5.2, 2.8 Hz, 1H), 1.77 (dt, J = 12.8, 3.5 Hz, 1H), 1.74 – 1.68 (m, 1H), 1.64 (ddt, J = 12.8, 8.7, 4.7 Hz, 3H), 1.60 – 1.56 (m, 2H), 1.54 – 1.47 (m, 2H), 1.46 – 1.41 (m, 1H), 1.40 – 1.31 (m, 3H), 1.27 (d, J = 4.7 Hz, 9H), 1.21 (s, 3H), 1.16 (d, J = 6.4 Hz, 3H), 1.09 – 0.98 (m, 3H), 0.84 (s, 3H).

**$^{13}$C NMR** (151 MHz, Chloroform-d) δ 186.34, 173.86, 168.84, 158.04, 156.95, 155.68, 138.11, 127.67, 124.05, 111.77, 102.59, 82.10, 52.32, 49.99, 47.51, 43.58, 42.87, 37.30, 36.64, 35.43, 34.61, 33.16, 32.81, 29.65, 29.47, 29.27, 29.18, 27.57, 26.11, 25.15, 24.24, 23.77, 22.45, 20.93, 18.84, 12.26.

**HPLC:** (ADH, 95:5:0.25 hexanes/IPA/DEA, 1.0 mL/min, 300 nm) indicated 93:7 dr: $t_R$ (major) = 47.0 min, $t_R$ (minor) = 54.3 min.

**$[\alpha]_D^{25}$:** +18.1 (*c* = 3.5, $CH_2Cl_2$).

**HRMS (*m/z*):** (ESI) calc'd $[M+H]^+$: 561.4051, found: 561.4050.

**Compound 43b**

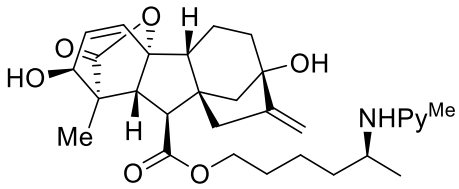


According to **Condition A** at 60 °C for 65h, compound **43a** (43 mg, 0.10 mmol) was allowed to react, and the product was purified by flash column chromatography ($SiO_2$; 66:33:1 DCM:MeCN:$NH_4OH$) to afford compound **43b** (42 mg, 79%) as a white solid. The dr was determined to be 12:1 by $^1$H NMR spectroscopy.

**$^1$H NMR** (600 MHz, Methylene Chloride-$d_2$) δ 7.35 (dd, J = 8.4, 7.3 Hz, 1H), 6.39 (d, J = 7.3 Hz, 1H), 6.31 (dd, J = 9.2, 0.8 Hz, 1H), 6.20 (d, J = 8.3 Hz, 1H), 5.90 (dd, J = 9.3, 3.7 Hz, 1H), 5.32 – 5.32 (m, 1H), 4.93 (d, J = 2.2 Hz, 1H), 4.81 (d, J = 8.3 Hz, 1H), 4.36 (ddd, J = 11.0, 8.9, 3.2 Hz, 1H), 4.15 (d, J = 3.7 Hz, 1H), 3.93 (ddd, J = 10.9, 5.8, 4.0 Hz, 1H), 3.64 – 3.56 (m, 1H), 3.29 (d, J = 10.8 Hz, 1H), 2.75 (d, J = 10.8 Hz, 1H), 2.31 (s, 3H), 2.26 – 2.19 (m, 2H), 2.08 (ddd, J = 12.8, 8.2, 1.9 Hz, 1H), 2.00 (dd, J = 10.8, 1.6 Hz, 1H), 1.95 (dd, J = 11.8, 5.8 Hz, 1H), 1.92 – 1.83 (m, 1H), 1.81 – 1.64 (m, 5H), 1.63 – 1.53 (m, 3H), 1.44 (ddq, J = 14.1, 7.0, 3.3, 2.9 Hz, 2H), 1.21 (s, 3H), 1.16 (d, J = 6.4 Hz, 3H).

**$^{13}$C NMR** (151 MHz, Methylene Chloride-$d_2$) δ 178.89, 172.36, 158.93, 158.38, 156.86, 138.92, 133.34, 132.69, 112.06, 106.73, 102.79, 90.98, 77.99, 69.65, 64.79, 53.95, 53.06, 51.94, 51.71, 50.69, 47.64, 44.83, 43.29, 39.05, 36.60, 28.85, 23.90, 22.36, 21.03, 17.28, 14.87.

**$[\alpha]_D^{25}$:** +70.7 (*c* = 2.7, $CH_2Cl_2$).

**HRMS (*m/z*):** (ESI) calc'd $[M+H]^+$: 537.2959, found: 537.2969.

**Compound 44b**

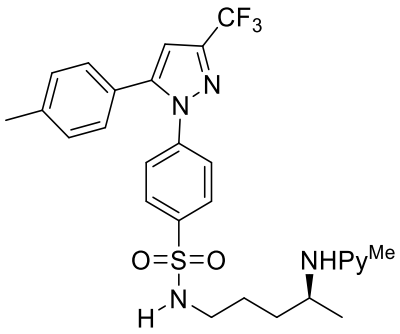


According to **Condition A** at 65 °C for 78h, compound **44a** (45 mg, 0.10 mmol) was allowed to react, and the product was purified by flash column chromatography ($SiO_2$; 50:50 hexanes:EA) to afford compound **44b** (50 mg, 89%) as a yellow oil.

**$^1$H NMR** (600 MHz, Chloroform-d) δ 7.85 – 7.78 (m, 2H), 7.45 – 7.40 (m, 2H), 7.29 (dd, J = 8.3, 7.2 Hz, 1H), 7.16 (d, J = 7.9 Hz, 2H), 7.11 – 7.06 (m, 2H), 6.73 (s, 1H), 6.37 (d, J = 7.2 Hz, 1H), 6.13 (d, J = 8.3 Hz, 1H), 4.90 (s, 1H), 3.66 (dq, J = 13.6, 6.5, 6.0 Hz, 1H), 2.99 (t, J = 6.2 Hz, 2H), 2.36 (s, 3H), 2.31 (s, 3H), 1.60 – 1.41 (m, 4H), 1.12 (d, J = 6.3 Hz, 3H).

**$^{13}$C NMR** (151 MHz, Chloroform-d) δ 157.57, 156.29, 145.25, 144.01 (q, J = 38.5 Hz), 142.29, 139.95, 139.76, 138.43, 129.74, 128.71, 128.01, 125.72, 125.50, 121.10 (q, J = 269.0 Hz), 111.84, 106.22 (q, J = 2.1 Hz), 103.70, 46.61, 43.10, 34.07, 25.69, 23.74, 21.31, 21.03.

**HPLC:** (IF, 95:5:0.25 hexanes/IPA/DEA, 1.0 mL/min, 300 nm) indicated 95:5 er: $t_R$ (major) = 34.0 min, $t_R$ (minor) = 32.5 min.

**$[\alpha]_D^{25}$:** +6.2 (*c* = 3.3, $CH_2Cl_2$).

**HRMS (*m/z*):** (ESI) calc'd $[M+H]^+$: 558.2145, found: 558.2139.

**Compound 45b**

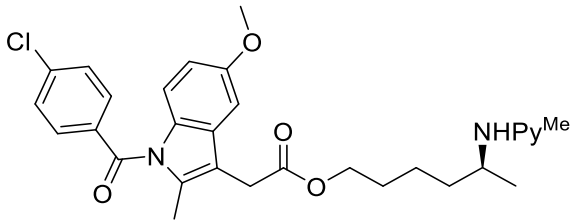


According to **Condition A** at 60 °C for 60h, compound **45a** (44 mg, 0.10 mmol) was allowed to react, and the product was purified by flash column chromatography ($SiO_2$; 65:35 hexanes:EA) to afford compound **45b** (44 mg, 80%) as a yellow solid.

**$^1$H NMR** 1H NMR (600 MHz, Chloroform-d) δ 7.68 – 7.60 (m, 2H), 7.48 – 7.42 (m, 2H), 7.31 (dd, J = 8.4, 7.2 Hz, 1H), 6.96 (d, J = 2.5 Hz, 1H), 6.87 (d, J = 9.0 Hz, 1H), 6.66 (dd, J = 9.0, 2.6 Hz, 1H), 6.37 (d, J = 7.2 Hz, 1H), 6.13 (d, J = 8.3 Hz, 1H), 5.08 (d, J = 42.1 Hz, 1H), 4.09 (t, J = 6.6 Hz, 2H), 3.81 (s, 3H), 3.64 (s, 2H), 3.54 (q, J = 6.5 Hz, 1H), 2.37 (s, 3H), 2.33 (s, 3H), 2.04 (d, J = 5.9 Hz, 1H), 1.63 (p, J = 7.0 Hz, 2H), 1.56 – 1.49 (m, 1H), 1.49 – 1.42 (m, 1H), 1.42 – 1.34 (m, 1H), 1.13 (d, J = 6.4 Hz, 3H).

**$^{13}$C NMR** (151 MHz, Chloroform-d) δ 170.98, 168.35, 157.74, 156.47, 156.13, 139.32, 138.47, 135.97, 134.02, 131.25, 130.91, 130.77, 129.20, 115.02, 112.80, 111.75, 111.67, 102.93, 101.51, 64.98, 55.77, 47.35, 36.67, 30.50, 28.68, 23.80, 22.54, 20.80, 13.44.

**HPLC:** (IF, 95:5:0.25 hexanes/IPA/DEA, 1.0 mL/min, 300 nm) indicated 92:8 er: $t_R$ (major) = 41.0 min, $t_R$ (minor) = 44.8 min.

$[\boldsymbol{\alpha}]_{\boldsymbol{D}}^{\mathbf{25}}$**:** +10.1 (*c* = 2.8, $CH_2Cl_2$).

**HRMS (*m/z*):** (ESI) calc'd $[M+H]^+$: 548.2311, found: 548.2300.

**Compound 46b**

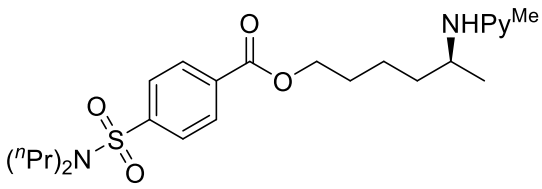


According to **Condition A** at 60 °C for 49h, compound **46a** (37 mg, 0.10 mmol) was allowed to react, and the product was purified by flash column chromatography ($SiO_2$; 65:35 hexanes:EA) to afford compound **46b** (37 mg, 78%) as a yellow oil.

**$^1$H NMR** (600 MHz, Methylene Chloride-d2) δ 8.20 – 8.02 (m, 2H), 7.92 – 7.75 (m, 2H), 7.29 (dd, J = 8.3, 7.3 Hz, 1H), 6.38 (d, J = 7.2 Hz, 1H), 6.16 (d, J = 8.3 Hz, 1H), 4.47 (d, J = 8.7 Hz, 1H), 4.34 (t, J = 6.6 Hz, 1H), 3.75 (h, J = 6.4 Hz, 1H), 3.15 – 3.00 (m, 4H), 2.29 (s, 3H), 1.85 – 1.74 (m, 2H), 1.64 – 1.49 (m, 8H), 1.19 (d, J = 6.4 Hz, 3H), 0.86 (t, J = 7.4 Hz, 6H).

**$^{13}$C NMR** (151 MHz, Methylene Chloride-d2) δ 165.60, 158.43, 157.29, 144.53, 138.04, 134.26, 130.48, 127.37, 111.84, 103.45, 65.90, 50.35, 47.29, 37.16, 29.00, 24.36, 23.01, 22.33, 21.13, 11.31.

**HPLC:** (ODH, 90:10:0.1 hexanes/IPA/DEA, 1.0 mL/min, 300 nm) indicated 94:6 er: $t_R$ (major) = 17.6 min, $t_R$ (minor) = 10.4 min.

$[\boldsymbol{\alpha}]_{\boldsymbol{D}}^{\mathbf{25}}$**:** +14.3 (*c* = 2.4, $CH_2Cl_2$).

**HRMS (*m/z*):** (ESI) calc'd $[M+H]^+$: 476.2578, found: 476.2600.

### 3.4.13 Unsuccessful substrates

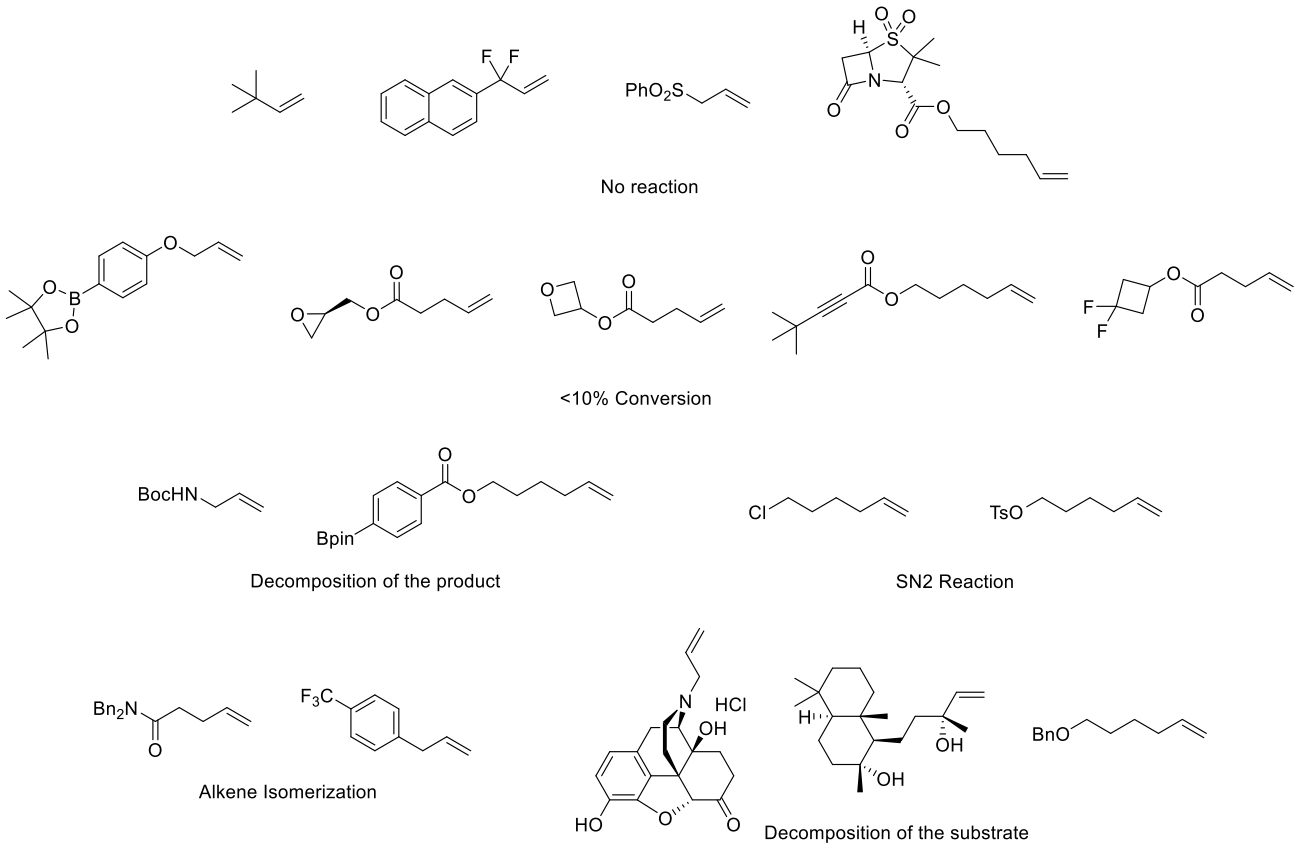


**Figure 3.12.** Unsuccessful substrate for hydroamination.

### 3.4.13. Determination of the Absolute Configuration

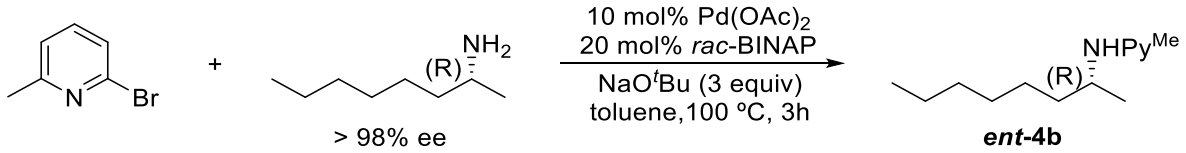


The absolute configuration of compound **4b** was unambiguously determined to be S at the nitrogen-bound stereocenter by comparison of the chiral HPLC traces of the standard sample ***ent*-4b** prepared by the following procedure. The absolute configurations of all other hydroamination products were assigned by analogy.

**Condition F: Palladium-catalyzed Amination of 2-Bromopyridine[33]**

**Condition F:** In a nitrogen-filled glovebox, a 20-mL vial was charged with $Pd(OAc)_2$ (22.5 mg, 10 mol% ), rac-BINAP (125 mg, 20 mol %), NaOtBu (288 mg, 3 equiv), (R)-2-aminooctane (> 98% ee, 129 mg, 1 equiv, 1.00 mmol), a magnetic stir bar, and 3 mL of toluene. 2-Bromo-6-methylpyridine (172 µL, 1 equiv, 1.00 mmol) was added, and the vial was capped, taped, and removed from the glovebox. The reaction was heated at 100 °C for 3 hours. The mixture was filtered with celite and purified by flash column chromatography ($SiO_2$; 75:25 hexanes:EA) to

afford compound ***ent*-4b** (181 mg, 82%) as a yellow oil. The ee was determined to be > 99% by HPLC.

### 3.4.14. Removal of the Pyridyl Group

**Condition G: Protection, Methylation and SNAr[49]**

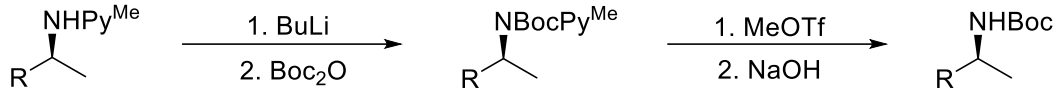


**Condition G:**

**Protection:** An oven-dried flask was charged with dry THF (15 mL), product from hydroamination (1.0 equiv), and a magnetic stir bar. Under nitrogen, *n*-BuLi (2.7M solution in toluene, 1.1 equiv) was added dropwise at 0°C and the reaction was allowed to stir for 15 minutes. At 0°C, $Boc_2O$ (3 equiv) was slowly added, and the reaction mixture was allowed warmed to room temperature and stirred for 4h. The reaction was quenched with stoichiometric amount of water and the crude residue was directly purified by flash column chromatography to yield the Boc-protect aminopyridine.

**Methylation and SNAr:** An oven-dried flask was charged with dry DCM (5 mL), Boc-protect aminopyridine (1.0 equiv), and a magnetic stir bar. Under nitrogen, a solution of MeOTf (1.1 equiv) in DCM (5 mL) was added dropwise at 0°C and the reaction was allowed to stir at 0°C overnight. The solvent was then removed followed by the addition of EtOH (8 mL) and NaOH (2M, 4 mL). The mixture was allowed to stir at 80°C overnight. The mixture was extracted with DCM (50 mL) three times and by flash column chromatography to yield the Boc-protect amine.

**Condition H: Hydrogenation and Reduction[50]**

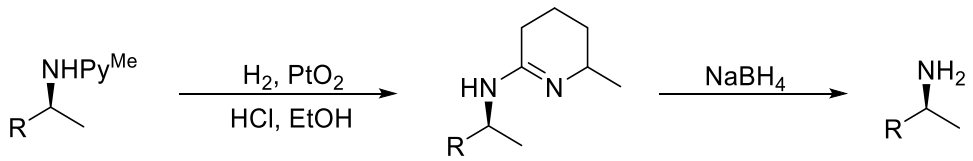


**Condition H:**

**Hydrogenation:** A 10-mL reaction tube was charged with product from hydroamination (1 equiv), a magnetic stir bar, 2 mL of ethanol, and HCl (4M solution in dioxane, 4 equiv). The mixture was allowed to stir for 15 minutes at room temperature before the addition of $PtO_2$ (10 mol%). The reaction tube was then sealed and purged with hydrogen for 15 minutes. The mixture was stirred at room temperature overnight, filtered through a pad of celite, and concentrated in vacuo.

**Reduction:** This above residue was dissolved in THF (2 mL) and EtOH (0.5 mL). Sodium borohydride (20 equiv) was added in two portions at 0 °C. The reaction was allowed to stir vigorously at room temperature overnight. The reaction was quenched with excess water and extracted with DCM (10 mL) three times. The crude product was purified by flash column chromatography to yield the amine.

### 3.4.15 Compounds Examined for Pyridyl Group Removal

**Compound 4c**

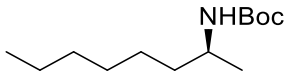


According to **Condition G**, compound **4b** (31 mg, 0.10 mmol) was allowed to react, and the product was purified by flash column chromatography ($SiO_2$; 90:10 hexanes:EA) to afford compound **4c** (17 mg, 70%) as a colorless oil. The $^{1}H$ and $^{13}C$ NMR spectra of compound **4c** matched those reported in literature. The er of compound **4c** was determined to be 94:6 by the following. Compound **4c** (17 mg, 0.074 mmol) was dissolved in EtOH (2 mL), HCl (4M solution in dioxane, 10 equiv) was added and the mixture was heated at 50 °C overnight. The solvent was then removed, and the residue was subjected to **Condition F** to afford compound **4b** for measurement of er.

**Compound 6c**

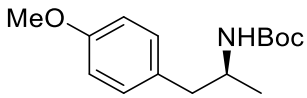


According to **Condition G**, compound **6b** (107 mg, 0.42 mmol) was allowed to react, and the product was purified by flash column chromatography ($SiO_2$; 80:20 hexanes:EA) to afford compound **6c** (77 mg, 74%) as a white solid. The $^{1}H$ and $^{13}C$ NMR spectra of compound **6c** matched those reported in literature. The er of compound **6c** was determined to be 93:7 by the following. Compound **6c** (77 mg, 0.29 mmol) was dissolved in EtOH (2 mL), HCl (4M solution in dioxane, 10 equiv) was added and the mixture was heated at 50 °C overnight. The solvent was then removed, and the residue was subjected to **Condition F** to afford compound **6b** for measurement of er.

**Compound 28c**

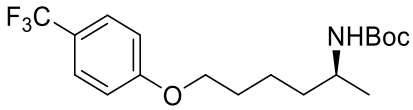


According to **Condition G**, compound **28b** (132 mg, 0.38 mmol) was allowed to react, and the product was purified by flash column chromatography ($SiO_2$; 80:20 hexanes:EA) to afford compound **28c** (103 mg, 82%) as a white solid. The er of compound **28c** was determined to be 98:2 by the following. Compound **28c** (103 mg, 0.29 mmol) was dissolved in EtOH (2 mL), HCl (4M solution in dioxane, 10 equiv) was added and the mixture was heated at 50 °C overnight. The solvent was then removed, and the residue was subjected to **Condition F** to afford compound **28b** for measurement of er.

**$^1$H NMR** (600 MHz, Chloroform-d) δ 7.52 (d, J = 8.6 Hz, 2H), 6.93 (d, J = 8.7 Hz, 2H), 4.32 (s, 1H), 3.99 (td, J = 6.4, 1.6 Hz, 2H), 3.68 (s, 1H), 1.88 – 1.73 (m, 2H), 1.57 – 1.46 (m, 4H), 1.44 (s, 9H), 1.13 (d, J = 6.6 Hz, 3H).

**$^{13}$C NMR** (151 MHz, Chloroform-d) δ 161.66, 155.55, 126.98 (q, J = 3.8 Hz), 124.63 (q, J = 270.9 Hz), 122.81 (q, J = 32.6 Hz), 114.56, 79.17, 68.14, 46.47, 37.21, 29.07, 28.58, 22.71, 21.41.

**$[\alpha]_D^{25}$:** +1.3 (*c* = 6.6, $CH_2Cl_2$).

**HRMS (*m/z*):** (ESI) calc'd $[M+Na]^+$: 384.1757, found: 384.1766.

**Compound 18c**

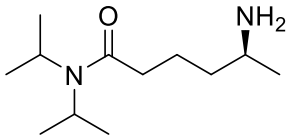


According to **Condition H**, compound **18c** (41 mg, 0.14 mmol) was allowed to react, and the product was purified by flash column chromatography ($SiO_2$; 2:1:0.02 DCM:MeOH:$NH_4OH$) to afford compound **18c** (22 mg, 75%) as a white solid. The er of compound **18c** was determined to be 90:10 by converting compound **18c** into compound **18b** following **Condition F**.

**$^1$H NMR** (500 MHz, Chloroform-d) δ 3.94 (p, J = 7.0 Hz, 1H), 3.40 (s, 1H), 2.90 (h, J = 6.4 Hz, 1H), 2.26 (t, J = 7.6 Hz, 2H), 1.63 (tq, J = 13.5, 6.7, 6.1 Hz, 4H), 1.40 – 1.28 (m, 8H), 1.18 (d, J = 6.8 Hz, 6H), 1.06 (d, J = 6.3 Hz, 3H).

**$^{13}$C NMR** (126 MHz, Chloroform-d) δ 171.76, 48.30, 47.01, 45.66, 39.92, 35.34, 23.88, 22.32, 21.14, 20.84.

**$[\alpha]_D^{25}$:** The optical rotation of compound **18c** is too low to be accurately measured.

**HRMS (*m/z*):** (ESI) calc'd $[M+H]^+$: 215.3605, found: 215.3602.

### 3.4.16. Comparison of Iridium-catalyzed and Ruthenium-catalyzed Hydroamination of Selected Substrates

Alkene (0.10 mmol, 1.0 equiv), 2-amino-5-methylpyridine (11 mg, 0.10 mmol), 1,3,5-trimethoxybenzene (5.6 mg, 0.033 mmol), and $Ru(PEt_3)_3(NTf_2)_2$ (5.0 mg, 0.010 mmol, 5.0 mol%) were combined with DCB (50 µL) and a magnetic stir bar in a one dram vial. The vial threads were wrapped with 1 layer of Teflon tape, and the resulting mixture was heated at 80 ˚C with stirring for 48 hours. The reaction was allowed to cool and an aliquot (5 µL) was then taken from the reaction and analyzed by $^1$H NMR spectroscopy.

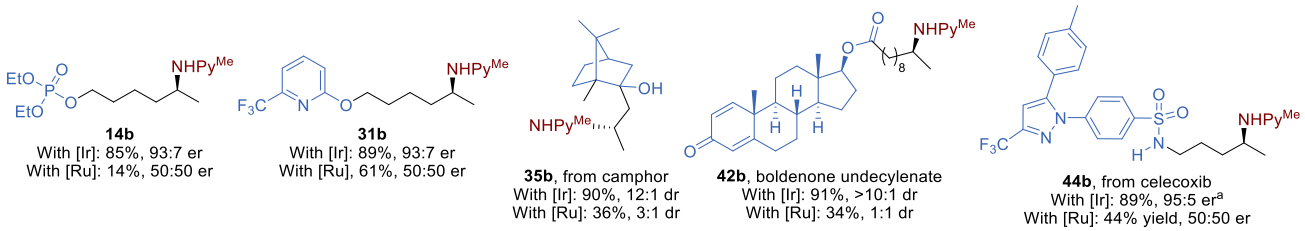


**Figure 3.13.** Comparison of Iridium-catalyzed and ruthenium-catalyzed hydroamination of selected substrates.

## 3.5 References

Parts of this chapter were reprinted with permission from:

"Enantioselective Hydroamination of Unactivated Terminal Alkenes"

Ma, S.; Xi, Y.; Fan, H.; Roediger, S.; Hartwig, J. F. *Chem* **2022**, *8*, 535-542.

1. Crudden, Cathleen M., and Edwards, D. (2003). Catalytic Asymmetric Hydroboration: Recent Advances and Applications in Carbon−Carbon Bond-Forming Reactions. Eur. J. Org. Chem. 2003, 4695-4712. https://doi.org/10.1002/ejoc.200300433.

2. Guo, J., Cheng, Z., Chen, J., Chen, X., and Lu, Z. (2021). Iron- and Cobalt-Catalyzed Asymmetric Hydrofunctionalization of Alkenes and Alkynes. Acc. Chem. Res. 54, 2701-2716. 10.1021/acs.accounts.1c00212.

3. Chen, J., and Lu, Z. (2018). Asymmetric hydrofunctionalization of minimally functionalized alkenes via earth abundant transition metal catalysis. Org. Chem. Front. 5, 260-272. 10.1039/C7QO00613F.

4. Liu, R.Y., and Buchwald, S.L. (2020). CuH-Catalyzed Olefin Functionalization: From Hydroamination to Carbonyl Addition. Acc. Chem. Res. 53, 1229-1243. 10.1021/acs.accounts.0c00164.

5. Mlynarski, S.N., Schuster, C.H., and Morken, J.P. (2014). Asymmetric synthesis from terminal alkenes by cascades of diboration and cross-coupling. Nature 505, 386-390. 10.1038/nature12781.

6. Coombs, J.R., and Morken, J.P. (2016). Catalytic Enantioselective Functionalization of Unactivated Terminal Alkenes. Angew. Chem. Int. Ed. 55, 2636-2649. https://doi.org/10.1002/anie.201507151.

7. Fuentes, A.V., Pineda, M.D., and Venkata, K.C.N. (2018). Comprehension of Top 200 Prescribed Drugs in the US as a Resource for Pharmacy Teaching, Training and Practice. Pharmacy 6. 10.3390/pharmacy6020043.

8. Steinhuebel, D., Sun, Y., Matsumura, K., Sayo, N., and Saito, T. (2009). Direct Asymmetric Reductive Amination. J. Am. Chem. Soc. 131, 11316-11317. 10.1021/ja905143m.

9. Storer, R.I., Carrera, D.E., Ni, Y., and MacMillan, D.W.C. (2006). Enantioselective Organocatalytic Reductive Amination. J. Am. Chem. Soc. 128, 84-86. 10.1021/ja057222n.

10. Tararov, V.I., and Börner, A. (2005). Approaching Highly Enantioselective Reductive Amination. Synlett 2005, 203-211.

11. Li, C., Villa-Marcos, B., and Xiao, J. (2009). Metal−Brønsted Acid Cooperative Catalysis for Asymmetric Reductive Amination. J. Am. Chem. Soc. 131, 6967-6969. 10.1021/ja9021683.

12. Wang, C., Pettman, A., Bacsa, J., and Xiao, J. (2010). A Versatile Catalyst for Reductive Amination by Transfer Hydrogenation. Angew. Chem. Int. Ed. 49, 7548-7552. https://doi.org/10.1002/anie.201002944.

13. Verendel, J.J., Pàmies, O., Diéguez, M., and Andersson, P.G. (2014). Asymmetric Hydrogenation of Olefins Using Chiral Crabtree-type Catalysts: Scope and Limitations. Chem. Rev. 114, 2130-2169. 10.1021/cr400037u.

14. Mutti, F.G., Knaus, T., Scrutton, N.S., Breuer, M., and Turner, N.J. (2015). Conversion of alcohols to enantiopure amines through dual-enzyme hydrogen-borrowing cascades. Science 349, 1525. 10.1126/science.aac9283.

15. Robak, M.T., Herbage, M.A., and Ellman, J.A. (2010). Synthesis and Applications of tert-Butanesulfinamide. Chem. Rev. 110, 3600-3740. 10.1021/cr900382t.

16. Xi, Y., Ma, S., and Hartwig, J.F. (2020). Catalytic asymmetric addition of an amine N–H bond across internal alkenes. Nature 588, 254-260. 10.1038/s41586-020-2919-z.

17. Pan, S., Endo, K., and Shibata, T. (2012). Ir(I)-Catalyzed Intermolecular Regio- and Enantioselective Hydroamination of Alkenes with Heteroaromatic Amines. Org. Lett. 14, 780-783. 10.1021/ol203318z.

18. Reznichenko, A.L., Nguyen, H.N., and Hultzsch, K.C. (2010). Asymmetric Intermolecular Hydroamination of Unactivated Alkenes with Simple Amines. Angew. Chem. Int. Ed. 49, 8984-8987. 10.1002/anie.201004570.

19. Zhang, Z., Lee, S.D., and Widenhoefer, R.A. (2009). Intermolecular Hydroamination of Ethylene and 1-Alkenes with Cyclic Ureas Catalyzed by Achiral and Chiral Gold(I) Complexes. J. Am. Chem. Soc. 131, 5372-5373. 10.1021/ja9001162.

20. Vanable, E.P., Kennemur, J.L., Joyce, L.A., Ruck, R.T., Schultz, D.M., and Hull, K.L. (2019). Rhodium-Catalyzed Asymmetric Hydroamination of Allyl Amines. J. Am. Chem. Soc. 141, 739-742. 10.1021/jacs.8b09811.

21. Ma, S., Hill, C.K., Olen, C.L., and Hartwig, J.F. (2021). Ruthenium-Catalyzed Hydroamination of Unactivated Terminal Alkenes with Stoichiometric Amounts of Alkene and an Ammonia Surrogate by Sequential Oxidation and Reduction. J. Am. Chem. Soc. 143, 359-368. 10.1021/jacs.0c11043.

22. Sevov, C.S., Zhou, J., and Hartwig, J.F. (2012). Iridium-Catalyzed Intermolecular Hydroamination of Unactivated Aliphatic Alkenes with Amides and Sulfonamides. J. Am. Chem. Soc. 134, 11960-11963. 10.1021/ja3052848.

23. Rucker, R.P., Whittaker, A.M., Dang, H., and Lalic, G. (2012). Synthesis of Tertiary Alkyl Amines from Terminal Alkenes: Copper-Catalyzed Amination of Alkyl Boranes. J. Am. Chem. Soc. 134, 6571-6574. 10.1021/ja3023829.

24. Miki, Y., Hirano, K., Satoh, T., and Miura, M. (2013). Copper-Catalyzed Intermolecular Regioselective Hydroamination of Styrenes with Polymethylhydrosiloxane and Hydroxylamines. Angew. Chem. Int. Ed. 52, 10830-10834. https://doi.org/10.1002/anie.201304365.

25. Strom, A.E., and Hartwig, J.F. (2013). One-Pot Anti-Markovnikov Hydroamination of Unactivated Alkenes by Hydrozirconation and Amination. J. Org. Chem. 78, 8909-8914. 10.1021/jo401498w.

26. Zhu, S., Niljianskul, N., and Buchwald, S.L. (2013). Enantio- and Regioselective CuH-Catalyzed Hydroamination of Alkenes. J. Am. Chem. Soc. 135, 15746-15749. 10.1021/ja4092819.

27. Shen, X., Chen, X., Chen, J., Sun, Y., Cheng, Z., and Lu, Z. (2020). Ligand-promoted cobalt-catalyzed radical hydroamination of alkenes. Nat. Commun. 11, 783. 10.1038/s41467-020-14459-x.

28. Johns, A.M., Sakai, N., Ridder, A., and Hartwig, J.F. (2006). Direct Measurement of the Thermodynamics of Vinylarene Hydroamination. J. Am. Chem. Soc. 128, 9306-9307. 10.1021/ja062773e.

29. Ohmura, T., Yagi, K., Torigoe, T., and Suginome, M. Intramolecular Addition of a Dimethylamino C(sp3)–H Bond across C–C Triple Bonds Using IrCl(DTBM-SEGPHOS)(ethylene) Catalyst: Synthesis of Indoles from 2-Alkynyl-N-methylanilines. Synthesis.

30. Dastbaravardeh, N., Schnürch, M., and Mihovilovic, M.D. (2012). Ruthenium(0)-Catalyzed sp3 C–H Bond Arylation of Benzylic Amines Using Arylboronates. Org. Lett. 14, 1930-1933. 10.1021/ol300627p.

31. Smout, V., Peschiulli, A., Verbeeck, S., Mitchell, E.A., Herrebout, W., Bultinck, P., Vande Velde, C.M.L., Berthelot, D., Meerpoel, L., and Maes, B.U.W. (2013). Removal of the Pyridine Directing Group from α-Substituted N-(Pyridin-2-yl)piperidines Obtained via Directed Ru-Catalyzed sp3 C–H Functionalization. J. Org. Chem. 78, 9803-9814. 10.1021/jo401521y.

32. Wang, J.-W., Li, Y., Nie, W., Chang, Z., Yu, Z.-A., Zhao, Y.-F., Lu, X., and Fu, Y. (2021). Catalytic asymmetric reductive hydroalkylation of enamides and enecarbamates to chiral aliphatic amines. Nat. Commun. 12, 1313. 10.1038/s41467-021-21600-x.

33. Xi, Y.; Ma, S.; Hartwig, J. F., Catalytic asymmetric addition of an amine N–H bond across internal alkenes. *Nature* **2020,** *588* (7837), 254-260.

34. Ma, S.; Hill, C. K.; Olen, C. L.; Hartwig, J. F., Ruthenium-Catalyzed Hydroamination of Unactivated Terminal Alkenes with Stoichiometric Amounts of Alkene and an Ammonia Surrogate by Sequential Oxidation and Reduction. *J. Am. Chem. Soc.* **2021,** *143* (1), 359-368.

35. Ohmura, T.; Yagi, K.; Torigoe, T.; Suginome, M., Intramolecular Addition of a Dimethylamino C(sp3)–H Bond across C–C Triple Bonds Using IrCl(DTBM-SEGPHOS)(ethylene) Catalyst: Synthesis of Indoles from 2-Alkynyl-N-methylanilines. *Synthesis* **2021,** *53* (EFirst), A-H.

36. Walker, S. R. Design, Synthesis and Characterisation of Inhibitors of 3-Deoxy-D-arabino-Heptulosonate 7-Phosphate. University of Canterbury, 2007.

37. Boschi, F. New routes to enantioenriched substances through small organic molecules. University of Bologna, 2009.

38. Beak, P.; Hunter, J. E.; Jun, Y. M.; Wallin, A. P., Complex-induced proximity effects: remote lithiations of carboxamides. *J. Am. Chem. Soc.* **1987,** *109* (18), 5403-5412.

39. Wang, F.; Xu, P.; Cong, F.; Tang, P., Silver-mediated oxidative functionalization of alkylsilanes. *Chemical Science* **2018,** *9* (47), 8836-8841.

40. Song, C.; Dong, X.; Yi, H.; Chiang, C.-W.; Lei, A., DDQ-Catalyzed Direct C(sp3)–H Amination of Alkylheteroarenes: Synthesis of Biheteroarenes under Aerobic and Metal-Free Conditions. *ACS Catalysis* **2018,** *8* (3), 2195-2199.

41. Li, D.; Mao, T.; Huang, J.; Zhu, Q., Copper-Catalyzed Bromodifluoroacetylation of Alkenes with Ethyl Bromodifluoroacetate. *J. Org. Chem.* **2018,** *83* (17), 10445-10452.

42. Yan, L.; Meng, Y.; Haeffner, F.; Leon, R. M.; Crockett, M. P.; Morken, J. P., Carbohydrate/DBU Cocatalyzed Alkene Diboration: Mechanistic Insight Provides Enhanced Catalytic Efficiency and Substrate Scope. *J. Am. Chem. Soc.* **2018,** *140* (10), 3663-3673.

43. Rotsides, C. Z.; Woerpel, K. A., Diastereoselective silylene transfer reactions to chiral enantiopure alkenes: effects of ligand size and substrate bias. *Dalton Transactions* **2017,** *46* (27), 8763-8768.

44. Taber, D. F.; Berry, J. F.; Martin, T. J., Convenient Synthetic Route to an Enantiomerically Pure FMOC α-Amino Acid. *J. Org. Chem.* **2008,** *73* (23), 9334-9339.

45. Xu, J.; Fu, Y.; Luo, D.-F.; Jiang, Y.-Y.; Xiao, B.; Liu, Z.-J.; Gong, T.-J.; Liu, L., Copper-Catalyzed Trifluoromethylation of Terminal Alkenes through Allylic C–H Bond Activation. *J. Am. Chem. Soc.* **2011,** *133* (39), 15300-15303.

46. Descotes, G.; Ramza, J.; Basset, J.-M.; Pagano, S., Metathesis of Ω-unsaturated glucosides with chloro-aryloxide complexes of tungsten, as a new way leading to unsaturated bolaamphiphiles. *Tetrahedron Lett.* **1994,** *35* (40), 7379-7382.

47. Xu, C.; Huang, W.; Zhang, R.; Gao, C.; Li, Y.; Wang, M., Trifluoromethylations of Alkenes Using PhICF3Cl as Bifunctional Reagent. *J. Org. Chem.* **2019,** *84* (21), 14209-14216.

48. Wu, X.; Chu, L.; Qing, F.-L., Silver-Catalyzed Hydrotrifluoromethylation of Unactivated Alkenes with CF3SiMe3. *Angew. Chem. Int. Ed.* **2013,** *52* (8), 2198-2202.

49. Dastbaravardeh, N.; Schnürch, M.; Mihovilovic, M. D., Ruthenium(0)-Catalyzed sp3 C–H Bond Arylation of Benzylic Amines Using Arylboronates. *Org. Lett.* **2012,** *14* (7), 1930-1933.

50. Smout, V.; Peschiulli, A.; Verbeeck, S.; Mitchell, E. A.; Herrebout, W.; Bultinck, P.; Vande Velde, C. M. L.; Berthelot, D.; Meerpoel, L.; Maes, B. U. W., Removal of the Pyridine Directing Group from α-Substituted N-(Pyridin-2-yl)piperidines Obtained via Directed Ru-Catalyzed sp3 C–H Functionalization. *J. Org. Chem.* **2013,** *78* (19), 9803-9814.

# CHAPTER 4
# Remote Hydroamination of Disubstituted Alkenes by a Combination of Isomerization and Regioselective N-H Addition

## 4.1 Introduction

Amines and their derivatives are important as both pharmaceuticals and agrochemicals.[1-3] The selective functionalization at electronically and sterically similar methylene carbons distal to a reactive site has been a longstanding goal in organic synthesis but has been challenging to develop because of the similar reactivity of unactivated methylene groups.[1-5] The remote hydrofunctionalization of alkenes, which places a hydrogen on the alkene and a functional group distal to the alkene, is a potential approach to this synthetic goal (Scheme 4.1A). Remote hydrosilylation[6-12] by chain walking is a classic reaction, and remote hydrofunctionalization with boranes,[13-22] as well as arenes or heteroarenes,[23-26] is known. Nickel–catalyzed formal remote hydroarylation[27-39] and hydroalkylation[40-42] has also been reported, but the remote hydrofunctionalization of alkenes with more polar X–H bonds, especially those of amines,[43-44] remains underdeveloped. The few reported transformations occur in a formal sense by combining silanes as the hydride donor and esters of hydroxylamine or dioxazolone as the aminating reagents (Scheme 4.1B).[45-48]

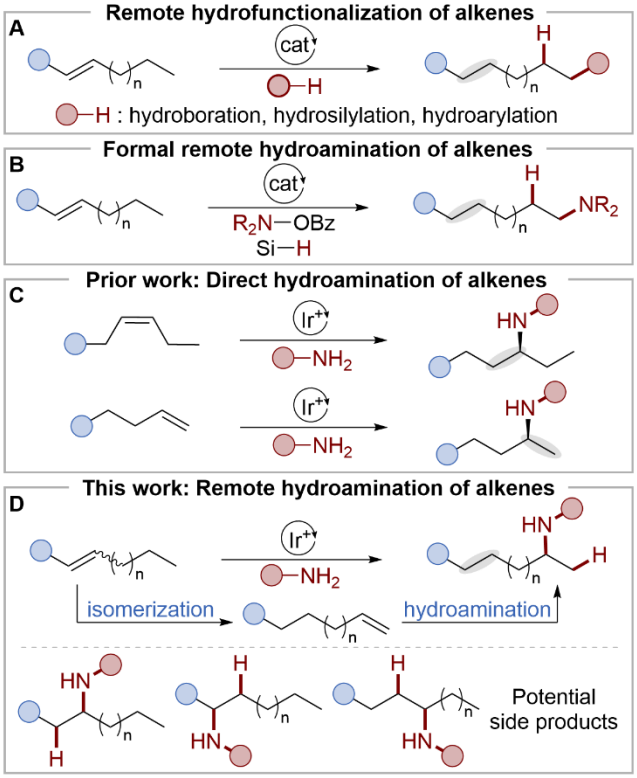


**Scheme 4.1.** (A) Remote hydrofunctionalization of alkenes. (B) Formal remote hydroamination of alkenes. (C) Prior work: Direct hydroamination of alkenes. (D) This work: Remote hydroamination of disubstituted alkenes.

We envisioned a reaction in which a single reagent containing an N-H bond could trigger alkene isomerization and deliver an amino group to form the product. While synthetically appealing, this reaction could generate a mixture of products with the amino group at multiple internal sites.[49] Our group recently reported catalytic hydroamination of internal and terminal alkenes with a 2-aminopyridine (Scheme 4.1C)[50-52] that suppressed isomerization and led to direct hydroamination. We envisioned that appropriate modifications to the amine and catalyst could increase the rate of

isomerization over that of hydroamination at internal sites thereby creating a remote hydroamination of internal alkenes by selective addition to the terminal alkene (Scheme 4.1D). Herein, we report the remote hydroamination of unactivated, internal alkenes to place the amino group at the unactivated subterminal carbon of an alkyl chain. This process was enabled by varying the electronic properties of the N-H donor to retard the rate of migratory insertion and varying the backbone and aryl fragment of the bisphosphine ligand to promote the desired remote hydroamination regioselectively.

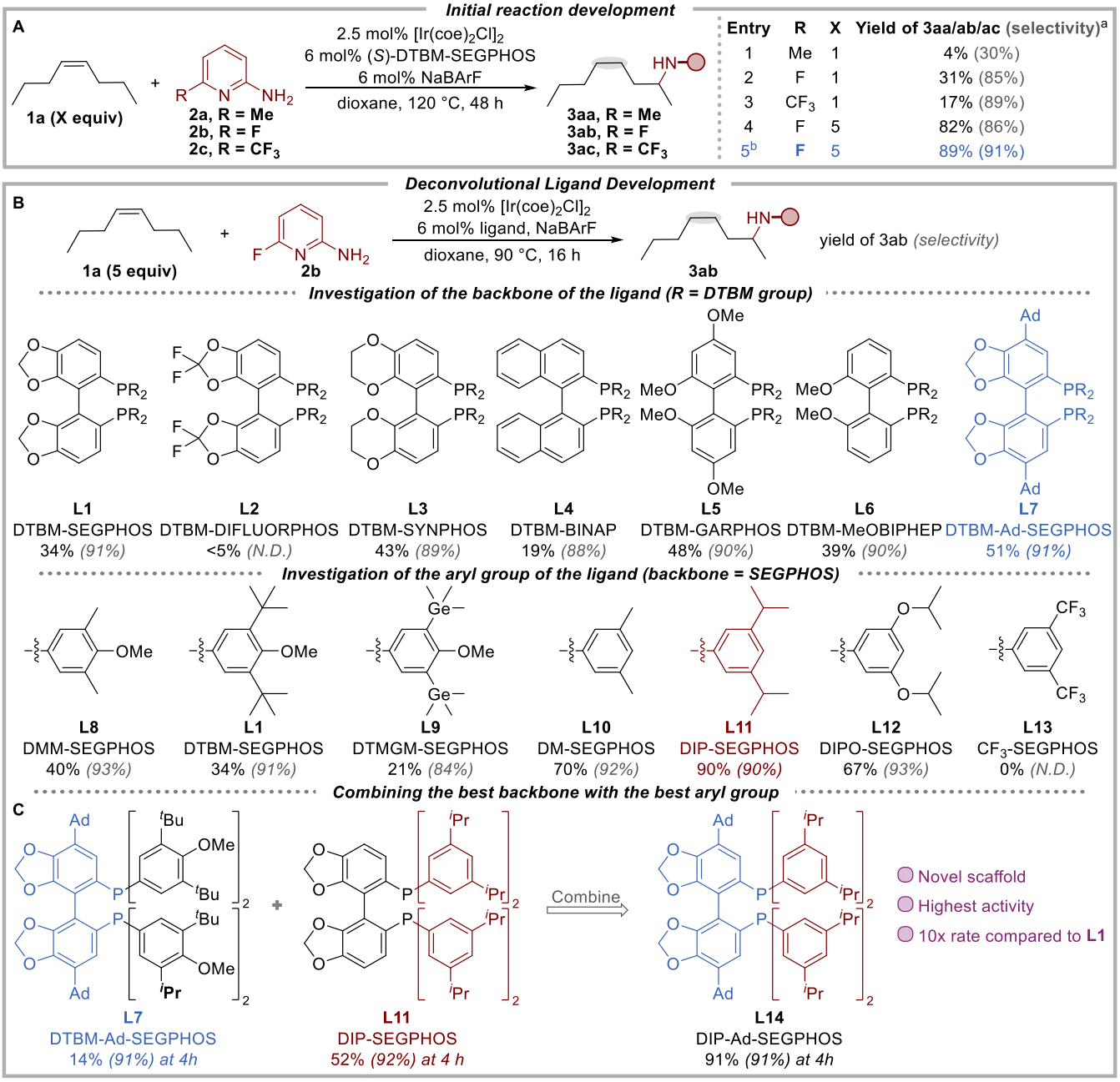


**Scheme 4.2.** Investigation of the Reaction Conditions for the Remote Hydroamination of *Cis*-4-octene. [a]Yield represents the yield of 2-amine with respect to 2-aminopyridine as the limiting reagent. selectivity = 2-amine/all amines. [b]The reaction was performed at 90 °C for 72 h.

## 4.2 Results and Discussion

To achieve remote hydroamination of internal alkenes, we first sought to identify an aminopyridine that would change the selectivity from the hydroamination we reported previously. To do so, we conducted the reactions of a model alkene, *cis*-4-octene (**1a**) with a series of 2-aminopyridines in combination with our previously developed cationic iridium catalyst.[50-51] The reaction with the electron-rich, 6-methyl-2-aminopyridine (**2a**) led to slow isomerization of *cis*-4-octene, the formation of the 2-aminoalkane (**3aa**) with low selectivity (30%), and the 4-aminoalkane from direct addition of the N–H bond to the internal alkene as the major product (Scheme 4.2A, entry 1). We hypothesized that the selectivity for the 2-aminoalkane would increase if the rate of hydroamination could be retarded to enable more complete isomerization of the alkene. Building on the precedent that migratory insertions of alkenes into late transition–metal amido bonds are faster when the amido group is more electron donating,[53-54] we examined the remote hydroamination with 2-aminopyridines bearing electron-withdrawing substituents. Rapid isomerization occurred, and the desired 2-amine was observed as the major product with the electron-deficient 6-fluoro- and 6-trifluoromethyl-2-aminopyridines (**2b** and **2c**) as the N–H donor (Scheme 4.2A, entry 2, 3). 6-Fluoro-2- aminopyridine (**2b**) was selected as the amine for further reaction development because it reacted in higher yield than did **2c** and with comparable selectivity. In addition, the pyridyl fluoride in the product would enable further derivatization by nucleophilic aromatic substitution.

To improve the yield of the reaction between *cis*-4-octene and 6-fluoro-2-aminopyridine to form amine **3ab**, we evaluated the effect of reaction time, temperature, solvent, and bisphosphine. However, the product formed in lower or similar yields (ca. 34%) in all cases (see the supporting information for details). Instead, the yield of the product increased to 89% when an excess of *cis*-4-octene (5 equiv) was used (Scheme 4.2A, entry 4). These results prompted us to assess whether the remote hydroamination was reversible and if a thermodynamic equilibrium between the isomeric alkenes and the 2-amine (**3ab**) affected the yield. To test for reversible hydroamination, we subjected 2-aminoalkane **3ab** to the catalytic conditions. Dehydroamination of **3ab** occurred to form octene isomers as well as **2b** and 37% of **3ab** remained. This result suggested that the low yield of 2-aminoalkene from a 1:1 ratio of *cis*-4-octene and 6-fluoro-2-aminopyridine resulted from unfavorable thermodynamics, rather than low activity or stability of the iridium catalyst. The regioselectivity of the reaction between *cis*-4-octene (5 equivalent) and **2b** was further increased to 91% by conducting the reaction at 90 °C instead of at 120 °C (Scheme 4.2A, entry 5). However, prolonged reaction time (72 h) was required for the reaction to reach equilibrium at this temperature. Thus, an iridium complex that would catalyze the remote hydroamination with higher rates at the lower temperature was needed.

To do so, we sought to exploit the modularity of the ligand backbone and phosphine aryl groups by an approach that could survey the effects within a broad range of structures. Because of the challenge of synthesizing a library of bisphosphine ligands, particularly with biaryl backbones,[55-59] we individually varied the components of the bisphosphines. We separately evaluated the effects of the electronic and steric properties of a series of backbones and a series of substituents on the aryl groups (Scheme 4.2B). After identifying the backbone and the aryl groups leading to the highest yield and selectivity, we combined these components to form a new ligand that would benefit from the properties of both components.

To evaluate the effect of the ligand backbone, we conducted the remote hydroamination with iridium catalysts of ligands possessing the same aryl group (DTBM group) but different backbones

(**L1-L7**). The effect of the backbone of the ligand on the selectivity of the reaction was negligible, but the effect of the backbone on the rate was significant. The rate of the reaction was fastest with the ligand containing the electron-rich and bulky Ad-SEGPHOS backbone (**L7**).

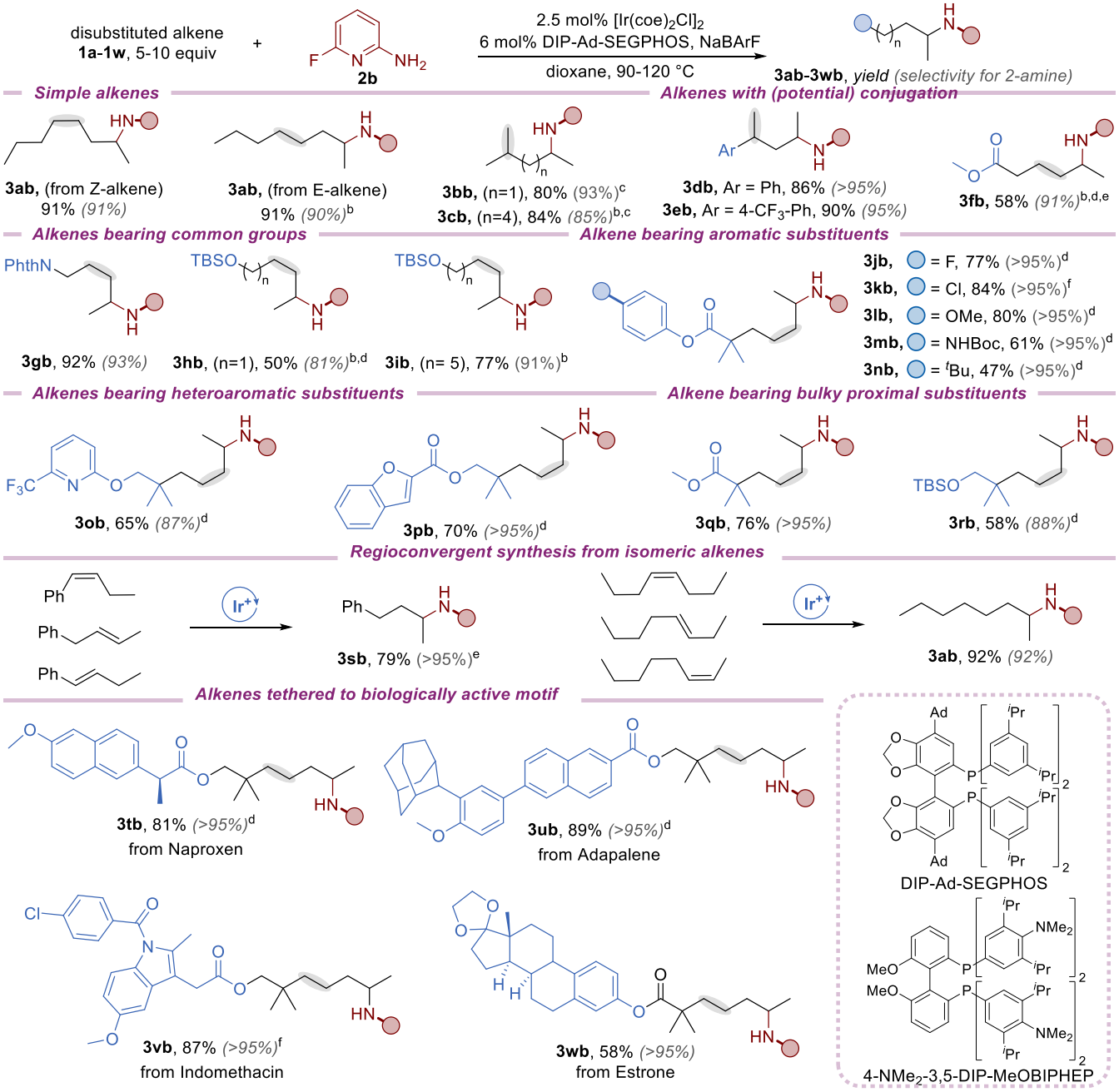


. **Scheme 4.3.** Scope of the Remote Hydroamination with Different Alkenes. [a]Products **3db-3eb, 3tb**, and **3wb** were formed in 1:1 dr. [b](4-$NMe_2$-3,5-DIP)-MeOBIPHEP as the ligand. [c]7.5 equivalents of alkene. [d]3.75 mol% $[Ir(coe_2)Cl]_2$, 9 mol% ligand and NaBArF. [e]10 equivalents of alkene. [f]5 mol% $[Ir(coe)_2Cl]_2$, 12 mol% ligand and NaBArF

The effect of the aryl group of the ligand on the reaction was assessed by conducting the remote hydroamination with iridium catalysts of ligands possessing the same backbone (SEGPHOS) but

different aryl groups (**L8**-**L13**). This effect was determined with the SEGPHOS backbone because it is present in commonly used bisphosphines, including several commercially available versions, and because the racemic ligand is readily accessible by the homocoupling of benzodioxolyl diethyl phosphonate.[57] The size of the *meta*-substituents on the aryl rings significantly affected the selectivity of the reaction (**L1**, **L8**, **L9**) and the electronic properties of the *meta* and *para* substituents affected the rate (**L8**, **L9**, **L12**, **L13**). A mid-sized, slightly electron-donating, diisopropyl substituted aryl group (DIP, **L11**) was determined to possess the properties leading to high selectivity and high rate for the remote hydroamination.

Having identified the backbone (Ad-SEGPHOS) and aryl group (3,5-diisopropylphenyl, DIP) that individually led to the highest yield and selectivity, we prepared DIP-Ad-SEGPHOS (**L14**) and discovered that the reaction catalyzed by iridium and **L14** yielded the product with selectivity equally high and with rates 6.5 and 1.8 times higher than of those of the reactions performed with the parent ligands **L7** and **L11**, respectively (Scheme 4.2C). This new ligand, DIP-Ad-SEGPHOS (**L14**), was synthesized in a high 34% overall yield on gram scale. Moreover, the remote hydroamination of *cis*-4-octene required 4 h to reach equilibrium, whereas the reaction with widely used, commercially available DTBM-SEGPHOS (**L11)** required 72 h. This modular approach to the new ligand experimentally assessed a wide space of bisphosphine ligands with 13 representative examples and revealed a structure with enhanced catalytic performance in a rapid and rational manner.

Having identified a suitable N–H donor and ligand to realize the remote hydroamination, the scope of the reaction with varied alkenes was investigated (Scheme 4.3). Remote hydroamination occurred in high yields and with high regioselectivity with *Z*-alkenes, *E*-alkenes, and 1,1-disubstitued alkenes, including those requiring multiple isomerizations (**3ab**-**3cb**); 2-amino product **3cb** formed from six consecutive isomerizations prior to hydroamination. The remote hydroamination also occurred with alkenes requiring contrathermodynamic isomerizations; the remote hydroamination of vinylarenes formed products **3db** and **3eb**, without competing generation of products from hydroamination at the benzylic position, even though the isomerization to generate the reactive alkene requires deconjugation. The hydroamination of a β,γ–unsaturated ester (**3fb**) furnished the product of remote amination without the formation of the β–aminoalkyl product from conjugate addition of the aminopyridine into an α,β–unsaturated ester that formed from isomerization. Less than 20% of the alkene isomerized to the α,β–unsaturated ester, indicating that isomerization in the direction of the carbonyl unit is slower than isomerization to further deconjugated positions, and N–H addition to the more electron- rich alkene is faster than that to the conjugated alkene. The remote hydroamination also occurred with alkenes bearing a variety of suitably protected and free functional groups, including protected amine (**3gb, 3mb**), alcohols (**3hb**-**3ib**), esters (**3jb**-**3nb**, **3pb**-**3rb)** as well as arenes (**3jb**-**3nb**) and heteroarenes (**3ob**-**3pb**) bearing electron-donating and electron-withdrawing substituents. It also occurred with alkenes containing proximal, fully substituted β-carbons (**3jb**-**3rb**). The reaction even occurred with mixtures of alkenes to form a single product. Regioconvergent generation of 2-substituted amines from isomeric mixtures of alkenes occurred in high yield with excellent regioselectivity (**3sb**, **3ab**). Finally, this reaction is compatible with the functionalization of alkenes derived from biologically relevant compounds (**3ub**-**3xb**). For certain substrates (**1c**, **1f**, **1h**, **1i**), the reactions with DIP-MeOBIPHEP as ligand afforded products with higher regioselectivity than those obtained from the reaction with the DIP-Ad-SEGPHOS ligand. For the reaction of β, γ–unsaturated

ester (**1f**) and alkenes containing fully substituted β-carbons (**1j-1p**, **1r-1v**), an increase in catalyst loading was required to achieve high yields.

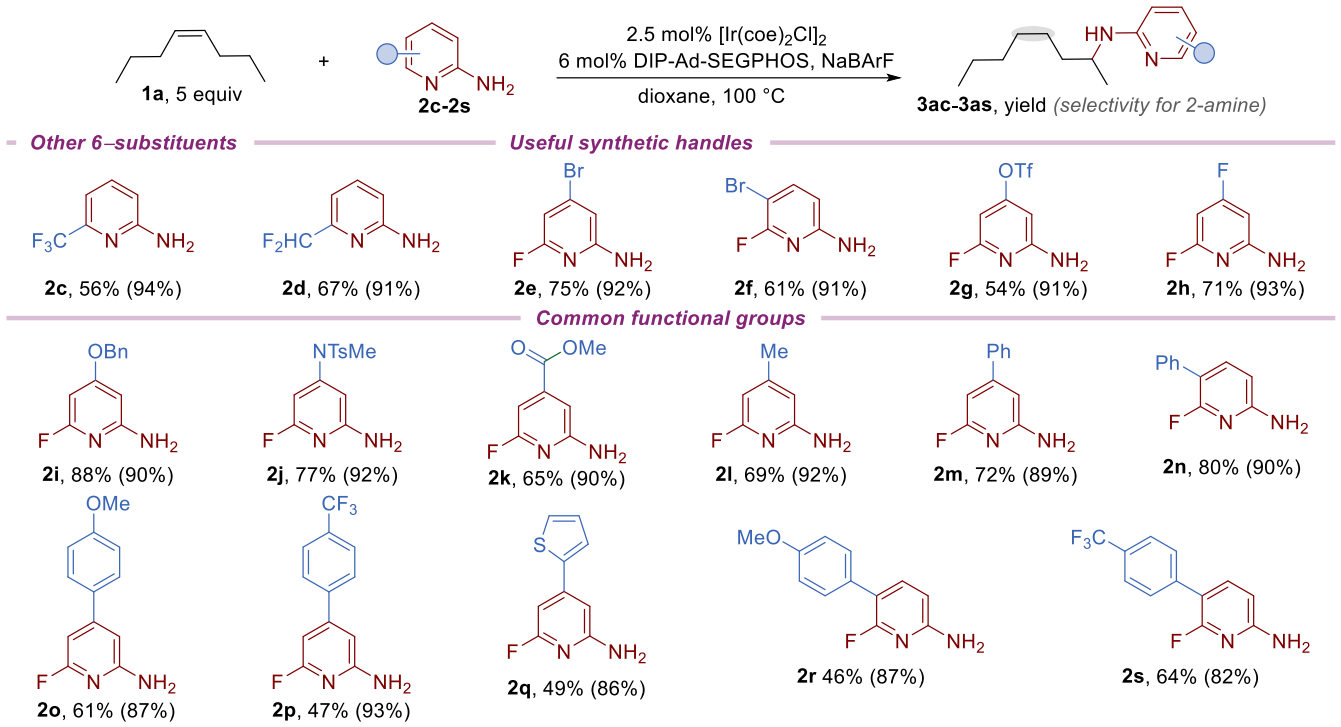


**Scheme 4.4.** Scope of the Remote Hydroamination with Different Aminopyridines. [a]5 mol% $[Ir(coe)_2Cl]_2$, 12 mol% ligand and NaBArF.

The scope of aminopyridines undergoing the remote hydroamination is shown in Scheme 4.4. Aminopyridines containing electron-withdrawing trifluoromethyl and difluoromethyl substituents at the 6–position underwent the remote hydroamination to afford the corresponding amines (**2c-2d**) in good yield with high regioselectivity. The remote hydroamination of *cis*-4-octene with aminopyridines containing synthetic handles for cross–coupling and $S_NAr$ reactions (**2e-2h**) also occurred in good yield. The remote hydroamination with aminopyridines containing a series of suitably protected or free functional groups, such as a protected alcohol (**2i**), protected amine (**2j**), ester (**2k**), alkyl (**2l**), aryl, and heteroaryl groups (**2m-2s**), also occurred.

Subsequent functionalization of the remote hydroamination products containing pyridyl fluorides occurred by nucleophilic aromatic substitutions (Scheme 4.5). $S_NAr$ reactions of amine **3ab** with sulfur-, oxygen-, and nitrogen-based nucleophiles proceeded smoothly to afford the substituted products (**4ab-9ab**), although deprotonation of the acidic N–H proton in **3ab** under basic conditions significantly decreased its reactivity towards $S_NAr$ reactions.

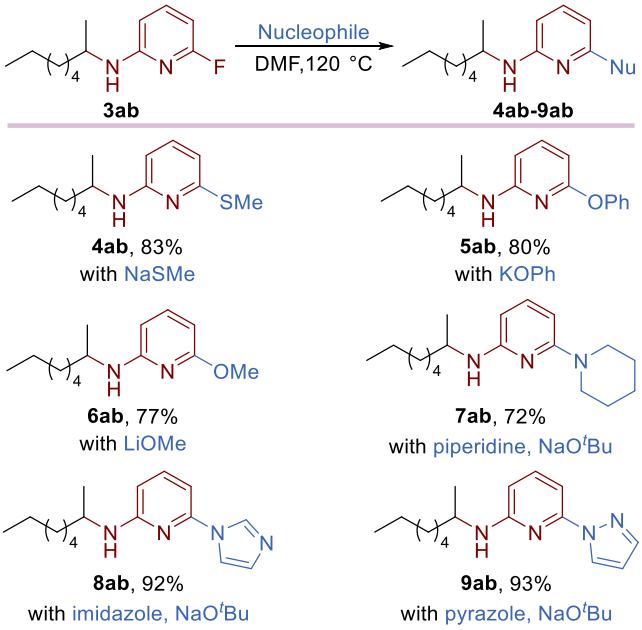


**Scheme 4.5.** Diversification of the product through nucleophilic aromatic substitutions.

### 4.3 Conclusion

In summary, we have discovered iridium-catalyzed remote hydroaminations of unactivated disubstituted alkenes with electron-poor 2-aminopyridines. Keys to this development are the use of aminopyridines bearing electron-withdrawing substituents at the 6 position to increase the selectivity for the remote amine product by changing the relative rates for hydroamination versus isomerization of the alkene and the creation of a new DIP-Ad-SEGPHOS ligand by evaluating the steric and electronic effects of ligand modules on reactivity and selectivity. Further work on elucidating the mechanism of the reaction is ongoing, and we anticipate that this work will inspire the development of other remote hydrofunctionalizations and the development of bisphosphines by experimental assessment of the components of such modular ligands.

### 4.4 Experimental

#### 4.4.1 General Experimental Procedures

All manipulations were performed in a nitrogen-filled glovebox or on a Schlenk manifold unless otherwise noted. Glassware was dried at 150 °C for at least 4 h before use. All liquid alkenes were stored over 4 Å molecular sieves in the glovebox for at least 12 h prior to use. All solid alkenes were used as received without further purification. All aminopyridines were purified by column chromatography to remove oxidized impurities prior to use. All catalytic reactions were assembled in a nitrogen-filled glovebox with oven-dried glassware and were stirred with Teflon-coated magnetic stirring bars.

#### 4.4.2 Reagents and Solvents

DCM, $Et_2O$, THF, and hexanes were collected from a solvent purification system containing a 0.33 m column of activated alumina under nitrogen and stored over 4 Å molecular sieves for at least 12 h prior to use. Anhydrous 1,4-dioxane was purchased from Acros, stored in a glovebox, and stored over 4 Å molecular sieves for at least 12 h prior to use. Phosphine ligands were used as received from Takasago or Strem. Aminopyridines was purchased from Aldrich, columned with ethyl acetate/hexanes, and stored in a glovebox. $[Ir(coe)_2Cl]_2$ was used as received from Strem.

### 4.4.3 Chromatography and Data Analysis

**Flash column chromatography** was carried out with a Teledyne Isco CombiFlash Rf system using RediSep Rf Gold columns.

**$^1$H, $^{13}$C and $^{19}$F NMR Spectra** were recorded on a Bruker 500 or 600 MHz spectrometer. $^1$H chemical shifts are reported in parts per million, relative residual protiated solvent as a reference. $^{13}$C chemical shifts are reported in parts per million, relative to the deuterated solvent as a reference. $^{19}$F chemical shifts were reported in parts per million, relative to an external standard of $CFCl_3$. $^{31}$P chemical shifts were reported in parts per million, relative to an 85% $H_3PO_4$ external standard.

**High-resolution mass spectral (HRMS)** data were obtained with PerkinElmer AxION 2 TOF (ESI and APCI), Thermo LTQ-FTICR (ESI) and Waters Autospec Premier (EI) mass spectrometers at the QB3/Chemistry Mass Spectrometry Facility at UC Berkeley at the LBNL Catalysis Facility.

**Gas Chromatography (GC)** was performed on an Agilent 7890 GC with an FID detector.

**Liquid Chromatography (LC)** was performed on a Waters ACQUITY UPLC System with a UV detector.

### 4.4.4 Naming of Compounds

Compound names are those generated by ChemDraw 16.0 software (PerkinElmer), following the IUPAC nomenclature.

### 4.4.5. General Procedures for the Remote Hydroamination of Alkenes

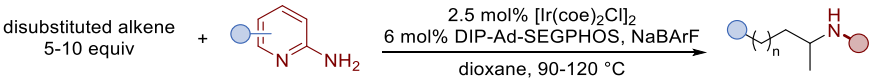


**Condition A:** In a nitrogen-filled glovebox, a 1-dram vial was charged sequentially with $[Ir(coe)_2Cl]_2$ (2.3 mg, 2.5 μmol, 2.5 mol%), aminopyridine (0.10 mmol, 1.0 equiv), DIP-Ad-SEGPHOS (7.3 mg, 6.0 μmol, 6.0 mol%), sodium tetrakis[3,5-bis(trifluoromethyl)phenyl]borate (5.4 mg, 6.0 μmol, 6.0 mol%), alkene (0.50 to 1.0 mmol, 5.0 to 10 equiv) 1,4-dioxane (0.2 mL), and a magnetic stir bar. The vial was capped and removed from the glovebox. The reaction was heated at 90 to 120 °C in an aluminium heating block. The ratio between the product and aminopyridine was monitored by $^1$H NMR spectroscopy periodically, and the reaction was diluted with 1 mL of DCM after this ratio was great than 10:1 or this ratio remained unchanged for two

consecutive aliquots. The last aliquot was analyzed by GC or LC to determine the regioselectivity of the reaction. The crude material was concentrated in vacuo and purified by flash column chromatography to afford the product.

### 4.4.6 Reaction Development for the Remote Hydroamination of Alkenes

In a nitrogen-filled glovebox, a 1-dram vial was charged sequentially with $[Ir(coe)_2Cl]_2$ (2.3 mg, 2.5 μmol, 2.5 mol%), aminopyridine (0.10 mmol, 1.0 equiv), ligand (6.0 μmol, 6.0 mol%), additive (6.0 μmol, 6.0 mol%), 1,3,5-trimethoxybenzene (5.6 mg, 0.033 mmol), cis-4-octene (**1a**) (16 to 78 μL, 0.10 to 0.50 mmol, 1.0 to 5.0 equiv) solvent (0.2 mL), and a magnetic stir bar. The vial was capped and removed from the glovebox. The reaction was heated at the designated temperature in an aluminium heating block. An aliquot (5 μL) was then taken from the reaction and analyzed by $^1$H NMR spectroscopy and GC.

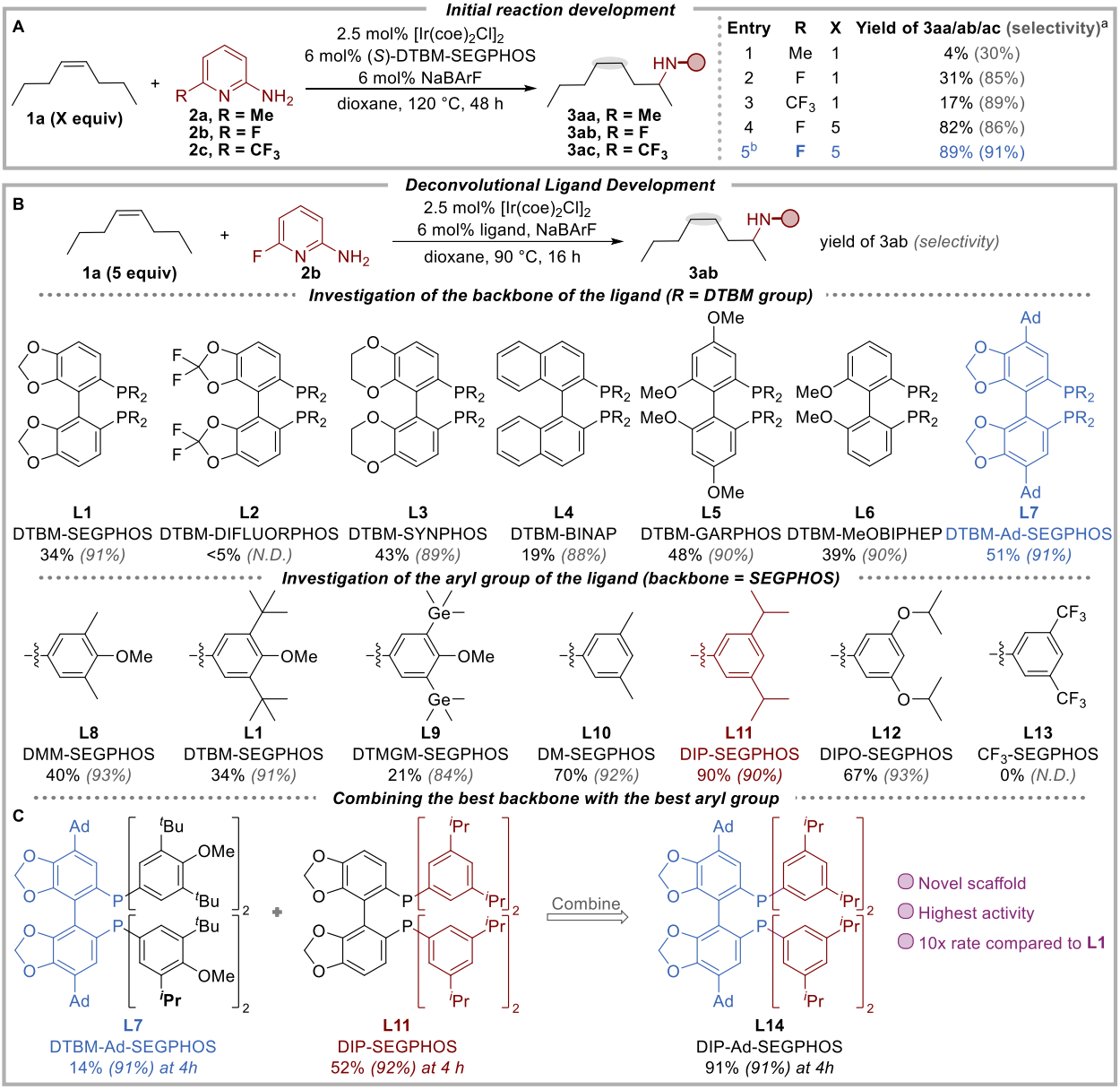


**Figure 4.1.** (A) Identification of suitable aminopyridine of the remote hydroamination of *cis*-4-octene. (B) Investigation effect of backbones and aryl fragments of the bisphosphine ligand on the remote hydroamination of *cis*-4-octene. (C) Identification of suitable ligand for the remote hydroamination of *cis*-4-octene. [a]Yield represents the yield of 2-amine with respect to 2-aminopyridine as the limiting reagent. selectivity = 2-amine/all amines. [b]The reaction was performed at 90 °C for 72 h.

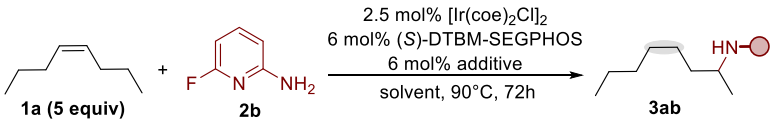


| Entry | solvent | Additive | Yield of 3ab (selectivity)[a] |
|---|---|---|---|
| 1 | dioxane | NaBArF | 89% (91%) |
| 2 | dioxane | $NaNTf_2$ | 7% (92%) |
| 3 | dioxane | NaOTf | 0% (N.D.) |
| 4 | PhF | NaBArF | 83% (88%) |
| 5 | PhCl | NaBArF | 82% (88%) |
| 6 | $PhCF_3$ | NaBArF | 83% (85%) |
| 7 | THF | NaBArF | 13% (89%) |
| 8 | 2-Me-THF | NaBArF | 14% (89%) |
| 9 | DME | NaBArF | 7% (85%) |
| 10 | CPME | NaBArF | 23% (89%) |

**Figure 4.2.** Investigation of the reaction conditions for the remote hydroamination of *cis*-4-octene. [a]Yield represents the yield of 2-amine with respect to 2-aminopyridine as the limiting reagent. selectivity = 2-amine/all amines.

### 4.4.7. Investigation for the Possibility of Reversible Hydroamination

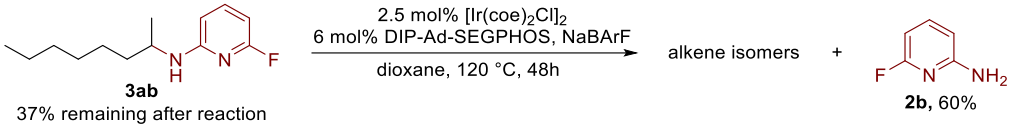


In a nitrogen-filled glovebox, a 1-dram vial was charged sequentially with $[Ir(coe)_2Cl]_2$ (2.3 mg, 2.5 µmol, 2.5 mol%), aminopyridine 6-fluoro-N-(octan-2-yl)pyridin-2-amine (**3ab**) (22 mg, 0.10 mmol, 1.0 equiv), DIP-Ad-SEGPHOS (7.3 mg, 6.0 µmol, 6.0 mol%), sodium tetrakis[3,5-bis(trifluoromethyl)phenyl]borate (5.4 mg, 6.0 µmol, 6.0 mol%), 1,3,5-trimethoxybenzene (5.6 mg, 0.033 mmol), dioxane (0.2 mL), and a magnetic stir bar. The vial was capped and removed from the glovebox. The reaction was heated at 120 °C in an aluminium heating block for 72 h. The reaction was cooled to room temperature, and a 5 µL aliquot was taken. The aliquot was analyzed by $^1$H NMR spectroscopy. Analysis by what type $^1$H NMR spectroscopy showed that **2b** was formed in 60% yield along with the formation of octene isomers. 37% of **3ab** was detected after the reaction.

### 4.4.8. Synthesis of Substrates and DIP-Ad-SEGPHOS

**Condition B:** An oven-dried flask was charged with dry DCM (15 mL), carboxylic acid (1.0 to 1.1 equiv), 4-dimethylamino pyridine (DMAP) (0.10 equiv), alcohol (1.0 to 1.1 equiv), *N*,*N*'-diisopropylcarbodiimide (DIC) (1.0 equiv), and a magnetic stir bar. The reaction mixture was allowed to stir at room temperature for 24 h, before filtering and concentrating under reduced pressure. The crude residue was directly purified by flash column chromatography to yield pure ester. **Notes:** No attempts were made to optimize for yield.

**Compound 1e**


An oven-dried flask was charged with dry THF (15 mL), $MePPh_3Br$ (2.6 g, 7.4 mmol), and a magnetic stir bar. At 0 °C, a dry THF solution (20 ml) of potassium *tert*-butoxide (830 mg, 7.4 mmol) was added dropwise. The mixture was warmed to room temperature and stirred for 1 h. At room temperature, A THF solution (20 ml) of 1-(3-(trifluoromethyl)phenyl)butan-1-one (1.3 g, 6.2 mmol) was added dropwise. The reaction mixture was allowed to stir at room temperature for 24 h, before concentrating under reduced pressure. The product was purified by flash column chromatography ($SiO_2$; Hexanes) to afford the corresponding alkene **1e** (944 mg, 72%) as a colorless oil. Note: Contains 15% of an inseparable trisubstituted isomer.

**$^1$H NMR** 1H NMR (600 MHz, $CDCl_3$) δ 7.65 (app-s, 1H), 7.58 (d, J = 7.9 Hz, 1H), 7.53 (d, J = 7.7 Hz, 1H), 7.42 (t, J = 7.7 Hz, 1H), 5.33 (d, J = 1.3 Hz, 1H), 5.15 (q, J = 1.3 Hz, 1H), 2.51 (td, J = 7.8, 1.2 Hz, 2H), 1.49 (h, J = 7.4 Hz, 2H), 0.94 (t, J = 7.4 Hz, 3H).

**$^{13}$C NMR** (151 MHz, $CDCl_3$) δ 147.51, 142.49, 132.07, 130.82 (q, J = 32.0 Hz) 128.83, 124.40 (q, J = 272.0 Hz), 124.07 (q, J = 3.7 Hz), 123.05 (q, J = 3.9 Hz), 113.88, 37.40, 21.34, 13.81.

**HRMS (*m/z*):** (EI) calc'd $[M]^+$: 214.0969, found: 214.0972.

**Compound 1j**

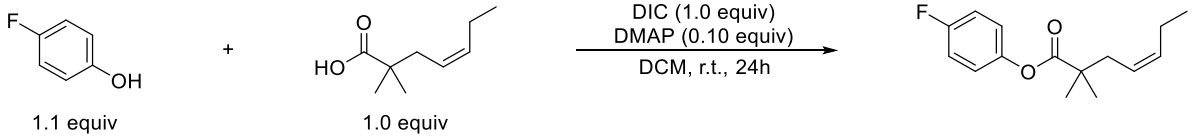


According to **Condition B**, (Z)-2,2-dimethylhept-4-enoic acid[60] (313 mg, 2.00 mmol) and 4-fluorophenol (247 mg, 2.20 mmol) were coupled, and the product was purified by flash column chromatography ($SiO_2$; 95:5 Hexanes:EA) to afford the corresponding ester **1j** (413 mg, 66%) as a colorless oil.

**$^1$H NMR** (500 MHz, $CDCl_3$) δ 7.09 – 6.95 (m, 4H), 5.59 – 5.50 (m, 1H), 5.42 – 5.35 (m, 1H), 2.43 (d, J = 7.5 Hz, 2H), 2.08 (p, J = 7.5 Hz, 2H), 1.33 (s, 6H), 0.97 (t, J = 7.5 Hz, 3H).

**$^{13}$C NMR** (126 MHz, $CDCl_3$) δ 176.32, 160.14 (d, J = 243.95 Hz) 146.89 (d, J = 3.0 Hz), 134.87, 123.64, 122.91 (d, J = 8.4 Hz), 115.97 (d, J = 23.4 Hz), 42.77, 37.69, 24.82, 20.68, 14.14.

**HRMS (*m/z*):** (EI) calc'd for $[M]^+$: 250.1369, found: 250.1371.

**Compound 1k**

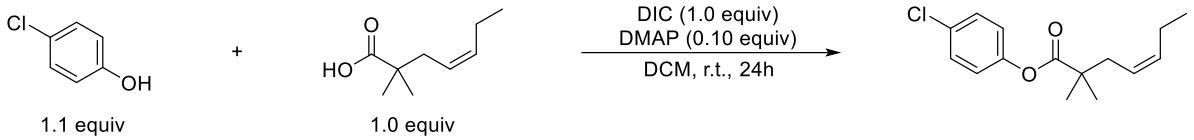


According to **Condition B**, (Z)-2,2-dimethylhept-4-enoic acid (391 mg, 2.50 mmol) and 4-chlorophenol (354 mg, 2.75 mmol) were coupled, and the product was purified by flash column chromatography ($SiO_2$; 95:5 Hexanes:EA) to afford the corresponding ester **1k** (320 mg, 48%) as a colorless oil.

**$^1$H NMR** (500 MHz, $CDCl_3$) δ 7.36 – 7.31 (m, 2H), 7.04 – 6.86 (m, 2H), 5.67 – 5.49 (m, 1H), 5.43 – 5.33 (m, 1H), 2.53 – 2.30 (d, J = 7.6 Hz, 2H), 2.08 (p, J = 7.5, 2H), 1.32 (s, 6H), 0.96 (t, J = 7.5 Hz, 3H).

**$^{13}$C NMR** (126 MHz, $CDCl_3$) δ 176.06, 149.56, 134.92, 130.96, 129.39, 123.58, 122.94, 42.83, 37.68, 24.80, 20.68, 14.14.

**HRMS (*m/z*):** (EI) calc'd for $[M]^+$: 266.1074, found: 266.1077.

**Compound 1l**

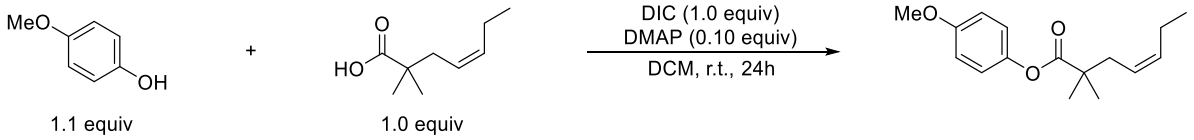


According to **Condition B**, (Z)-2,2-dimethylhept-4-enoic acid (391 mg, 2.50 mmol) and 4-methoxyphenol (341 mg, 2.75 mmol) were coupled, and the product was purified by flash column chromatography ($SiO_2$; 95:5 Hexanes:EA) to afford the corresponding ester **1l** (395 mg, 56%) as a colorless oil.

**$^1$H NMR** (500 MHz, $CDCl_3$) δ 7.01 – 6.91 (m, 2H), 6.91 – 6.76 (m, 2H), 5.61 – 5.47 (m, 1H), 5.45 – 5.34 (m, 1H), 3.79 (s, 3H), 2.43 (d, J = 7.6 Hz, 2H), 2.09 (p, J = 7.5 Hz, 2H), 1.32 (s, 6H), 0.97 (t, J = 7.5 Hz, 3H).

**$^{13}$C NMR** (126 MHz, $CDCl_3$) δ 176.63, 157.10, 144.58, 134.73, 123.83, 122.26, 114.39, 55.60, 42.71, 37.72, 24.86, 20.68, 14.16.

**HRMS (*m/z*):** (EI) calc'd $[M]^+$: 262.1569, found: 262.1572.

**Compound 1m**

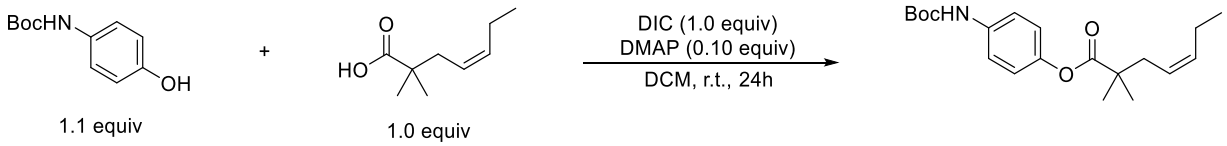


According to **Condition B**, (Z)-2,2-dimethylhept-4-enoic acid (391 mg, 2.50 mmol) and tert-butyl (4-hydroxyphenyl)carbamate (575 mg, 2.75 mmol) were coupled, and the product was purified by

flash column chromatography ($SiO_2$; 90:10 Hexanes:EA) to afford the corresponding ester **1m** (576 mg, 66%) as a colorless oil.

**$^1$H NMR** (500 MHz, $CDCl_3$) δ 7.34 (d, J = 8.4 Hz, 2H), 7.00 – 6.90 (m, 2H), 6.47 (s, 1H), 5.57 – 5.50 (m, 1H), 5.44 – 5.35 (m, 1H), 2.42 (d, J = 7.6 Hz, 2H), 2.08 (p, J = 7.5 Hz, 2H), 1.51 (s, 9H), 1.31 (s, 6H), 0.96 (t, J = 7.5 Hz, 3H).

**$^{13}$C NMR** (126 MHz, $CDCl_3$) δ 176.42, 152.72, 146.41, 135.82, 134.78, 123.76, 121.92, 119.31, 42.74, 37.70, 28.34, 24.83, 20.68, 14.15.

**HRMS (*m/z*):** (ESI) calc'd for $[2M+Na]^+$: 717.4086, found: 717.4088.

**Compound 1n**

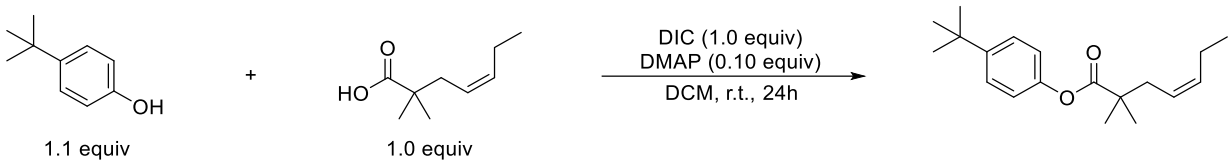


According to **Condition B**, (Z)-2,2-dimethylhept-4-enoic acid (391 mg, 2.50 mmol) and 4-(tert-butyl)phenol (413 mg, 2.75 mmol) were coupled, and the product was purified by flash column chromatography ($SiO_2$; 95:5 Hexanes:EA) to afford the corresponding ester **1n** (296 mg, 41%) as a colorless oil.

**$^1$H NMR** (500 MHz, $CDCl_3$) δ 7.39 – 7.35 (m, 2H), 7.01 – 6.94 (m, 2H), 5.64 – 5.48 (m, 1H), 5.44 – 5.37 (m, 1H), 2.43 (d, J = 7.6 Hz, 2H), 2.09 (p, J = 7.4 Hz, 2H), 1.33 (s, 6H), 1.31 (s, 9H), 0.97 (t, J = 7.5 Hz, 3H).

**$^{13}$C NMR** (126 MHz, $CDCl_3$) δ 176.42, 148.72, 148.38, 134.71, 126.22, 123.86, 120.81, 42.75, 37.71, 34.46, 31.43, 24.86, 20.69, 14.17.

**HRMS (*m/z*):** (EI) calc'd $[M]^+$: 288.2089, found: 288.2089.

**Compound 1o**

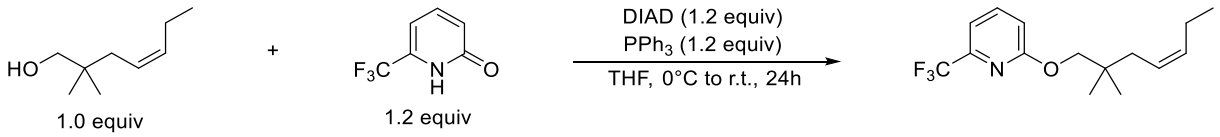


An oven-dried flask was charged with (Z)-2,2-dimethylhept-4-en-1-ol (370 mg, 2.62 mmol), triphenylphosphine (824 mg 3.16 mmol), 6-(trifluoromethyl)pyridin-2(1H)-one (512 mg, 3.16 mmol ), 15 mL of dry THF, and a magnetic stir bar. The solution was cooled to 0 °C, and diisopropyl azodicarboxylate (DIAD) (617 µL, 3.14 mmol) was added dropwise. The resulting mixture was slowly warmed to room temperature. After stirring for 24 h, the reaction was concentrated under reduced pressure. The crude material was purified by flash column chromatography ($SiO_2$; 97:3 Hexanes:EA) to afford the corresponding ether **1o** (540 mg, 72%) as a colorless oil.

**$^1$H NMR** (500 MHz, $CDCl_3$) δ 7.67 (t, J = 7.8 Hz, 1H), 7.22 (d, J = 7.2 Hz, 1H), 6.91 (d, J = 8.4 Hz, 1H), 5.51 – 5.44 (m, 1H), 5.43 – 5.36 (m, 1H), 4.04 (s, 2H), 2.13 (d, J = 7.7 Hz, 2H), 2.03 (p, J = 7.4, 2H), 1.01 (s, 6H), 0.91 (t, J = 7.5 Hz, 3H).

**$^{13}$C NMR** (151 MHz, $CDCl_3$) δ 164.32, 145.49 (q, J = 34.5 Hz), 139.08, 133.99, 124.53, 121.42 (q, J = 273.6 Hz), 114.58, 112.89 (q, J = 3.2 Hz), 74.14, 36.19, 34.78, 24.37, 20.51, 14.13.

**HRMS (*m/z*):** (ESI) calc'd for $[M+Na]^+$: 300.1389, found: 300.1399.

**Compound 1p**

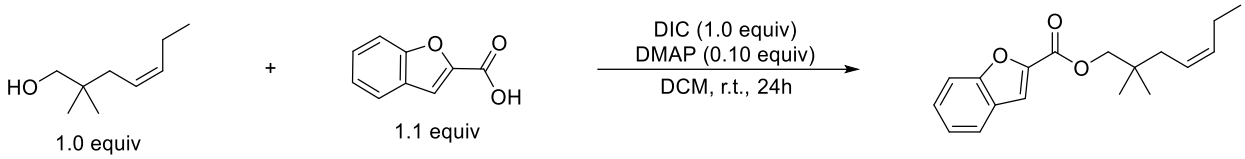


According to **Condition B**, benzofuran-2-carboxylic acid (446 mg, 2.75 mmol) and (Z)-2,2-dimethylhept-4-en-1-ol (356 mg, 2.50 mmol) were coupled, and the product was purified by flash column chromatography ($SiO_2$; 90:10 Hexanes:EA) to afford the corresponding ester **1p** (626 mg, 87%) as a colorless oil.

**$^1$H NMR** (500 MHz, $CDCl_3$) δ 7.69 (dt, J = 8.0, 1.0 Hz, 1H), 7.60 (dq, J = 8.4, 0.9 Hz, 1H), 7.51 (d, J = 1.0 Hz, 1H), 7.45 (ddd, J = 8.5, 7.2, 1.3 Hz, 1H), 7.31 (ddd, J = 8.0, 7.2, 0.9 Hz, 1H), 5.59 – 5.47 (m, 1H), 5.44 – 5.37 (m, 1H), 4.11 (s, 2H), 2.14 (d, J = 7.6 Hz, 2H), 2.07 (pd, J = 7.5, 1.6 Hz, 2H), 1.03 (s, 6H), 0.94 (t, J = 7.5 Hz, 3H).

**$^{13}$C NMR** (126 MHz, $CDCl_3$) δ 159.85, 155.94, 145.82, 134.57, 127.68, 127.13, 124.13, 123.91, 122.92, 113.65, 112.56, 72.96, 36.34, 34.99, 24.38, 20.70, 14.32.

**HRMS (*m/z*):** (EI) calc'd for $[M]^+$: 286.1569, found: 286.1566.

**Compound 1r**

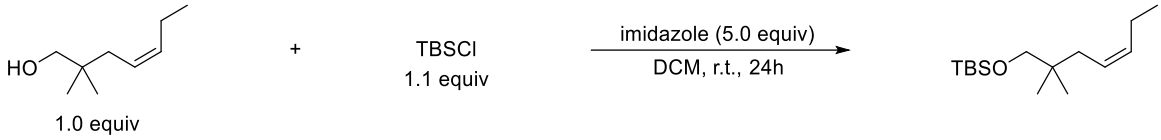


An oven-dried flask was charged with dry DCM (15 mL), TBSCl (332mg, 2.20 mmol), (Z)-2,2-dimethylhept-4-en-1-ol (284 mg, 2.00 mmol), imidazole (681 mg, 10.0 mmol) and a magnetic stir bar. The reaction mixture was allowed to stir at room temperature for 24 h, before concentrating under reduced pressure. The crude residue was directly purified by flash column chromatography ($SiO_2$; Hexanes) to afford the corresponding ether **1r** (415 mg, 81%) as a colorless oil. Note: Contains 7% of inseparable TBS siloxane.

**$^1$H NMR** (500 MHz, $CDCl_3$) δ 5.47 – 5.38 (m, 1H), 5.37 – 5.30 (m, 1H), 3.21 (s, 2H), 2.02 (p, J = 7.5 Hz, 2H), 1.95 (d, J = 7.8 Hz, 2H), 0.92 (t, J = 7.5 Hz, 3H), 0.87 (s, 9H), 0.80 (s, 6H), 0.00 (s, 6H).

**$^{13}$C NMR** (126 MHz, $CDCl_3$) δ 133.44, 125.61, 71.49, 36.19, 35.87, 26.07, 24.06 (two carbons), 20.67, 14.43, -5.34.

**HRMS (*m/z*):** (EI) calc'd $[M-CH_3]^+$: 241.1988, found: 241.1988.

**Compound 1t**

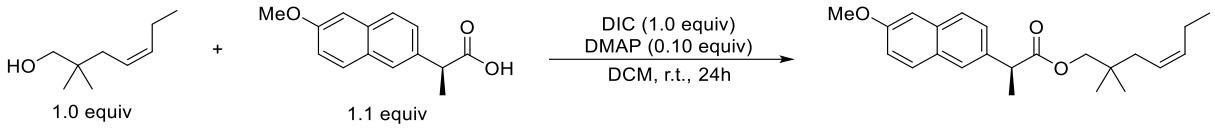


According to **Condition B**, naproxen (507 mg, 2.20 mmol) and (Z)-2,2-dimethylhept-4-en-1-ol (284 mg, 2.00 mmol) were coupled, and the product was purified by flash column chromatography ($SiO_2$; 85:15 Hexanes:EA) to afford the corresponding ester **1t** (547 mg, 77%) as a colorless oil.

**$^1$H NMR** (500 MHz, $CDCl_3$) δ 7.69 (d, J = 8.6 Hz, 2H), 7.68 – 7.66 (m, 1H), 7.42 (dd, J = 8.4, 1.9 Hz, 1H), 7.17 – 7.08 (m, 2H), 5.44 – 5.36 (m, 1H), 5.29 – 5.20 (m, 1H), 3.91 (s, 3H), 3.88 (q, J = 7.2 Hz, 1H), 3.84 – 3.73 (m, 2H), 1.94 – 1.80 (m, 4H), 1.60 (d, J = 7.1 Hz, 3H), 0.85 (t, J = 7.5 Hz, 3H), 0.81 (d, J = 6.2 Hz, 6H).

**$^{13}$C NMR** (126 MHz, $CDCl_3$) δ 174.61, 157.60, 135.75, 134.12, 133.68, 129.27, 128.94, 127.03, 126.41, 126.00, 124.13, 118.92, 105.59, 72.28, 55.30, 45.68, 36.02, 34.65, 24.07, 24.02, 20.41, 18.29, 14.13.

HRMS (*m/z*): (EI) calc'd for $[M]^+$: 354.2195, found: 354.2189.

**Compound 1u**

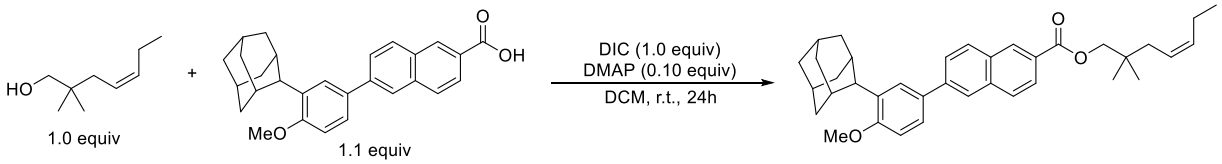


According to **Condition B**, adapalene (991 mg, 2.40 mmol) and (Z)-2,2-dimethylhept-4-en-1-ol (311 mg, 2.18 mmol) were coupled, and the product was purified by flash column chromatography ($SiO_2$; 90:10 Hexanes:EA) to afford the corresponding ester **1u** (871 mg, 74%) as a white solid.

**$^1$H NMR** (500 MHz, $CDCl_3$) δ 8.62 (s, 1H), 8.09 (dd, J = 8.5, 1.7 Hz, 1H), 8.03 – 8.01 (m, 1H), 8.00 (d, J = 8.6 Hz, 1H), 7.93 (d, J = 8.6 Hz, 1H), 7.81 (dd, J = 8.5, 1.8 Hz, 1H), 7.62 (d, J = 2.4 Hz, 1H), 7.55 (dd, J = 8.4, 2.4 Hz, 1H), 7.00 (d, J = 8.4 Hz, 1H), 5.57 – 5.50 (m, 1H), 5.49 – 5.41 (m, 1H), 4.13 (s, 2H), 3.91 (s, 3H), 2.22 – 2.18 (m, 8H), 2.14 – 2.05 (m, 5H), 1.81 (app-s, 6H), 1.08 (s, 6H), 0.95 (t, J = 7.5 Hz, 3H).

**$^{13}$C NMR** (126 MHz, $CDCl_3$) δ 166.83, 158.94, 141.37, 139.03, 135.96, 134.31, 132.59, 131.29, 130.72, 129.72, 128.24, 127.31, 126.48, 126.00, 125.75, 125.57, 124.76, 124.24, 112.13, 72.64, 55.18, 40.63 (two carbons), 37.24, 37.15 (two carbons), 36.40, 34.91, 29.14 (two carbons), 24.45, 20.61, 14.21.

**HRMS (*m/z*):** (EI) calc'd for $[M]^+$: 536.3290, found: 536.3290.

**Compound 1v**

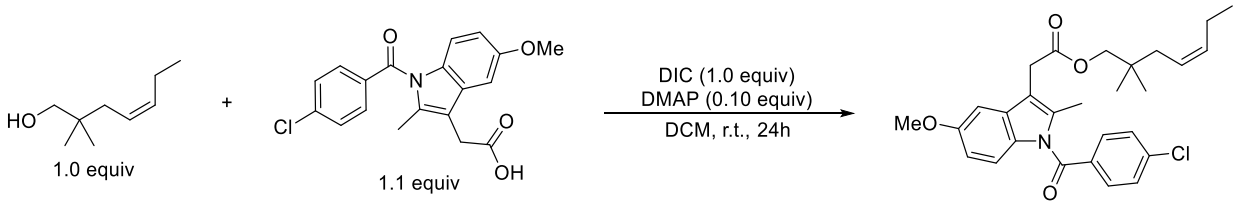


According to **Condition B**, indomethacin (787 mg, 2.20 mmol) and (Z)-2,2-dimethylhept-4-en-1-ol (284 mg, 2.00 mmol) were coupled, and the product was purified by flash column chromatography ($SiO_2$; 85:15 Hexanes:EA) to afford the corresponding ester **1v** (317 mg, 33%) as a yellow oil.

**$^1$H NMR** (500 MHz, $CDCl_3$) δ 7.67 – 7.59 (m, 2H), 7.49 – 7.43 (m, 2H), 6.97 (d, J = 2.6 Hz, 1H), 6.87 (d, J = 9.0 Hz, 1H), 6.67 (dd, J = 9.0, 2.6 Hz, 1H), 5.48 – 5.39 (m, 1H), 5.32 – 5.23 (m, 1H), 3.83 (s, 3H), 3.82 (s, 2H), 3.68 (s, 2H), 2.40 (s, 3H), 1.97 – 1.88 (m, 4H), 0.89 (t, J = 7.6 Hz, 3H), 0.85 (s, 6H).

**$^{13}$C NMR** (126 MHz, $CDCl_3$) δ 170.87, 168.28, 156.09, 139.26, 135.74, 134.26, 133.95, 131.17, 130.80, 130.64, 129.12, 123.98, 114.97, 112.78, 111.85, 101.19, 72.63, 55.69, 36.06, 34.52, 30.47, 24.09, 20.45, 14.17, 13.34.

**HRMS (*m/z*):** (EI) calc'd for $[2M+Na]^+$: 985.3932, found: 985.3941.

**Compound 1w**

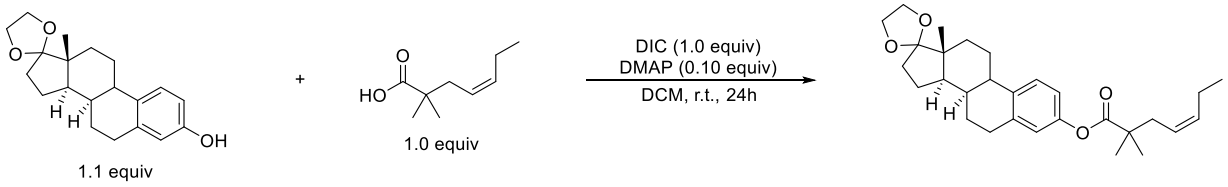


According to **Condition B**, (Z)-2,2-dimethylhept-4-enoic acid (391 mg, 2.50 mmol) and (8R,13R,14R)-13-methyl-6,7,8,9,11,12,13,14,15,16-decahydrospiro[cyclopenta[a]phenanthrene-17, 2' [1,3]dioxolan]-3-ol (847 mg, 2.75 mmol) were coupled, and the product was purified by flash column chromatography ($SiO_2$; 95:5 Hexanes:EA) to afford the corresponding ester **1w** (552 mg, 49%) as a colorless oil.

**$^1$H NMR** (500 MHz, $CDCl_3$) δ 7.27 (d, J = 8.4 Hz, 1H), 6.80 (d, J = 8.5 Hz, 1H), 6.75 (s, 1H), 5.61 – 5.51 (m, 1H), 5.45 – 5.36 (m, 1H), 4.01 – 3.85 (m, 4H), 2.91 – 2.79 (m, 2H), 2.42 (d, J = 7.6 Hz,

2H), 2.37 – 2.22 (m, 2H), 2.14 – 2.07 (m, 2H), 2.07 – 1.99 (m, 1H), 1.86 – 1.80 (m, 4H), 1.70 – 1.33 (m, 6H), 1.32 (s, 6H), 0.97 (t, J = 7.5 Hz, 3H), 0.88 (s, 3H).

**$^{13}$C NMR** (126 MHz, $CDCl_3$) δ 176.50, 148.77, 138.18, 137.79, 134.69, 126.29, 123.89, 121.41, 119.41, 118.49, 65.28, 64.60, 49.41, 46.12, 43.83, 42.72, 38.73, 37.70, 34.24, 30.70, 29.54, 26.82, 26.01, 24.86 (two carbons), 22.38, 20.68, 14.33, 14.17.

**HRMS (*m/z*):** (ESI) calc'd for $[2M+Na]^+$: 927.5746, found: 927.5724.

**Aminopyridine Substrates**

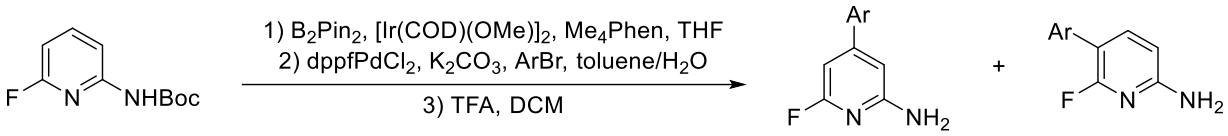


**Condition C**[61]: In a nitrogen-filled glovebox, a 20mL vial was charged sequentially with $[Ir(COD)(OMe)]_2$ (6.6 mg, 0.010 mmol, 1.0 mol%), tetramethylphenanthroline (5.2 mg, 0.022 mmol, 2.2 mol%), $B_2pin_2$ (380 mg, 1.5 mmol, 1.5 equiv), HBpin (20 µL), dried THF (2.0 mL), and a magnetic stir bar. The vial was capped and removed from the glovebox. The reaction was heated at 80 °C for 0.5 h and brought back into the glovebox. Tert-butyl (6-fluoropyridin-2-yl)carbamate (210 mg, 1.0 mmol, 1.0 equiv) was added and the vial was capped and removed from the glovebox. The reaction was heated at 50 °C for 0.75 h, brought back into the glovebox, filtered, and concentrated in vacuo. Aryl bromide (1.2 mmol, 1.2 equiv), $dppfPdCl_2$ (37 mg, 0.050 mmol, 5 mol%), $K_2CO_3$ (350 mg, 2.5 mmol, 2.5 equiv), toluene (2.0 mL), and water (0.2 mL) were then added. The vial was capped and removed from the glovebox. The reaction was heated at 100 °C for 24 h, filtered, concentrated under reduced pressure, and redissolved in DCM (2.0 mL). At room temperature, TFA (766 µL, 10.0 mmol, 10.0 equiv) was added dropwise. The reaction mixture was allowed to stir overnight before quenched with $NaHCO_3$ and extracted with DCM. The reaction mixture was concentrated under reduced pressure and purified by flash column chromatography ($SiO_2$) to afford correspond arylated aminopyridines as yellow solids.

**Compound 2g-NHBoc**

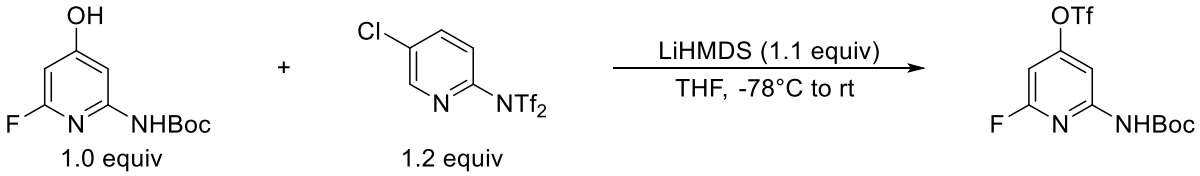


An oven-dried flask was charged with dry THF (15 mL), tert-butyl (6-fluoro-4-hydroxypyridin-2-yl)carbamate (84 mg, 0.37 mmol) and a magnetic stir bar. At -78 °C, LiHMDS (1M solution, 410 µL, 0.41 mmol) was added dropwise. The reaction mixture was allowed to stir -78 °C for 0.5 h and a THF solution of Comin's reagent (170 mg, 0.44 mmol) was added dropwise -78 °C. The reaction mixture was allowed to slowly warm to room temperature and stirred overnight. The reaction mixture was concentrated under reduced pressure and the crude residue was directly

purified by flash column chromatography ($SiO_2$; 95:5 Hexanes:EA) to afford compound **2g-NHBoc** (120 mg, 93%) as a white solid.

**$^1$H NMR** (600 MHz, $CDCl_3$) δ 7.84 (s, 1H), 7.31 (s, 1H), 6.53 (s, 1H), 1.53 (s, 9H).

**$^{13}$C NMR** (151 MHz, $CDCl_3$) δ 162.56 (d, J = 241.5 Hz), 159.85 (d, J = 11.6 Hz), 152.10 (d, J = 18.3 Hz), 151.33, 118.56 (q, J = 321.0 Hz), 101.70 (d, J = 5.4 Hz), 96.37 (d, J = 40.9 Hz), 82.62, 28.11.

**HRMS (*m/z*):** (ESI) calc'd for $[M+Na]^+$: 383.0295, found: 383.0292.

**Compound 2g**

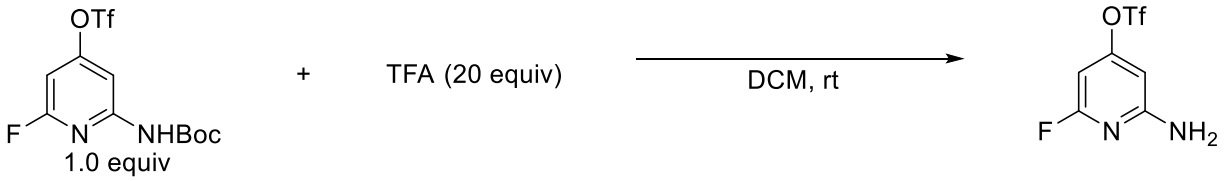


A 20mL vial was charged with DCM (0.5 mL), compound **2g-NHBoc** (90 mg, 0.25 mmol) and a magnetic stir bar. At room temperature, TFA (380 μL, 5.0 mmol, 20 equiv) was added dropwise. The reaction mixture was allowed to stir overnight before quenched with $NaHCO_3$ and extracted with DCM. The reaction mixture was concentrated under reduced pressure and purified by flash column chromatography ($SiO_2$; 75:25 Hexanes:EA) to afford compound **2g** (59 mg, 90%) as a white solid.

**$^1$H NMR** (600 MHz, $CDCl_3$) δ 6.24 (s, 1H), 6.17 (s, 1H), 4.89 (s, 2H).

**$^{13}$C NMR** (151 MHz, $CDCl_3$) δ 163.98 (d, J = 239.1 Hz), 159.80 (d, J = 12.9 Hz), 158.67 (d, J = 20.2 Hz), 118.70 (q, J = 320.9 Hz), 96.74 (d, J = 5.5 Hz), 91.01 (d, J = 42.0 Hz).

**HRMS (*m/z*):** (ESI) calc'd for $[2M+K]^+$: 558.9390, found: 558.9377.

**Compound 2i**

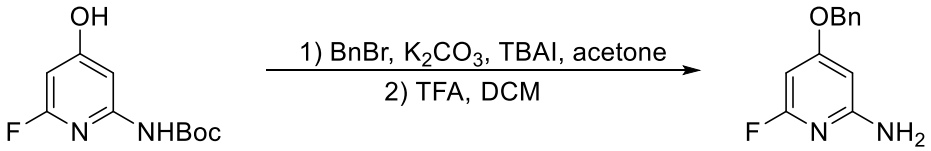


A 20mL vial was charged with dry acetone (2.0 mL), compound **2g-NHBoc** (69 mg, 0.30 mmol), TBAI (5.5 mg, 0.015 mmol, 5 mol%), BnBr (38 μL, 0.32 mmol, 1.1 equiv), $K_2CO_3$ (62 mg, 0.45 mmol, 3.0 equiv) and a magnetic stir bar. The reaction mixture was allowed to stir overnight and extracted with EA. The reaction mixture was filtered, concentrated under reduced pressure, and redissolved in DCM (0.5 mL). At room temperature, TFA (460 μL, 6.0 mmol, 20 equiv) was added dropwise. The reaction mixture was allowed to stir overnight before quenched with $NaHCO_3$ and extracted with DCM. The reaction mixture was concentrated under reduced pressure and purified

by flash column chromatography ($SiO_2$; 75:25 Hexanes:EA) to afford compound **2i** (56 mg, 85%) as a white solid.

**$^1$H NMR** (600 MHz, $CDCl_3$) δ 7.43 – 7.32 (m, 5H), 5.88 (app-s, 2H), 5.04 (app-s, 2H), 4.51 (s, 2H).

**$^{13}$C NMR** (151 MHz, $CDCl_3$) δ 169.97 (d, J = 12.7 Hz), 164.68 (d, J = 233.0 Hz), 158.37 (d, J = 21.0 Hz), 135.73, 128.86, 128.52, 127.57, 90.36 (d, J = 4.2 Hz), 85.66 (d, J = 40.9 Hz), 70.38.

**HRMS (*m/z*):** (ESI) calc'd for $[M+Na]^+$: 241.0747, found: 241.0736.

**Compound 2j**

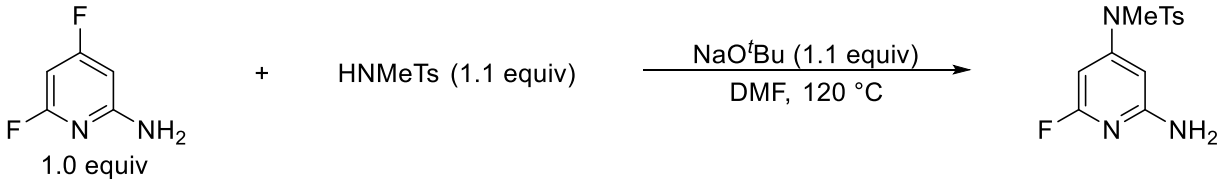


In a nitrogen-filled glovebox, a 1-dram vial was charged sequentially with 4,6-difluoropyridin-2-amine (33 mg, 0.25 mmol, 1.0 equiv), N,4-dimethylbenzenesulfonamide (55 mg, 0.27 mmol, 1.1 equiv), (NaO$^t$Bu) (24 mg, 0.27 mmol, 1.1 equiv), DMF (2.5 mL), and a magnetic stir bar. The vial was capped and removed from the glovebox. The reaction was heated at 120 °C for 24 h. The crude material was extracted with EA/$H_2O$ 5 times to remove residual DMF, concentrated in vacuo, and purified by flash column chromatography ($SiO_2$; 95:5 DCM:EA) to afford compound **2j** (58 mg, 78%) as a white solid.

**$^1$H NMR** (600 MHz, $CDCl_3$) δ 7.55 (d, J = 7.9 Hz, 2H), 7.29 (d, J = 7.8 Hz, 2H), 6.35 (s, 1H), 6.04 (s, 1H), 4.59 (s, 2H), 3.20 (s, 3H), 2.43 (s, 3H).

**$^{13}$C NMR** (151 MHz, $CDCl_3$) δ 163.70 (d, J = 234.8 Hz), 157.66 (d, J = 19.6 Hz), 154.08 (d, J = 11.4 Hz), 144.42, 133.73, 129.76, 127.39, 98.75 (d, J = 4.4 Hz), 91.48 (d, J = 40.5 Hz), 36.61, 21.58.

**HRMS (*m/z*):** (ESI) calc'd for $[M+ACN+H]^+$: 337.1129, found: 337.1120.

**Compound 2o and 2r**

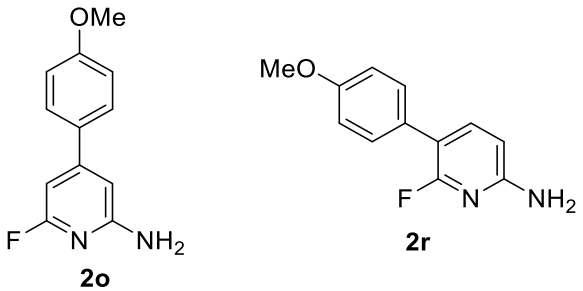

According to **Condition C**, 1-bromo-4-methoxybenzene (220 mg, 1.2 mmol) was used as the aryl bromide coupling partner, and the product was purified by flash column chromatography ($SiO_2$; 50:50 Hexanes:ether) to afford compound **2o** (57 mg, 26%) as a yellow solid and **2r** (90 mg, 41%) as a yellow solid.

**Compound 2o**

**$^1$H NMR** (600 MHz, $CDCl_3$) δ 7.55 – 7.50 (m, 2H), 7.00 – 6.96 (m, 2H), 6.49 (s, 1H), 6.42 (s, 1H), 4.54 (s, 2H), 3.86 (s, 3H).

**$^{13}$C NMR** (151 MHz, $CDCl_3$) δ 164.14 (d, J = 235.9 Hz), 160.80, 157.86 (d, J = 18.1 Hz), 154.92 (d, J = 9.1 Hz), 130.40 (d, J = 3.6 Hz), 128.24, 114.52, 102.01 (d, J = 3.9 Hz), 95.29 (d, J = 37.2 Hz), 55.55.

**HRMS (*m/z*):** (ESI) calc'd $[M+ACN+H]^+$: 260.1193, found: 260.1187.

**Compound 2r**

**$^1$H NMR** (600 MHz, $CDCl_3$) δ 7.62 (t, J = 10.1 Hz, 1H), 7.45 (d, J = 8.2 Hz, 2H), 6.98 (d, J = 8.3 Hz, 2H), 6.43 (d, J = 8.0 Hz, 1H), 4.61 (s, 2H), 3.86 (s, 3H).

**$^{13}$C NMR** (151 MHz, $CDCl_3$) δ 159.38 (d, J = 238.8 Hz), 158.84, 156.10 (d, J = 16.5 Hz), 142.03 (d, J = 5.2 Hz), 129.42 (d, J = 3.2 Hz), 127.07 (d, J = 5.0 Hz), 114.03, 111.34 (d, J = 27.1 Hz), 105.34 (d, J = 4.4 Hz), 55.33.

**HRMS (*m/z*):** (ESI) calc'd $[M+Na]^+$: 241.0747, found: 241.0746.

**Compound 2p and 2s**

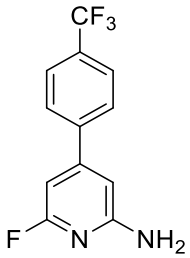


**2p**

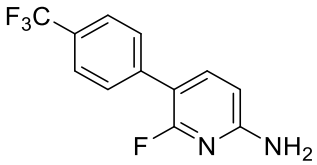


**2s**

According to **Condition C**, 1-bromo-4-trifluoromethylbenzene (270 mg, 1.2 mmol) was used as the aryl bromide coupling partner,, and the product was purified by flash column chromatography ($SiO_2$; 80:20 Hexanes:EA) to afford compound **2p** (87 mg, 34%) as a yellow solid and **2s** (77 mg, 30%) as a yellow solid.

**Compound 2p**

**$^1$H NMR** (600 MHz, $CDCl_3$) δ 7.74 (d, J = 8.1 Hz, 2H), 7.68 (d, J = 8.1 Hz, 2H), 6.54 (s, 1H), 6.46 (s, 1H), 4.72 (s, 2H).

**$^{13}$C NMR** (151 MHz, $CDCl_3$) δ 163.94 (d, J = 237.1 Hz), 157.98 (d, J = 17.8 Hz), 153.76 (d, J = 8.8 Hz), 141.59, 131.23 (q, J = 32.7 Hz), 127.34, 125.96 (q, J = 3.7 Hz), 123.94 (q, J = 272.4 Hz), 102.73 (d, J = 4.3 Hz), 95.74 (d, J = 37.6 Hz).

**HRMS (*m/z*):** (ESI) calc'd $[2M+ACN+Na]^+$: 576.1406, found: 576.1433.

**Compound 2s**

**$^1$H NMR** (600 MHz, $CDCl_3$) δ 7.70 – 7.65 (m, 3H), 7.63 (t, J = 8.1 Hz, 2H), 6.47 (dd, J = 8.2, 1.6 Hz, 1H), 4.83 (s, 2H).

**$^{13}$C NMR** (151 MHz, $CDCl_3$) δ 159.70 (d, J = 239.8 Hz), 157.42 (d, J = 17.3 Hz), 142.22 (d, J = 4.6 Hz), 138.48 (d, J = 5.3 Hz), 129.19 (q, J = 32.6 Hz), 128.57 (d, J = 3.6 Hz), 125.59 (q, J = 3.7 Hz), 124.33 (q, J = 272.0 Hz), 110.00 (d, J = 26.9 Hz), 105.67 (d, J = 4.3 Hz).

**HRMS (*m/z*):** (ESI) calc'd $[M+ACN+Na]^+$: 320.0782, found: 320.0772.

**Compound 2q**

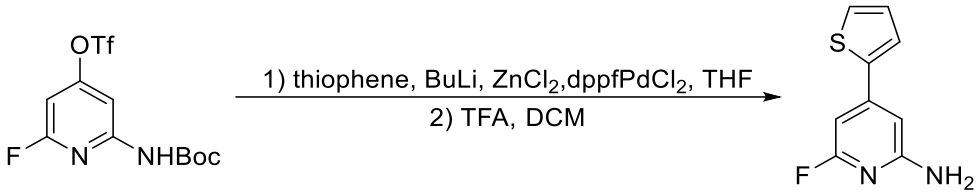


An oven-dried flask was charged with dry THF (3.0 mL), thiophene (76 mg, 0.90 mmol) and a magnetic stir bar. At -78 °C, BuLi (2.5M solution, 400 μL, 1.0 mmol, 1.1 equiv) was added dropwise. The reaction mixture was allowed to stir -78 °C for 0.5 h, and a THF suspension of $ZnCl_2$ (240 mg, 1.8 mmol, 2.0 equiv) was added dropwise -78 °C. The reaction mixture was allowed to slowly warm to 0 °C, stirred for 0.5 h, and brought into the glovebox. In a nitrogen-filled glovebox, a 20mL vial was charged sequentially $dppfPdCl_2$ (11 mg, 0.015 mmol, 5.0 mol%), compound **2g-NHBoc** (110 mg, 0.3 mmol), and the arylzinc solution. The vial was capped and removed from the glovebox. The reaction was heated at 65 °C for 24 h, filtered, concentrated under reduced pressure, and redissolved in DCM (2.0 mL). At room temperature, TFA (766 μL, 10.0 mmol, 10.0 equiv) was added dropwise. The reaction mixture was allowed to stir overnight before quenched with $NaHCO_3$ and extracted with DCM. The reaction mixture was concentrated under reduced pressure and purified by flash column chromatography ($SiO_2$; 75:25 Hexanes:EA) to afford compound **2q** (36 mg, 62%) as a yellow solid.

**$^1$H NMR** (600 MHz, $CDCl_3$) δ 7.50 – 7.37 (m, 2H), 7.13 (app-s, 1H), 6.56 (s, 1H), 6.49 (s, 1H), 4.34 (s, 2H).

**$^{13}$C NMR** (151 MHz, $CDCl_3$) δ 164.10 (d, J = 236.3 Hz), 157.98 (d, J = 17.9 Hz), 147.86 (d, J = 9.5 Hz), 140.96 (d, J = 4.0 Hz), 128.36, 127.24, 125.70, 100.98 (d, J = 3.9 Hz), 94.31 (d, J = 38.5 Hz).

**HRMS (*m/z*):** (ESI) calc'd $[M+K]^+$: 232.9946, found: 232.9952.

**diethyl (7-((3r,5r,7r)-adamantan-1-yl)benzo[d][1,3]dioxol-5-yl)phosphonate**

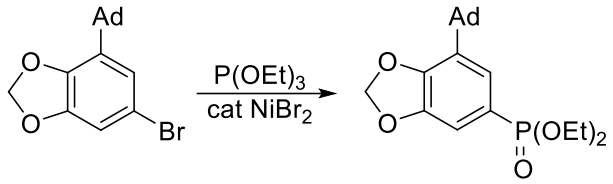


**Adapted from a reported procedure[62]:** 4-((3r,5r,7r)-adamantan-1-yl)-6-bromobenzo [d][1,3]dioxole[63] (4.7 g, 14 mmol) and nickel dibromide (180 mg, 1.4 mmol, 10 mol%) were placed in a two-necked flask provided with a distillation apparatus and a dropping funnel. The suspension was heated at 160 °C, after what triethylphosphite (2.9 mL, 17 mmol, 1.2 equiv) was added dropwise over 1 h. The reaction mixture was stirred at 160 °C for 1 h. The ethyl bromide formed was continuously distilled all along the reaction. After cooling down the mixture, 50 mL of diethyl ether and 50 mL of ethyl acetate were added and the precipitate was filtered off. The filtrate was concentrated under reduced pressure and the crude oil was purified by flash column chromatography ($SiO_2$; 50:50 hexanes:EA) to afford the target compound (4.2 g, 76%) as a yellow oil. The NMR spectra of the target compound matched those reported in the literature.[64]

**Ad-SEGPHOS-POEt$_2$**

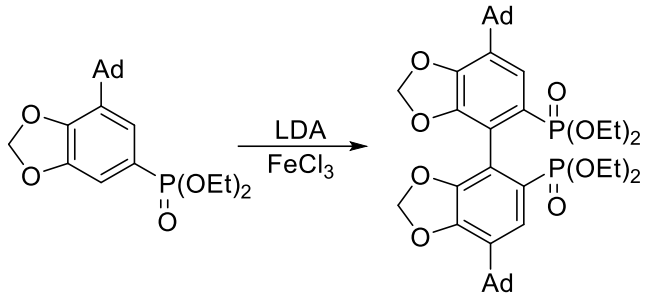


**Adapted from a reported procedure[62]:** To a solution of diethyl (7-((3r,5r,7r)-adamantan-1-yl)benzo[d][1,3]dioxol-5-yl)phosphonate (4.8 g, 12 mmol) in dry THF (15 mL) was added dropwise a solution of freshly prepared LDA (13 mmol, 1.1 equiv) at -78 °C. The reaction mixture was stirred at -78 °C for 15 minutes and at -15°C for 15 minutes. The mixture was cooled to -78 °C and a THF solution of anhydrous $FeCl_3$ (2.7 g, 16 mmol, 1.3 equiv) was added dropwise. The reaction temperature was allowed to rise to r.t and the mixture was stirred overnight. The solution was concentrated in vacuum, and the brown residue was diluted with $CH_2Cl_2$ (50 mL) and treated with 50 mL of 2 M aqueous NaOH. After stirring for 1 h, the resulting suspension was filtered on celite. The organic layer was washed with water and brine, dried over MgSO4, filtered, and concentrated under reduced pressure. The obtained brown solid was purified by flash column chromatography ($SiO_2$; 90:10 DCM:MeOH) to afford the target compound (4.1 g, 87%) as white solid. The NMR spectra of the target compound matched those reported in the literature.[64]

**Ad-SEGPHOS-POCl$_2$**

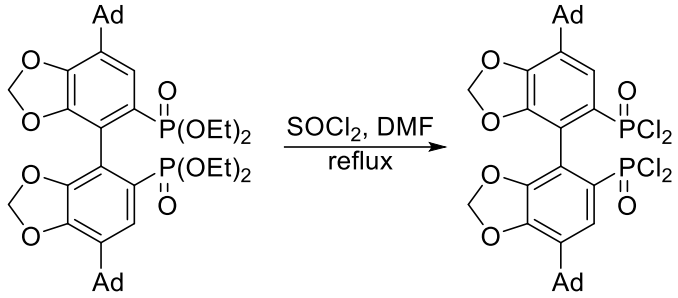


**Adapted from a reported procedure**[65]**:** In a nitrogen-filled glovebox, an oven dried round-bottom flask (50 ml) was charged **Ad-SEGPHOS-POEt2** (2.0 g, 2.5 mmol) and a magnetic stir bar. A reflux condenser was attached to the flask. Thionyl chloride was added to the flask via syringe (18 mL, 250 mmol), followed by dropwise addition of DMF (1.9 ml, 25 mmol). The solution was allowed to reflux (96 °C) for 17 h. Upon completion, the flask was allowed to cool to room temperature, and the solvents were distilled away under high vacuum to yield a brown solid. The flask was taken into the glovebox, and the solid was redissolved in DCM and dried under high vacuum for 48 h to yield the title compound as a pale solid (1.8 g, 98% yield). Note: The crude solid was used directly for the next step without further purification.

**$^{1}$H NMR** (600 MHz, $CDCl_3$) δ 7.58 (d, J = 22.6 Hz, 2H), 6.09 (d, J = 1.5 Hz, 2H), 6.03 (d, J = 1.4 Hz, 2H), 2.13 – 2.08 (m, 6H), 2.08 – 2.04 (m, 12H), 1.82 – 1.75 (m, 12H).

**$^{31}$P NMR** (243 MHz, $CDCl_3$) δ 33.68.

**HRMS (*m/z*):** (ESI) calc'd $[M+Na]^+$: 765.0633, found: 765.0633.

**Ad-SEGPHOS-POAr2**

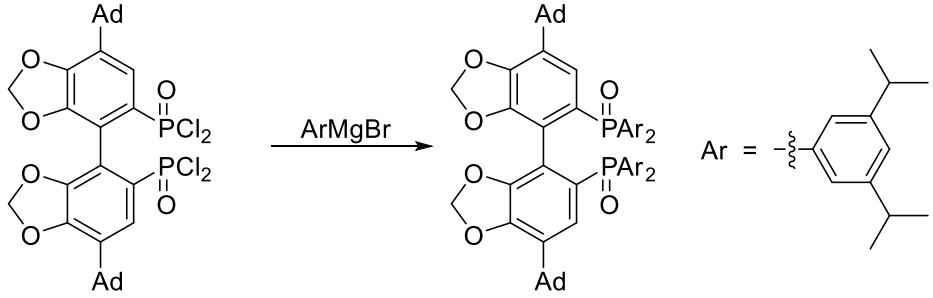


**Adapted from a reported procedure**[65]**:** In a nitrogen-filled glovebox, a 20 ml vial was charged with Mg turnings (350 mg, 14 mmol), 1-bromo-3,5-diisopropylbenzene (2.9 g, 12 mmol), a crystal of iodine, THF (5.0 mL) and a magnetic stir bar. The vial was capped and stirred at 65 °C for 3 h. The Grignard was then brought back into the back and was added dropwise to a 20 ml vial containing a THF solution (5 mL) of **Ad-SEGPHOS-POCl2** (890 mg, 1.2 mmol) at -35 °C. The reaction was heated at 65 °C for 24 h. Upon completion, the reaction was allowed to cool to room temperature, quenched with $NH_4Cl$ (aq), extracted with EA and concentrated under high vacuum. The obtained crude solid was purified by flash column chromatography ($SiO_2$; 70:30 Hexanes:EA) to afford the target compound (1.1 g, 70%) as white solid.

**$^{1}$H NMR** (600 MHz, $CDCl_3$) δ 7.37 (dd, J = 11.9, 1.7 Hz, 4H), 7.26 (dd, J = 12.3, 1.7 Hz, 4H), 7.13 (s, 2H), 7.03 (s, 2H), 6.78 (d, J = 15.2 Hz, 2H), 5.82 (d, J = 1.8 Hz, 2H), 5.61 (d, J = 1.8 Hz, 2H), 2.87 (hept, J = 6.9 Hz, 4H), 2.69 (hept, J = 6.9 Hz, 4H), 1.95 (app-s, 6H), 1.87 – 1.79 (m, 12H), 1.71 – 1.62 (m, 12H), 1.20 (dd, J = 6.9, 4.8 Hz, 24H), 1.05 (dd, J = 8.5, 6.9 Hz, 24H).

**$^{31}$P NMR** (243 MHz, $CDCl_3$) δ 30.50.

**HRMS (*m/z*):** (ESI) calc'd $[M+H]^+$: 1247.7381, found: 1247.7404.

**DIP-Ad-SEGPHOS (Ad-SEGPHOS-PAr$_2$)**

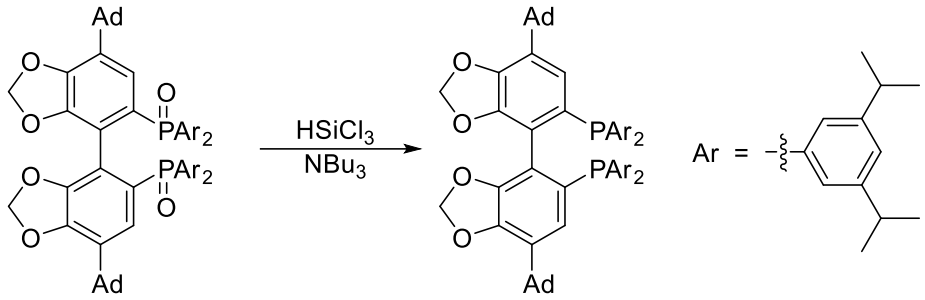


**Adapted from a reported procedure[6]:** In a nitrogen-filled glovebox, a 40 ml vial was charged with **Ad-SEGPHOS-POAr$_2$** (2.0 g, 1.6 mmol) and a magnetic stir bar. Dry mesitylene (5.0 ml) and dry $Bu_3N$ (4.6 mL, 19 mmol) were added to the vial. Trichlorosilane (1.9 mL, 19 mmol) was added dropwise to the solution. Once the evolution of gas ceased, the vial was sealed with a Teflon-lined cap and placed in a 120 °C heating block. After 24 h, the vial was removed from the heating block and the reaction mixture was transferred into a 250 mL round-bottom flask placed in an ice bath. Under a stream of nitrogen and vigorous stirring, an aqueous solution of NaOH (25%, 10 ml) was added to the flask dropwise. The reaction was stirred at room temperature for 1 h, quenched with HCl (aq), extracted with EA and concentrated under high vacuum. The obtained crude solid was purified by flash column chromatography ($SiO_2$; 97:3 Hexanes:EA) to afford the target compound (1.5 g, 83%) as white solid.

**$^{1}$H NMR** (600 MHz, $CDCl_3$) δ 7.26 (s, 1H), 7.00 – 6.96 (m, 7H), 6.95 – 6.93 (m, 2H), 6.91 – 6.89 (m, 2H), 6.63 – 6.58 (m, 2H), 5.74 (d, J = 1.7 Hz, 2H), 5.14 (d, J = 1.7 Hz, 2H), 2.80 (hept, J = 6.9 Hz, 4H), 2.72 (hept, J = 6.9 Hz, 4H), 1.95 – 1.91 (m, 6H), 1.87 – 1.78 (m, 12H), 1.72 – 1.61 (m, 12H), 1.17 (dd, J = 6.9, 3.7 Hz, 24H), 1.12 (dd, J = 6.9, 5.9 Hz, 24H).

**$^{31}$P NMR** (243 MHz, $CDCl_3$) δ -13.90.

**HRMS (*m/z*):** (ESI) calc'd $[M+H]^+$: 1215.7483, found: 1215.7477.

### 4.4.9. Scope of Hydroamination

**Compound 3ab**

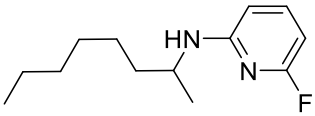


From *cis*-4-octene: According to **Condition A** at 90 °C for 4.5 h. *cis*-4-octene (78 µL, 0.50 mmol) and aminopyridine **2b** (11 mg, 0.10 mmol) was allowed to react, and the product was purified by flash column chromatography ($SiO_2$; 97.5:2.5 hexanes:EA) to afford compound **3ab** (20 mg, 91%) as a yellow oil. The regioselectivity of the reaction was determined to be 91% by GC.

From *trans*-4-octene: According to **Condition A** at 90 °C for 44 h. *trans*-4-octene (78 µL, 0.50 mmol) and aminopyridine **2b** (11 mg, 0.10 mmol) was allowed to react, and the product was purified by flash column chromatography ($SiO_2$; 97.5:2.5 hexanes:EA) to afford compound **3ab** (20 mg, 91%) as a yellow oil. The regioselectivity of the reaction was determined to be 90% by GC. Note: 4-$NMe_2$-3,5-DIP-MeOBIPHEP was used as the ligand instead of DIP-Ad-SEGPHOS.

From an equimolar mixture of *cis*-4-octene, *cis*-3-octene, and *cis*-2-octene: According to **Condition A** at 90 °C for 5 h. *cis*-4-octene (26 µL, 0.17 mmol), *cis*-3-octene (26 µL, 0.17 mmol), *cis*-2-octene (26 µL, 0.17 mmol) and aminopyridine **2b** (11 mg, 0.10 mmol) was allowed to react, and the product was purified by flash column chromatography ($SiO_2$; 97.5:2.5 hexanes:EA) to afford compound **3ab** (20 mg, 89%) as a yellow oil. The regioselectivity of the reaction was determined to be 92% by GC.

**$^1$H NMR** (600 MHz, $CDCl_3$) δ 7.42 (q, J = 8.1 Hz, 1H), 6.14 (dd, J = 8.1, 2.4 Hz, 1H), 6.07 (dd, J = 7.8, 2.3 Hz, 1H), 4.38 (s, 1H), 3.70 (h, J = 6.4 Hz, 1H), 1.56 – 1.41 (m, 2H), 1.40 – 1.31 (m, 2H), 1.31 – 1.22 (m, 6H), 1.17 (d, J = 6.6 Hz, 3H), 0.87 (t, J = 6.8 Hz, 3H).

**$^{13}$C NMR** (151 MHz, $CDCl_3$) δ 163.43 (d, J = 236.0 Hz), 157.75 (d, J = 16.9 Hz), 141.71 (d, J = 8.7 Hz), 102.54 (d, J = 4.0 Hz), 95.09 (d, J = 36.6 Hz), 47.48, 37.21, 31.90, 29.37, 26.08, 22.71, 20.90, 14.17.

**$^{19}$F NMR** (565 MHz, $CDCl_3$) δ -69.72.

**HRMS (*m/z*):** (ESI) calc'd $[M+H]^+$: 225.1762, found: 225.1758.

**Compound 3bb**

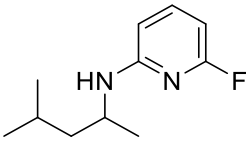


According to **Condition A** at 90 °C for 14 h. alkene **1b** (92 µL, 0.75 mmol) and aminopyridine **2b** (11 mg, 0.10 mmol) was allowed to react, and the product was purified by flash column chromatography ($SiO_2$; 97.5:2.5 hexanes:EA) to afford compound **3bb** (16 mg, 80%) as a yellow oil. The regioselectivity of the reaction was determined to be 93% by GC. Note: 4-$NMe_2$-3,5-DIP-MeOBIPHEP was used as the ligand instead of DIP-Ad-SEGPHOS.

**$^{1}$H NMR** (600 MHz, $CDCl_3$) δ 7.44 (q, J = 8.1 Hz, 1H), 6.15 (d, J = 8.1 Hz, 1H), 6.08 (d, J = 7.7 Hz, 1H), 4.33 (s, 1H), 3.79 (h, J = 6.4 Hz, 1H), 1.75 – 1.66 (m, 1H), 1.47 – 1.37 (m, 1H), 1.33 – 1.22 (m, 1H), 1.17 (d, J = 6.3 Hz, 3H), 0.92 (dd, J = 12.8, 6.6 Hz, 6H).

**$^{13}$C NMR** (151 MHz, $CDCl_3$) δ 163.45 (d, J = 236.0 Hz), 157.73 (d, J = 16.8 Hz), 141.77 (d, J = 8.7 Hz), 102.47 (d, J = 3.9 Hz), 95.15 (d, J = 36.8 Hz), 46.82, 45.65, 25.16, 22.86, 22.82, 21.36.

**$^{19}$F NMR** (565 MHz, $CDCl_3$) δ -69.67.

**HRMS (*m/z*):** (ESI) calc'd $[M+H]^+$: 197.1449, found: 197.1446.

**Compound 3cb**

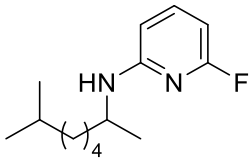


According to **Condition A** at 90 °C for 24 h. alkene **1c** (94 mg, 0.75 mmol) and aminopyridine **2b** (11 mg, 0.10 mmol) was allowed to react, and the product was purified by flash column chromatography ($SiO_2$; 97.5:2.5 hexanes:EA) to afford compound **3cb** (20 mg, 84%) as a yellow oil. The regioselectivity of the reaction was determined to be 85% by GC. Note: 4-$NMe_2$-3,5-DIP-MeOBIPHEP was used as the ligand instead of DIP-Ad-SEGPHOS.

**$^{1}$H NMR** (600 MHz, $CDCl_3$) δ 7.36 (q, J = 8.1 Hz, 1H), 6.07 (d, J = 8.1 Hz, 1H), 6.01 (d, J = 7.7 Hz, 1H), 4.31 (d, J = 8.4 Hz, 1H), 3.70 – 3.55 (m, 1H), 1.48 – 1.36 (m, 3H), 1.31 – 1.19 (m, 4H), 1.13 – 1.05 (m, 5H), 0.78 (d, J = 6.6 Hz, 6H).

**$^{13}$C NMR** (151 MHz, $CDCl_3$) δ 163.33 (d, J = 236.0 Hz), 157.63 (d, J = 16.8 Hz), 141.60 (d, J = 8.7 Hz), 102.40 (d, J = 4.4 Hz), 95.00 (d, J = 36.9 Hz), 47.37, 38.92, 37.14, 27.91, 27.34, 26.25, 22.61(two carbons), 20.81.

**$^{19}$F NMR** (565 MHz, $CDCl_3$) δ -69.74.

**HRMS (*m/z*):** (ESI) calc'd $[2M+K]^+$: 515.3322, found: 515.3313.

**Compound 3db**

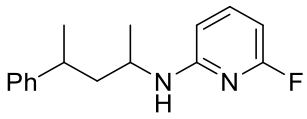


According to **Condition A** at 90 °C for 24 h. alkene **1d** (73 mg, 0.50 mmol) and aminopyridine **2b** (11 mg, 0.10 mmol) was allowed to react, and the product was purified by flash column chromatography ($SiO_2$; 97.5:2.5 hexanes:EA) to afford compound **3db** (22 mg, 86%) as a yellow oil. The regioselectivity of the reaction was determined to be >95% by GC. The d.r. of the product was determined to be 1:1 by GC.

**$^{1}$H NMR** (600 MHz, $CDCl_3$) δ 7.42 (p, J = 8.3 Hz, 2H, both diastereomers), 7.35 (t, J = 7.6 Hz, 2H, diastereomer 1), 7.32 – 7.28 (m, 2H, diastereomer 2), 7.27 – 7.20 (m, 4H, both diastereomers), 7.18 (d, J = 7.5 Hz, 2H, both diastereomers), 6.12 (ddd, J = 8.2, 6.4, 2.3 Hz, 2H, both diastereomer), 5.98 (dd, J = 8.0, 2.4 Hz, 1H, diastereomer 1), 5.94 (dd, J = 8.1, 2.4 Hz, 1H, diastereomer 2), 4.38 (d, J = 8.8 Hz, 2H, both diastereomers), 3.63 (hept, J = 6.9 Hz, 1H, diastereomer 1), 3.56 (h, J = 6.5, 5.9 Hz, 1H, diastereomer 2), 3.01 – 2.92 (m, 1H, diastereomer 2), 2.91 – 2.82 (m, 1H, diastereomer 1), 1.99 – 1.90 (m, 1H, diastereomer 1), 1.86 – 1.75 (m, 2H, both diastereomers), 1.74 – 1.65 (m, 1H, diastereomer 2), 1.31 (dd, J = 8.9, 6.9 Hz, 6H, both diastereomers), 1.24 (d, J = 6.4 Hz, 3H, diastereomer 1), 1.17 (d, J = 6.4 Hz, 3H, diastereomer 2).

**$^{13}$C NMR** 13C NMR (151 MHz, $CDCl_3$) δ 163.38 (d, J = 236.1 Hz, diastereomer 1), 163.36 (d, J = 236.0 Hz, diastereomer 2), 157.66 (d, J = 16.7 Hz, diastereomer 1), 157.51 (d, J = 16.8 Hz, diastereomer 2), 146.92 (diastereomer 1), 146.79 (diastereomer 2), 141.76 (d, J = 8.8 Hz, diastereomer 1), 141.73 (d, J = 8.7 Hz, diastereomer 2), 128.68 (diastereomer 1), 128.59 (diastereomer 2), 127.19 (diastereomer 1), 127.04 (diastereomer 2), 126.36 (diastereomer 1), 126.29 (diastereomer 2), 102.39 (d, J = 4.3 Hz, diastereomer 1), 102.32 (d, J = 3.9 Hz, diastereomer 2), 95.29 (d, J = 36.7 Hz, both diastereomers), 46.25 (diastereomer 1), 45.94 (diastereomer 2), 45.76 (diastereomer 1), 45.74 (diastereomer 2), 37.13 (diastereomer 1), 36.90 (diastereomer 2), 22.88 (diastereomer 1), 22.67 (diastereomer 2), 21.38 (diastereomer 1), 21.05 (diastereomer 2).

**$^{19}$F NMR** (565 MHz, $CDCl_3$) δ -69.72 (diastereomer 1), -69.78 (diastereomer 2).

**HRMS (*m/z*):** (ESI) calc'd $[2M+ACN+Na]^+$: 580.3222, found: 580.3239.

**Compound 3eb**

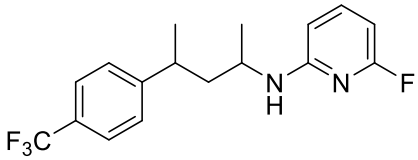


According to **Condition A** at 90 °C for 48 h. alkene **1e** (110 mg, 0.50 mmol) and aminopyridine **2b** (11 mg, 0.10 mmol) was allowed to react, and the product was purified by flash column chromatography ($SiO_2$; 97.5:2.5 hexanes:EA) to afford compound **3eb** (29 mg, 88%) as a yellow oil. The regioselectivity of the reaction was determined to be >95% by GC. The d.r. of the product was determined to be 1:1 by GC.

**$^{1}$H NMR** (600 MHz, $CDCl_3$) δ 7.53 – 7.30 (m, 10H, both diastereomers), 6.16 – 6.04 (m, 2H, both diastereomers), 6.00 – 5.88 (m, 2H, both diastereomers), 4.32 (dd, J = 14.6, 9.0 Hz, 2H, both diastereomers), 3.65 (p, J = 7.0 Hz, 1H, diastereomer 1), 3.51 (p, J = 6.9 Hz, 1H, diastereomer 2), 2.99 (h, J = 7.2 Hz, 1H, diastereomer 2), 2.92 (h, J = 7.1 Hz, 1H, diastereomer 1), 1.91 (dt, J = 14.7, 7.6 Hz, 1H, diastereomer 1), 1.78 (t, J = 7.1 Hz, 2H, both diastereomers), 1.71 – 1.63 (m, 1H, diastereomer 2), 1.29 (dd, J = 10.0, 6.9 Hz, 6H, both diastereomers), 1.20 (d, J = 6.4 Hz, 3H, diastereomer 2), 1.13 (d, J = 6.3 Hz, 3H, diastereomer 1).

**$^{13}$C NMR** (151 MHz, $CDCl_3$) δ 163.43 (d, J = 236.1 Hz, diastereomer 1), 163.39 (d, J = 236.2 Hz, diastereomer 2), 157.54 (d, J = 14.0 Hz, diastereomer 1), 157.42 (d, J = 14.0 Hz, diastereomer 2), 147.98 (diastereomer 1), 147.69 (diastereomer 2), 141.88 (d, J = 8.5 Hz, diastereomer 1), 141.79

(d, J = 8.6 Hz, diastereomer 2), 130.61 (both diastereomers), 129.12 (diastereomer 1), 129.02 (diastereomer 2), 124.39 (q, J = 272.1 Hz, diastereomer 1), 124.38 (q, J = 272.1 Hz, diastereomer 1), 124.02 (q, J = 3.8 Hz, diastereomer 2), 123.67 (q, J = 3.7 Hz, diastereomer 1), 123.24 (q, J = 3.6 Hz, diastereomer 2), 102.55 (d, J = 3.7 Hz, diastereomer 1), 102.37 (d, J = 3.7 Hz, diastereomer 2), 95.65 (d, J = 10.8 Hz, diastereomer 1), 95.41 (d, J = 10.7 Hz, diastereomer 2), 46.17 (diastereomer 2), 45.71 (diastereomer 1), 45.55 (both diastereomers), 37.13 (diastereomer 1), 36.88 (diastereomer 2), 22.71 (diastereomer 1), 22.42 (diastereomer 2), 21.54 (diastereomer 1), 21.17 (diastereomer 2).

**$^{19}$F NMR** (565 MHz, $CDCl_3$) δ -62.48 (diastereomer 1), -62.52 (diastereomer 2), -69.66 (diastereomer 1), -69.74 (diastereomer 2).

**HRMS (*m/z*):** (ESI) calc'd $[M+Na]^+$: 349.1298, found: 349.1285.

**Compound 3fb**

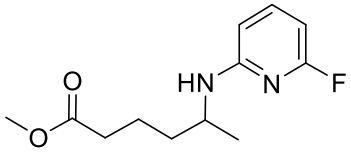


According to **Condition A** at 120 °C for 44 h. alkene **1f** (130 mg, 1.0 mmol) and aminopyridine **2b** (11 mg, 0.10 mmol) was allowed to react, and the product was purified by flash column chromatography ($SiO_2$; 90:10 hexanes:EA) to afford compound **3fb** (14 mg, 58%) as a yellow oil. The regioselectivity of the reaction was determined to be 91% by GC. Note: 4-$NMe_2$-3,5-DIP-MeOBIPHEP was used as the ligand instead of DIP-Ad-SEGPHOS. 3.75 mol% $[Ir(coe)_2Cl]_2$, 9 mol% ligand, and 9 mol% NaBArF were used.

**$^1$H NMR** (600 MHz, $CDCl_3$) δ 7.43 (q, J = 8.1 Hz, 1H), 6.15 (dd, J = 8.0, 2.4 Hz, 1H), 6.08 (dd, J = 7.8, 2.3 Hz, 1H), 4.38 (s, 1H), 3.79 (q, J = 6.4 Hz, 1H), 3.66 (s, 3H), 2.33 (t, J = 7.3 Hz, 2H), 1.77 – 1.63 (m, 2H), 1.59 – 1.46 (m, 2H), 1.20 (d, J = 6.4 Hz, 3H).

**$^{13}$C NMR** (151 MHz, $CDCl_3$) δ 173.88, 163.31 (d, J = 236.1 Hz), 157.49 (d, J = 16.6 Hz), 141.60 (d, J = 8.5 Hz), 102.77 (d, J = 4.0 Hz), 95.18 (d, J = 36.9 Hz), 51.54, 46.96, 36.33, 33.79, 21.39, 20.84.

**$^{19}$F NMR** (565 MHz, $CDCl_3$) δ -69.70.

**HRMS (*m/z*):** (ESI) calc'd $[M+H]^+$: 241.1347, found: 241.1346.

**Compound 3gb**

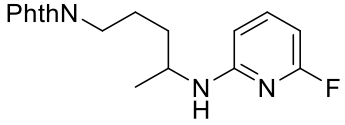


According to **Condition A** at 100 °C for 40 h. alkene **1g** (110 mg, 0.50 mmol) and aminopyridine **2b** (11 mg, 0.10 mmol) was allowed to react, and the product was purified by flash column

chromatography ($SiO_2$; 95:5 DCM:MeCN) to afford compound **3gb** (30 mg, 92%) as a yellow oil. The regioselectivity of the reaction was determined to be 93% by GC.

**$^1$H NMR** (600 MHz, $CDCl_3$) δ 7.82 (dd, J = 5.4, 3.0 Hz, 2H), 7.73 – 7.65 (m, 2H), 7.40 (q, J = 8.1 Hz, 1H), 6.14 (dd, J = 8.0, 2.3 Hz, 1H), 6.05 (dd, J = 7.7, 2.3 Hz, 1H), 4.42 (s, 1H), 3.83 (q, J = 6.5 Hz, 1H), 3.69 (t, J = 7.1 Hz, 2H), 1.85 – 1.69 (m, 2H), 1.60 – 1.48 (m, 2H), 1.17 (d, J = 6.4 Hz, 3H).

**$^{13}$C NMR** (151 MHz, $CDCl_3$) δ 168.54, 163.38 (d, J = 236.1 Hz), 157.54 (d, J = 17.0 Hz), 141.68 (d, J = 8.7 Hz), 134.04, 132.18, 123.32, 102.92 (d, J = 3.9 Hz), 95.28 (d, J = 36.9 Hz), 47.02, 37.95, 34.13, 25.40, 21.07.

**$^{19}$F NMR** (565 MHz, $CDCl_3$) δ -69.66.

**HRMS (*m/z*):** (ESI) calc'd $[M+H]^+$: 328.1456, found: 328.1455.

**Compound 3hb**

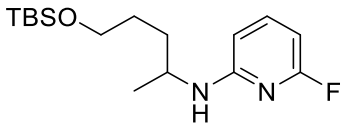


According to **Condition A** at 90 °C for 44 h. alkene **1h** (100 mg, 0.50 mmol) and aminopyridine **2b** (11 mg, 0.10 mmol) was allowed to react, and the product was purified by flash column chromatography ($SiO_2$; 95:5 hexanes:EA) to afford compound **3hb** (16 mg, 50%) as a yellow oil. The regioselectivity of the reaction was determined to be 81% by GC. Note: 4-$NMe_2$-3,5-DIP-MeOBIPHEP was used as the ligand instead of DIP-Ad-SEGPHOS. 3.75 mol% $[Ir(coe)_2Cl]_2$, 9 mol% ligand, and 9 mol% NaBArF were used.

**$^1$H NMR** (600 MHz, $CDCl_3$) δ 7.43 (q, J = 8.1 Hz, 1H), 6.15 (dd, J = 8.0, 2.4 Hz, 1H), 6.08 (dd, J = 7.8, 2.3 Hz, 1H), 4.44 (s, 1H), 3.76 (q, J = 6.2 Hz, 1H), 3.66 – 3.59 (m, 2H), 1.65 – 1.51 (m, 4H), 1.20 (d, J = 6.4 Hz, 3H), 0.89 (s, 9H), 0.04 (s, 6H).

**$^{13}$C NMR** (151 MHz, $CDCl_3$) δ 163.30 (d, J = 236.0 Hz), 157.57 (d, J = 16.7 Hz), 141.58 (d, J = 8.5 Hz), 102.57 (d, J = 3.9 Hz), 95.04 (d, J = 36.6 Hz), 62.91, 47.17, 33.28, 29.20, 25.95, 20.86, 18.33, -5.30.

**$^{19}$F NMR** (565 MHz, $CDCl_3$) δ -69.75.

**HRMS (*m/z*):** (ESI) calc'd $[M+H]^+$: 313.2106, found: 313.2107.

**Compound 3ib**

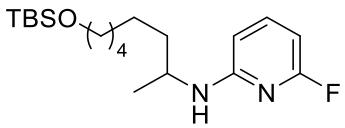

According to **Condition A** at 90 °C for 21 h. alkene **1i** (130 mg, 0.50 mmol) and aminopyridine **2b** (11 mg, 0.10 mmol) was allowed to react, and the product was purified by flash column chromatography ($SiO_2$; 95:5 hexanes:EA) to afford compound **3hb** (20 mg, 77%) as a yellow oil. The regioselectivity of the reaction was determined to be 91% by GC. Note: 4-$NMe_2$-3,5-DIP-MeOBIPHEP was used as the ligand instead of DIP-Ad-SEGPHOS.

**$^1$H NMR** (600 MHz, $CDCl_3$) δ 7.43 (q, J = 8.1 Hz, 1H), 6.14 (dd, J = 8.0, 2.4 Hz, 1H), 6.08 (dd, J = 7.8, 2.3 Hz, 1H), 4.36 (s, 1H), 3.71 (q, J = 6.4 Hz, 1H), 3.58 (t, J = 6.6 Hz, 2H), 1.59 – 1.44 (m, 4H), 1.40 – 1.35 (m, 2H), 1.33 – 1.28 (m, 4H), 1.18 (d, J = 6.3 Hz, 3H), 0.89 (s, 9H), 0.04 (s, 6H).

**$^{13}$C NMR** (151 MHz, $CDCl_3$) δ 163.43 (d, J = 236.1 Hz), 157.73 (d, J = 16.9 Hz), 141.76 (d, J = 8.6 Hz), 102.56 (d, J = 4.3 Hz), 95.16 (d, J = 36.8 Hz), 63.36, 47.48, 37.17, 32.92, 29.52, 26.12 (two carbons), 25.89, 20.94, 18.51, -5.13.

**$^{19}$F NMR** (565 MHz, $CDCl_3$) δ -69.72.

**HRMS (*m/z*):** (ESI) calc'd $[M+H]^+$: 369.2732, found: 369.2733.

**Compound 3jb**

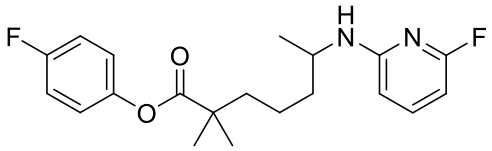


According to **Condition A** at 120 °C for 24 h. alkene **1j** (130 mg, 0.50 mmol) and aminopyridine **2b** (11 mg, 0.10 mmol) was allowed to react, and the product was purified by flash column chromatography ($SiO_2$; 90:10 hexanes:EA) to afford compound **3jb** (28 mg, 77%) as a yellow oil. The regioselectivity of the reaction was determined to be >95% by GC. Note: 3.75 mol% $[Ir(coe)_2Cl]_2$, 9 mol% ligand, and 9 mol% NaBArF were used.

**$^1$H NMR** 1H NMR (600 MHz, $CDCl_3$) δ 7.43 (q, J = 8.1 Hz, 1H), 7.07 – 6.98 (m, 2H), 6.97 – 6.91 (m, 2H), 6.14 (dd, J = 8.0, 2.4 Hz, 1H), 6.09 (dd, J = 7.7, 2.3 Hz, 1H), 4.36 (s, 1H), 3.80 (q, J = 6.4 Hz, 1H), 1.73 – 1.62 (m, 2H), 1.59 – 1.48 (m, 2H), 1.48 – 1.37 (m, 2H), 1.30 (d, J = 2.0 Hz, 6H), 1.19 (d, J = 6.4 Hz, 3H).

**$^{13}$C NMR** (151 MHz, $CDCl_3$) δ 176.59, 163.44 (d, J = 236.1 Hz), 160.25 (d, J = 244.0 Hz), 157.66 (d, J = 16.8 Hz), 146.91 (d, J = 2.8 Hz), 141.75 (d, J = 8.5 Hz), 122.98 (d, J = 8.4 Hz), 116.12 (d, J = 23.3 Hz), 102.80 (d, J = 4.2 Hz), 95.31 (d, J = 36.9 Hz), 47.13, 42.73, 40.61, 37.58, 25.25 (two carbons), 21.66, 21.04.

**$^{19}$F NMR** (565 MHz, $CDCl_3$) δ -69.62.

**HRMS (*m/z*):** (ESI) calc'd $[M+H]^+$: 363.1879, found: 363.1878.

**Compound 3kb**

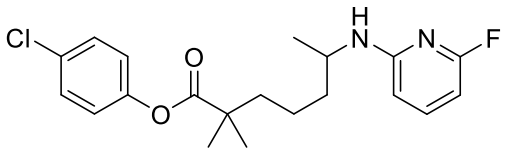

According to **Condition A** at 120 °C for 24 h. alkene **1k** (130 mg, 0.50 mmol) and aminopyridine **2b** (11 mg, 0.10 mmol) was allowed to react, and the product was purified by flash column chromatography ($SiO_2$; 90:10 hexanes:EA) to afford compound **3kb** (32 mg, 84%) as a yellow oil. The regioselectivity of the reaction was determined to be >95% by GC. Note: 5 mol% $[Ir(coe)_2Cl]_2$, 12 mol% ligand, and 12 mol% NaBArF were used.

**$^1$H NMR** (600 MHz, $CDCl_3$) δ 7.43 (q, J = 8.0 Hz, 1H), 7.30 (d, J = 8.3 Hz, 2H), 6.93 (d, J = 8.3 Hz, 2H), 6.19 – 6.13 (m, 1H), 6.11 – 6.05 (m, 1H), 4.35 (s, 1H), 3.80 (q, J = 6.5 Hz, 1H), 1.73 – 1.63 (m, 2H), 1.60 – 1.51 (m, 2H), 1.47– 1.37 (m, 2H), 1.29 (s, 3H), 1.28 (s, 3H), 1.19 (d, J = 6.4 Hz, 3H).

**$^{13}$C NMR** (151 MHz, $CDCl_3$) δ 176.34, 163.45 (d, J = 236.0 Hz), 157.66 (d, J = 16.6 Hz), 149.59, 141.76 (d, J = 8.6 Hz), 131.11, 129.54, 123.01, 102.82 (d, J = 4.4 Hz), 95.33 (d, J = 36.7 Hz), 47.12, 42.79, 40.58, 37.57, 29.84, 25.24, 21.66, 21.06.

**$^{19}$F NMR** (565 MHz, $CDCl_3$) δ -69.61.

**HRMS (*m/z*):** (ESI) calc'd $[M+H]^+$: 379.1583, found: 379.1584.

**Compound 3lb**

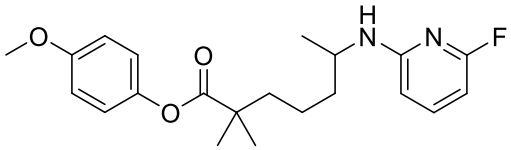

According to **Condition A** at 120 °C for 24 h. alkene **1l** (130 mg, 0.50 mmol) and aminopyridine **2b** (11 mg, 0.10 mmol) was allowed to react, and the product was purified by flash column chromatography ($SiO_2$; 85:15 hexanes:EA) to afford compound **3lb** (30 mg, 80%) as a yellow oil. The regioselectivity of the reaction was determined to be >95% by GC. Note: 3.75 mol% $[Ir(coe)_2Cl]_2$, 9 mol% ligand, and 9 mol% NaBArF were used.

**$^1$H NMR** (600 MHz, $CDCl_3$) δ 7.43 (q, J = 8.1 Hz, 1H), 6.90 (d, J = 8.6 Hz, 2H), 6.86 (d, J = 8.7 Hz, 2H), 6.14 (dd, J = 8.0, 2.3 Hz, 1H), 6.08 (dd, J = 7.7, 2.3 Hz, 1H), 4.38 (s, 1H), 3.79 (s, 4H), 1.72 – 1.60 (m, 2H), 1.59 – 1.48 (m, 2H), 1.48 – 1.38 (m, 2H), 1.30 (s, 3H), 1.29 (s, 3H), 1.19 (d, J = 6.4 Hz, 3H).

**$^{13}$C NMR** (151 MHz, $CDCl_3$) δ 176.79, 163.31 (d, J = 236.0 Hz), 157.55 (d, J = 16.9 Hz), 157.12, 144.47, 141.64 (d, J = 8.5 Hz), 122.21, 114.43, 102.65 (d, J = 3.9 Hz), 95.15 (d, J = 36.6 Hz), 55.59, 47.07, 42.55, 40.55, 37.46, 25.21, 25.16, 21.55, 20.88.

**$^{19}$F NMR** (565 MHz, $CDCl_3$) δ -69.66.

**HRMS (*m/z*):** (ESI) calc'd $[M+H]^+$: 375.2078, found: 375.2079.

**Compound 3mb**

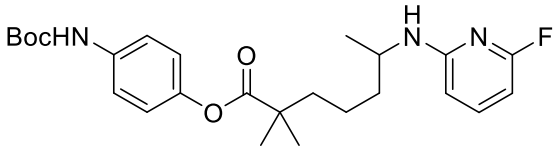


According to **Condition A** at 120 °C for 48 h. alkene **1m** (170 mg, 0.50 mmol) and aminopyridine **2b** (11 mg, 0.10 mmol) was allowed to react, and the product was purified by flash column chromatography ($SiO_2$; 85:15 hexanes:EA) to afford compound **3mb** (28 mg, 61%) as a yellow oil. The regioselectivity of the reaction was determined to be >95% by GC. Note: 3.75 mol% $[Ir(coe)_2Cl]_2$, 9 mol% ligand, and 9 mol% NaBArF were used.

**$^1$H NMR** (600 MHz, $CDCl_3$) δ 7.43 (q, J = 8.1 Hz, 1H), 7.33 (d, J = 8.4 Hz, 2H), 6.91 (d, J = 8.7 Hz, 2H), 6.52 (s, 1H), 6.14 (dd, J = 8.1, 2.3 Hz, 1H), 6.08 (dd, J = 7.7, 2.2 Hz, 1H), 4.38 (s, 1H), 3.78 (q, J = 6.4 Hz, 1H), 1.72 – 1.62 (m, 2H), 1.57 – 1.48 (m, 11H), 1.47 – 1.38 (m, 2H), 1.29 (s, 3H), 1.28 (s, 3H), 1.19 (d, J = 6.4 Hz, 3H).

**$^{13}$C NMR** (151 MHz, $CDCl_3$) δ 176.59, 163.27 (d, J = 236.1 Hz), 157.52 (d, J = 16.7 Hz), 152.74, 146.30, 141.67 (d, J = 8.6 Hz), 135.88, 121.84, 119.37, 102.68 (d, J = 3.9 Hz), 95.14 (d, J = 36.7 Hz), 47.07, 42.58, 40.50, 37.44, 29.71, 28.34, 25.18, 25.13, 21.53, 20.86.

**$^{19}$F NMR** (565 MHz, $CDCl_3$) δ -69.69.

**HRMS (*m/z*):** (ESI) calc'd $[M+H]^+$: 460.2606, found: 460.2609.

**Compound 3nb**

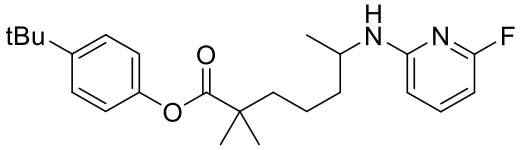


According to **Condition A** at 120 °C for 48 h. alkene **1n** (140 mg, 0.50 mmol) and aminopyridine **2b** (11 mg, 0.10 mmol) was allowed to react, and the product was purified by flash column chromatography ($SiO_2$; 92:8 hexanes:EA) to afford compound **3nb** (19 mg, 47%) as a yellow oil. The regioselectivity of the reaction was determined to be >95% by GC. Note: 5 mol% $[Ir(coe)_2Cl]_2$, 12 mol% ligand, and 12 mol% NaBArF were used.

**$^1$H NMR** (600 MHz, $CDCl_3$) δ 7.33 (q, J = 8.1 Hz, 1H), 7.26 (d, J = 8.5 Hz, 2H), 6.82 (d, J = 8.5 Hz, 2H), 6.05 (dd, J = 8.0, 2.4 Hz, 1H), 5.99 (dd, J = 7.8, 2.3 Hz, 1H), 4.28 (s, 1H), 3.73 – 3.64 (m, 1H), 1.63 – 1.54 (m, 2H), 1.50 – 1.39 (m, 2H), 1.39 – 1.29 (m, 2H), 1.21 (s, 9H), 1.21 (s, 3H), 1.20 (s, 3H), 1.10 (d, J = 6.4 Hz, 3H).

**$^{13}$C NMR** (151 MHz, $CDCl_3$) δ 176.56, 163.31 (d, J = 236.1 Hz), 157.53 (d, J = 16.7 Hz), 148.61, 148.42, 141.63 (d, J = 8.5 Hz), 126.26, 120.75, 102.62 (d, J = 4.0 Hz), 95.17 (d, J = 36.9 Hz), 47.10, 42.59, 40.57, 37.47, 34.45, 31.42, 25.21, 25.17, 21.56, 20.88.

**$^{19}$F NMR** (565 MHz, $CDCl_3$) δ -69.66.

**HRMS (*m/z*):** (ESI) calc'd $[M+H]^+$: 401.2599, found: 401.2698.

**Compound 3ob**

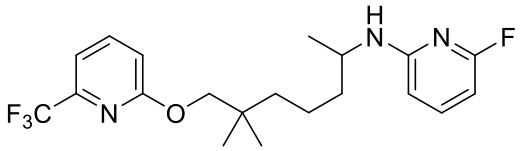

According to **Condition A** at 120 °C for 24 h. alkene **1o** (140 mg, 0.50 mmol) and aminopyridine **2b** (11 mg, 0.10 mmol) was allowed to react, and the product was purified by flash column chromatography ($SiO_2$; 97:3 hexanes:EA) to afford compound **3ob** (26 mg, 65%) as a yellow oil. The regioselectivity of the reaction was determined to be 87% by GC. Note: 3.75 mol% $[Ir(coe)_2Cl]_2$, 9 mol% ligand, and 9 mol% NaBArF were used.

**$^1$H NMR** (600 MHz, $CDCl_3$) δ 7.66 (t, J = 7.9 Hz, 1H), 7.43 (q, J = 8.1 Hz, 1H), 7.21 (d, J = 7.3 Hz, 1H), 6.87 (d, J = 8.5 Hz, 1H), 6.14 (d, J = 8.0 Hz, 1H), 6.08 (d, J = 7.7 Hz, 1H), 4.36 (s, 1H), 4.03 (s, 2H), 3.74 (q, J = 6.5 Hz, 1H), 1.55 – 1.43 (m, 2H), 1.41 – 1.34 (m, 4H), 1.17 (d, J = 6.3 Hz, 3H), 0.97 (s, 6H).

**$^{13}$C NMR** (151 MHz, $CDCl_3$) δ 164.29, 163.28 (d, J = 235.9 Hz), 157.58 (d, J = 16.9 Hz), 145.42 (q, J = 34.6 Hz), 141.62 (d, J = 8.7 Hz), 139.13, 121.42 (q, J = 273.5 Hz), 114.63, 112.93 (q, J = 3.3 Hz), 102.49 (d, J = 4.0 Hz), 95.05 (d, J = 36.8 Hz), 74.32, 47.24, 39.05, 37.93, 34.08, 24.48, 24.45, 20.83, 20.39.

**$^{19}$F NMR** (565 MHz, $CDCl_3$) δ -68.42, -69.74.

**HRMS (*m/z*):** (ESI) calc'd $[M+H]^+$: 400.2007, found: 400.2007.

**Compound 3pb**

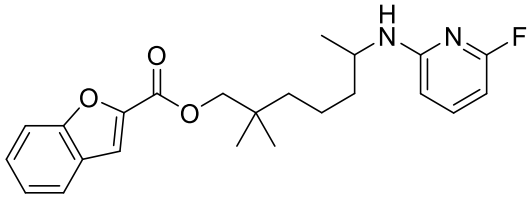

According to **Condition A** at 120 °C for 24 h. alkene **1p** (140 mg, 0.50 mmol) and aminopyridine **2b** (11 mg, 0.10 mmol) was allowed to react, and the product was purified by flash column chromatography ($SiO_2$; 90:10 hexanes:EA) to afford compound **3pb** (28 mg, 70%) as a yellow oil. The regioselectivity of the reaction was determined to be >95% by GC. Note: 3.75 mol% $[Ir(coe)_2Cl]_2$, 9 mol% ligand, and 9 mol% NaBArF were used.

**$^1$H NMR** (600 MHz, $CDCl_3$) δ 7.67 (d, J = 7.8 Hz, 1H), 7.58 (d, J = 8.5 Hz, 1H), 7.49 (s, 1H), 7.44 (t, J = 8.4 Hz, 1H), 7.40 (q, J = 8.1 Hz, 1H), 7.33 – 7.27 (m, 1H), 6.13 (dd, J = 8.1, 2.3 Hz, 1H),

6.06 (dd, J = 7.7, 2.3 Hz, 1H), 4.37 (s, 1H), 4.09 (s, 2H), 3.77 (q, J = 6.4 Hz, 1H), 1.56 – 1.44 (m, 2H), 1.45 – 1.31 (m, 4H), 1.19 (d, J = 6.4 Hz, 3H), 0.99 (s, 6H).

**$^{13}$C NMR** (151 MHz, $CDCl_3$) δ 163.29 (d, J = 236.0 Hz), 159.71, 157.57 (d, J = 16.9 Hz), 155.80, 145.60, 141.61 (d, J = 8.7 Hz), 127.57, 126.98, 123.78, 122.81, 113.60, 112.40, 102.60 (d, J = 4.2 Hz), 95.09 (d, J = 36.6 Hz), 73.12, 47.19, 39.08, 37.86, 34.17, 24.29 (two carbons), 20.88, 20.38.

**$^{19}$F NMR** (565 MHz, $CDCl_3$) δ -69.69.

**HRMS (*m/z*):** (ESI) calc'd $[M+H]^+$: 399.2078, found: 399.2076.

**Compound 3qb**

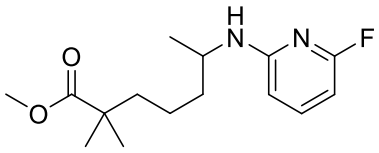


According to **Condition A** at 120 °C for 58 h. alkene **1q** (85 mg, 0.50 mmol) and aminopyridine **2b** (11 mg, 0.10 mmol) was allowed to react, and the product was purified by flash column chromatography ($SiO_2$; 90:10 hexanes:EA) to afford compound **3qb** (22 mg, 76%) as a yellow oil. The regioselectivity of the reaction was determined to be >95% by GC.

**$^{1}$H NMR** (600 MHz, $CDCl_3$) δ 7.43 (q, J = 8.0 Hz, 1H), 6.18 – 6.10 (m, 1H), 6.10 – 6.02 (m, 1H), 4.36 (s, 1H), 3.73 (q, J = 6.4 Hz, 1H), 3.62 (s, 3H), 1.55 – 1.40 (m, 4H), 1.35 – 1.21 (m, 2H), 1.16 (d, J = 6.5 Hz, 3H), 1.14 (d, J = 3.1 Hz, 6H).

**$^{13}$C NMR** (151 MHz, $CDCl_3$) δ 178.52, 163.42 (d, J = 235.9 Hz), 157.67 (d, J = 16.9 Hz), 141.74 (d, J = 8.6 Hz), 102.70 (d, J = 3.9 Hz), 95.20 (d, J = 36.8 Hz), 51.78, 47.21, 42.39, 40.68, 37.52, 25.31, 25.26, 21.56, 20.90.

**$^{19}$F NMR** (565 MHz, $CDCl_3$) δ -69.73.

**HRMS (*m/z*):** (ESI) calc'd $[M+H]^+$: 283.1816, found: 283.1815.

**Compound 3rb**

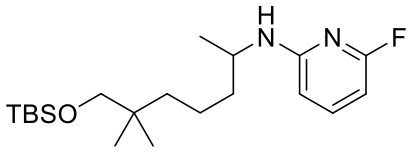


According to **Condition A** at 120 °C for 24 h. alkene **1r** (130 mg, 0.50 mmol) and aminopyridine **2b** (11 mg, 0.10 mmol) was allowed to react, and the product was purified by flash column chromatography ($SiO_2$; 97:3 hexanes:EA) to afford compound **3rb** (22 mg, 58%) as a yellow oil. The regioselectivity of the reaction was determined to be 88% by GC. Note: 3.75 mol% $[Ir(coe)_2Cl]_2$, 9 mol% ligand, and 9 mol% NaBArF were used.

**$^{1}$H NMR** (600 MHz, $CDCl_3$) δ 7.44 (q, J = 8.1 Hz, 1H), 6.14 (dd, J = 8.1, 2.4 Hz, 1H), 6.08 (dd, J = 7.8, 2.3 Hz, 1H), 4.38 (s, 1H), 3.72 (q, J = 6.4 Hz, 1H), 3.21 (s, 2H), 1.54 – 1.38 (m, 2H), 1.36 – 1.27 (m, 2H), 1.21 (d, J = 8.6 Hz, 2H), 1.18 (d, J = 6.5 Hz, 3H), 0.88 (s, 9H), 0.80 (s, 6H), 0.01 (s, 6H).

**$^{13}$C NMR** (151 MHz, $CDCl_3$) δ 163.30 (d, J = 236.1 Hz), 157.59 (d, J = 16.8 Hz), 141.62 (d, J = 8.7 Hz), 102.39 (d, J = 4.1 Hz), 95.02 (d, J = 36.6 Hz), 71.44, 47.40, 38.70, 38.08, 35.21, 25.89, 24.12, 24.10, 20.78, 20.41, 18.28, -5.53.

**$^{19}$F NMR** (565 MHz, $CDCl_3$) δ -69.75.

**HRMS (*m/z*):** (ESI) calc'd $[M+H]^+$: 369.2732, found: 369.2734.

**Compound 3sb**

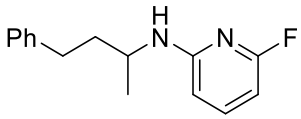


According to **Condition A** at 90 °C for 24 h. (Z)-but-1-en-1-ylbenzene (44 mg, 0.34 mmol), (E)-but-2-en-1-ylbenzene (44 mg, 0.34 mmol), (E)-but-1-en-1-ylbenzene (44 mg, 0.34 mmol) and aminopyridine **2b** (11 mg, 0.10 mmol) was allowed to react, and the product was purified by flash column chromatography ($SiO_2$; 97.5:2.5 hexanes:EA) to afford compound **3sb** (19 mg, 79%) as a yellow oil. The regioselectivity of the reaction was determined to be >95% by GC. Note: 3.75 mol% $[Ir(coe)_2Cl]_2$, 9 mol% ligand, and 9 mol% NaBArF were used.

**$^{1}$H NMR** (600 MHz, $CDCl_3$) δ 7.43 (q, J = 8.1 Hz, 1H), 7.28 (t, J = 7.6 Hz, 2H), 7.21 – 7.15 (m, 3H), 6.17 – 6.09 (m, 1H), 6.09 – 6.05 (m, 1H),, 4.42 (d, J = 8.9 Hz, 1H), 3.81 – 3.75 (m, 1H), 2.75 – 2.67 (m, 2H), 1.89 – 1.78 (m, 2H), 1.24 (d, J = 6.4 Hz, 3H).

**$^{13}$C NMR** (151 MHz, $CDCl_3$) δ 163.32 (d, J = 236.1 Hz), 157.53 (d, J = 16.7 Hz), 141.73 (d, J = 4.1 Hz), 141.66, 128.44, 128.39, 125.94, 102.49 (d, J = 4.0 Hz), 95.29 (d, J = 36.9 Hz), 46.91, 38.78, 32.39, 20.90.

**$^{19}$F NMR** (565 MHz, $CDCl_3$) δ -69.67.

**HRMS (*m/z*):** (ESI) calc'd $[2M+ACN+H]^+$: 530.3090, found: 530.3077.

**Compound 3tb**

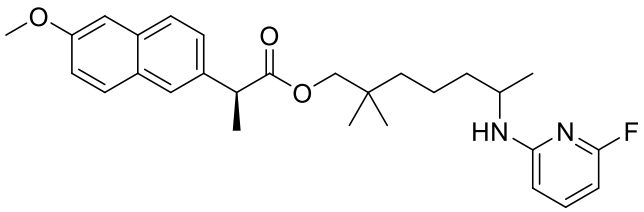


According to **Condition A** at 120 °C for 48 h. alkene **1t** (180 mg, 0.50 mmol) and aminopyridine **2b** (11 mg, 0.10 mmol) was allowed to react, and the product was purified by flash column

chromatography ($SiO_2$; 95:5 hexanes:EA) to afford compound **3tb** (38 mg, 81%) as a yellow oil. The regioselectivity of the reaction was determined to be >95% by GC. The d.r. of the product was determined to be 1:1 by GC. Note: 3.75 mol% $[Ir(coe)_2Cl]_2$, 9 mol% ligand, and 9 mol% NaBArF were used. Note: The two diastereomers have identical NMR chemical shifts.

**$^1$H NMR** (600 MHz, $CDCl_3$) δ 7.72 – 7.66 (m, 3H), 7.42 – 7.38 (m, 2H), 7.15 – 7.11 (m, 1H), 7.11 (s, 1H), 6.09 – 6.04 (m, 2H), 4.22 (s, 1H), 3.92 – 3.85 (m, 4H), 3.82 (dd, J = 10.8, 2.8 Hz, 1H), 3.71 (dd, J = 10.8, 3.0 Hz, 1H), 3.62 – 3.52 (m, 1H), 1.59 (d, J = 7.2 Hz, 3H), 1.29 – 1.08 (m, 5H), 1.06 – 1.02 (m, 4H), 0.80 (s, 3H), 0.77 (d, J = 3.2 Hz, 3H).

**$^{13}$C NMR** (151 MHz, $CDCl_3$) δ 174.59, 163.31 (d, J = 235.7 Hz), 157.64, 157.55 (d, J = 16.7, 2.5 Hz), 141.57 (d, J = 8.7, 2.6 Hz), 135.83, 133.69, 129.27, 128.93, 127.03, 126.43, 126.00, 118.98, 105.61, 102.54 (d, J = 8.3, 3.9 Hz), 95.00 (d, J = 36.9, 2.1 Hz), 72.26, 55.30, 47.10, 45.63, 38.77, 37.68, 33.89, 24.44, 24.17, 20.70, 20.24, 18.05.

**$^{19}$F NMR** (565 MHz, $CDCl_3$) δ -69.72.

**HRMS (*m/z*):** (ESI) calc'd $[M+H]^+$: 467.2704, found: 467.2702.

**Compound 3ub**

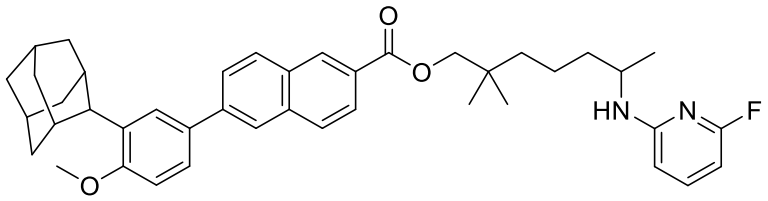


According to **Condition A** at 120 °C for 24 h. alkene **1u** (270 mg, 0.50 mmol) and aminopyridine **2b** (11 mg, 0.10 mmol) was allowed to react, and the product was purified by flash column chromatography ($SiO_2$; 80:20 hexanes:EA) to afford compound **3ub** (58 mg, 89%) as a white solid. The regioselectivity of the reaction was determined to be >95% by LCMS. Note: 3.75 mol% $[Ir(coe)_2Cl]_2$, 9 mol% ligand, and 9 mol% NaBArF were used.

**$^1$H NMR** (600 MHz, $CDCl_3$) δ 8.61 (s, 1H), 8.08 (d, J = 8.4 Hz, 1H), 8.03 (s, 1H), 8.00 (d, J = 8.5 Hz, 1H), 7.92 (d, J = 8.6 Hz, 1H), 7.81 (dd, J = 8.6, 1.8 Hz, 1H), 7.63 (d, J = 2.4 Hz, 1H), 7.55 (dd, J = 8.3, 2.3 Hz, 1H), 7.39 (q, J = 8.1 Hz, 1H), 7.00 (d, J = 8.4 Hz, 1H), 6.13 (dd, J = 8.1, 2.3 Hz, 1H), 6.07 (dd, J = 7.7, 2.2 Hz, 1H), 4.44 (s, 1H), 4.12 (s, 2H), 3.91 (s, 3H), 3.79 (q, J = 6.4 Hz, 1H), 2.21 (s, 6H), 2.12 (s, 3H), 1.89 – 1.77 (m, 6H), 1.61 – 1.36 (m, 6H), 1.20 (d, J = 6.4 Hz, 3H), 1.06 (s, 6H).

**$^{13}$C NMR** (151 MHz, $CDCl_3$) δ 166.90, 163.39 (d, J = 236.0 Hz), 159.04, 157.68 (d, J = 16.7 Hz), 141.68 (d, J = 8.7 Hz), 141.45, 139.11, 136.05, 132.63, 131.36, 130.80, 129.81, 128.35, 127.33, 126.56, 126.04, 125.83, 125.62, 124.80, 112.23, 102.66 (d, J = 4.4 Hz), 95.14 (d, J = 36.9 Hz), 73.00, 67.18, 55.25, 47.33, 40.72, 39.41, 38.00, 37.32, 37.24, 34.29, 29.80, 29.22 (two carbons), 24.61, 24.57, 20.94, 20.56.

**$^{19}$F NMR** (565 MHz, $CDCl_3$) δ -69.69.

**HRMS (*m/z*):** (ESI) calc'd $[M+H]^+$: 649.3800, found: 649.3810.

**Compound 3vb**

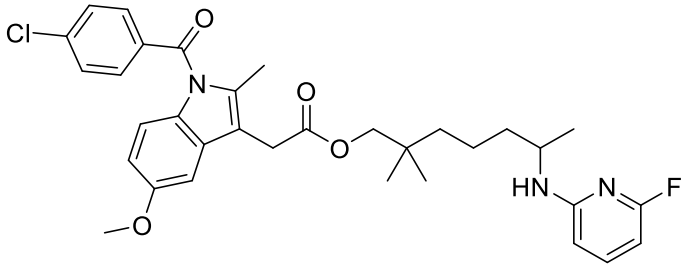

According to **Condition A** at 120 °C for 24 h. alkene **1v** (240 mg, 0.50 mmol) and aminopyridine **2b** (11 mg, 0.10 mmol) was allowed to react, and the product was purified by flash column chromatography ($SiO_2$; 80:20 hexanes:EA) to afford compound **3vb** (52 mg, 87%) as a yellow oil. The regioselectivity of the reaction was determined to be >95% by LCMS. Note: 5 mol% $[Ir(coe)_2Cl]_2$, 12 mol% ligand, and 12 mol% NaBArF were used.

**$^1$H NMR** (600 MHz, $CDCl_3$) δ 7.63 (d, J = 8.1 Hz, 2H), 7.45 (d, J = 8.1 Hz, 2H), 7.41 (q, J = 8.2 Hz, 1H), 6.98 (d, J = 2.5 Hz, 1H), 6.88 (d, J = 8.9 Hz, 1H), 6.66 (dd, J = 8.9, 2.6 Hz, 1H), 6.11 (dd, J = 7.9, 2.3 Hz, 1H), 6.06 (dd, J = 7.8, 2.3 Hz, 1H), 4.35 (s, 1H), 3.82 (s, 3H), 3.79 (s, 2H), 3.66 (s, 3H), 2.39 (s, 3H), 1.28 – 1.24 (m, 4H), 1.14 – 1.07 (m, 5H), 0.81 (s, 6H).

**$^{13}$C NMR** (151 MHz, $CDCl_3$) δ 170.83, 168.30, 163.32 (d, J = 235.7 Hz), 157.62 (d, J = 16.7 Hz), 156.05, 141.55 (d, J = 8.8 Hz), 139.31, 135.75, 133.89, 131.17, 130.83, 130.65, 129.13, 114.95, 112.85, 111.69, 102.68 (d, J = 3.9 Hz), 101.44, 94.98 (d, J = 36.8 Hz), 72.56, 55.71, 47.11, 38.82, 37.78, 33.80, 30.48, 24.29, 24.20, 20.87, 20.32, 13.33.

**$^{19}$F NMR** (565 MHz, $CDCl_3$) δ -69.70.

**HRMS (*m/z*):** (ESI) calc'd $[M+H]^+$: 594.2529, found: 594.2534.

**Compound 3wb**

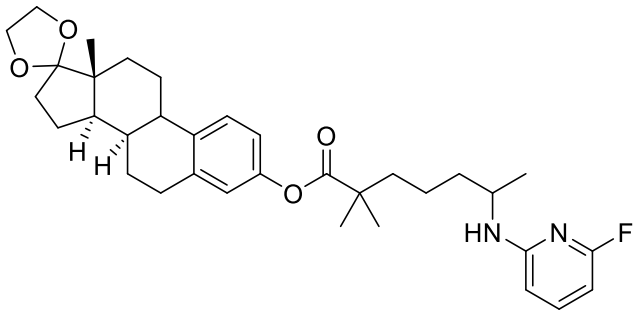

According to **Condition A** at 120 °C for 19 h. alkene **1w** (230 mg, 0.50 mmol) and aminopyridine **2b** (11 mg, 0.10 mmol) was allowed to react, and the product was purified by flash column chromatography ($SiO_2$; 80:20 hexanes:EA) to afford compound **3wb** (33 mg, 58%) as a yellow oil. The regioselectivity of the reaction was determined to be >95% by GC. The d.r. of the product was determined to be 1:1 by GC. Note: The two diastereomers have identical NMR chemical shifts.

**$^{1}$H NMR** (600 MHz, $CDCl_3$) δ 7.42 (q, J = 8.1 Hz, 1H), 7.25 (d, J = 8.9 Hz, 1H), 6.75 (d, J = 8.4 Hz, 1H), 6.71 (s, 1H), 6.14 (d, J = 8.0 Hz, 1H), 6.08 (d, J = 7.7 Hz, 1H), 4.39 (s, 1H), 4.04 – 3.83 (m, 4H), 3.79 (q, J = 6.6 Hz, 1H), 2.84 (t, J = 8.1 Hz, 2H), 2.40 – 2.19 (m, 2H), 2.08– 1.98 (m, 1H), 1.96 – 1.81 (m, 2H), 1.81 – 1.72 (m, 2H), 1.72 – 1.60 (m, 3H), 1.60 – 1.32 (m, 9H), 1.29 (d, J = 3.8 Hz, 6H), 1.19 (d, J = 6.4 Hz, 3H), 0.88 (s, 3H).

**$^{13}$C NMR** (151 MHz, $CDCl_3$) δ 176.65, 163.30 (d, J = 236.1 Hz), 157.54 (d, J = 16.9 Hz), 148.68, 141.62 (d, J = 8.6 Hz), 138.21, 137.83, 126.32, 121.34, 119.39, 118.41, 102.65 (d, J = 3.9 Hz), 95.13 (d, J = 36.7 Hz), 65.27, 64.59, 49.40, 47.10, 46.12, 43.83, 42.56, 40.53, 38.73, 37.47, 34.24, 30.71, 29.53, 26.81, 26.01, 25.24, 25.16, 22.38, 21.55, 20.85, 14.33.

**$^{19}$F NMR** (565 MHz, $CDCl_3$) δ -69.65.

**HRMS (*m/z*):** (ESI) calc'd $[M+H]^+$: 565.3436, found: 565.3431.

**Compound 3ac**

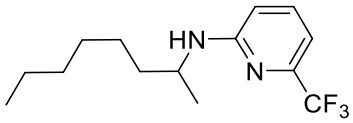


According to **Condition A** at 100 °C for 36 h. *cis*-4-octene (78 µL, 0.50 mmol) and aminopyridine **2c** (16 mg, 0.10 mmol) was allowed to react, and the product was purified by flash column chromatography ($SiO_2$; 98:2 hexanes:EA) to afford compound **3ac** (16 mg, 56%) as a yellow oil. The regioselectivity of the reaction was determined to be 94% by GC. Note: 5 mol% $[Ir(coe)_2Cl]_2$, 12 mol% ligand, and 12 mol% NaBArF were used.

**$^{1}$H NMR** (600 MHz, $CDCl_3$) δ 7.50 (t, J = 7.9 Hz, 1H), 6.87 (d, J = 7.4 Hz, 1H), 6.48 (d, J = 8.5 Hz, 1H), 4.61 (d, J = 8.1 Hz, 1H), 3.74 (hept, J = 6.6 Hz, 1H), 1.60 – 1.44 (m, 2H), 1.41 – 1.33 (m, 2H), 1.33 – 1.24 (m, 6H), 1.20 (d, J = 6.4 Hz, 3H), 0.88 (t, J = 6.8 Hz, 3H).

**$^{13}$C NMR** (151 MHz, $CDCl_3$) δ 158.17, 146.74 (q, J = 33.7 Hz), 138.10, 121.66 (q, J = 274.1 Hz), 109.28, 108.38 (q, J = 3.3 Hz), 47.37, 37.08, 31.77, 29.24, 25.98, 22.59, 20.69, 14.04.

**$^{19}$F NMR** (565 MHz, $CDCl_3$) δ -68.84.

**HRMS (*m/z*):** (ESI) calc'd $[M+K]^+$: 313.1289, found: 313.1276.

**Compound 3ad**

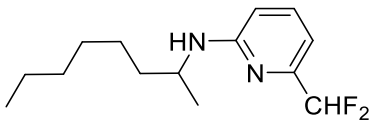


According to **Condition A** at 100 °C for 18 h. *cis*-4-octene (78 µL, 0.50 mmol) and aminopyridine **2d** (14 mg, 0.10 mmol) was allowed to react, and the product was purified by flash column chromatography ($SiO_2$; 97.5:2.5 hexanes:EA) to afford compound **3ad** (15 mg, 67%) as a yellow oil. The regioselectivity of the reaction was determined to be 91% by GC.

**$^{1}$H NMR** (600 MHz, $CDCl_3$) δ 7.42 (t, J = 7.8 Hz, 1H), 6.75 (d, J = 7.3 Hz, 1H), 6.34 (d, J = 8.4 Hz, 1H), 6.32 (t, J = 55.9 Hz, 1H), 4.42 (d, J = 8.4 Hz, 1H), 3.66 (p, J = 6.7 Hz, 1H), 1.53 – 1.37 (m, 2H), 1.34 – 1.26 (m, 2H), 1.25 – 1.16 (m, 6H), 1.12 (d, J = 6.4 Hz, 3H), 0.81 (t, J = 6.8 Hz, 3H).

**$^{13}$C NMR** (151 MHz, $CDCl_3$) δ 158.08, 151.30 (t, J = 24.9 Hz), 138.21, 114.03 (t, J = 240.0 Hz), 108.17 (t, J = 3.7 Hz), 47.29, 37.14, 31.78, 29.7 (t, J = 319.1 Hz) 29.27, 26.01, 22.60, 20.77, 14.06.

**$^{19}$F NMR** (565 MHz, $CDCl_3$) δ -116.65 (app-d, J = 55.3 Hz).

**HRMS (*m/z*):** (ESI) calc'd $[M+Na]^+$: 279.1643, found: 279.1663.

**Compound 3ae**

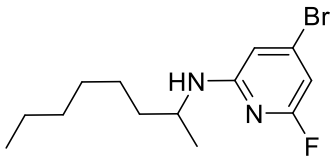


According to **Condition A** at 100 °C for 12 h. *cis*-4-octene (78 µL, 0.50 mmol) and aminopyridine **2e** (19 mg, 0.10 mmol) was allowed to react, and the product was purified by flash column chromatography ($SiO_2$; 97.5:2.5 hexanes:EA) to afford compound **3ae** (23 mg, 75%) as a yellow oil. The regioselectivity of the reaction was determined to be 92% by GC.

**$^{1}$H NMR** (600 MHz, $CDCl_3$) δ 6.31 (s, 1H), 6.27 (s, 1H), 4.48 (d, J = 8.4 Hz, 1H), 3.68 (hept, J = 6.8 Hz, 1H), 1.54 – 1.43 (m, 2H), 1.40 – 1.22 (m, 8H), 1.18 (d, J = 6.4 Hz, 3H), 0.88 (t, J = 6.8 Hz, 3H).

**$^{13}$C NMR** (151 MHz, $CDCl_3$) δ 163.29 (d, J = 238.4 Hz), 157.77 (d, J = 19.1 Hz), 135.79 (d, J = 10.9 Hz), 105.50, 99.16 (d, J = 40.9 Hz), 47.66, 37.10, 31.89, 29.33, 26.03, 22.72, 20.85, 14.19.

**$^{19}$F NMR** (565 MHz, $CDCl_3$) δ -68.66.

**HRMS (*m/z*):** (ESI) calc'd $[2M+H]^+$: 605.1661, found: 605.1671.

**Compound 3af**

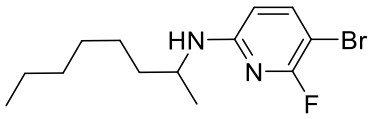


According to **Condition A** at 100 °C for 12 h. *cis*-4-octene (78 µL, 0.50 mmol) and aminopyridine **2f** (19 mg, 0.10 mmol) was allowed to react, and the product was purified by flash column chromatography ($SiO_2$; 97.5:2.5 hexanes:EA) to afford compound **3af** (17 mg, 61%) as a yellow oil. The regioselectivity of the reaction was determined to be 91% by GC.

**$^{1}$H NMR** 1H NMR (600 MHz, $CDCl_3$) δ 7.53 (t, J = 8.7 Hz, 1H), 6.09 (d, J = 8.5 Hz, 1H), 4.40 (d, J = 8.3 Hz, 1H), 3.77 – 3.63 (m, 1H), 1.55 – 1.41 (m, 2H), 1.39 – 1.21 (m, 8H), 1.17 (d, J = 6.4 Hz, 3H), 0.87 (t, J = 6.8 Hz, 3H).

**$^{13}$C NMR** (151 MHz, $CDCl_3$) δ 158.73 (d, J = 233.2 Hz), 156.36 (d, J = 15.9 Hz), 144.10 (d, J = 2.8 Hz), 104.59 (d, J = 4.4 Hz), 86.93 (d, J = 37.9 Hz), 47.60, 36.99, 31.76, 29.22, 25.92, 22.58, 20.71, 14.05.

**$^{19}$F NMR** (565 MHz, $CDCl_3$) δ -67.25.

**HRMS (*m/z*):** (ESI) calc'd $[2M+H]^+$: 605.1661, found: 605.1671.

**Compound 3ag**

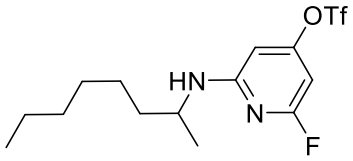


According to **Condition A** at 100 °C for 18 h. *cis*-4-octene (78 µL, 0.50 mmol) and aminopyridine **2g** (26 mg, 0.10 mmol) was allowed to react, and the product was purified by flash column chromatography ($SiO_2$; 97.5:2.5 hexanes:EA) to afford compound **3ag** (20 mg, 54%) as a yellow oil. The regioselectivity of the reaction was determined to be 91% by GC. Note: 3.75 mol% $[Ir(coe)_2Cl]_2$, 9 mol% ligand, and 9 mol% NaBArF were used.

**$^{1}$H NMR** 1H NMR (600 MHz, $CDCl_3$) δ 6.04 (s, 1H), 6.02 (s, 1H), 4.71 (d, J = 8.3 Hz, 1H), 3.75 – 3.66 (m, 1H), 1.56 – 1.45 (m, 2H), 1.40 – 1.22 (m, 8H), 1.20 (d, J = 6.4 Hz, 3H), 0.88 (t, J = 6.8 Hz, 3H).

**$^{13}$C NMR** (151 MHz, $CDCl_3$) δ 163.85 (d, J = 237.5 Hz), 159.54 (d, J = 13.2 Hz), 158.16 (d, J = 20.5 Hz), 118.58 (q, J = 320.8 Hz), 94.65, 88.87 (d, J = 43.0 Hz), 47.80, 36.83, 31.71, 29.15, 25.88, 22.55, 20.54, 14.01.

**$^{19}$F NMR** (565 MHz, $CDCl_3$) δ -64.23, -72.85.

**HRMS (*m/z*):** (ESI) calc'd $[M+Na]^+$: 395.1023, found: 395.1020.

**Compound 3ah**

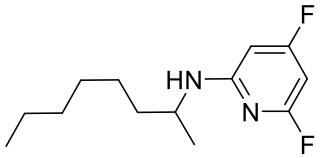


According to **Condition A** at 100 °C for 12 h. *cis*-4-octene (78 µL, 0.50 mmol) and aminopyridine **2h** (13 mg, 0.10 mmol) was allowed to react, and the product was purified by flash column chromatography ($SiO_2$; 97.5:2.5 hexanes:EA) to afford compound **3ah** (17 mg, 71%) as a yellow oil. The regioselectivity of the reaction was determined to be 93% by GC.

**$^{1}$H NMR** (600 MHz, $CDCl_3$) δ 5.86 (s, 1H), 5.84 (t, J = 2.8 Hz, 1H), 4.56 (d, J = 8.3 Hz, 1H), 3.65 – 3.58 (m, 1H), 1.54 – 1.42 (m, 2H), 1.38 – 1.23 (m, 8H), 1.18 (d, J = 6.4 Hz, 3H), 0.88 (t, J = 6.8 Hz, 3H).

**$^{13}$C NMR** (151 MHz, $CDCl_3$) δ 172.63 (dd, J = 255.8, 14.1 Hz), 164.29 (dd, J = 234.6, 17.4 Hz), 158.53 (dd, J = 21.2, 14.2 Hz), 89.30 (dd, J = 22.9, 5.3 Hz), 85.00 (dd, J = 42.2, 24.6 Hz), 47.82, 37.08, 31.90, 29.34, 26.05, 22.72, 20.80, 14.18.

**$^{19}$F NMR** (565 MHz, $CDCl_3$) δ -66.22 (d, J = 22.8 Hz), -98.96.

**HRMS (*m/z*):** (ESI) calc'd $[M+H]^+$: 243.1668, found: 243.1663.

**Compound 3ai**

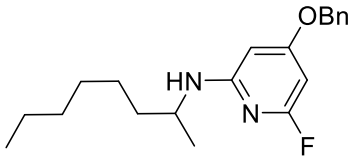


According to **Condition A** at 100 °C for 12 h. *cis*-4-octene (78 µL, 0.50 mmol) and aminopyridine **2i** (22 mg, 0.10 mmol) was allowed to react, and the product was purified by flash column chromatography ($SiO_2$; 97:3 hexanes:EA) to afford compound **3ai** (29 mg, 88%) as a yellow oil. The regioselectivity of the reaction was determined to be 90% by GC.

**$^{1}$H NMR** (600 MHz, $CDCl_3$) δ 7.40 (d, J = 4.4 Hz, 4H), 7.37 – 7.32 (m, 1H), 5.78 (d, J = 1.7 Hz, 1H), 5.72 (s, 1H), 5.05 (s, 2H), 4.37 (d, J = 8.3 Hz, 1H), 3.59 (p, J = 6.7 Hz, 1H), 1.52 – 1.42 (m, 2H), 1.39 – 1.20 (m, 8H), 1.16 (d, J = 6.4 Hz, 3H), 0.88 (t, J = 6.8 Hz, 3H).

**$^{13}$C NMR** (151 MHz, $CDCl_3$) δ 169.85 (d, J = 13.0 Hz), 164.70 (d, J = 231.8 Hz), 158.21 (d, J = 21.1 Hz), 135.96, 128.85, 128.47, 127.64, 88.14 (d, J = 4.2 Hz), 83.72 (d, J = 41.8 Hz), 70.31, 47.67, 37.17, 31.91, 29.38, 26.07, 22.72, 20.86, 14.19.

**$^{19}$F NMR** (565 MHz, $CDCl_3$) δ -69.20.

**HRMS (*m/z*):** (ESI) calc'd $[2M+Na]^+$: 683.4106, found: 683.4096.

**Compound 3aj**

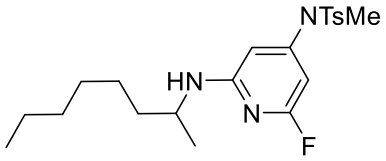


According to **Condition A** at 100 °C for 6 h. *cis*-4-octene (78 µL, 0.50 mmol) and aminopyridine **2j** (30 mg, 0.10 mmol) was allowed to react, and the product was purified by flash column chromatography ($SiO_2$; 91:9 hexanes:EA) to afford compound **3aj** (31 mg, 77%) as a yellow oil. The regioselectivity of the reaction was determined to be 92% by GC.

**$^{1}$H NMR** (600 MHz, $CDCl_3$) δ 7.27 (d, J = 7.8 Hz, 2H), 6.99 (d, J = 7.4 Hz, 2H), 5.91 (s, 1H), 5.55 (s, 1H), 4.18 (d, J = 8.3 Hz, 1H), 3.43 – 3.31 (m, 1H), 2.90 (s, 3H), 2.14 (s, 3H), 1.26 – 1.14 (m, 2H), 1.14 – 0.96 (m, 8H), 0.89 (d, J = 6.4 Hz, 3H), 0.61 (t, J = 6.8 Hz, 3H).

**$^{13}$C NMR** 13C NMR (151 MHz, $CDCl_3$) δ 163.73 (d, J = 233.5 Hz), 157.54 (d, J = 19.8 Hz), 153.70 (d, J = 11.6 Hz), 144.23, 133.83, 129.66, 127.45, 97.60, 89.77 (d, J = 41.3 Hz), 47.45, 36.99, 36.70, 31.78, 29.25, 25.90, 22.59, 21.56, 20.69, 14.06.

**$^{19}$F NMR** (565 MHz, $CDCl_3$) δ -68.72.

**HRMS (*m/z*):** (ESI) calc'd $[2M+ACN+H]^+$: 878.4244, found: 878.4236.

**Compound 3ak**

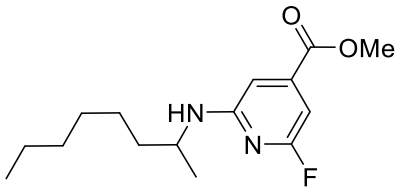


According to **Condition A** at 100 °C for 12 h. *cis*-4-octene (78 µL, 0.50 mmol) and aminopyridine **2k** (17 mg, 0.10 mmol) was allowed to react, and the product was purified by flash column chromatography ($SiO_2$; 97:3 hexanes:EA) to afford compound **3ak** (18 mg, 65%) as a yellow oil. The regioselectivity of the reaction was determined to be 90% by GC.

**$^{1}$H NMR** (600 MHz, $CDCl_3$) δ 6.76 (s, 1H), 6.59 (s, 1H), 4.57 (d, J = 8.4 Hz, 1H), 3.91 (s, 3H), 3.79 (t, J = 7.0 Hz, 1H), 1.56 – 1.43 (m, 2H), 1.41 – 1.23 (m, 8H), 1.19 (d, J = 6.4 Hz, 3H), 0.87 (t, J = 6.7 Hz, 3H).

**$^{13}$C NMR** (151 MHz, $CDCl_3$) δ 165.42 (d, J = 4.3 Hz), 163.90 (d, J = 236.4 Hz), 158.06 (d, J = 17.4 Hz), 143.39 (d, J = 9.0 Hz), 103.34, 94.88 (d, J = 39.7 Hz), 52.76, 47.65, 37.15, 31.89, 29.35, 26.04, 22.72, 20.91, 14.18.

**$^{19}$F NMR** (565 MHz, $CDCl_3$) δ -68.83.

**HRMS (*m/z*):** (ESI) calc'd $[M+ACN+Na]^+$: 346.1902, found: 349.1905.

**Compound 3al**

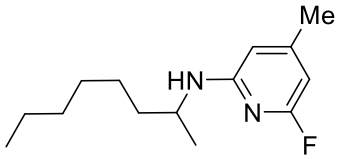


According to **Condition A** at 100 °C for 24 h. *cis*-4-octene (78 µL, 0.50 mmol) and aminopyridine **2l** (12 mg, 0.10 mmol) was allowed to react, and the product was purified by flash column chromatography ($SiO_2$; 98:2 hexanes:EA) to afford compound **3al** (17 mg, 69%) as a yellow oil. The regioselectivity of the reaction was determined to be 92% by GC.

**$^{1}$H NMR** (600 MHz, $CDCl_3$) δ 5.96 (s, 1H), 5.93 (s, 1H), 4.29 (d, J = 8.5 Hz, 1H), 3.68 (app-dq, J = 8.2, 6.3 Hz, 1H), 2.23 (s, 3H), 1.53 – 1.42 (m, 2H), 1.39 – 1.32 (m, 2H), 1.30 – 1.23 (s, 6H), 1.17 (d, J = 6.4 Hz, 3H), 0.87 (t, J = 6.8 Hz, 3H).

**$^{13}$C NMR** (151 MHz, $CDCl_3$) δ 163.79 (d, J = 234.5 Hz), 157.59 (d, J = 17.8 Hz), 153.45 (d, J = 8.9 Hz), 102.89 (d, J = 3.6 Hz), 96.32 (d, J = 36.6 Hz), 47.46, 37.28, 31.92, 29.40, 26.09, 22.73, 21.35 (d, J = 3.5 Hz), 21.00, 14.20.

**$^{19}$F NMR** (565 MHz, $CDCl_3$) δ -72.35.

**HRMS (*m/z*):** (ESI) calc'd $[M+H]^+$: 239.1918, found: 239.1909.

**Compound 3am**

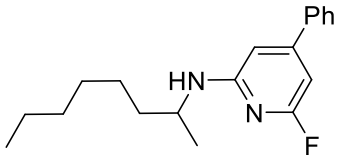


According to **Condition A** at 100 °C for 6 h. *cis*-4-octene (78 µL, 0.50 mmol) and aminopyridine **2m** (19 mg, 0.10 mmol) was allowed to react, and the product was purified by flash column chromatography ($SiO_2$; 97.5:2.5 hexanes:EA) to afford compound **3am** (22 mg, 72%) as a yellow oil. The regioselectivity of the reaction was determined to be 89% by GC. Notes: Contain 10% inseparable isomers.

**$^{1}$H NMR** (600 MHz, $CDCl_3$) δ 7.60 – 7.53 (m, 2H), 7.48 – 7.38 (m, 3H), 6.35 (s, 1H), 6.32 (s, 1H), 4.47 (d, J = 8.3 Hz, 1H), 3.84 – 3.76 (m, 1H), 1.58 – 1.47 (m, 2H), 1.42 – 1.35 (m, 2H), 1.34 – 1.24 (m, 6H), 1.22 (d, J = 6.4 Hz, 3H), 0.88 (t, J = 6.8 Hz, 3H).

**$^{13}$C NMR** (151 MHz, $CDCl_3$) δ 164.17 (d, J = 234.8 Hz), 157.94 (d, J = 18.3 Hz), 154.97 (d, J = 9.0 Hz), 138.79 (d, J = 3.5 Hz), 129.17, 129.04, 127.06, 100.75 (d, J = 3.9 Hz), 93.96 (d, J = 38.0 Hz), 47.61, 37.28, 31.93, 29.42, 26.11, 22.74, 21.03, 14.20.

**$^{19}$F NMR** (565 MHz, $CDCl_3$) δ -70.71.

**HRMS (*m/z*):** (ESI) calc'd $[M+K]^+$: 339.1634, found: 339.1635.

**Compound 3an**

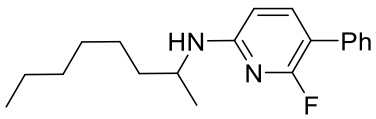


According to **Condition A** at 100 °C for 6 h. *cis*-4-octene (78 µL, 0.50 mmol) and aminopyridine **2n** (19 mg, 0.10 mmol) was allowed to react, and the product was purified by flash column chromatography ($SiO_2$; 97.5:2.5 hexanes:EA) to afford compound **3an** (24 mg, 80%) as a yellow oil. The regioselectivity of the reaction was determined to be 90% by GC. Notes: Contain 10% inseparable isomers.

**$^{1}$H NMR** (600 MHz, $CDCl_3$) δ 7.61 (dd, J = 10.1, 8.2 Hz, 1H), 7.53 – 7.47 (m, 2H), 7.40 (t, J = 7.6 Hz, 2H), 7.32 – 7.27 (m, 1H), 6.27 (dd, J = 8.2, 1.8 Hz, 1H), 4.44 (s, 1H), 3.77 (p, J = 6.1 Hz,

1H), 1.60 – 1.46 (m, 2H), 1.43 – 1.36 (m, 2H), 1.34 – 1.25 (m, 6H), 1.22 (d, J = 6.2 Hz, 3H), 0.88 (t, J = 6.8 Hz, 3H).

**$^{13}$C NMR** 13C NMR (151 MHz, $CDCl_3$) δ 160.46, 158.88, 156.59 (d, J = 17.1 Hz), 141.81 (d, J = 5.1 Hz), 135.14 (d, J = 5.4 Hz), 128.48, 126.76, 109.58 (d, J = 27.7 Hz), 103.30 (d, J = 4.1 Hz), 47.52, 37.16, 31.79, 29.27, 25.99, 22.61, 20.91, 14.07.

**$^{19}$F NMR** (565 MHz, $CDCl_3$) δ -73.27.

**HRMS (*m/z*):** (ESI) calc'd $[M+Na]^+$: 323.1894, found: 323.1887.

**Compound 3ao**

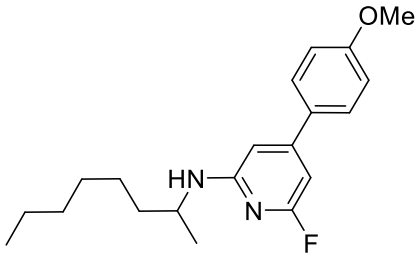


According to **Condition A** at 100 °C for 6 h. *cis*-4-octene (78 µL, 0.50 mmol) and aminopyridine **2o** (22 mg, 0.10 mmol) was allowed to react, and the product was purified by flash column chromatography ($SiO_2$; 95:5 hexanes:EA) to afford compound **3ao** (20 mg, 61%) as a yellow oil. The regioselectivity of the reaction was determined to be 87% by GC.

**$^{1}$H NMR** 1H NMR (600 MHz, $CDCl_3$) δ 7.54 – 7.50 (m, 2H), 6.99 – 6.95 (m, 2H), 6.31 (s, 1H), 6.29 (s, 1H), 4.46 (s, 1H), 3.85 (s, 3H), 3.78 (q, J = 6.4 Hz, 1H), 1.59 – 1.45 (m, 2H), 1.56 – 1.46 (m, 2H), 1.34 – 1.24 (m, 6H), 1.22 (d, J = 6.4 Hz, 3H), 0.88 (t, J = 6.9 Hz, 3H).

**$^{13}$C NMR** (151 MHz, $CDCl_3$) δ 164.17 (d, J = 234.7 Hz), 160.63, 157.88 (d, J = 18.0 Hz), 154.45 (d, J = 9.1 Hz), 131.02 (d, J = 3.4 Hz), 128.23, 114.44, 100.06 (d, J = 3.4 Hz), 93.42 (d, J = 37.7 Hz), 55.52, 47.61, 37.29, 31.93, 29.42, 26.12, 22.74, 21.03, 14.20.

**$^{19}$F NMR** (565 MHz, $CDCl_3$) δ -71.17.

**HRMS (*m/z*):** (ESI) calc'd $[M+ACN+Na]^+$: 394.2264, found: 394.2266.

**Compound 3ap**

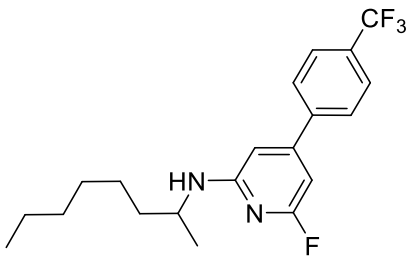

According to **Condition A** at 100 °C for 6 h. *cis*-4-octene (78 µL, 0.50 mmol) and aminopyridine **2p** (26 mg, 0.10 mmol) was allowed to react, and the product was purified by flash column chromatography ($SiO_2$; 97.5:2.5 hexanes:EA) to afford compound **3ap** (17 mg, 47%) as a yellow oil. The regioselectivity of the reaction was determined to be 93% by GC.

**$^1$H NMR** (600 MHz, $CDCl_3$) δ 7.71 (d, J = 8.1 Hz, 2H), 7.66 (d, J = 8.0 Hz, 2H), 6.33 (s, 1H), 6.30 (s, 1H), 4.52 (d, J = 8.2 Hz, 1H), 3.83 – 3.76 (m, 1H), 1.58 – 1.49 (m, 2H), 1.44 – 1.36 (m, 2H), 1.34 – 1.24 (m, 6H), 1.23 (d, J = 6.4 Hz, 3H), 0.88 (t, J = 6.8 Hz, 3H).

**$^{13}$C NMR** (151 MHz, $CDCl_3$) δ 164.06 (d, J = 235.5 Hz), 157.92 (d, J = 18.1 Hz), 153.26 (d, J = 9.1 Hz), 142.22 (d, J = 3.1 Hz), 131.01 (q, J = 32.6 Hz), 127.34, 125.88 (q, J = 3.8 Hz), 123.99 (q, J = 272.1 Hz), 100.88, 93.85 (d, J = 38.4 Hz), 47.50, 37.11, 31.78, 29.26, 25.97, 22.60, 20.85, 14.05.

**$^{19}$F NMR** (565 MHz, $CDCl_3$) δ -62.64, -69.78.

**HRMS (*m/z*):** (ESI) calc'd $[M+H]^+$: 369.1949, found: 369.1951.

**Compound 3aq**

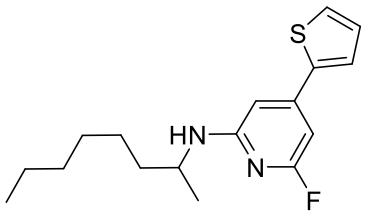


According to **Condition A** at 100 °C for 12 h. *cis*-4-octene (78 µL, 0.50 mmol) and aminopyridine **2q** (19 mg, 0.10 mmol) was allowed to react, and the product was purified by flash column chromatography ($SiO_2$; 97.5:2.5 hexanes:EA) to afford compound **3aq** (15 mg, 49%) as a yellow oil. The regioselectivity of the reaction was determined to be 86% by GC.

**$^1$H NMR** (600 MHz, $CDCl_3$) δ 7.41 (d, J = 3.6 Hz, 1H), 7.37 (d, J = 5.0 Hz, 1H), 7.10 (dd, J = 5.1, 3.7 Hz, 1H), 6.35 (s, 1H), 6.33 (s, 1H), 4.45 (d, J = 8.4 Hz, 1H), 3.79 (p, J = 6.7 Hz, 1H), 1.58 – 1.46 (m, 2H), 1.42 – 1.34 (m, 2H), 1.34 – 1.23 (m, 6H), 1.21 (d, J = 6.4 Hz, 3H), 0.88 (t, J = 6.8 Hz, 3H).

**$^{13}$C NMR** 13C NMR (151 MHz, $CDCl_3$) δ 164.12 (d, J = 234.3 Hz), 157.89 (d, J = 18.5 Hz), 147.14 (d, J = 9.8 Hz), 141.47 (d, J = 4.4 Hz), 128.10, 126.67, 125.21, 99.03, 92.31 (d, J = 39.1 Hz), 47.44, 37.14, 31.79, 29.28, 25.97, 22.61, 20.89, 14.07.

**$^{19}$F NMR** (565 MHz, $CDCl_3$) δ -70.54.

**HRMS (*m/z*):** (ESI) calc'd $[2M+Na]^+$: 635.3024, found: 635.3037.

**Compound 3ar**

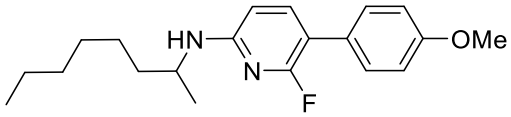


According to **Condition A** at 100 °C for 6 h. *cis*-4-octene (78 µL, 0.50 mmol) and aminopyridine **2r** (22 mg, 0.10 mmol) was allowed to react, and the product was purified by flash column chromatography ($SiO_2$; 95:5 hexanes:EA) to afford compound **3ar** (15 mg, 46%) as a yellow oil. The regioselectivity of the reaction was determined to be 92% by GC.

**$^1$H NMR** (600 MHz, $CDCl_3$) δ 7.57 (t, J = 10.2 Hz, 1H), 7.42 (d, J = 8.2 Hz, 2H), 6.94 (d, J = 8.4 Hz, 2H), 6.26 (dd, J = 8.2, 1.8 Hz, 1H), 3.83 (s, 3H), 3.75 (q, J = 6.4 Hz, 1H), 1.56 – 1.45 (m, 2H), 1.43 – 1.34 (m, 2H), 1.34 – 1.24 (m, 7H), 1.21 (d, J = 6.4 Hz, 3H), 0.88 (t, J = 6.8 Hz, 3H).

**$^{13}$C NMR** 13C NMR (151 MHz, $CDCl_3$) δ 159.60 (d, J = 238.0 Hz), 158.73, 156.31 (d, J = 16.7 Hz), 141.75 (d, J = 5.3 Hz), 129.43 (d, J = 3.0 Hz), 127.64 (d, J = 5.1 Hz), 114.12, 109.47 (d, J = 27.8 Hz), 103.40 (d, J = 4.2 Hz), 55.45, 47.68, 37.28, 31.93, 29.41, 26.12, 22.74, 21.03, 14.20.

**$^{19}$F NMR** (565 MHz, $CDCl_3$) δ -73.73.

**HRMS (*m/z*):** (ESI) calc'd $[M+Na]^+$: 353.1999, found: 353.2004.

**Compound 3as**

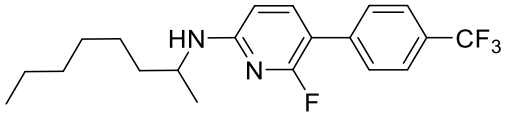


According to **Condition A** at 100 °C for 6 h. *cis*-4-octene (78 µL, 0.50 mmol) and aminopyridine **2s** (26 mg, 0.10 mmol) was allowed to react, and the product was purified by flash column chromatography ($SiO_2$; 97.5:2.5 hexanes:EA) to afford compound **3as** (17 mg, 47%) as a yellow oil. The regioselectivity of the reaction was determined to be 93% by GC.

**$^1$H NMR** (600 MHz, $CDCl_3$) δ 7.70 – 7.52 (m, 5H), 6.29 (d, J = 8.3 Hz, 1H), 4.55 (s, 1H), 3.79 (p, J = 6.2 Hz, 1H), 1.57 – 1.48 (m, 2H), 1.42 – 1.35 (m, 2H), 1.34 – 1.26 (m, 6H), 1.23 (d, J = 6.4 Hz, 3H), 0.88 (t, J = 6.9 Hz, 3H).

**$^{13}$C NMR** (151 MHz, $CDCl_3$) δ 159.75 (d, J = 238.9 Hz), 157.15 (d, J = 17.5 Hz), 141.55 (d, J = 4.8 Hz), 138.81 (d, J = 5.3 Hz), 128.66 (q, J = 32.5 Hz), 128.26 (d, J = 3.4 Hz), 125.41 (q, J = 3.8 Hz), 124.28 (q, J = 271.9 Hz), 107.96 (d, J = 27.3 Hz), 103.61, 47.55, 37.10, 31.78, 29.25, 25.98, 22.60, 20.86, 14.06.

**$^{19}$F NMR** (565 MHz, $CDCl_3$) δ -62.44, -72.49.

**HRMS (*m/z*):** (ESI) calc'd $[2M+H]^+$: 737.3825, found: 737.3846.

### 4.4.10. Product Derivatization by $S_NAr$

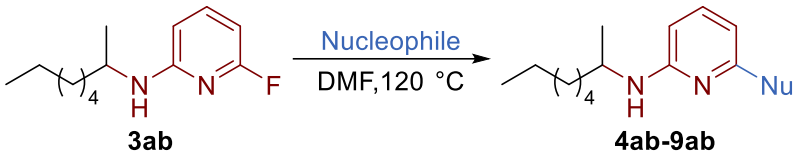


**Condition D:** In a nitrogen-filled glovebox, a 1-dram vial was charged sequentially with 6-fluoro-N-(octan-2-yl)pyridin-2-amine (**3ab**) (22 mg, 0.10 mmol, 1.0 equiv), nucleophile (0.30 to 1.0 mmol, 3.0 to 10.0 equiv), DMF (0.2 mL), and a magnetic stir bar. The vial was capped and removed from the glovebox. The reaction was heated at 120 to 130 °C in an aluminium heating block. The crude material was extracted with ether/$H_2O$ 5 times to remove residual DMF, concentrated in vacuo, and purified by flash column chromatography to afford the product.

**Compound 4ab**

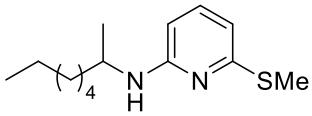


According to **Condition D** at 120 °C for 18 h. sodium methanethiolate (NaSMe) (71 mg, 1.0 mmol) was used as the nucleophile, and the product was purified by flash column chromatography ($SiO_2$; 97.5:2.5 hexanes:EA) to afford compound **4ab** (21 mg, 83%) as a yellow oil.

**$^1$H NMR** (600 MHz, $CDCl_3$) δ 7.22 (t, J = 7.8 Hz, 1H), 6.43 (d, J = 7.5 Hz, 1H), 6.02 (d, J = 8.2 Hz, 1H), 4.33 (s, 1H), 3.73 (h, J = 7.4, 7.0 Hz, 1H), 2.49 (s, 3H), 1.58 – 1.51 (m, 1H), 1.50 – 1.41 (m, 1H), 1.40 – 1.33 (m, 2H), 1.32 – 1.25 (m, 6H), 1.18 (d, J = 6.4 Hz, 3H), 0.88 (t, J = 6.7 Hz, 3H).

**$^{13}$C NMR** (151 MHz, $CDCl_3$) δ 158.11, 158.06, 137.50, 109.24, 101.66, 47.34, 37.38, 31.95, 29.47, 26.23, 22.75, 21.01, 14.20, 13.41.

**HRMS (*m/z*):** (ESI) calc'd $[2M+ACN+Na]^+$: 568.3478, found: 568.3472.

**Compound 5ab**

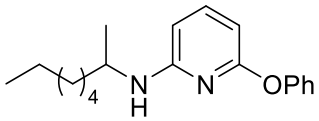


According to **Condition D** at 120 °C for 36 h. potassium phenoxide (KOPh) (39 mg, 0.30 mmol) was used as the nucleophile, and the product was purified by flash column chromatography ($SiO_2$; 97.5:2.5 hexanes:EA) to afford compound **5ab** (24 mg, 80%) as a yellow oil.

**$^1$H NMR** (600 MHz, $CDCl_3$) δ 7.36 (q, J = 7.8 Hz, 3H), 7.17 – 7.12 (m, 3H), 6.03 (d, J = 8.0 Hz, 1H), 5.97 (d, J = 7.8 Hz, 1H), 4.30 (d, J = 8.1 Hz, 1H), 3.62 (hept, J = 6.5 Hz, 1H), 1.53 – 1.46 (m, 1H), 1.44 – 1.37 (m, 1H), 1.36 – 1.20 (m, 8H), 1.14 (d, J = 6.4 Hz, 3H), 0.88 (t, J = 6.9 Hz, 3H).

**$^{13}$C NMR** (151 MHz, $CDCl_3$) δ 163.28, 157.85, 154.86, 140.54, 129.51, 124.17, 121.17, 100.30, 97.54, 47.45, 37.30, 31.95, 29.44, 26.15, 22.74, 20.93, 14.21.

**HRMS (*m/z*):** (ESI) calc'd $[2M+Na]^+$: 619.3982, found: 619.3962.

**Compound 6ab**

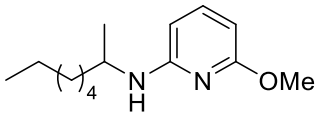

According to **Condition D** at 130 °C for 36 h. lithium methoxide (LiOMe) (11 mg, 0.30 mmol) was used as the nucleophile, and the product was purified by flash column chromatography ($SiO_2$; 97.5:2.5 hexanes:EA) to afford compound **4ab** (18 mg, 77%) as a yellow oil.

**$^1$H NMR** (600 MHz, $CDCl_3$) δ 7.31 (t, J = 7.9 Hz, 1H), 5.97 (d, J = 7.8 Hz, 1H), 5.89 (d, J = 7.9 Hz, 1H), 4.20 (s, 1H), 3.84 (s, 3H), 3.71 (hept, J = 6.6 Hz, 1H), 1.61 – 1.51 (m, 1H), 1.48 – 1.42 (m, 1H), 1.41 – 1.34 (m, 2H), 1.32 – 1.24 (m, 6H), 1.19 (d, J = 6.4 Hz, 3H), 0.88 (t, J = 6.8 Hz, 3H).

**$^{13}$C NMR** (151 MHz, $CDCl_3$) δ 163.81, 157.51, 140.02, 97.78, 96.78, 53.15, 47.43, 37.43, 31.97, 29.49, 26.26, 22.76, 21.06, 14.21.

**HRMS (*m/z*):** (ESI) calc'd $[M+Na]^+$: 259.1781, found: 259.1768.

**Compound 7ab**

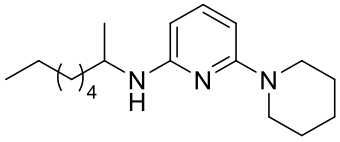

According to **Condition D** at 130 °C for 18 h. piperidine (29 μL, 0.30 mmol) and sodium *tert*-butoxide ($NaO^tBu$) (29 mg, 0.30 mmol) were used as the nucleophile, and the product was purified by flash column chromatography ($SiO_2$; 97.5:2.5 hexanes:EA) to afford compound **7ab** (21 mg, 72%) as a yellow oil.

**$^1$H NMR** (600 MHz, $CDCl_3$) δ 7.25 (app-d, J = 7.8 Hz, 1H), 5.92 (d, J = 7.8 Hz, 1H), 5.86 (d, J = 7.9 Hz, 1H), 4.05 (s, 1H), 3.75 (q, J = 6.5 Hz, 1H), 1.56 (s, 10H), 1.48 – 1.40 (m, 1H), 1.39 – 1.33 (m, 2H), 1.33 – 1.24 (m, 7H), 1.18 (d, J = 6.4 Hz, 3H), 0.88 (d, J = 6.7 Hz, 3H).

**$^{13}$C NMR** (151 MHz, $CDCl_3$) δ 163.37, 157.13, 139.53, 100.26, 98.35, 78.74, 47.34, 37.49, 31.98, 29.50, 29.11, 26.32, 22.76, 21.19, 14.21.

**HRMS (*m/z*):** (ESI) calc'd $[M+ACN+Na]^+$: 353.2676, found: 535.2666.

**Compound 8ab**

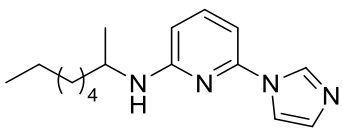

According to **Condition D** at 130 °C for 24 h. imidazole (20 mg, 0.30 mmol) and sodium *tert*-butoxide ($NaO^tBu$) (29 mg, 0.30 mmol) were used as the nucleophile, and the product was purified by flash column chromatography ($SiO_2$; 97.5:2.5 hexanes:EA) to afford compound **8ab** (25 mg, 92%) as a yellow oil.

**$^1$H NMR** (500 MHz, $CD_2Cl_2$) δ 8.26 (s, 1H), 7.48 (t, J = 7.9 Hz, 1H), 7.09 (s, 1H), 6.55 (d, J = 7.6 Hz, 1H), 6.28 (d, J = 8.3 Hz, 1H), 4.57 (d, J = 8.2 Hz, 1H), 3.89 (hept, J = 6.6 Hz, 1H), 1.60 – 1.55 (m, 1H), 1.55 – 1.46 (m, 1H), 1.40 – 1.35 (m, 2H), 1.34 – 1.26 (m, 6H), 1.22 (d, J = 6.4 Hz, 3H), 0.88 (t, J = 6.7 Hz, 3H).

**$^{13}$C NMR** (126 MHz, $CD_2Cl_2$) δ 158.33, 148.32, 139.93, 135.20, 129.98, 116.54, 105.49, 99.43, 47.55, 37.46, 32.24, 29.72, 26.50, 23.02, 20.95, 14.24.

**HRMS (*m/z*):** (ESI) calc'd $[M+H]^+$: 273.2074, found: 273.2075.

**Compound 9ab**

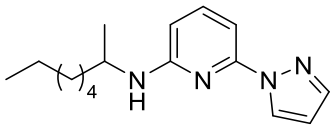

According to **Condition D** at 130 °C for 24 h. pyrazole (20 mg, 0.30 mmol) and sodium *tert*-butoxide ($NaO^tBu$) (29 mg, 0.30 mmol) were used as the nucleophile, and the product was purified by flash column chromatography ($SiO_2$; 97.5:2.5 hexanes:EA) to afford compound **9ab** (25 mg, 93%) as a yellow oil.

**$^1$H NMR** (500 MHz, $CD_2Cl_2$) δ 8.30 (d, J = 2.6 Hz, 1H), 7.48 (s, 1H), 7.32 (t, J = 7.9 Hz, 1H), 6.94 (d, J = 7.7 Hz, 1H), 6.23 (t, J = 2.1 Hz, 1H), 6.08 (d, J = 8.2 Hz, 1H), 4.27 (s, 1H), 3.70 (p, J = 6.3 Hz, 1H), 1.42 (ddt, J = 12.3, 9.3, 6.1 Hz, 1H), 1.37 – 1.29 (m, 1H), 1.23 (hept, J = 5.9 Hz, 2H), 1.19 – 1.08 (m, 6H), 1.05 (d, J = 6.4 Hz, 3H), 0.70 (t, J = 6.6 Hz, 3H).

**$^{13}$C NMR** (151 MHz, $CDCl_3$) δ 157.43, 150.50, 141.58, 139.79, 126.91, 107.01, 104.32, 99.76, 47.40, 37.35, 31.96, 29.47, 26.26, 22.76, 21.00, 14.20.

**HRMS (*m/z*):** (ESI) calc'd $[M+H]^+$: 273.2074, found: 273.2077.

## 4.5 References

Parts of this chapter were submitted to *J. Am. Chem. Soc.* for consideration for potential publication:

"Remote Hydroamination of Disubstituted Alkenes by a Combination of Isomerization and Regioselective N-H Addition"

1. Vasseur, A.; Bruffaerts, J.; Marek, I., Remote functionalization through alkene isomerization. *Nat. Chem.* **2016,** *8* (3), 209-219.

2. Sommer, H.; Juliá-Hernández, F.; Martin, R.; Marek, I., Walking Metals for Remote Functionalization. *ACS Cent. Sci.* **2018,** *4* (2), 153-165.

3. Janssen-Müller, D.; Sahoo, B.; Sun, S.-Z.; Martin, R., Tackling Remote sp3 C−H Functionalization via Ni-Catalyzed "chain-walking" Reactions. *Isr. J. Chem.* **2020,** *60* (3-4), 195-206.

4. Ghosh, S.; Patel, S.; Chatterjee, I., Chain-walking reactions of transition metals for remote C–H bond functionalization of olefinic substrates. *Chem. Commun.* **2021,** *57* (85), 11110-11130.

5. Wang, X.-X.; Lu, X.; Li, Y.; Wang, J.-W.; Fu, Y., Recent advances in nickel-catalyzed reductive hydroalkylation and hydroarylation of electronically unbiased alkenes. *Sci. China Chem.* **2020,** *63* (11), 1586-1600.

6. Buslov, I.; Becouse, J.; Mazza, S.; Montandon-Clerc, M.; Hu, X., Chemoselective Alkene Hydrosilylation Catalyzed by Nickel Pincer Complexes. *Angew. Chem. Int. Ed.* **2015,** *54* (48), 14523-14526.

7. Buslov, I.; Song, F.; Hu, X., An Easily Accessed Nickel Nanoparticle Catalyst for Alkene Hydrosilylation with Tertiary Silanes. *Angew. Chem. Int. Ed.* **2016,** *55* (40), 12295-12299.

8. Chen, C.; Hecht, M. B.; Kavara, A.; Brennessel, W. W.; Mercado, B. Q.; Weix, D. J.; Holland, P. L., Rapid, Regioconvergent, Solvent-Free Alkene Hydrosilylation with a Cobalt Catalyst. *J. Am. Chem. Soc.* **2015,** *137* (41), 13244-13247.

9. Jia, X.; Huang, Z., Conversion of alkanes to linear alkylsilanes using an iridium–iron-catalysed tandem dehydrogenation–isomerization–hydrosilylation. *Nat. Chem.* **2016**, *8* (2), 157-161.

10. Noda, D.; Tahara, A.; Sunada, Y.; Nagashima, H., Non-Precious-Metal Catalytic Systems Involving Iron or Cobalt Carboxylates and Alkyl Isocyanides for Hydrosilylation of Alkenes with Hydrosiloxanes. *J. Am. Chem. Soc.* **2016**, *138* (8), 2480-2483.

11. Hanna, S.; Butcher, T. W.; Hartwig, J. F., Contra-thermodynamic Olefin Isomerization by Chain-Walking Hydrofunctionalization and Formal Retro-hydrofunctionalization. *Org. Lett.* **2019**, *21* (17), 7129-7133.

12. Ye, W.-T.; Zhu, R., Dioxygen-promoted cobalt-catalyzed oxidative hydroamination using unactivated alkenes and free amines. *Chem Catal.* **2022**, *2* (2), 345-357.

13. Crudden, Cathleen M.; Edwards, D., Catalytic Asymmetric Hydroboration: Recent Advances and Applications in Carbon−Carbon Bond-Forming Reactions. *Eur. J. Org. Chem.* **2003**, *2003* (24), 4695-4712.

14. Cipot, J.; Vogels, C. M.; McDonald, R.; Westcott, S. A.; Stradiotto, M., Catalytic Alkene Hydroboration Mediated by Cationic and Formally Zwitterionic Rhodium(I) and Iridium(I) Derivatives of a P,N-Substituted Indene. *Organometallics* **2006,** *25* (25), 5965-5968.

15. Ghebreyessus, K. Y.; Angelici, R. J., Isomerizing-Hydroboration of the Monounsaturated Fatty Acid Ester Methyl Oleate. *Organometallics* **2006,** *25* (12), 3040-3044.

16. Lata, C. J.; Crudden, C. M., Dramatic Effect of Lewis Acids on the Rhodium-Catalyzed Hydroboration of Olefins. *J. Am. Chem. Soc.* **2010,** *132* (1), 131-137.

17. Obligacion, J. V.; Chirik, P. J., Bis(imino)pyridine Cobalt-Catalyzed Alkene Isomerization–Hydroboration: A Strategy for Remote Hydrofunctionalization with Terminal Selectivity. *J. Am. Chem. Soc.* **2013**, *135* (51), 19107-19110.

18. Palmer, W. N.; Diao, T.; Pappas, I.; Chirik, P. J., High-Activity Cobalt Catalysts for Alkene Hydroboration with Electronically Responsive Terpyridine and α-Diimine Ligands. *ACS Catal.* **2015**, *5* (2), 622-626.

19. Scheuermann, M. L.; Johnson, E. J.; Chirik, P. J., Alkene Isomerization–Hydroboration Promoted by Phosphine-Ligated Cobalt Catalysts. *Org. Lett.* **2015**, *17* (11), 2716-2719.

20. Ogawa, T.; Ruddy, A. J.; Sydora, O. L.; Stradiotto, M.; Turculet, L., Cobalt- and Iron-Catalyzed Isomerization–Hydroboration of Branched Alkenes: Terminal Hydroboration with Pinacolborane and 1,3,2-Diazaborolanes. *Organometallics* **2017**, *36* (2), 417-423.

21. Obligacion, J. V.; Chirik, P. J., Earth-abundant transition metal catalysts for alkene hydrosilylation and hydroboration. *Nat. Rev. Chem.* **2018**, *2* (5), 15-34.

22. Hanna, S.; Bloomer, B.; Ciccia, N. R.; Butcher, T. W.; Conk, R. J.; Hartwig, J. F., Contra-thermodynamic Olefin Isomerization by Chain-Walking Hydroboration and Dehydroboration. *Org. Lett.* **2022**, *24* (4), 1005-1010.

23. Lim, Y.-G.; Kang, J.-B.; Kim, Y. H., Regioselective alkylation of 2-phenylpyridines with terminal alkenes via C–H bond activation by a rhodium catalyst. *J. Chem. Soc., Perkin Trans.* 1 1996, (17), 2201-2206.

24. Bair, J. S.; Schramm, Y.; Sergeev, A. G.; Clot, E.; Eisenstein, O.; Hartwig, J. F., Linear-Selective Hydroarylation of Unactivated Terminal and Internal Olefins with Trifluoromethyl-Substituted Arenes. *J. Am. Chem. Soc.* **2014**, *136* (38), 13098-13101.

25. Borah, A. J.; Shi, Z., Rhodium-Catalyzed, Remote Terminal Hydroarylation of Activated Olefins through a Long-Range Deconjugative Isomerization. *J. Am. Chem. Soc.* **2018**, *140* (19), 6062-6066.

26. Zhang, M.; Hu, L.; Lang, Y.; Cao, Y.; Huang, G., Mechanism and Origins of Regio- and Enantioselectivities of Iridium-Catalyzed Hydroarylation of Alkenyl Ethers. *J. Org. Chem.* **2018**, *83* (5), 2937-2947.

27. Lee, W.-C.; Wang, C.-H.; Lin, Y.-H.; Shih, W.-C.; Ong, T.-G., Tandem Isomerization and C–H Activation: Regioselective Hydroheteroarylation of Allylarenes. *Org. Lett.* **2013**, *15* (20), 5358-5361.

28. Yamakawa, T.; Yoshikai, N., Alkene Isomerization–Hydroarylation Tandem Catalysis: Indole C2-Alkylation with Aryl-Substituted Alkenes Leading to 1,1-Diarylalkanes. *Chem. Asian J.* **2014**, *9* (5), 1242-1246.

29. He, Y.; Cai, Y.; Zhu, S., Mild and Regioselective Benzylic C–H Functionalization: Ni-Catalyzed Reductive Arylation of Remote and Proximal Olefins. *J. Am. Chem. Soc.* **2017**, *139* (3), 1061-1064.

30. He, Y.; Liu, C.; Yu, L.; Zhu, S., Ligand-Enabled Nickel-Catalyzed Redox-Relay Migratory Hydroarylation of Alkenes with Arylborons. *Angew. Chem. Int. Ed.* 2020, *59* (23), 9186-9191.

31. He, Y.; Han, B.; Zhu, S., Terminal-Selective C(sp3)–H Arylation: NiH-Catalyzed Remote Hydroarylation of Unactivated Internal Olefins. *Organometallics* **2021**, *40* (14), 2253-2264.

32. He, Y.; Ma, J.; Song, H.; Zhang, Y.; Liang, Y.; Wang, Y.; Zhu, S., Regio- and enantioselective remote hydroarylation using a ligand-relay strategy. *Nat. Commun.* **2022**, *13* (1), 2471.

33. Zhang, Y.; Han, B.; Zhu, S., Rapid Access to Highly Functionalized Alkyl Boronates by NiH-Catalyzed Remote Hydroarylation of Boron-Containing Alkenes. *Angew. Chem. Int. Ed.* **2019**, *58* (39), 13860-13864.

34. Cheng, Q.; Liu, W.; Dang, Y., Insights into the mechanism and regioselectivity in Ni-catalysed redox-relay migratory hydroarylation of alkenes with arylborons. *Chem. Commun.* **2021**, *57* (99), 13610-13613.

35. Liu, J.; Gong, H.; Zhu, S., BH3 · Me2S: An Alternative Hydride Source for NiH-Catalyzed Reductive Migratory Hydroarylation and Hydroalkenylation of Alkenes. *Eur. J. Org. Chem.* **2021**, *2021* (10), 1543-1546.

36. Zhang, Y.; Ma, J.; Chen, J.; Meng, L.; Liang, Y.; Zhu, S., A relay catalysis strategy for enantioselective nickel-catalyzed migratory hydroarylation forming chiral α-aryl alkylboronates. *Chem* **2021**, *7* (11), 3171-3188.

37. Werner, E. W.; Mei, T.-S.; Burckle, A. J.; Sigman, M. S., Enantioselective Heck Arylations of Acyclic Alkenyl Alcohols Using a Redox-Relay Strategy. *Science* **2012**, *338* (6113), 1455-1458.

38. Mei, T.-S.; Werner, E. W.; Burckle, A. J.; Sigman, M. S., Enantioselective Redox-Relay Oxidative Heck Arylations of Acyclic Alkenyl Alcohols using Boronic Acids. *J. Am. Chem. Soc.* **2013**, *135* (18), 6830-6833.

39. Mei, T.-S.; Patel, H. H.; Sigman, M. S., Enantioselective construction of remote quaternary stereocentres. *Nature* **2014**, *508* (7496), 340-344.

40. Qian, D.; Hu, X., Ligand-Controlled Regiodivergent Hydroalkylation of Pyrrolines. *Angew. Chem. Int. Ed.* **2019**, *58* (51), 18519-18523.

41. Zhou, F.; Zhang, Y.; Xu, X.; Zhu, S., NiH-Catalyzed Remote Asymmetric Hydroalkylation of Alkenes with Racemic α-Bromo Amides. *Angew. Chem. Int. Ed.* **2019**, *58* (6), 1754-1758.

42. Wang, J.-W.; Liu, D.-G.; Chang, Z.; Li, Z.; Fu, Y.; Lu, X., Nickel-Catalyzed Switchable Site-Selective Alkene Hydroalkylation by Temperature Regulation. *Angew. Chem. Int. Ed.* **2022**, *61* (31), e202205537.

43. Li, P.; Lee, B. C.; Zhang, X.; Koh, M. J., Base-Mediated Site-Selective Hydroamination of Alkenes. *Synthesis* **2021**, *54* (06), 1566-1576.

44. Miao, H.-Z.; Liu, Y.; Chen, Y.-W.; Lu, H.-Y.; Li, J.; Lin, G.-Q.; He, Z.-T., Stereoselective Pd-Catalyzed Remote Hydroamination of Skipped Dienes with Azoles. *Synlett* **2022**, *33*, A-F. DOI: 10.1055/a-1916-2937

45. Zhang, Y.; He, J.; Song, P.; Wang, Y.; Zhu, S., Ligand-Enabled NiH-Catalyzed Migratory Hydroamination: Chain Walking as a Strategy for Regiodivergent/Regioconvergent Remote sp3C–H Amination. *CCS Chem.* **2020,** *3* (9), 2259-2268.

46. Lee, C.; Seo, H.; Jeon, J.; Hong, S., γ-Selective C(sp3)–H amination via controlled migratory hydroamination. *Nat. Commun.* **2021**, *12* (1), 5657.

47. Du, B.; Ouyang, Y.; Chen, Q.; Yu, W.-Y., Thioether-Directed NiH-Catalyzed Remote γ-C(sp3)–H Hydroamidation of Alkenes by 1,4,2-Dioxazol-5-ones. *J. Am. Chem. Soc.* **2021**, *143* (37), 14962-14968.

48. Wagner-Carlberg, N.; Rovis, T., Rhodium(III)-Catalyzed Anti-Markovnikov Hydroamidation of Unactivated Alkenes Using Dioxazolones as Amidating Reagents. *J. Am. Chem. Soc.* **2022**, *144* (49), 22426-22432.

49. Rosenfeld, D. C.; Shekhar, S.; Takemiya, A.; Utsunomiya, M.; Hartwig, J. F., Hydroamination and Hydroalkoxylation Catalyzed by Triflic Acid. Parallels to Reactions Initiated with Metal Triflates. *Org. Lett.* **2006,** *8* (19), 4179-4182.

50. Xi, Y.; Ma, S.; Hartwig, J. F., Catalytic asymmetric addition of an amine N–H bond across internal alkenes. *Nature* **2020,** *588* (7837), 254-260.

51. Ma, S.; Xi, Y.; Fan, H.; Roediger, S.; Hartwig, J. F., Enantioselective hydroamination of unactivated terminal alkenes. *Chem* **2022**, *8* (2), 532-542.

52. Ma, S.; Hill, C. K.; Olen, C. L.; Hartwig, J. F., Ruthenium-Catalyzed Hydroamination of Unactivated Terminal Alkenes with Stoichiometric Amounts of Alkene and an Ammonia Surrogate by Sequential Oxidation and Reduction. *J. Am. Chem. Soc.* **2021**, *143* (1), 359-368.

53. Hanley, P. S.; Hartwig, J. F., Intermolecular Migratory Insertion of Unactivated Olefins into Palladium–Nitrogen Bonds. Steric and Electronic Effects on the Rate of Migratory Insertion. *J. Am. Chem. Soc.* **2011,** *133* (39), 15661-15673.

54. Hanley, P. S.; Hartwig, J. F., Migratory Insertion of Alkenes into Metal–Oxygen and Metal–Nitrogen Bonds. *Angew. Chem. Int. Ed.* **2013**, *52* (33), 8510-8525.

55. Miyashita, A.; Yasuda, A.; Takaya, H.; Toriumi, K.; Ito, T.; Souchi, T.; Noyori, R., Synthesis of 2,2'-bis(diphenylphosphino)-1,1'-binaphthyl (BINAP), an atropisomeric chiral bis(triaryl)phosphine, and its use in the rhodium(I)-catalyzed asymmetric hydrogenation of .alpha.-(acylamino)acrylic acids. *J. Am. Chem. Soc.* **1980,** *102* (27), 7932-7934.

56. Müller, D.; Umbricht, G.; Weber, B.; Pfaltz, A., C2-Symmetric 4,4′,5,5′-Tetrahydrobi(oxazoles) and 4,4′,5,5′-Tetrahydro-2,2′-methylenebis[oxazoles] as Chiral Ligands for Enantioselective Catalysis Preliminary Communication. *Helv. Chim. Acta* **1991,** *74* (1), 232-240.

57. Saito, T.; Yokozawa, T.; Ishizaki, T.; Moroi, T.; Sayo, N.; Miura, T.; Kumobayashi, H., New Chiral Diphosphine Ligands Designed to have a Narrow Dihedral Angle in the Biaryl Backbone. *Adv. Synth. Catal.* **2001,** *343* (3), 264-267.

58. Pai, C.-C.; Li, Y.-M.; Zhou, Z.-Y.; Chan, A. S. C., Synthesis of new chiral diphosphine ligand (BisbenzodioxanPhos) and its application in asymmetric catalytic hydrogenation. *Tetrahedron Lett.* **2002,** *43* (15), 2789-2792.

59. Duprat de Paule, S.; Jeulin, S.; Ratovelomanana-Vidal, V.; Genêt, J.-P.; Champion, N.; Deschaux, G.; Dellis, P., SYNPHOS: a New Atropisomeric Diphosphine Ligand. From

Laboratory-scale Synthesis to Scale-up Development. *Org. Process Res. Dev.* **2003**, *7* (3), 399-406.

60. Shen, K.; Wang, Q., Copper-Catalyzed Alkene Aminoazidation as a Rapid Entry to 1,2-Diamines and Installation of an Azide Reporter onto Azahetereocycles. *J. Am. Chem. Soc.* **2017,** *139* (37), 13110-13116.

61 .Robbins, D. W.; Hartwig, J. F., A C–H Borylation Approach to Suzuki–Miyaura Coupling of Typically Unstable 2–Heteroaryl and Polyfluorophenyl Boronates. *Org. Lett.* **2012,** *14* (16), 4266-4269.

62. Berhal, F.; Esseiva, O.; Martin, C.-H.; Tone, H.; Genet, J.-P.; Ayad, T.; Ratovelomanana-Vidal, V., (R)-3,5-diCF3-SYNPHOS and (R)-p-CF3-SYNPHOS, Electron-Poor Diphosphines for Efficient Room Temperature Rh-Catalyzed Asymmetric Conjugate Addition of Arylboronic Acids. *Org. Lett.* **2011,** *13* (11), 2806-2809.

63.Cincinelli, R.; Dallavalle, S.; Nannei, R.; Merlini, L.; Penco, S.; Giannini, G.; Pisano, C.; Vesci, L.; Ferrara, F. F.; Zuco, V.; Zanchi, C.; Zunino, F., Synthesis and structure–activity relationships of new antiproliferative and proapoptotic retinoid-related biphenyl-4-yl-acrylic acids. *Biorg. Med. Chem.* **2007,** *15* (14), 4863-4875.

64. Sevov, C. S.; Hartwig, J. F., Iridium-Catalyzed Oxidative Olefination of Furans with Unactivated Alkenes m, R. S.; Watson, D. A., Synthesis of Axially Chiral 2,2′-Bisphosphobiarenes via a Nickel-Catalyzed Asymmetric Ullmann Coupling: General Access to Privileged Chiral Ligands without Optical Resolution. *J. Am. Chem. Soc.* **2021,** *143* (3), 1328-1333.

65. Sevov, C. S.; Hartwig, J. F., Iridium-Catalyzed Oxidative Olefination of Furans with Unactivated Alkenes. *J. Am. Chem. Soc.* **2014,** *136* (30), 10625-10631.